AD623630

Naval
Air
Engineering
Center
philadelphia

FOUNDATIONAL RESEARCH PROGRAM

DEPARTMENT OF THE NAVY

BUREAU OF NAVAL WEAPONS

DDC
NOV 3
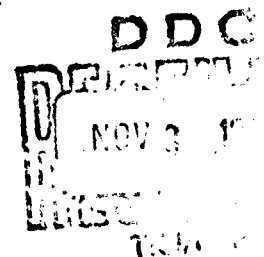
NOTICE

Discussions concerning any commercial products in this publica-

tion do not constitute an endorsement by the Government, nor

are they intended to convey or imply the license or right to

use such products.

Reviewed and Approved

A. H. CLANCY, JR.
Commanding Officer, NAVATREMCEN
27 August 1965

U. S. NAVAL AIR ENGINEERING CENTER

FOREWORD

A Foundational Research Program was initiated at the U. S. Naval Air Engineering Center by the Bureau of Aeronautics in May 1959 and has had continued support by the Bureau of Naval Weapons. The Program supports the Navy's general policy that Research and Development Activities directly control a portion of their research capacity to exploit new ideas related to their fields of interest.

At the NAVAIRENGCEN, Foundational Research is defined generally as research to develop knowledge useful in the current and future development of systems, weapons, and components; to establish the feasibility of applying new ideas; or to foster the creative productivity of the Center Staff in military problems. Normally, this research includes basic and applied research up to the stage of indicating that normal development and application may be successfully undertaken. However, no restrictive or ironclad definition of research has been indicated or even considered desirable.

The Foundational Research Program endeavors to provide:

     1. A stimulating research and development atmosphere conducive to the formulation of new concepts and ideas;

     2. Continuing programs of research which will establish a reservoir of knowledge that can be drawn upon for the solution of immediate and long-term naval air problems;

     3. Opportunities for preliminary investigation of the more speculative problems unsuitable for study under specific task assignments;

     4. Flexibility of operation which will enable programs to be started or stopped as deemed appropriate by NAVAIRENGCEN.

This report gives a brief summary of each task undertaken during Fiscal Year 1965. Of the twenty-six tasks in progress during Fiscal Year 1965, twenty-five have carried over into Fiscal Year 1966.
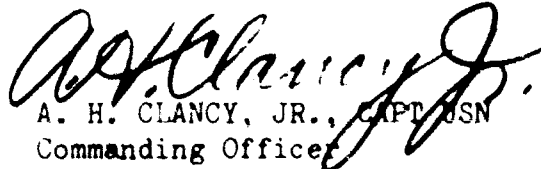
A. H. CLANCY, JR., CAPT USN
Commanding Officer

i

TABLE OF CONTENTS

ii

RESEARCH ON THE STATICS AND DYNAMICS OF FLUIDS

FRIEDRICH O. RINGLEB

BACKGROUND.

Former investigations under the same title (see reference 1/) dealt with the following topics: Studies on vortex motion, flow control by standing vortices, air flow over the deck of an aircraft carrier, control of stack gases using standing vortices, flow over blast deflectors, the geometry of flow in general and others. A result of the early studies on vortex motion was the development of the three dimensional smoke tunnel of the Naval Air Engineering Laboratory, which served as a powerful research instrument for most of the later investigations under the Foundational Research Project No. 1.

OBJECTIVES.

The successful solution of problems, as discussed in the foundational research reports 1963 and 1964, automatically lead to new problems and investigations, which formed the objectives for the foundational research project No. 1 during the year 1965. Particular attention was paid or intended to pay to:

(1) Continued investigations on carrier airflow,
(2) study of scale effects influencing the streamline patterns of smoke tunnel observations,
(3) flow visualization in water by dyed longitudinal vortices,
(4) flow visualization in two phase flow, and,
(5) studies of air entrainment in water.

ACCOMPLISHMENTS.

(1) Control of airflow over an aircraft carrier.

The three dimensional smoke tunnel provided the possibility of studying the airflow over an aircraft carrier, and especially of finding the origin of the dangerous air disturbances met by landing aircraft near the stern - called the "burble." The moving carrier influences the air above the water like a low aspect ratio air plane wing influences the air beside the fuselage. In general, a wing tip vortex forms, which results in a rotation of the air on the down stream side of the ship, unless the aerodynamic angle of attack between the ship and the air flow is zero. In the latter case, the distortion of the airflow over the carrier is smallest. The flow is then similar to the almost parallel flow over a ridge. It is this case which yields the most favorable conditions for landing aircraft.

- 1 -
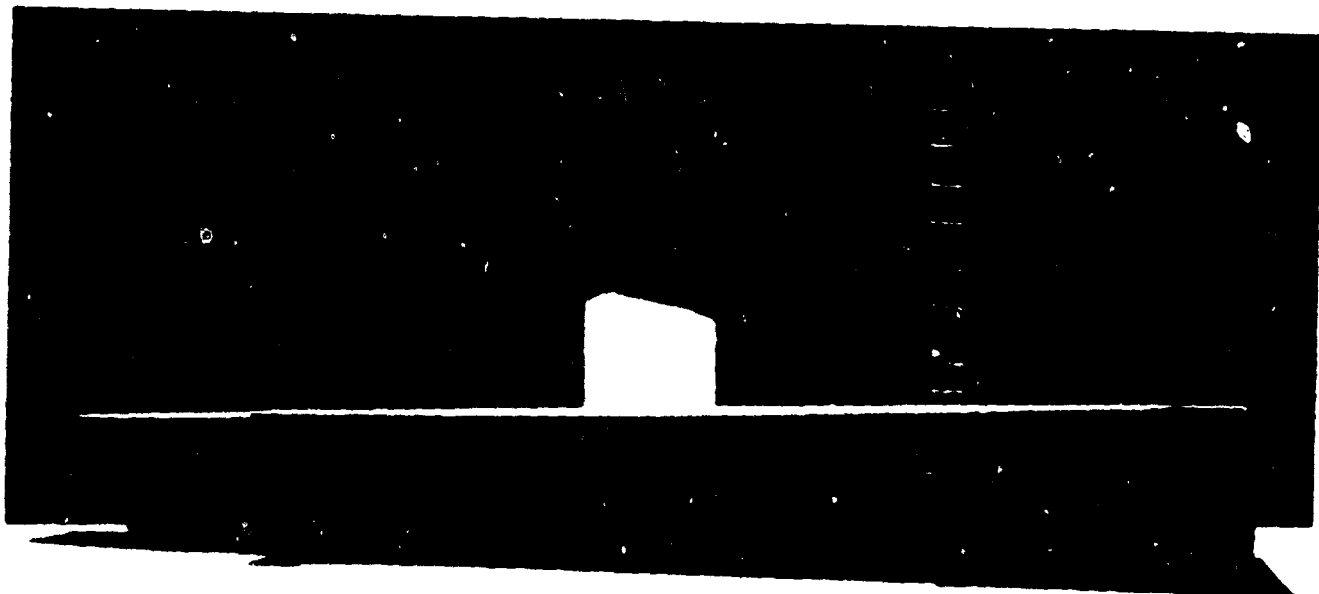
FIGURE 1. AIRFLOW OVER AN AIRCRAFT CARRIER PARALLEL TO CANTED DECK AXIS. ISLAND PARALLEL TO SHIP AXIS.
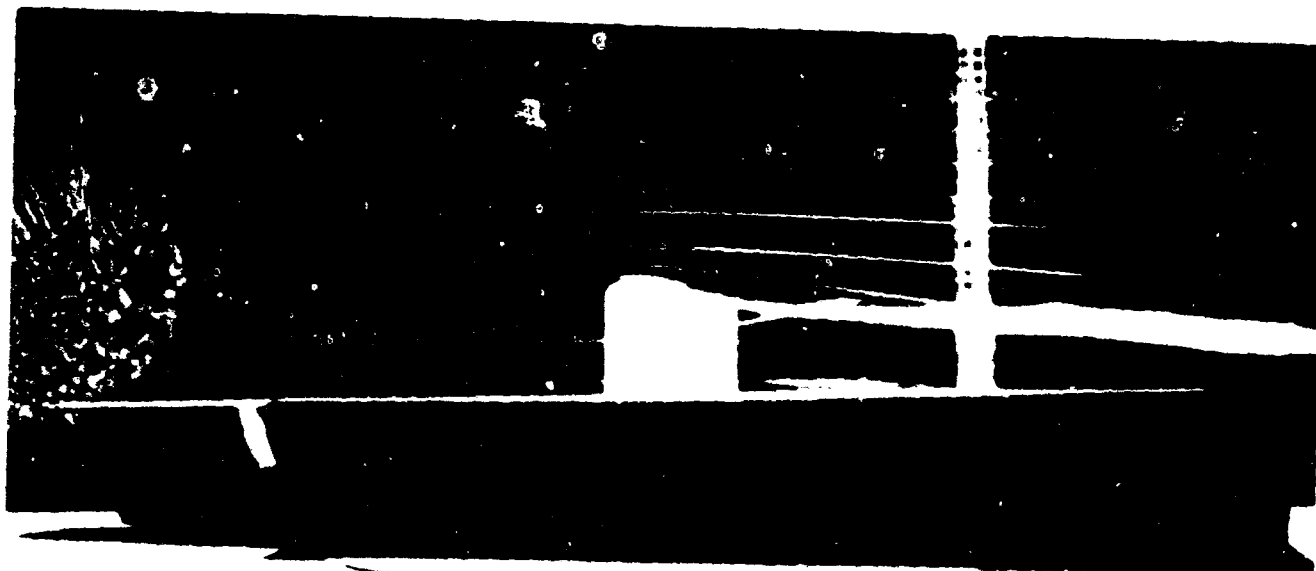
FIGURE 2. LIKE FIGURE 1. THE CORE OF THE TIP VORTEX IS MADE VISIBLE BY TITANIUM TETRA-CHLORIDE SMOKE EMANATING FROM THE TIP.

- 2 -

FIGURE 3. AIRFLOW OVER AN AIRCRAFT CARRIER PARALLEL TO CANTED DECK AXIS. ISLAND TURNED SO THAT NO TIP VORTEX IS FORMED.

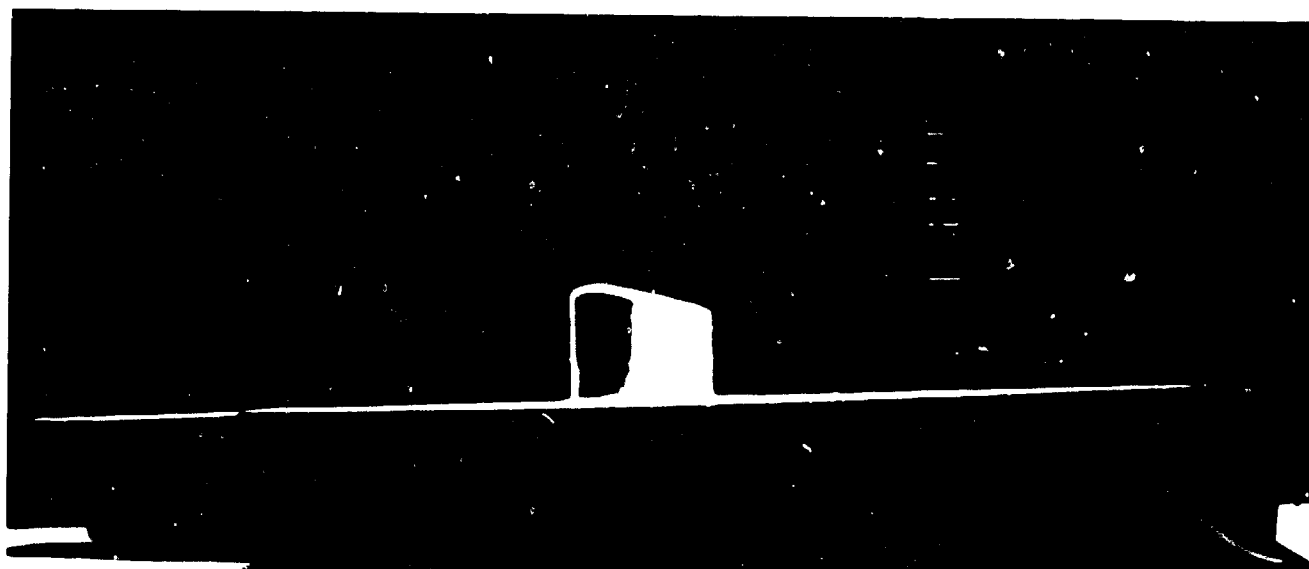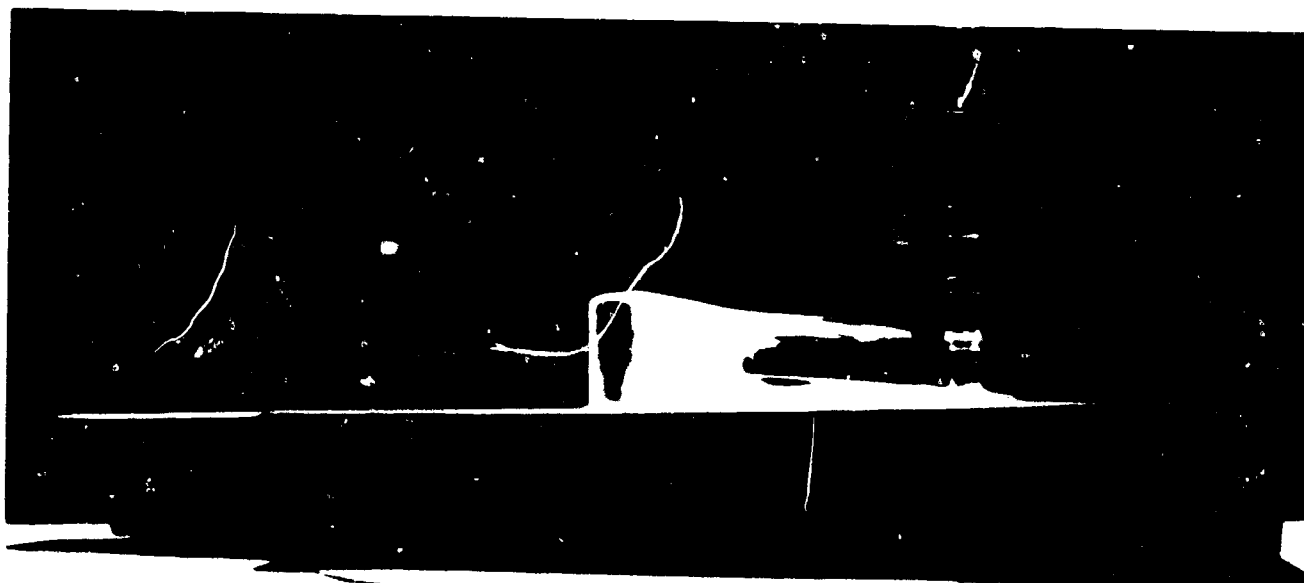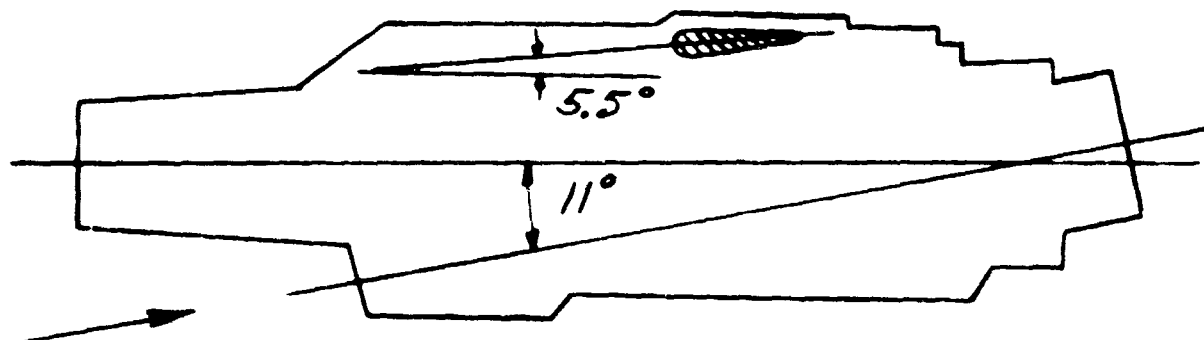FIGURE 4. LIKE FIGURE 3 WITH TITANIUM TETRACHLORIDE SMOKE EMANATING FROM TIP SHOWING THE WAKE OF THE ISLAND.

Wind over deck

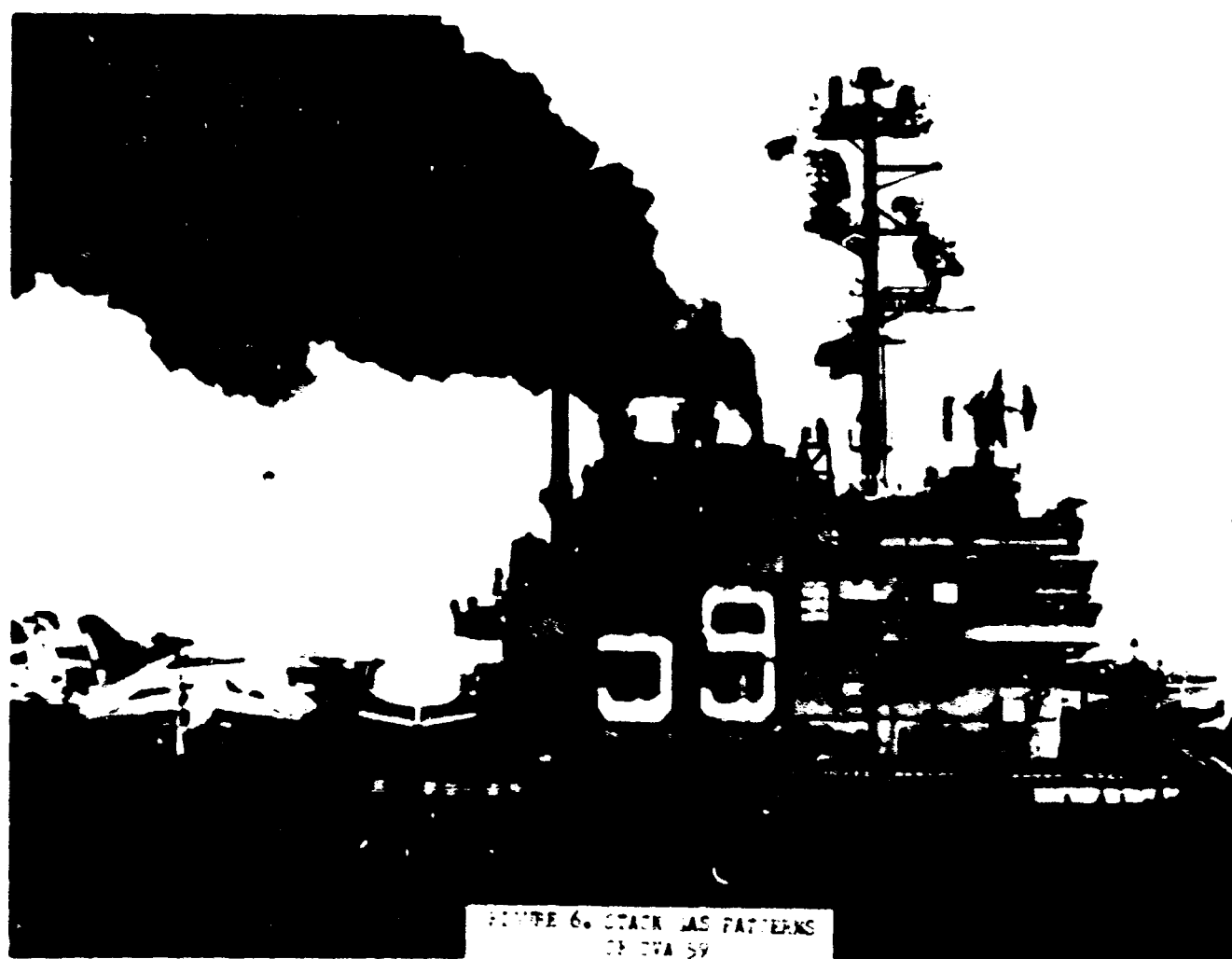FIGURE 5. POSITION OF ISLAND WITHOUT WING TIP VORTEX

FIGURE 6. STACK GAS PATTERNS ON CVA 59

- 4 -

In order to obtain this case, the landing operation must be carried out under zero aerodynamic angle of attack between the carrier and the resulting airflow over the carrier. This can be achieved by turning the island into a direction in which the wind, which is assumed to be parallel to the axis of the canted deck, forms a zero aerodynamic angle of attack with the ship. Smoke tunnel observations show that the nose of the island must be turned about one half of the angle between the ship axis and the axis of the canted deck, toward the canted deck axis in order to obtain the proper position (see Fig. 5).

In order to demonstrate this amazingly simple solution of a particularly serious problem of Naval Aviation, a simplified streamlined aircraft carrier model is shown in the three dimensional smoke tunnel (see Figures 1 through 4). The streamlining, especially of the island, clearly shows the essential features of the overall flow, not disturbed by the confusing influences of many little protuberances. Figure 1 shows the carrier airflow under a wind direction which is about parallel to the axis of the canted deck. Here the island has the conventional position parallel to the ship axis. The airflow downstream of the island shows the effect of the wing tip vortex. The air is rotating around a horizontal axis. This can be recognized by observing the smoke lines incoming from the left within a vertical plane under an angle of about 11° with the symmetry plane of the carrier hull. Downstream of the island these streamlines become spirals, and wind around the core of the wing tip vortex (shown in Figure 2) by Titanium tetrachloride smoke emanating from the wing tip. The figures 3 and 4 correspond to the Figures 1 and 2. However, the nose of the island has now been turned (about 5°) toward the canted deck axis until the wing tip vortex disappeared, and the flow over the deck became almost undisturbed. The veil of smoke seen in Fig. 4 indicates the wake of the island.

This method of removing a severe disturbance of the airflow near the stern has been accepted by BuShips for application at the new carrier CVA-68. Its island will have a vertical plane of symmetry under a non-zero angle with the ship axis. It also will have a rounded nose in order to reduce the width of its wake, schematically shown in Figure 5 (compare also reference 2).

The results of these investigations will be presented by the principal investigator under the title "Effects of the Configuration of an Aircraft Carrier on Starting and Landing Aircraft", at the Fifth Annual National Conference on Environmental Effects on Aircraft and Propulsion Systems at Princeton, N. J., September 1965.

(2) Scale effects on streamline patterns.

It has been questioned frequently whether the model observations in the smoke tunnel under a rather moderate Reynolds number convey a true picture of the flow corresponding to a very high Reynolds number, as in the case of the airflow over an aircraft carrier. Since this question is important to the application of almost all smoke tunnel observations, it has been made the objective of a separate experimental and theoretical study. In particular, the question has been studied in how far the pattern
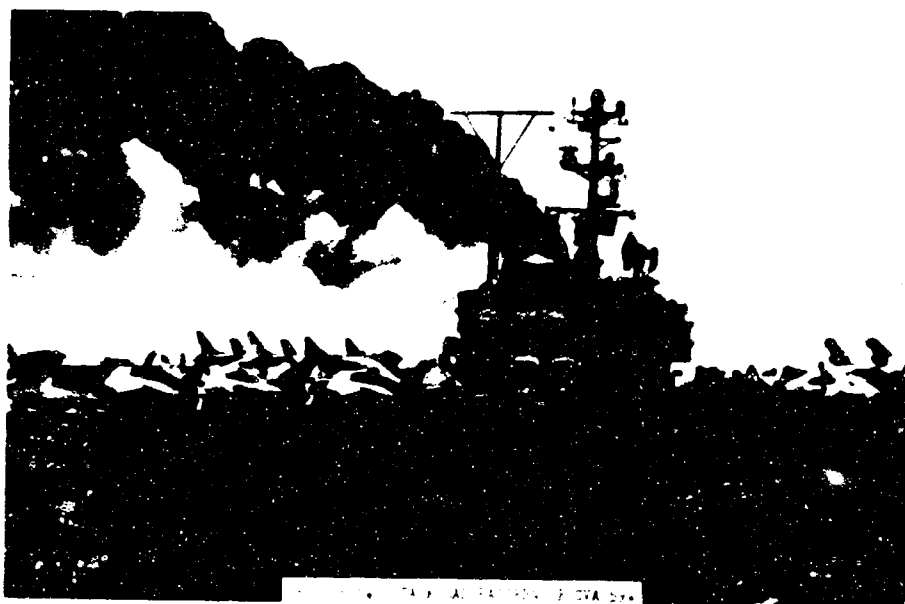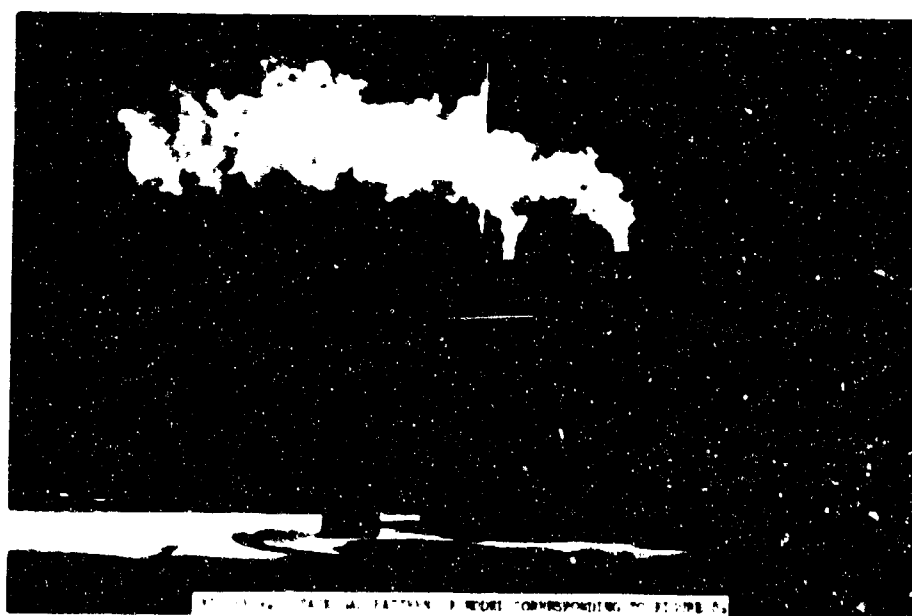
of the streamlines of a viscous flow depends on the scale. Theoretically, it can be shown that there exist steamline patterns of real, i.e. viscous, fluid flows which are independent of the Reynolds number. For instance, in a two-dimensional duct whose boundaries are two of the streamlines ψ = constant

where
$$\psi = f\left(A + B\ell_{nn}r + C\varphi\right)$$

(r, φ polar coordinates, A, B, C constants) and $f(\tau)$ is a function of τ which satisfies a special differential equation of fourth order and proper boundary conditions, the streamlines (logarithmic spirals) do not change with the Reynolds number. In the case of other solutions of Navier-Stokes equations they do, depending on the circumstances. A paper discussing such solutions is being prepared.

In the following, some examples of an experimental investigation of the same question are included, consisting in a comparison of the stack gas patterns of the CVA 59 (Forrestal). Figures 6 and 7 show two corresponding stack gas patterns-full scale and of a smoke tunnel model. Figures 8 and 9 show two other corresponding patterns. These examples demonstrate sufficiently, that under certain circumstances and by proper scaling of the boundary conditions, full scale properties can be predicted very well from smoke tunnel observations at much smaller Reynolds numbers.

A paper containing the details of this investigation is also being prepared.

(3) <u>Water tunnel for flow visualization</u>.

It was intended to develop and construct a gravity water tunnel for flow visualization, somewhat similar to that of Office National D'Etudes et de Recherches Aerospatiales in Paris, but with increased performance on the basis of the smoke tunnel experiences. Due to sickness of the principal investigator for about three quarters of a year, this project, the project on visualization of two phase flow, and the study on air entrainment in water, had to be postponed for a considerable time· These projects are now underway and will be continued during 1966.

<u>FUTURE PLANNING</u>.

In addition to the projects on flow visualization in water and in two-phase media, also theoretical studies on cavitation, air entrainment and air lubrication are planned, depending on the progress of the flow visualization studies in water.

<u>REFERENCES</u>.

1/ F. O. Ringleb, Research on the Statics and Dynamics of Fluids, The Foundation Research program at the Naval Air Engineering Center, Philadelphia, Pa., August 1963 and August 1964.

2/ D. Johnson, Airflow investigations on Model Aircraft Carriers, Royal Aircraft Establishment (Bedford), Technical Note No. Naval 59, June 1963.

BLANK PAGE

MECHANISM OF THE LUBRICATION OF METAL SURFACES WITH SOLID FILMS

MARTIN J. DEVINE

BACKGROUND.

The operating environments for space vehicles and missiles include: nuclear radiation, low pressures, oxidizing media and temperatures ranging from approximately minus 460°F to plus 2800°F. Analysis of lubrication research being conducted by Government and industrial laboratories covering greases, oils, gases and solid films indicates that the inorganic solid films developed by the Aeronautical Materials Laboratory (AML) offer the greatest potential for solving many problems of space lubrication. It should be noted that a hydrodynamic component exists in the mechanism of lubrication for oils, greases and gases. Accordingly, existing rheological theories can be utilized effectively for many design purposes involving these lubricants. Since viscosity is not associated with solid films such theories cannot be applied. Further, many factors which characterize important parameters basic to solid film lubrication have been uncovered only recently. These factors include: lubricant particle size, metal pretreatment, lubricant-bearing reactivity and surface asperities. To date, there is no complete quantitative definition relating the effectiveness of the solid film lubricant to these factors.

The specific aim of the program is to determine the mechanism by which metal surfaces are lubricated by solid films and to provide a definitive working theory.

OBJECTIVES.

Based on current Aerospace Industries Association estimates for space vehicle lubrication needs by 1970, and also on inquiries from missile manufacturers and bearing companies concerning solid film lubricants, it is considered that inorganic solid films may be the only satisfactory lubricant for many of the applications to be encountered. Accordingly, the results of a program which provides the physico-chemical mechanism of lubricity for solid films would accelerate the design of the optimum lubricant-bearing system. The work to be carried out under the program is to establish and define principles and scientific laws of solid film lubrication, and aid in establishing the basic technology of solid film lubrication.

ACCOMPLISHMENTS.

As a result of studies performed from the beginning of this project to the last annual report (30 June 1964), a number of scientific accomplishments have been achieved: e.g. (1) the reservoir theory for solid lubricants was postulated and established; (2) the interdependence concept for lubricant, bearing geometry and bearing composition was defined;

and (3) the synergistic effect for molybdenum metal and metallic sulfides was established. In addition, the effect of vacuum-temperature environment was explored for inorganic solid films.

Exploratory work conducted since 1 July 1964 has continued in four areas in an effort to provide a range of information pertinent to solid film mechanism and characteristics. This work is summarized as follows:

1. The study of internal and external changes for solid film lubricants under dynamic conditions of wear. A motion picture utilizing a stroboscopic technique provides for visual observation of blister formation and rupture in bonded solid film lubricants and burnished lubricating films.

2. The effect of liquid abrasion in the preparation of metal surfaces for solid lubrication. Five different grit compositions covering a wide range of particle size were employed to study the effect of wear characteristics for solid lubricants.

3. Experiments to determine the possibility of establishing a general equation to describe wear of solid lubricants and the contribution exhibited by the different phases of the wear process.

4. Wear characteristics at cryogenic temperatures.

Since the laboratory program covering the latter research area has been completed, details are provided below. Extensive data has been obtained for two of the remaining three areas; however, additional experiments will be required to project the findings. A detailed report will be prepared upon completion of test runs.

A. Solid Film Characteristics - Cryogenic Temperatures. It has been shown that cryogenic fluids exhibit lubricant capabilities for bearing systems with a short term operating interval. The limitations of such fluids in maintaining extended performance were established by using liquid oxygen as the source of lubricant in experiments conducted by AML, and in low temperature motor operation using liquid nitrogen in tests initiated by Naval Research Laboratory. Accordingly, it was considered necessary to develop knowledge covering the wear life and failure process for inorganic solid film lubricant exposed to sliding and rolling bearing surfaces at temperatures in the range of liquid helium.

1. The operation of a motor cooled to cryogenic temperatures requires a lubricant material exhibiting a minor or zero change in viscosity with decrease in temperature, which eliminates the use of known fluid or grease lubricants. It should be noted that the miniature ball bearings associated with a synchronous motor were designed specifically for conventional oils or grease. An analysis of the operating environment and bearing geometry imposes the following requirements on the lubricant:

a. No deterioration when subjected to extremes of temperature producing different dimensional characteristics for the substrate.

b. Provide extremely low torque values over a temperature range from -450°F to 77°F.

c. Resistant to mechanical abrasion.

d. Minimize friction and wear.

e. Capacity for being deposited in a thin adherent film.

2. It was also considered important, ba ?d on economic considerations, to explore a lubricant system compatible with the available miniature bearings. An inorganic solid film lubricant derived from $Na_2 O:SiO_2$ (1:2.90) binder and lubricating solids composed of molybdenum disulfide and graphite, was selected for the initial runs. This lubricant was the subject of a previous study and was found to exhibit the following characteristics: thermally stable from -300°F to +1000°F at 760 mm. Hg, resistant to nuclear radiation (gamma dosage = 5×10^9r), compatible with liquid oxygen and stable in the high-vacuum region.

3. In preparing the lubricant, MoS_2 powder and graphite powder are mixed in a beaker. While stirring the mixture thoroughly water is added slowly. Continue addition of water, stirring to insure complete wetting of the powder mixture, until a pourable slurry is obtained. (Note - An excess amount of water will result in separation. if separation is observed, the mixture should be discarded and a second preparation using fresh constituents started.)

4. The pourable slurry is added to sodium silicate solution with stirring to obtain a uniform sprayable mixture.

5. The means devised to utilize solid film lubricants in ball bearings consisted of:

a. Disassembling the miniature ball bearing.

b. Applying the solid film to retainers and races.

c. Curing the solid film.

d. Reassembling the bearing.

6. The assembled bearing is then subjected to rotation at several hundred rpm. Loose adhering particles of lubricant are removed by subjecting the internal areas of the bearing to a stream of nitrogen gas. The solid film lubricated bearings were then placed in the motor assembly and subjected to the low temperature-vacuum environment. The successful performance of the test bearings, as reported herein, further establishes the capabilities of solid lubricants for antifriction bearings.

7. The utilization of solid film lubricants in high speed miniature ball bearing applications is a relatively recent advance in the science of lubrication. Accordingly, not enough is yet known about the wear pattern encountered with such lubricants in ball sliding and rolling. Oxidation or other chemical degradation of liquid lubricants is a frequent cause of failure of oils and greases; however, the inorganic lubricating solid present in the solid film under investigation is, by comparison, more oxidation resistant and thermally stable. Therefore, it is hypothesized that ball bearing failure is due to the removal of the solid film by the continual rubbing action of the ball in contact with the lubricated surfaces. Prior to break-in, the lubricant film has a dull bluish-gray appearance; after break-in, the surface assumes a shiny metallic appearance in the wear zones of the ball-race and ball retainer contact. This difference is shown in Figure 1. Eventually a complete removal of film by mechanical action allows metal-to-metal contact, resulting in failure of the bearing assembly.

8. The first set of tests were made with MoS_2, graphite and sodium silicate lubricated miniature bearings that had only a nominal 0.0008 inch clearance. The tests were successful in showing that the bearing would operate, and by careful selection, would run continuously in excess of 160 hours in liquid nitrogen.

9. Since the internal radial clearance of the test bearings ranged from 0.0001 - 0.0008, it was considered that significant limitations would result for solid film lubricant performance.

10. Miniature bearings having a 0.0008 inch radial clearance were then obtained for additional runs. This reduced the rejection rate from 3 out of 4, to less than 1 to 10.

11. Continuous life tests on the latter bearings gave results in excess of 400 hours under the same test conditions. Lubricant deposition technique improvements provided for continuous operation in excess of 700 hours. At this point, the test procedure was changed to provide temperature cycling and to simulate on and off operation. In one long term cycling test, 900 running hours were obtained.

SUMMARY.

A. Publications - Thirteen technical publications and five reports have been completed to date:

"Inorganic Solid Film Lubricants," Journal of Chemical and Engineering Data, Vol. 6, No. 1 (Jan 1961)

"Dry Film Lubricants Research," Bureau of Naval Weapons Bulletin No. 3-60

"The Lubrication of Ball bearings with Solid Films," American Society of Mechanical Engineers ASME 61-LUBS-11, May 1961
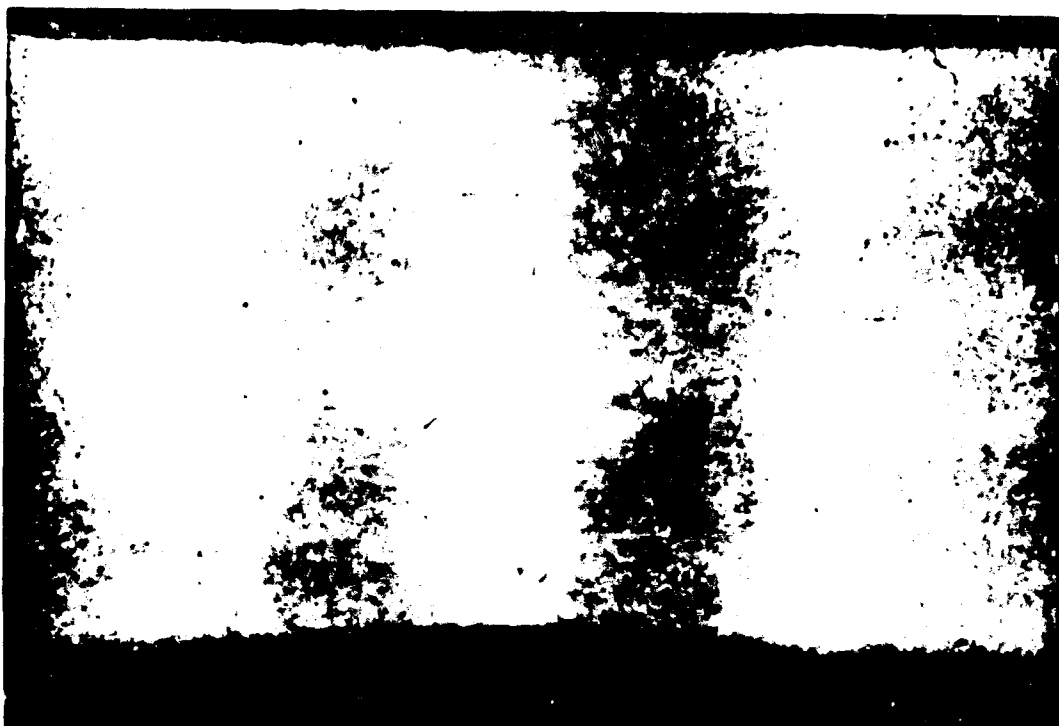
BEFORE BREAK-IN
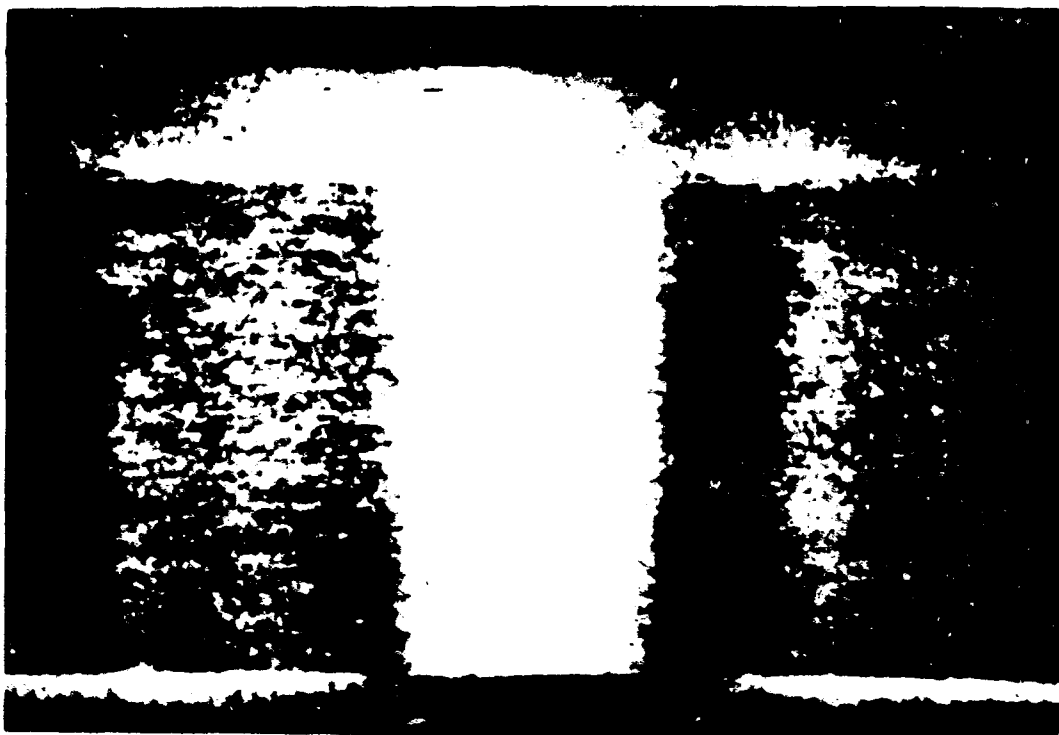
AFTER BREAK-IN

SURFACE APPEARANCE OF INORGANIC SOLID FILM LUBRICANT

FIGURE 1

- 13 -

"The Effect of the Chemical Composition of Metals and Lubrication by Solids," American Chemical Society Publication, April 1963

"Antifriction Bearing Design Considerations for Solid Lubrication," American Society of Mechanical Engineers ASME 63-MD-43, May 1963

"Naval Air Material Center Lubricants Research" (Motion Picture), Nov 1962

"Solids and Solid Lubrication," ASLE, 12th Annual Lubrication Course, Mar 1964

"Molybdenum Disulfide Diester Lubricating Greases," Journal of the National Lubricating Grease Institute, Vol. XXVII, No. 10 (Jan 1964)

"A Review of Aerospace Bearing Research," USAF-SWRI Bearing Conference, Mar 1964

"Naval Air Engineering Center's Solid Lubricants Program," BUWEPS Bulletin

"Aromatic Polyimide Compositions for Solid Lubrication" Lubrication Engineering, Vol. 20, No. 6 (Jun 1964)

"Solids and Solid Lubrication" Lubrication Engineering (Jan 1965)

AML Report No. NAMC-AML-RS-7045/7, 15 Dec 1959, Mar 1960, Jun 1960, Sep 1960, Dec 1960

    B. <u>Presentations</u> - Twenty-four technical presentations, each by invitation, have been made to sixteen technical societies.

    C <u>References by Other Investigators</u> - Over 100 references to the work under this program are contained in various technical reports, papers, journals, etc.

    D. <u>Reviews of Program</u> - Work in this program, has been the subject of eighty reviews by technical publications, engineering literature, etc.

    E. <u>Requests for Reports</u> - The interest of the military, industry, universities, etc., in this work is shown by their requests for copies of progress reports, publications, etc. Approximately 350 organizations have received these reports, including twenty in foreign countries.

FUTURE PLANS.

Laboratory work to be conducted in the near future will include:

1. Characterizing surface effects (chemical and physical).

2. A study of basic relationships for chemical reactivity, crystal properties, physical constants and lubricant wear characteristics.

3. Factors pertinent to lubricating effects for self lubricating solid sections: e.g., mechanical stability and wear rate.

BLANK PAGE

THE ROLE OF OXYGEN IN THE BRITTLE FRACTURE OF METALS

EDWIN S. TANKINS AND MARSHALL K. THOMAS

Background.

A considerable amount of discussion concerning the thermodynamic proper-
ties of dissolved oxygen has been presented in recent reports.[1] [2]
Previous and forthcoming publications contain detailed descriptions of
the apparatus and associated electrical system,[3] [4] [5] [6] and the
method of gas analysis.[7]

As a result of a joint effort between E. S. Tankins and Prof. G. R. Belton,
Metallurgy Department, University of Pennsylvania, a paper was recently
submitted [8] which describes a model that appears to predict the thermo-
dynamic behavior of dilute solutions of oxygen in liquid metals. It will
take awhile to analyze all the systems, but in all the checks made, the
agreement is excellent between the predicted and the experimental
results. It appears that the model will make a significant contribution
to the solution theory, and will enable metallurgists to make reasonable
estimates of thermodynamic properties of the systems of interest to
them.

The thermodynamic studies are important in understanding the activity of
oxygen in solution and being able to control the oxygen in solution.
Specimens with controlled oxygen can be subjected to a series of tests,
which will enable the researcher to understand what is happening in the
metal.

Within the last few years, there has been considerable interest in the
deformation mechanisms of the body centered cubic metals. They are
characterized by an increasing strength and strain rate sensitivity with
decreasing temperature, and a characteristic transition temperature from
ductile to brittle behavior. Interstitial impurities also have a
significant effect on this transition temperature.

These basic mechanisms are all related to each other, and several models
have been proposed to explain the low temperature strength character-
istics of the body centered cubic metals. At the present time, either
the Peierls-Nabarro Force or the non-conservative motion of jogs is
considered the rate controlling mechanism for plastic deformation.

Within the last year, the role of the interstitials in the deformation
and fracture process in body centered cubic metals has been studied at
the Aeronautical Materials Laboratory by investigating the correlation
between interstitial content (oxygen, nitrogen, and carbon) and strength
in high purity zone refined crystals of Cb and Ta of controlled

orientation, given different zone refining treatments and impure poly-crystalline Cb and Ta. Testing was accomplished over a range of temperatures from 4°K to 600°K in simple tension.

In addition to strength, the activation volumes and activation energies were also measured by strain rate cycling at a constant temperature and thermal cycling at a constant strain rate. The equation for calculating the activation volume is developed by first considering deformation in terms of a thermally activated process, where a dislocation overcomes an energy barrier by a combination of applied stress and thermal activation. This can be expressed by an Arhenius equation:

$$\dot{\mathcal{E}} = Ae^{(H - V^* \tau_a)/kT}$$

$\dot{\mathcal{E}}$ = Strain rate
τ_a = Applied shear stress
H = Activation energy
V^* = Lbd = activation volume
A = Frequency factor

Differentiating the above equation with respect to τ_a at a constant temperature and assuming no change in the energy barrier as a function of τ_a, the following expression is derived for determining the activation volume:

$$V^* = \frac{kT\,(\ln\dot{\mathcal{E}}_1 - \ln\dot{\mathcal{E}}_2)}{a_1 - a_2}$$

Differentiating the above expression in respect to T at a constant strain rate and assuming no change in the energy barrier:

$$H = \frac{V^* (T_1 \tau_{a_2} - T_2 \tau_{a_1})}{T_2 - T_1}$$

The results of this study of the activation volume, activation energy and deformation behavior are in good agreement with those of other investigators and are discussed in more detail in a paper to be submitted for publication. [9]

Objective.

One objective will be to find a workable model which will permit reason-able estimates to be made of the thermodynamic properties of dilute constituents in multicomponent systems; the primary objective of the project is to determine the effect of oxygen on the brittle fracture characteristics of iron, columbium, tantalum, molybdenum, and tungsten.

The information obtained will aid in expanding existing models or develop new models which will explain how interstitial elements such as oxygen affect body centered cubic elements and lead to brittle properties. The project is also concerned with fractographic studies which will give some correlation between gas conten , orientation, and the fracture surface. The over-all purpose is to gain a clearer insight into why metals are brittle in the presence of such impurities as oxygen.

Accomplishments.

The accomplishments prior to 31 July 1965 have been listed in detail in earlier reports. [1] [2] The important contributions in these reports are the number of papers published, the overwhelming evidence that Henry's Law is obeying all of the systems investigated, and that the existing dilute solution models were not adequate to explain the experimental results. T, model that is being proposed [8] will reduce the existing confusion.

Since 31 July 1965, the principal investigator has:

(1) Zone refined molybdenum, columbium, and tantalum in an electron beam zone refiner which was designed and built by Mr. Marshall K. Thomas. Columbium rods have been zone refined by induction heated zone refining methods.

(2) Shown that there is a correlation between rate of speed in zone refining, number of passes and gas content.

(3) Shown that there is carbon pick up with very slow speeds due to back streaming from the diffusion pump.

(4) Shown a correlation between orientation and impurities on twinning and work hardening.

(5) Participated in a round robin gas analysis of refractory metals for the Material Advisory Board.

(6) Submitted two progress reports.

(7) Been author or co-author of four papers presented during the year.

Published the following papers:

(8) E. S. Tankins, J. F. Erthal and M. K. Thomas, Jr., "The Thermodynamic Properties of Dilute Solutions of Oxygen in the Liquid Binary Cu-Ni Alloys," Jnl Electrochem Soc., 1965, Vol. 112, No. 4, p. 446-450.

(9) E. S. Tankins et. al., "The Activity of Oxygen in Liquid Iron-Molybdenum and Iron-Tungsten Alloys," scheduled for publication in the ASM Transactions Quarterly, September 1965.

(10) Submitted four additional papers for publication.

Future Planning.

During the next year, the emphasis will be on the zone refining of pure metal and alloys. The mechanical properties of the pure material will be studied. Then the pure metals and their alloys will be subjected to controlled oxygen atmospheres and the mechanical properties as a function of oxygen content will be studied. Single crystals of Cb and Ta have been prepared of controlled orientations. These are being studied to see what effect speed of zone refining and number of passes has on mechanical properties. This will also allow us to see the effect of orientation on mechanical properties. Plans are underway to run fractographic studies on the various refractory metals that have been studied. Plans are also underway to prepare Mo and W for the same type of studies.

References.

1/ "The Foundational Research Program at the Naval Air Engineering Center," Philadelphia, Pa., 1963, p. 46-47.

2/ Ibid. 1964, p. 21-25.

3/ E. S. Tankins and N. A. Gokcen, "Solubility of Oyxgen in Delta Iron," Trans ASM, 1961, Vol. 53, p. 843.

4/ E. S. Tankins, N. A. Gokcen, and G. R. Belton, "The Activity and Solubility of Oxygen in Liquid Iron, Nickel and Cobalt," Trans AIME, 1964, Vol. 230, p. 820-827.

5/ E. S. Tankins, G. R. Belton, and N. A. Gokcen, "The Thermodynamic Properties of Dilute Solutions of Oxygen in the Liquid Binary Alloys Fe-Ni, Fe-Co, and Ni-Co," submitted for publication.

6/ E. S. Tankins and G. R. Belton, "The Thermodynamic Properties of Oxygen in the Liquid Fe-Ni-Co Ternary Alloys," submitted for publication.

7/ N. A. Gokcen and E. S. Tankins, "Vacuum Analysis of Metals for Oxygen, Nitrogen, and Hydrogen," Jnl Metals, Aug 1962, p. 584.

8/ G. R. Belton and E. S. Tankins, "The Thermodynamic Behavior of Oxygen in Liquid Binary Alloys, A Simple Solution Model," submitted for publication Trans AIME.

9/ M. K. Thomas, Jr., and E. S. Tankins, "The Effect of Temperature and Orientation on the Yield and Flow Stress of Columbium and Tantalum," to be submitted for publication.

A STUDY TO DETERMINE THE OPTIMUM SYSTEM
FOR BOTH EJECTION AND NON-EJECTION TYPE SEAT DESIGN
FOR THE ATTENUATION OF HIGH G VERTICAL FORCES
WHICH RESULT FROM HIGH IMPACT LANDINGS OR CRASHES

CLIFFORD C. WOODWARD

BACKGROUND.

The problem of spinal injuries to pilot and aircrewmen as a result of high impact landings has been well recognized for a number of years, and is on the increase for both ejection and non-ejection type aircraft. It is also a fact that various energy absorption devices are available to attenuate these high G vertical forces. However, today's aircraft are not flying with energy absorption (E/A) built into the seats; since there is insufficient information concerning the behavior of the systems under dynamic crash-type loads to determine the optimum system and its proper design into the seat structure.

In order to obtain that information, this investigator proposed the construction of a 150 ft. vertical drop tower, with a unique method of arresting the seat and car through elongation of fully annealed stainless steel straps. The deceleration forces obtained would simulate essentially a square wave pattern resembling crash loads in magnitude and time duration, and would provide a relatively inexpensive method of obtaining reproducible crash-type loads. The device was constructed at the Aerospace Crew Equipment Laboratory (ACEL) and was completed in September 1961, with final acceptance in January 1962. The vertical drop tower, being of unique design and construction, required extensive calibration tests and establishment of instrumentation and photographic setup and recording methods, before the actual work on this project could be initiated. Following a period of operation from acceptance of the drop tower until early 1964, it became obvious that the braking system was limited. Although it did provide the designed crash-type loading, it did not provide the positive control of acceleration and variation in small increments of G required for conducting live drop tests safely on the tower. Without this capability it was not possible to determine the effects of vertical loadings on the human vertebra, and to correlate between humans and anthropomorphic dummies for extrapolation in the high G region where only dummies can be utilized. Therefore, in April 1964, a contract was let to convert the primary braking system from the stainless steel straps to one designed by Van Zelm Associates, consisting of various combinations of dies and metal bending elements. This braking system allows positive control of acceleration and variation of G's in increments as small as 1 G, from 5 G up to 50 G with the present drop car, and 100 G's with a redesigned car. Control is sufficient to allow live testing on this facility. The braking device was completed and calibration drops made, resulting in final acceptance in March 1965.

OBJECTIVES.

a. To determine systems and materials that can be used most effectively to attenuate to a tolerable limit the vertical forces imposed by high impact landings or crashes, in both ejection and non-ejection type seats.

FIGURE 1

DROP TOWER TEST #8
17 JUNE 1965

F7U-3 STAINLESS STEEL STRAP
ENERGY ABSORPTION SYSTEM

DOUGLASS A-4 EJECTION SEAT

INSTRUMENTATION OVERLOAD

VERTICAL RAILS (FRAME)
35.5 G/INCH
39 G
.063 SEC.

VERTICAL DUMMY CHEST
22.1 G/INCH
26 G
.046 SEC.
.054 SEC.
.01 SEC.

- 22 -
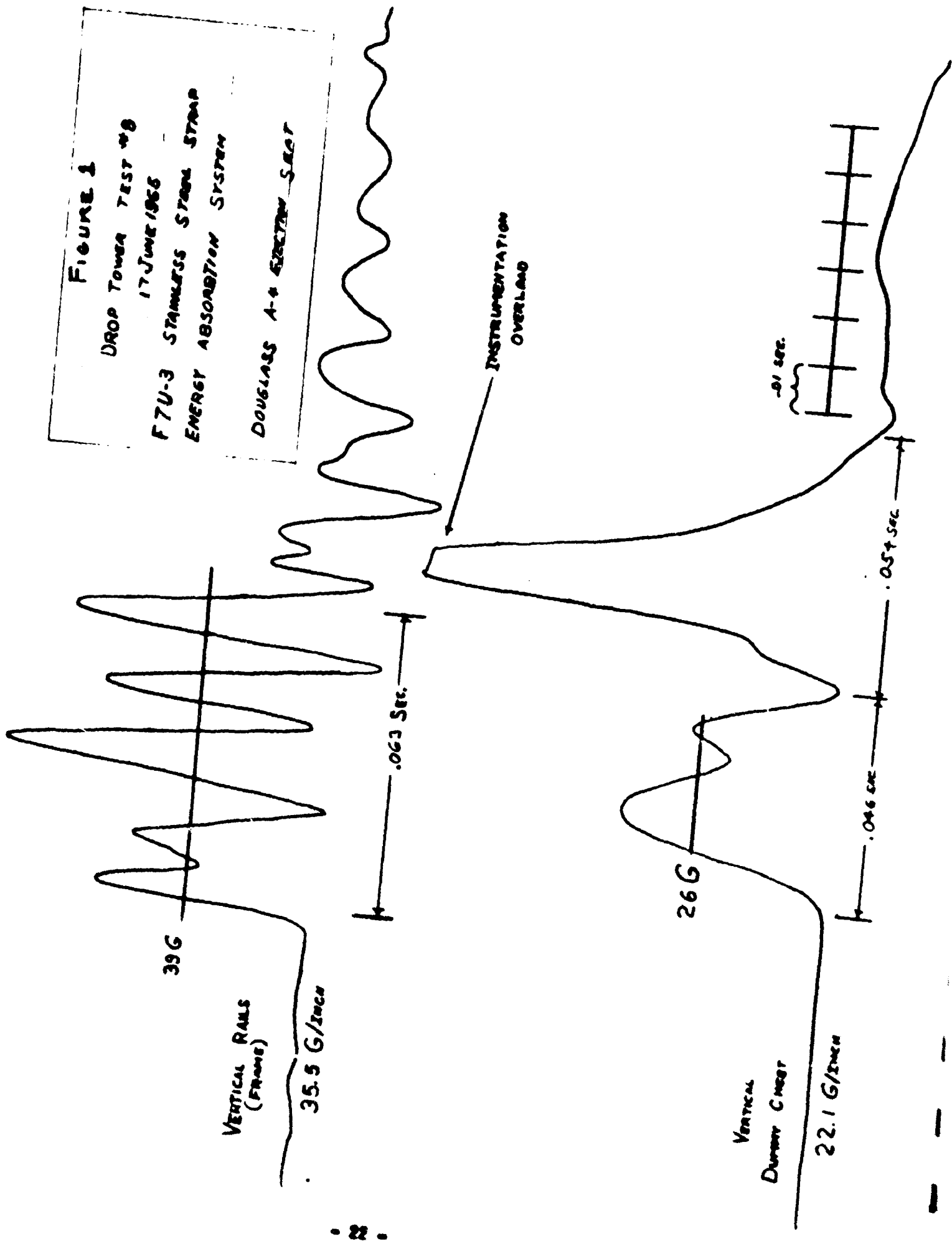
b. To determine the effects of various G loadings on the human vertebra, and to show more clearly the mechanisms responsible for spinal injury.

c. To determine the correlation between humans and anthropomorphic dummies when subjected to crash forces, for extrapolation in the high impact region where only dummies can be utilized.

ACCOMPLISHMENTS.

A. **Summary to 1 July 1964.** A limited number of 20 G drop tests were conducted, using the former braking system on an E/A system designed by Aerotherm Corporation for helicopter and transport type seating. Performance of the E/A system was determined by dropping two identical seats at the same time, one with and one without the E/A system installed. Results indicated that the seat structure was weak in several load carrying members which must be designed properly so that the E/A system will function. However, this particular design is not an optimum system, as double the static design load is required to start it moving, due to inherent friction and torsion in the seat members and the force required to overcome the inertia of the mass. Approximately 50 milliseconds of crash attenuation by the E/A system is sufficient to preclude bottoming out and consequent overshoot of the load into the seat occupant.

B. **From 1 July 1964 to 1 July 1965.** Following completion of the new Van Zelm braking system in September 1964, a number of calibration drops were conducted prior to acceptance. One failure of a 40 G strap element required investigation and resulted in closer material control, with a later change from black iron to fully annealed stainless steel. Final acceptance of the new braking system occurred in March 1965 following a final 40 G calibration drop.

An E/A system, consisting of a fully annealed stainless steel strap and slider mechanism as designed for the F7U-3 ejection seat, was mounted on an F7U-3 seat and drop tested on 5 May 1965 under a 35 G crash condition. The seat and car were fully instrumented. The E/A system is so designed to elongate and absorb energy above 20 G. A failure of some of the seat components prevented satisfactory operation of the E/A system. As the F7U-3 seat is obsolete and therefore difficult to obtain, an A4 Douglas seat was substituted and the system modified for compatibility. A 40 G drop was conducted on 17 June 1965; the results, as shown in Fig. 1, show energy attenuation from 39 G, as recorded on the vertical rails, to 26 G in the dummy's chest cavity, for a period of 46 milliseconds until the E/A system bottomed out. The crash loading was applied for a longer period of time than that for which the system was designed, to show the effect of E/A while functioning and when bottomed out. The fluctuation of the instrumentation trace recorded on the vertical rails is a result of the vibration and flexure of the rails during deceleration, and cannot easily be eliminated without losing performance data. Correlation with high speed photographic interpretation will perhaps supply the answer to better recording analysis.

FUTURE PLANS.

During the next fiscal year, it is planned to determine the E/A characteristics of other systems presently available for both ejection and non-ejection type seat design for attenuating high G vertical forces. When

- 2 -

enough data has been obtained on the various methods and materials available, it should be possible then to determine a system which will best perform the function of R/A in the various types of seat design, both ejection and non-ejection. Also, it is planned to conduct a controlled series of live and dummy drops together at the lower deceleration loads to correlate for prediction of human reactions at the higher G's where only dummies can be used. The effect of the vertical crash type forces on the human spine, particularly in the neck area, will be studied through high speed photography for use in crash type research and dummy simulation of human response.

THE PERMEATION OF SALT WATER THROUGH ORGANIC PROTECTIVE COATINGS
USING RADIOACTIVE TRACER TECHNIQUES

ALFRED L. GLASS

Background

The Navy Department is conducting extensive research programs to develop
barrier materials and organic protective coatings for minimizing deterioration
caused by corrosion. Since organic coatings and barrier materials are mem-
branes, they may be permeable to air, water and various electrolytes in solution.
Therefore, the laws of diffusion and electroendosmosis may be involved in the
mechanism of permeation and the resultant corrosion. In order to develop more
efficient barriers and protective coatings, the mechanisms of permeation through
these films must be more fully understood. Previous investigations did not
determine the quantities of permeating materials, since they were either too
minute to be measured accurately by analytical chemical means, or were in forms
that did not lend themselves to ordinary analytical techniques. However, with
the advent of radioactive tracer chemicals and techniques, a direct approach
is available, in which micro quantities of a tagged chemical may be accurately
determined and even followed through processes under environmental conditions
similar to those that exist when such materials are in use.

Objectives

The specific aims of this program then are: (1) to use radioisotopes to
establish fundamental data on the mechanism of salt water permeation through
organic protective films; (2) to investigate the effect of incorporated resins,
pigments and corrosion inhibitors on the permeation; and (3) to apply the radio-
active tracer techniques to obtain accurate fundamental data concerning protective
coatings used by the Bureau of Naval Weapons.

Accomplishments

A. Prior to 30 June 1964

Radioactive tracer procedures have been developed and evaluated for
measuring the rates of diffusion of the chloride ion, sodium ion and water
molecules through membranes.[1,2,3]

Employing these methods, determinations of the rates of diffusion of
these ions and water were made for eight films representing typical protective
coatings ar' barrier materials used by the Bureau of Naval Weapons for corrosion
protection. Experimental work was performed to investigate the effect on ionic
diffusion of various factors, such as the concentration of sodium chloride in
solution and the thickness of the film. A detailed analysis of all the diffusion
data indicated that an additional factor beside pore diameter and size of hydrated
ions is involved in the mechanism of diffusion through a membrane. This factor
is the concept of ionic charges appearing upon the walls of the pores of a mem-
brane as a result of the hydrolysis of certain groups which are a part of the
polymer molecule. Thus, a membrane can be perm-selective in that ions of the
same charge as that on the walls of the pores are prevented by electrical repulsion

EFFECT OF PIGMENT ON RATE OF DIFFUSION OF IONS

Film	Measured Rates of Sodium Diffusion*	Measured Rates of Chloride Diffusion*	Theoretical Rates** of Sodium Diffusion	Charge on Walls of Pores
Epoxy Polyamide	----	----	----	----
Clear Film	5.17×10^{-8}	1.23×10^{-8}	8.08×10^{-9}	Negative
1.6% pigment	1.83×10^{-9}	2.17×10^{-9}	1.41×10^{-9}	Negative
6.2% pigment	1.45×10^{-9}	1.66×10^{-9}	1.08×10^{-9}	Negative
31.0% pigment (spec. content)	1.39×10^{-9}	1.51×10^{-9}	9.92×10^{-10}	Negative
Lacquer: Acrylic Nitrocellulose	----	----	----	----
Clear Film	1.00×10^{-7}	5.15×10^{-5}	3.35×10^{-5}	Positive
1.2% pigment	None	2.55×10^{-8}	1.65×10^{-8}	Positive
4.8% pigment	None	9.64×10^{-9}	6.25×10^{-9}	Positive
24% pigment (spec. content)	None	7.29×10^{-9}	4.79×10^{-9}	Positive

*Rate of diffusion g. sq. cm^{-1} hr^{-1} mil^{-1}

**Theoretical Rate of diffusion calculated stoichiometrically from the chloride ion measured rate of diffusion

TABLE 1

-6-

from permeating through the film, allowing only the ions of opposite charge
to pass through. It was further demonstrated that the permeation is charac-
teristic of a Fickion diffusion process for which the simplified equation
$q = \dfrac{DAt}{l}$ is applicable, where:

q = the quantity transferred in time t
D = the permeability constant (diffusion coefficient, g. hr^{-1}, $sq.cm^{-1}$, mil^{-1})
A is the cross sectional area of the film and
l is the film thickness

The permeability constant D may be calculated from the above equation by
substituting the experimental values for q and t when a steady flow has been
reached.

B. Subsequent to 30 June 1964

The effect of a pigment in a protective coating on the diffusion of
ions through a film was investigated. The rates of diffusion of the chloride
ion and the sodium ion were determined through free films prepared from the
formulations shown in Table 1. The experimental results are also included in
this table. An analysis of these results shows that the rates of diffusion
for both ions decrease as the quantity of pigment increases. For each formulation,
the relationship between the measured rate of sodium ion diffusion and the theo-
retical rate of sodium ion diffusion (calculated from the measured rate of chloride
ion diffusion) remains unchanged. That is, for the epoxy polyamide films, the
measured rate of diffusion for the sodium ion is always greater so that the charge
on the walls of the pores remains negative. The opposite is noted in the case
of the acrylic nictrocellulose lacquer film where the charge on the walls of the
pores remains positive. From these observations, it is then concluded that the
TiO_2 pigment in these protective coatings diminishes the flow of ions through
the films by acting as a barrier in blocking the pores, and has no effect on the
hydrolysis reactions affecting the charges on the walls.

The radioactive tracer procedure for the determination of the diffusion
of water through a free film is described.[4] This procedure was used to determine
the rates of diffusion at various time intervals, through neoprene, acrylic-
nitrocellulose, and epoxy polyamide free films. The results are tabulated in
Table 2. These measurements were made to determine the possibility of obtaining
information concerning the structural changes that may take place in an organic
protective coating exposed to water. The data in Table 2 for each film were
examined statistically. It was found that for each film, less than 30% of the
values exceeded the standard deviation. This indicated compatibility with the
Gaussian curve for which the predicted value for the probability of observing
an error greater than the standard deviation is 31.7% of the observations. Thus,
it is shown statistically that the individual values in each set of figures do
not vary from that for a one day exposure time to that for a 40 day period,
indicating that any "swelling" action that water might have on these films does
not affect the "geometry" of the pores for should there have been an effect,
it would have resulted in either an increase or a decrease in the rate of dif-
fusion of water.

RATE OF DIFFUSION OF WATER THROUGH FREE FILMS AT VARIOUS TIME INTERVALS

Elapsed Time	Rate of Diffusion g hr^{-1} sq. cm^{-1} mil^{-1}		
	Neoprene Film	Nitrocellulose Acrylic Film	Epoxy Polyamide Film
1 day	1.01×10^{-3}	2.90×10^{-4}	1.25×10^{-4}
3 days	----	----	1.27×10^{-4}
4 days	1.00×10^{-3}	2.95×10^{-4}	1.27×10^{-4}
6 days	0.87×10^{-3}	----	----
7 days	----	----	1.31×10^{-4}
8 days	----	----	1.39×10^{-4}
11 days	----	3.05×10^{-4}	1.46×10^{-4}
15 days	----	2.35×10^{-4}	----
16 days	----	----	1.37×10^{-4}
20 days	0.88×10^{-3}	----	----
21 days	1.10×10^{-3}	----	----
22 days	----	----	1.15×10^{-4}
23 days	----	----	1.58×10^{-4}
25 days	----	3.15×10^{-4}	----
27 days	0.99×10^{-3}	3.45×10^{-4}	----
29 days	----	3.20×10^{-4}	----
30 days	0.95×10^{-3}	----	1.30×10^{-4}
31 days	----	----	1.22×10^{-4}
32 days	----	3.10×10^{-4}	----
35 days	----	3.05×10^{-4}	$1.2? \times 10^{-4}$
36 days	----	----	1.31×10^{-4}
40 days	1.10×10^{-3}	3.25×10^{-4}	1.29×10^{-4}

TABLE 2

-33-

Future Plans

Investigations will be made of the mechanisms by which slightly water soluble corrosion inhibitor pigments incorporated in a film affect the rates of diffusion of chloride and sodium ions.

REFERENCES
1/ Second Progress Report on F.R. Project NAMC AML RC 7045/17 of 15 Jun 1961
2/ Third Progress Report on F.R. Project NAMC AML RS 7045/17 of 15 Dec 1961
3/ Fifth Progress Report on F.R. Project NAMC AML RS 7045/17 of 15 Dec 1962
4/ Fourth Progress Report on F.R. Project NAMC AML RC 7045/17 of 15 Jun 1962

APPLICATION OF POTENTIOSTATIC AND GALVANOSTATIC TECHNIQUES TO THE STUDY OF INTERGRANULAR CORROSION IN HIGH STRENGTH ALUMINUM ALLOYS

MRS. SARA J. KETCHAM

Background.

The effect of metallurgical factors on the electrochemical behavior of high strength aluminum alloys is a subject of great interest in connection with the use of these alloys for naval aircraft. The most serious types of corrosion encountered are exfoliation and stress corrosion, both of which are due to preferential attack along grain boundaries.

Intergranular corrosion in the aluminum-copper alloys has been generally attributed to the depletion of copper from areas adjacent to grain boundaries during slow cooling following solution heat treatment. The depletion is a function of the free energy of formation of precipitates at the grain boundary and the diffusion of constituents to the grain boundaries. Both are dependent upon temperature, and the amount of depletion should, therefore, be a function of the quenching rate.

With this as the basic assumption, a comprehensive study has been made of the mechanism of intergranular corrosion as it is related to quenching rate, and the relationship between intergranular corrosion susceptibility and stress corrosion susceptibility. The effect of quenching rate on corrosion potentials, degree of intergranular corrosion susceptibility and microstructure in the commercial alloy, 2024, was determined first. The experience gained in that study led to the conclusion that for any real understanding of basic mechanisms, it was desirable to go back to an Al-4% copper binary material and add one element at a time in order to determine the effect each addition had on the precipitation process and on the electrochemical behavior of the alloy. Experiments have been conducted to determine the effect of quenching rate on susceptibility to intergranular and stress corrosion for an Al-4% Cu binary alloy and an Al-4% Cu-1.5 Mg ternary alloy.

To facilitate study of the electrode kinetics of reactions involved in intergranular corrosion, an electrochemical model for an Al-Cu-Mg alloy susceptible to intergranular corrosion was assumed. This consists of (1) homogeneous solid solution in the center of the grain represented by the ternary Al-Cu-Mg alloy cold water quenched, and therefore, not susceptible to intergranular corrosion; (2) the precipitate Al_2CuMg (referred to as the S phase in the Al-Cu-Mg equilibrium phase diagrams); and, (3) a depleted zone at the grain boundary represented by pure aluminum. Potential and polarization data were obtained on these three

phases separately, and results of the cooling rate-corrosion potential
experiments interpreted on the basis of this model.

Objective.

The objective of this investigation was to determine the effect of
metallurgical factors on the electrochemical behavior of structural
aluminum aircraft alloys, using potentiostatic and galvanostatic
techniques. The ultimate aim was to learn more about the mechanism
of intergranular corrosion in hopes of devising methods to avoid or
minimize it.

Accomplishments.

1. Prior to 30 June 1964

a. The relation between quenching rate, corrosion potential, and
intergranular corrosion susceptibility was determined for the commercial
2024 aluminum alloy in the solution heat treated and naturally aged
condition. With decreasing cooling rate, corrosion potentials became
more anodic and intergranular corrosion susceptibility became more
pronounced.

b. The kinetics of the depleted zone represented by pure aluminum,
was studied in NaCl solutions. Effect of variations in chloride ion
concentration and pH was included. Based on the results, a theory was
presented that the corrosion potential of aluminum and its alloys is
believed to be a function of the type of halide and its concentration,
as well as the activity of the basis metal. The rate of corrosion is
believed to be controlled by the cathodic limiting current for the
reduction of hydrogen, which is a function of the local hydrogen ion
concentration and the oxide film thickness.

c. Experiments relating quenching rate and corrosion potentials with
intergranular corrosion susceptibility have been repeated on high purity
binary (Al-4% Cu) and ternary (Al-4% Cu-1.5% Mg) alloys. The Al-Cu-Mg
showed the same dependence of intergranular corrosion susceptibility on
quenching rate as did the commercial material, and the same correlation
with corrosion potential measurements. The binary Al-Cu material showed
little or no susceptibility to intergranular corrosion except at very
slow quenching rates, and no correlation of corrosion potentials with
quenching rates.

2. From 1 July 1964

a. The relationship between intergranular and stress corrosion
susceptibility has been determined for the binary and ternary alloys in
neutral and acidified salt solutions. Electron transmission microscopy

EFFECT OF QUENCHING RATE ON STRESS CORROSION
ALTERNATE IMMERSION – 3.5 % NaCl
C – RING SPECIMEN

Al – Cu ALLOY

E_{CORR}

.545 V

PITTING

.545 V

STRESS

CORROSION

CRACKING

Al – Cu – Mg ALLOY

E_{CORR}

.550 V

.550 V

.5 .005 V

PITTING

STRESS

CORROSION

CRACKING

STRESS ACCELERATED CORROSION

| 1000 ⟶ 200 | 150 | 100 | 50 | 0 |

QUENCHING RATE – °C / SEC
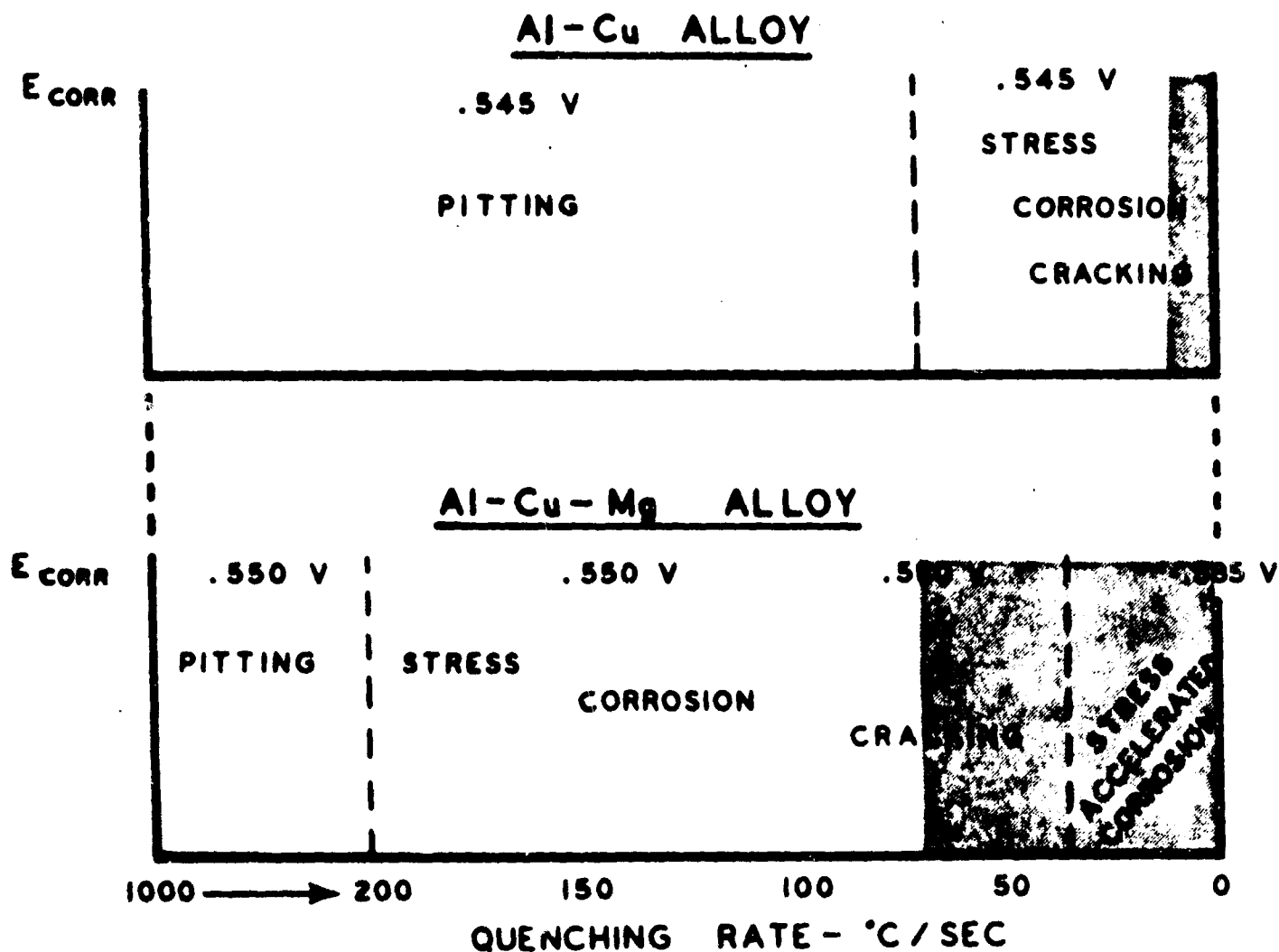
RANGE OF INTERGRANULAR CORROSION SUSCEPTIBILITY
(BASED ON NaCl – H_2O_2 TEST)

FIGURE 1.

studies have also been completed. Results, in neutral solutions, are presented graphically in Figure 1, and can be summarized as follows

(1) The binary Al-Cu alloy is susceptible to stress corrosion cracking when slowly quenched, even though corrosion potentials and accelerated corrosion tests indicate little or no susceptibility to intergranular corrosion, and the structure evinces very little sign of preferential precipitation.

(2) The slowly quenched ternary alloy is extremely susceptible to intergranular corrosion - as results of accelerated corrosion tests, and potential measurements would indicate. The application of stress accelerates the intergranular attack

(3) Intermediate quenching rates can produce stress corrosion cracking in the ternary alloy when, as with the binary alloy, results of accelerated corrosion tests, potential measurements, and degree of precipitation indicate a very slight propensity toward intergranular attack.

In other words, there is no indication of the existence of any continuous anodic paths without stress. Stress seems actually to initiate the intergranular attack, providing strong support for the theory of Hoar [1] and others, of the electrochemical effect of stress or so-called strain induced depolarization.

b. In acidified salt solutions, time to failure was decreased by a factor of ten.

c. Potential and polarization experiments on the separate phases indicated that potential differences between the phases are great enough to allow for the flow of fairly large galvanic currents providing the phases were behaving as independent electrodes as assumed by the electrochemical model. The validity of the model was proved experimentally by polarizing a slowly quenched specimen at a potential which should cathodically protect two phases and anodically dissolve the grain boundary areas. Results are given in Figure 2 Attack was produced at grain boundaries and other areas remained unattacked

d. Chemical inhomogeneity therefore is undoubtedly responsible for intergranular attack in slowly quenched Al-Cu-Mg alloys, but does not account for intergranular failures in material with faster quenching rates. An electrochemical mechanism for this requires the existence of a small anode area in relation to that of the cathode, so that high anodic current densities can produce and maintain highly localized attack and acidity. A possible sequence of reactions is proposed below

(1) Attack or crack initiation under stress in either neutral or acidified chloride solutions conceivably could be due to straining and

RESULTS OF POLARIZING C-RING SPECIMENS OF Al-Cu-Mg AT -.750V IN NEUTRAL AND ACIDIFIED* .2N NaCl

| Quench Media	Quench Rate	Condition	pH of Electrolyte	Type of Attack
Boiling Water	17°C/sec	Unstressed	6.4	Intergranular Attack
Boiling Water	17°C/sec	Unstressed	1.5	Intergranular Attack
Boiling Water	17°C/sec	Stressed	6.4	Intergranular Attack
Boiling Water	17°C/sec	Stressed	1.5	Intergranular Cracking
Alcohol	65°C/sec	Unstressed	6.4	Intergranular Attack
Alcohol	65°C/sec	Unstressed	1.5	Intergranular Attack
Alcohol	65°C/sec	Stressed	6.4	Intergranular Attack
Alcohol	65°C/sec	Stressed	1.5	Intergranular Cracking
Cold Water	800°C/sec	Unstressed	6.4	No Attack
Cold Water	800°C/sec	Unstressed	1.5	No Attack
Cold Water	800°C/sec	Stressed	6.4	No Attack
Cold Water	800°C/sec	Stressed	1.5	No Attack

*pH adjusted with conc. H_2SO_4

FIGURE 2

rupture of the oxide film at weak points, such as grain boundaries. Once started, attack will tend to continue downward along grain boundaries, producing crevices.

(2) Work by Lorking and Mayne [2] and others [3] has provided strong evidence that the corrosion product in neutral chloride solutions is aluminum chloride. Oxygen would not have read; access to the crevice, and the formation of aluminum chloride would contribute to localized acidity making film repair difficult. Ultimately, the cathodic reaction in the crevice could change from oxygen reduction to hydrogen ion discharge.

(3) Stern's [4] work points to the possibility that the cathodic area increases as the hydrogen ion activity increases (possibly caused by greater hydrogen adsorption), and a decrease in the anode area results. Uhlig [5] indicates that for metals of fairly high hydrogen overvoltage such as aluminum, the discharge of the hydrated hydrogen ion is apparently the slow step:

$$H^+ \longrightarrow H \text{ (ads)} - e^-$$
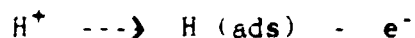
Work by Bockris and others [6] shows that stress in a steel membrane increases the surface coverage of hydrogen atoms. A change, then, of the cathodic reaction within the crevice to hydrogen ion discharge and an increase in the hydrogen coverage by stress, could decrease the anode area producing the necessary conditions for a high anodic current density at the root of the crevice, promoting intergranular penetration.

e. To summarize, as a result of this investigation, a theory has been proposed to explain intergranular stress corrosion failures in presumably non-susceptible Al-Cu-Mg alloys, based on the electrochemical effect of stress which is believed to be the result of strain induced depolarization of the anodic phase or phases and stress induced increase in the surface activity of hydrogen ions.

f. There are also several practical implications of this work

(1) Accelerated corrosion testing of unstressed specimens has been shown to be inadequate for predicting service behavior where parts will usually be under a stress.

(2) Initiation of intergranular attack and rate of penetration proceeds much more rapidly in acidified salt environments than in neutral salt environments. Since the corrosion environment of an aircraft carrier provides not only salt spray but also some sulfuric acid formed from the sulfur in the stack gases, consideration should b given to the possibility of incorporating a neutralizing substance into the water used to wash down aircraft while on carrier duty.

g. Three progress reports and two papers have been published to date. Two additional papers have been presented and will be combined for publication in the near future.

Future Planning.

None. Project terminated as of 30 June 1964. At the time this work was initiated, little use had been made of potentiostatic techniques for the study of intergranular corrosion in aluminum alloys. Since that time, their use has been growing steadily. It is believed that use of electrochemical techniques to study stress corrosion and hydrogen embrittlement in high strength steels is more in the interest of the Navy, at the present time, than to continue investigation on aluminum alloys which appears to be receiving adequate attention elsewhere.

References.

1/ T. P. Hoar, Corrosion, 19, 331t (1963).

2/ K. F. Lorking and J.E.O. Mayne, Jnl of Applied Chemistry, 11, 170-180, May 1961.

3/ H. L. Craig, Jr., Reynolds Metals Co., private communication.

4/ M. Stern and R. M. Roth, Jnl Electrochem. Soc., 104, 6, 390 (June 1957).

5/ H. H. Uhlig, Corrosion and Corrosion Control, Chap. 4,p. 47, John Wiley and Sons, New York, 1963.

6/ J. O'M. Bockris, J. McBreen, W. Beck and L. Nanis, Proc. Royal Society (in course of publication).

THE MEASUREMENT OF STRESS AND ITS RELATIONSHIP TO
AND EFFECTS ON HUMAN PERFORMANCE IN MENTAL AND MOTOR WORK

SHERWIN J. KLEIN and MALCOLM M. COHEN

Background.

The Aerospace Crew Equipment Laboratory (ACEL) is engaged in a variety of programs involving the development and evaluation of personal safety equipment for the naval aviator. Much of this equipment has a psychological as well as physical impact upon the user. How much of an impact is not always known because of a paucity of reliable criteria with which to measure it. Even where the fact of an impact is known, its effects upon precise motor performance and/or instantaneous decisions required in high performance aircraft cannot be determined easily. The present program was undertaken with these problems in mind.

Previous observations have indicated that conditions which induce stress in human subjects are associated with concomitant increases in tne tensions of skeletal muscles. It has also been observed that when tensions in muscles are increased, their electrical activities (Muscle Action Potentials or MAP) are likewise increased. By definition, then, muscles are said to be "stressed" whenever they are active above their normal basal levels. Therefore, it can be postulated that the electrical activities of active skeletal muscles are functionally related to the state of tension or "stress" in the muscles. The MAP can be picked off the surface of the skin with electrodes, amplified, and analyzed. Thus, MAP can be employed as an operational measure of the increased muscle tensions associated with stress-inducing conditions.

The tension in skeletal muscles can be induced in a variety of ways. Anything that induces tension in muscles is termed a "stressor." Stressors which have been employed in experimental settings may be divided into two broad categories - the physical and the psychological. Physical stressors include direct muscle loading, muscular exercise, thermal extremes, reduced oxygen intake, and a variety of other conditions in which physical variables are altered to produce elevated levels of MAP. Psychological stressors include mental effort, feelings of failure, and a variety of internally-generated anxieties resulting from stimuli which the individual believes to be a threat to his physical or psychological well-being. An important aspect of the program is to examine the functional relationships between the physical and the psychological stressors, and to attempt to determine whether some sort of functional equivalence between these two classes of stressors can be established with respect to their mutual effects upon performance.

Although in a theoretical context, other investigators 1J, 2J, 3J, have suggested that the relationships between muscle tensions and performance may be a function of the means by which the muscle tensions were induced, Klein 4J has obtained actual experiment evidence that the relationships were less dependent upon how the tensions (as measured by MAP) were induced than upon the specific aspect of performance which was measured.

-42-

Certain stressors have been studied experimentally; however, functions relating stress (as measured by MAP) to various kinds of stressors may differ widely. The purpose of the present program is to explore more fully, both in kind and in extent, the functional relationships between stress and various stressors and, where possible, to obtain functional relationships between stress and performance.

Based upon the preceding theoretical and empirical considerations, a Motor Theory of Stress was developed. The theory, in part, asserts that: (1) the MAP of musculature involved in any given action is a function of level of systemic stress during that action; and (2) irrespective of how induced, the directionality of the relationship between MAP and any given measure of performance is uniquely defined. A schematic diagram of our theoretical framework is presented in Figure 1.

A further conjecture was developed following this theoretical approach. It was hypothesized that not only the absolute level of MAP activity was a relevant variable in the analysis of the effects of MAP upon performance, but that the distributions of MAP throughout the body might also be of interest, particularly with respect to changes of visual perception. Certain stressors cause relatively greater increases in MAP at one location of the body than at another location. Thus, analyses of MAP as a function of body locus may be of particular value in exploring the effects of these stressors, especially as they influence visual perceptual functioning. Therefore, a separate phase of the program is concerned with bio-electric responses associated with visual perceptual changes.

In addition to the MAP parameters of intensity and location, a third parameter is also of interest. Since the MAP signal obtained by means of surface electrode recording techniques is comprised of the electrical activities of many discrete muscle fibers firing at different rates and with different degrees of synchrony or asynchrony, the frequency spectrum of the MAP signal may also be of interest. By employing frequency-intensity analyses of the MAP signal, further information concerning the underlying neuro-muscular substratum may be obtained. If precision and "smoothness" of motor skills depend upon the frequency response characteristics of the musculature employed in the performance of skilled tasks, then analyses of the type outlined above should provide a means of quantifying these aspects of the muscular activity.

Objective.

To explore the effects of various types of stressors on the bio-electric responses of human subjects and to study the relationships between bio-electric responses and their effects upon concomitant motor and mental performance.

Success in the overall program will lead to: (1) a better operational definition of systemic stress to include both momentary and long-term stresses. (2) the development of a simple and reliable stress index, and (3) the development of a method for quantifying and quantitatively expressing the effects of stress upon human performance.
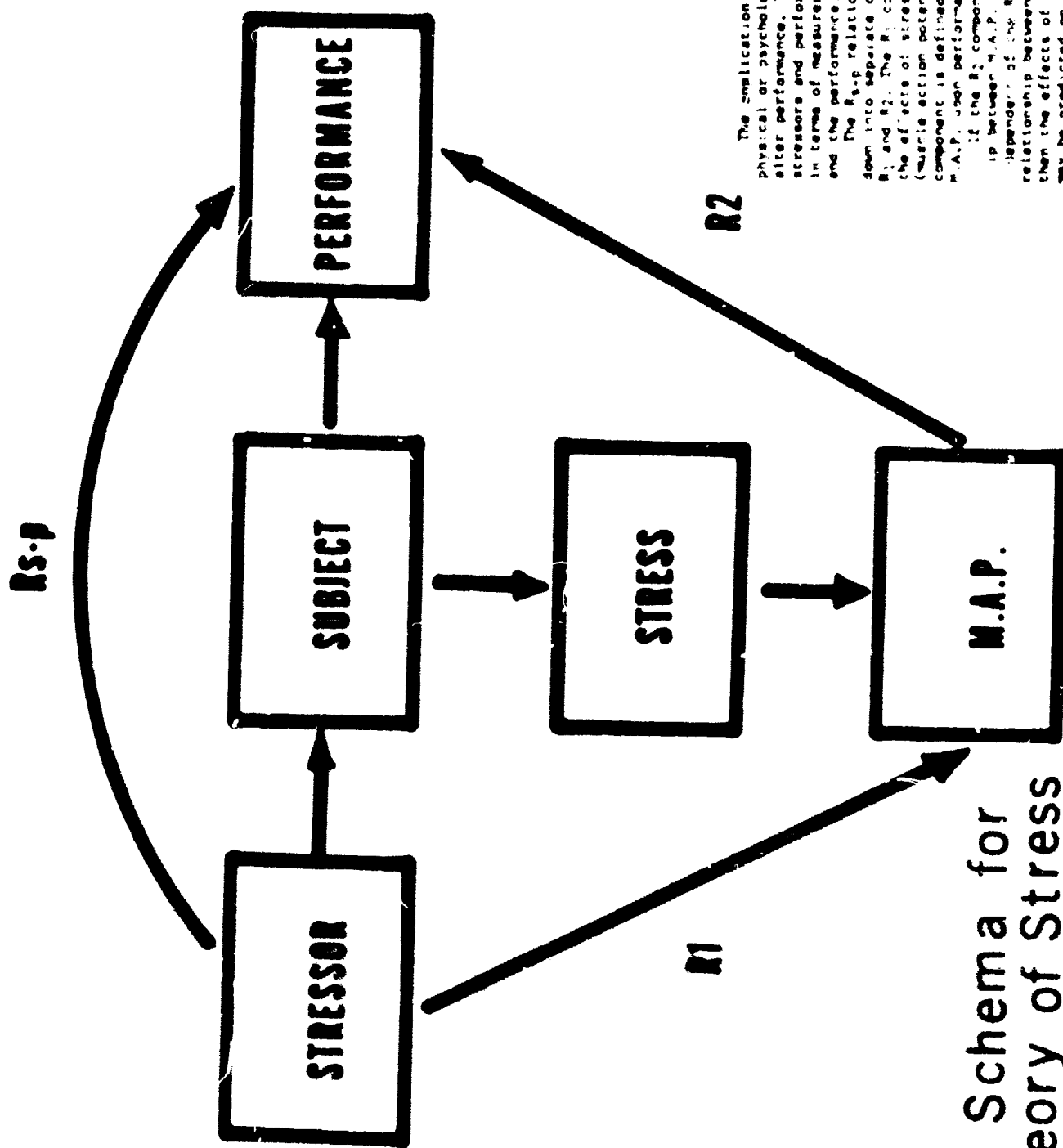
Conceptual Schema for
a Motor Theory of Stress

FIGURE 1

STRESSOR

SUBJECT

STRESS

M.A.P.

PERFORMANCE

Rs-p

R1

R2

The application of a stressor, either physical or psychological, will generally alter performance. This relationship between stressors and performance may be expressed in terms of measures of both the stressors and the performance, designated by R_{s-p}.

The R_{s-p} relationship may be broken down into separate components, designated R_1 and R_2. The R_1 component is designated the effects of stressors upon M.A.P. (muscle action potentials), and the R_2 component is defined by the effects of M.A.P. upon performance.

If the R_1 component (i.e. relationship between M.A.P. and performance is dependent on the R_1 component (i.e. the relationship between stressors and M.A.P.), then the effects of stressors upon performance may be predicted on the basis of the R_2 relationship alone. This would allow the establishment of a functional equivalence (on the basis of M.A.P. alone) between physical and psychological stressors in terms of their mutual effects upon performance.

ANATOMICAL SKETCHES USED
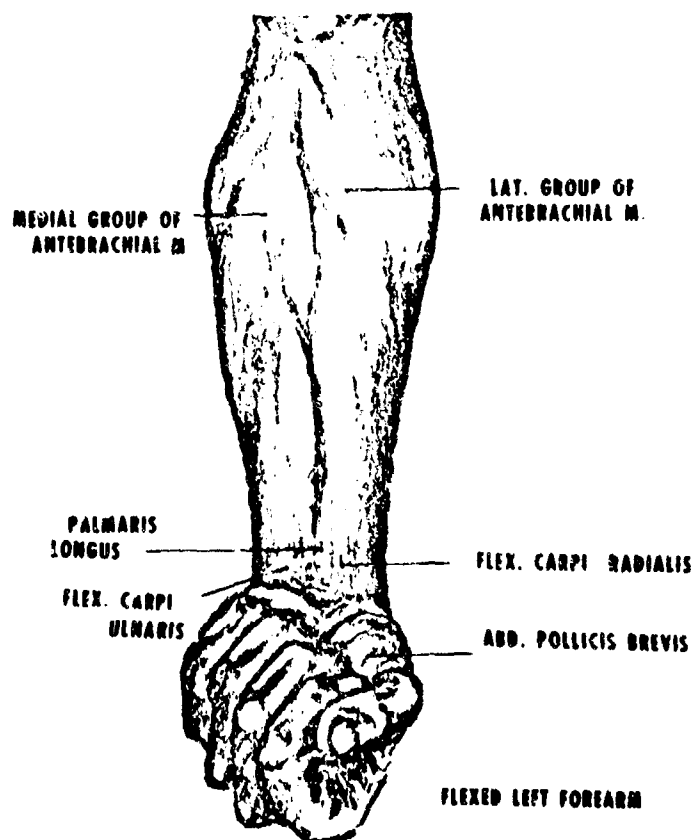# AS GUIDES FOR ELECTRODE PLACEMENT

BRACHIORADIALIS

ANCONAEUS

EXT. CARPI. RAD. LONG.

EXT. DIGITORUM COM.

EXT. CARPI RAD. BREV.

EXT. CARPI ULNARIS

EXT. DIGITI QUINTI PROPRIUS

LEFT FOREARM

THE SUPERFICIAL DORSAL ANTEBRACHIAL MUSCLES

PRONATOR TERES

FLEXOR CARPI RADIALIS

PALMARIS LONGUS

FLEXOR CARPI ULNARIS

FLEXOR DIGITORUM SUBLIMIS

RIGHT FOREARM

THE SUPERFICIAL VOLAR ANTEBRACHIAL MUSCLES

SUBMAXILLARY
TRIANGLE

HYOID BONE

THYROID
CARTILAGE

CRICOID
CARTILAGE

JUGULAR NOTCH

STERNOCLEIDO -
MASTOIDEUS

TRAPEZIUS

SUPRACLAVICULAR
FOSSA

STERNAL HEAD

CLAVICULAR HEAD

CLAVICLE

INFRACLAVICULAR
FOSSA

MEDIAL GROUP OF
ANTEBRACHIAL M

LAT. GROUP OF
ANTEBRACHIAL M.

PALMARIS
LONGUS

FLEX. CARPI
ULNARIS

FLEX. CARPI RADIALIS

ABD. POLLICIS BREVIS

FLEXED LEFT FOREARM
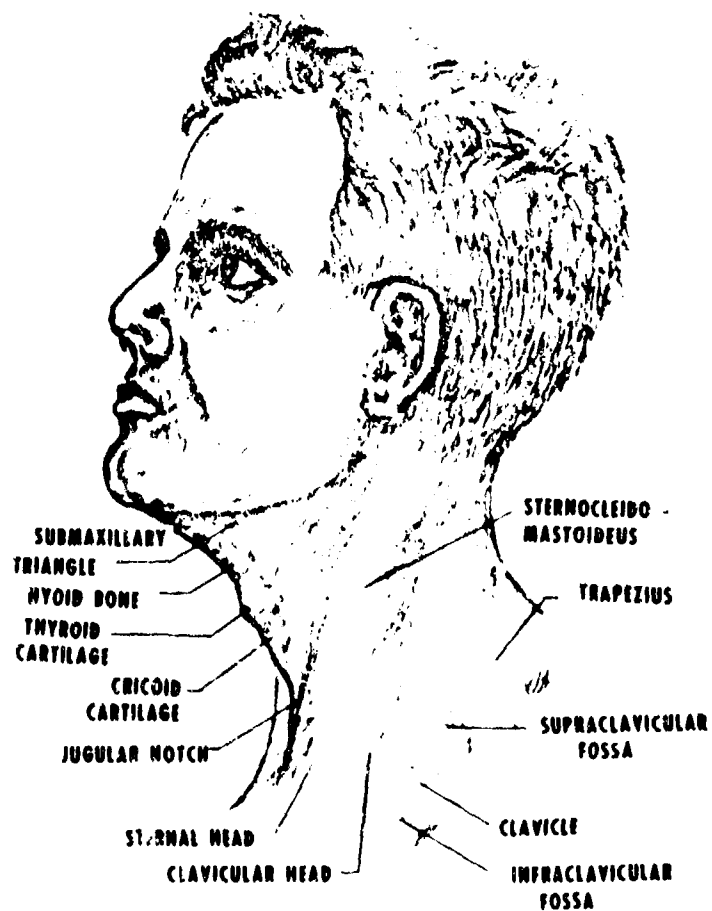
Figure
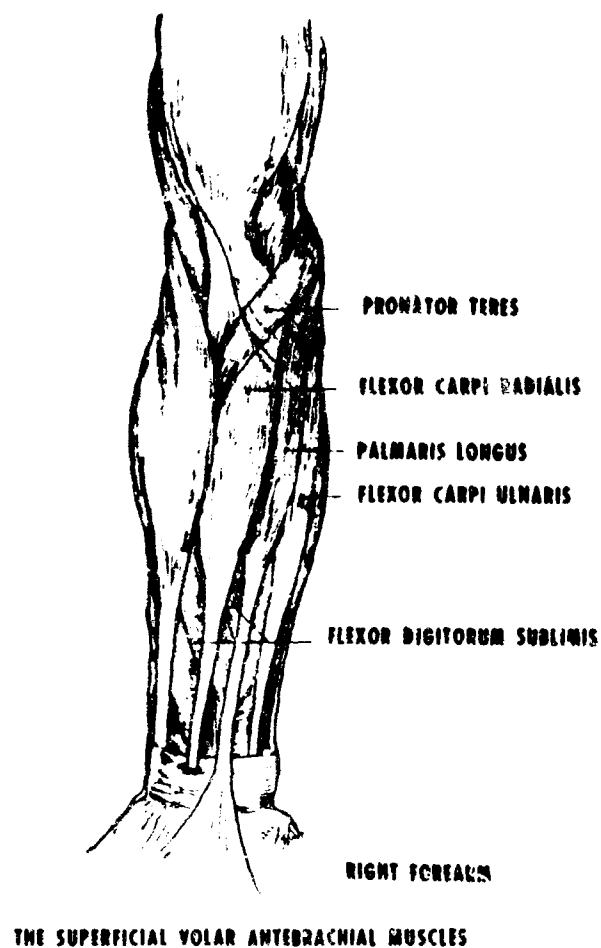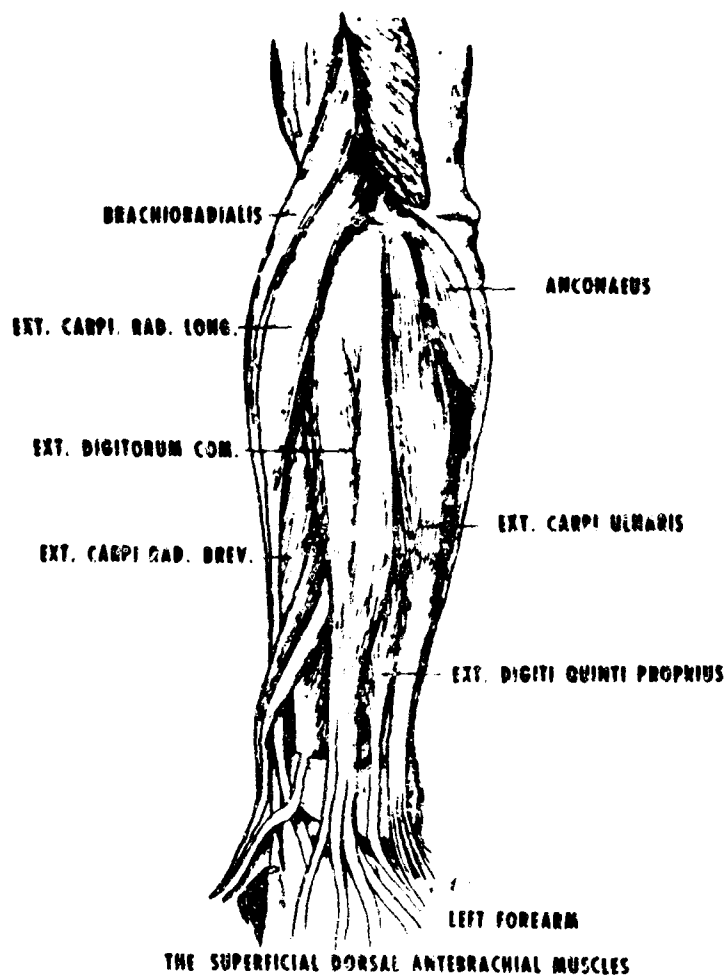
- 4 -

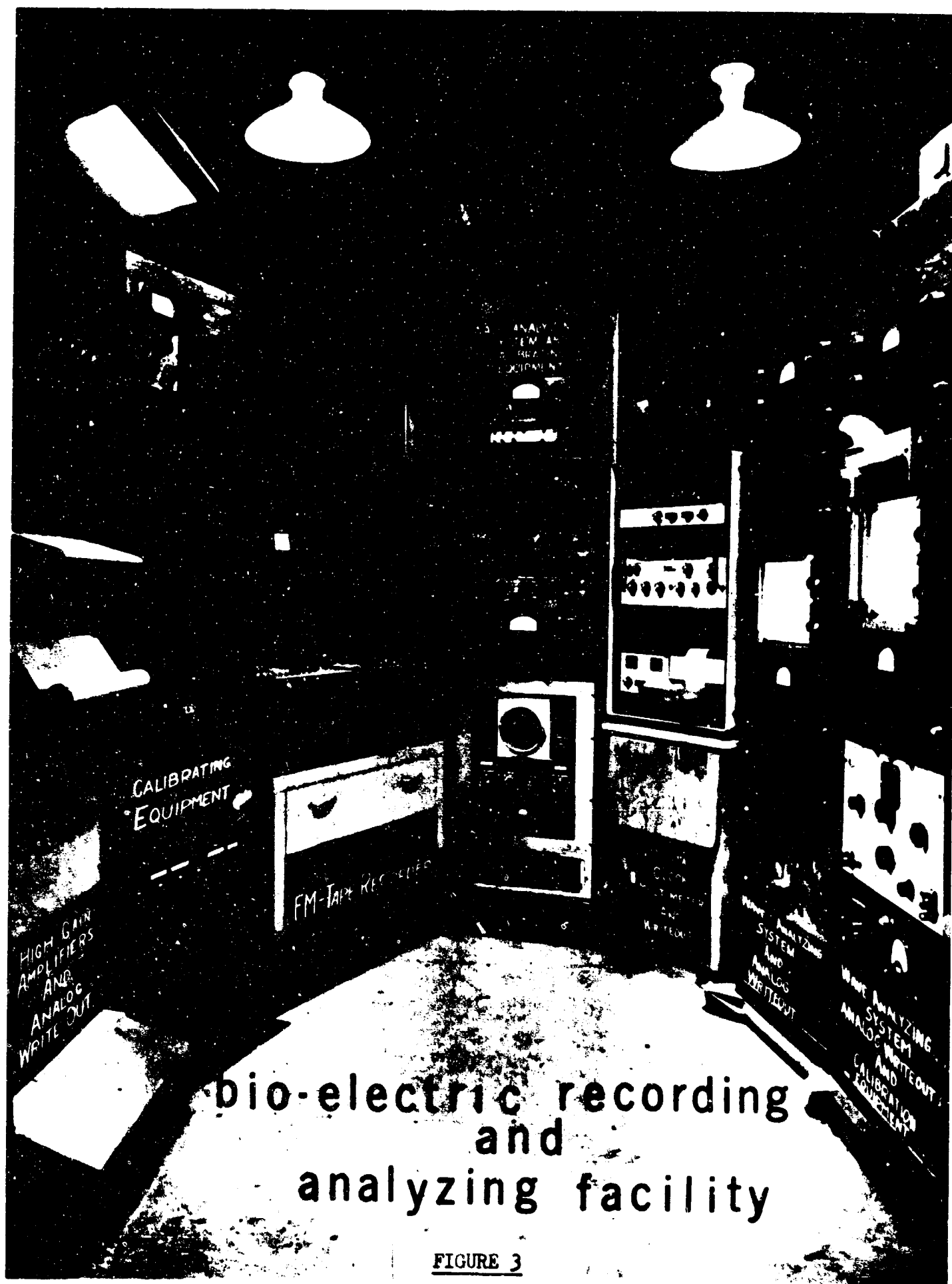bio-electric recording
and
analyzing facility

FIGURE 3

FLOW CHART OF BIO-ELECTRIC RECORDING AND ANALYZING FACILITY
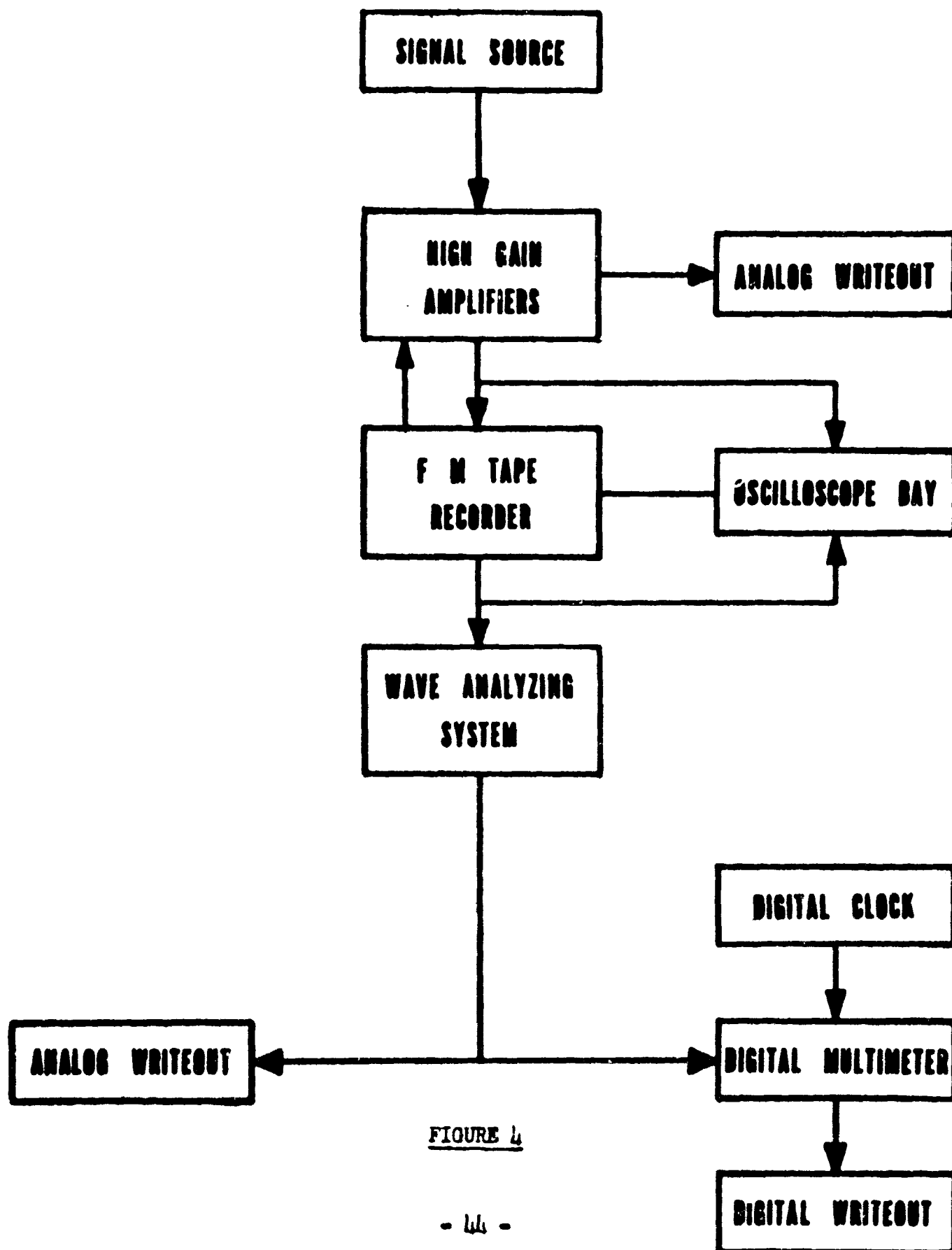

FIGURE 4

Methodological Requirements.

In order to obtain reliable quantitative data of the type outlined in the preceding section of this report, two fundamental requirements must be met: (1) the electrodes employed to pick up the bio-electric signals must be correctly positioned over the musculature; and (2) the equipment employed for amplifying and analyzing the bio-electric signals must be of high gain, of low internal noise, and extremely accurate.

To meet the first of these requirements, namely that of correct electrode placement, a series of anatomical studies of skeletal musculature was undertaken. Following these studies, several anatomical sketches, indicating the loci of various muscle groups, were prepared in order to facilitate correct electrode placement. Samples of these sketches are presented in Figure 2.

The second requirement, that of precise and accurate high-gain, low noise equipment has involved a continual program of development and improvement. Our present recording and analyzing facility is the result of several years of development. The facility is pictured in Figure 3, and a flow chart of its various operations is presented in Figure 4.

Accomplishments.

Summary to 1 July 1964. Previous findings indicate that:

1. The amount of energy expended in the performance of a simple motor task is affected by subjective feelings of success or failure. When the subject feels that he is successful, he expends less energy to perform a given task than when he feels that he is failing .5]

2. The amount of energy expended in the performance of a simple conceptual-motor task (card-sorting by means of a coded finger-tapping task) is influenced by the subject's estimated probability of his succeeding in the performance of the task. When Ss feel that there is a chance of succeeding in the performance of a task, their MAP levels tend to be higher than when they feel that there is no chance of succeeding in the performance of the task .6]

3a. In the performance of an isotonic work task, the MAP is a logarithmic function of the load employed; also, the amount of work output is a logarithmic function of the load employed .7]

3b. In the performance of an isotonic work task, the MAP is linearly related to the rate of work; also, the amount of work output is a linear function of the rate of work.

3c. Since both MAP and work output are logarithmic functions of load and linear functions of rate of work, they are linearly related to one another. Thus, work output is linearly related to MAP both as a function of load and as a function of rate of work.

4. In a series of experiments involving isometric work tasks in which Ss squeezed a hand dynamometer at various initial levels until they could no longer support as much as ½ of the initial load, the following results were obtained:

a. The average MAP intensity was a negatively accelerating monotonic increasing function of the initial load (8j

b. The frequency spectrum of the MAP signal is distributed with a modal frequency of between 40 to 60 cycles per second 8j, .9j

c. The frequency spectrum of the MAP signal is similar for both the flexor and extensor muscles of the working arm, although the absolute level of MAP activity for the flexors is greater than that for the extensors 9j, See Figure 5.

d. The frequency spectrum of the MAP signal changes as the subject becomes progressively more "fatigued." With increased time of isometric work, the absolute magnitude of the high frequency MAP components diminishes, but the magnitude of the low frequency components increases 8j, .9j See Figures 5 and 6.

e. With increased time, the precision of performance in isometric work decreases. The magnitude of isometric contractions becomes more variable, and hence, more imprecise. Associated with this performance "decrement" is a change in the frequency spectrum of the MAP signals so that higher frequency components decrease in mean amplitude and lower frequency components increase in mean amplitude .9j

5. The perception of the vertical is influenced by the relative distribution of MAP activity on contralateral sides of the body, as indicated by changes of the left-right distributions of MAP signals obtained from the left and right sternocleidomastoid muscles of the neck. When MAP activity of the left sternocleidomastoid is greater than that of the right sternocleidomastoid, the apparent vertical shifts relatively to the left of true vertical; but when the right sternocleidomastoid is more active than is the left sternocleidomastoid, the apparent vertical shifts to the right. This is true whether the imbalance of muscle activity is due to physically tilting the subject, or whether it is due to direct loading of the musculature without actually tilting the subject .10j

Summary from 1 July 1964 to 1 July 1965.

The following experiments were performed since the issuance of the previous annual progress report on this program .11j.

1. Previous observations by the authors have indicated that the frequency spectrum of the MAP signal is altered by prolonged isometric contractions. The alteration is such that the high frequency components decrease in mean amplitude, while the low frequency components increase in mean amplitude. Associated with these changes in the frequency spectrum of the MAP signal is a corresponding decrease in the precision of perf-rmance. While it is likely that the "fatigue" state of the subject is the relevant factor influencing the change in the frequency distribution of the MAP signals, it is also possible that the increased variability in the performance of the motor task is, in turn, dependent upon the frequency spectrum of the MAP signals. According to this conjecture, then, the performance of a motor task will be affected directly by the existent frequency spectrum

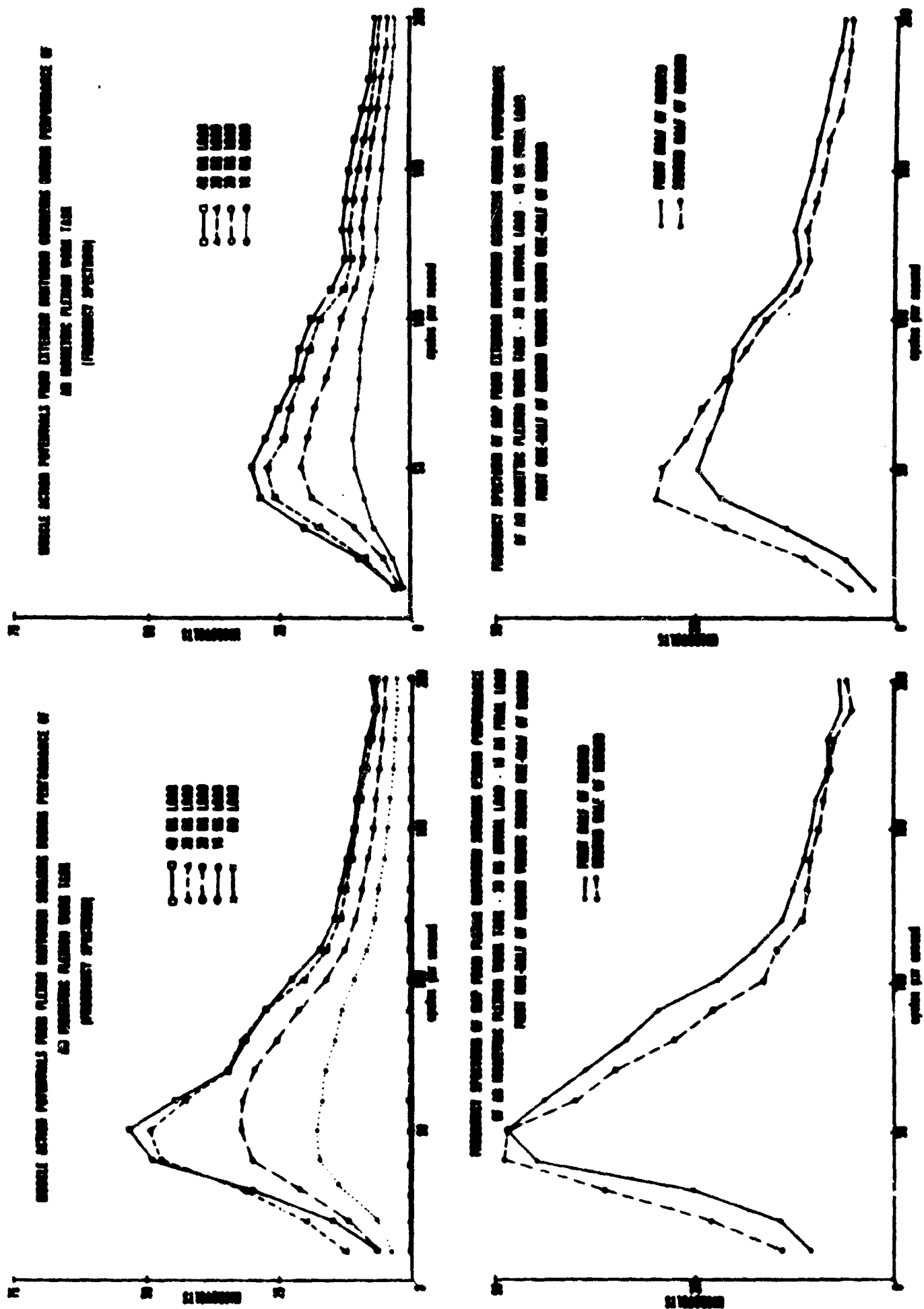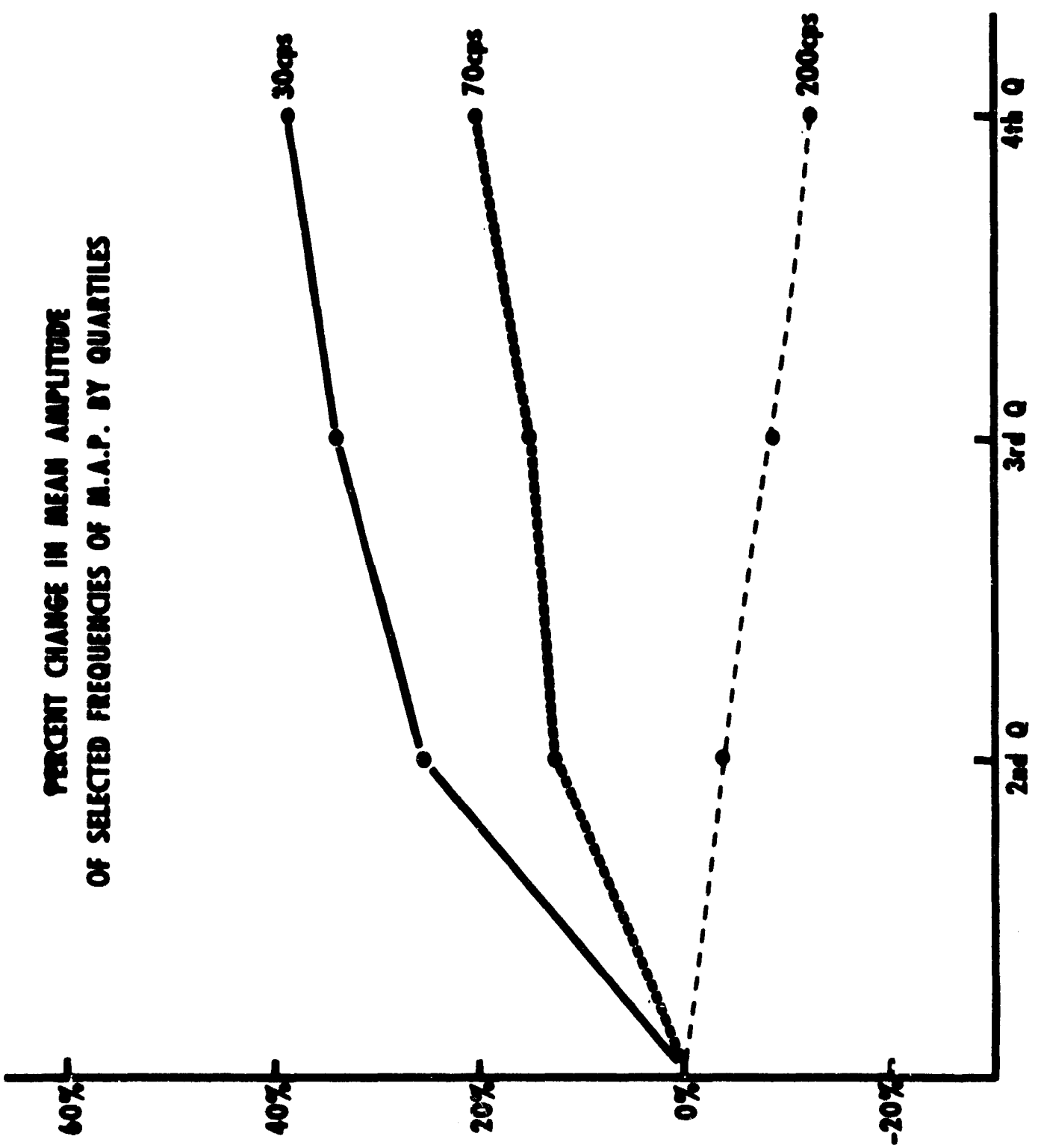CHANGES IN FREQUENCY SPECTRUM OF MUSCLE ACTION POTENTIALS

STIMULATED MUSCLE ACTION POTENTIALS

FIGURE 5

PERCENT CHANGE IN MEAN AMPLITUDE
OF SELECTED FREQUENCIES OF M.A.P. BY QUARTILES

quartile of time to fatigue

FIGURE 6

of the MAP signals - regardless of how the frequency spectrum was brought about
Thus, the hypothesis could be entertained that with increased precision of
performance in a motor task, the frequency spectrum of the associated MAP signals
would be altered in a manner opposite to that brought about in conjunction with
decreased precision of performance. To put the conjecture in somewhat dif-
ferent terms: If decreased precision is associated with a decreased amplitude
of high frequency MAP components and an increased amplitude of low frequency
MAP components, then increased precision should be associated with an increased
amplitude of high frequency MAP components and a decreased amplitude of low
frequency MAP components.

The problem, then, is to establish a condition in which the precision of
performance of a motor task can be increased. One such method involves the
acquisition of a motor skill through practice, i.e., motor learning.

Each of eight subjects attempted to trace the outlines of five different
geometric forms for a period of three minutes with each of the forms while
he viewed both his tracing hand and the forms in a mirror. On each of five
successive days, the subjects practiced the mirror tracing task; at the same
time, MAP signals were recorded from various muscle groups of the working arm.

The subjects were then confined for a period of 34 days, and, during that
period, practiced the same task daily for the same periods of time - without
MAP signals being recorded.

Following the 34-day confinement-practice period, the subjects were again
required to perform the same mirror tracing task for five additional days as
they did before practice; MAP signals were again recorded as in the
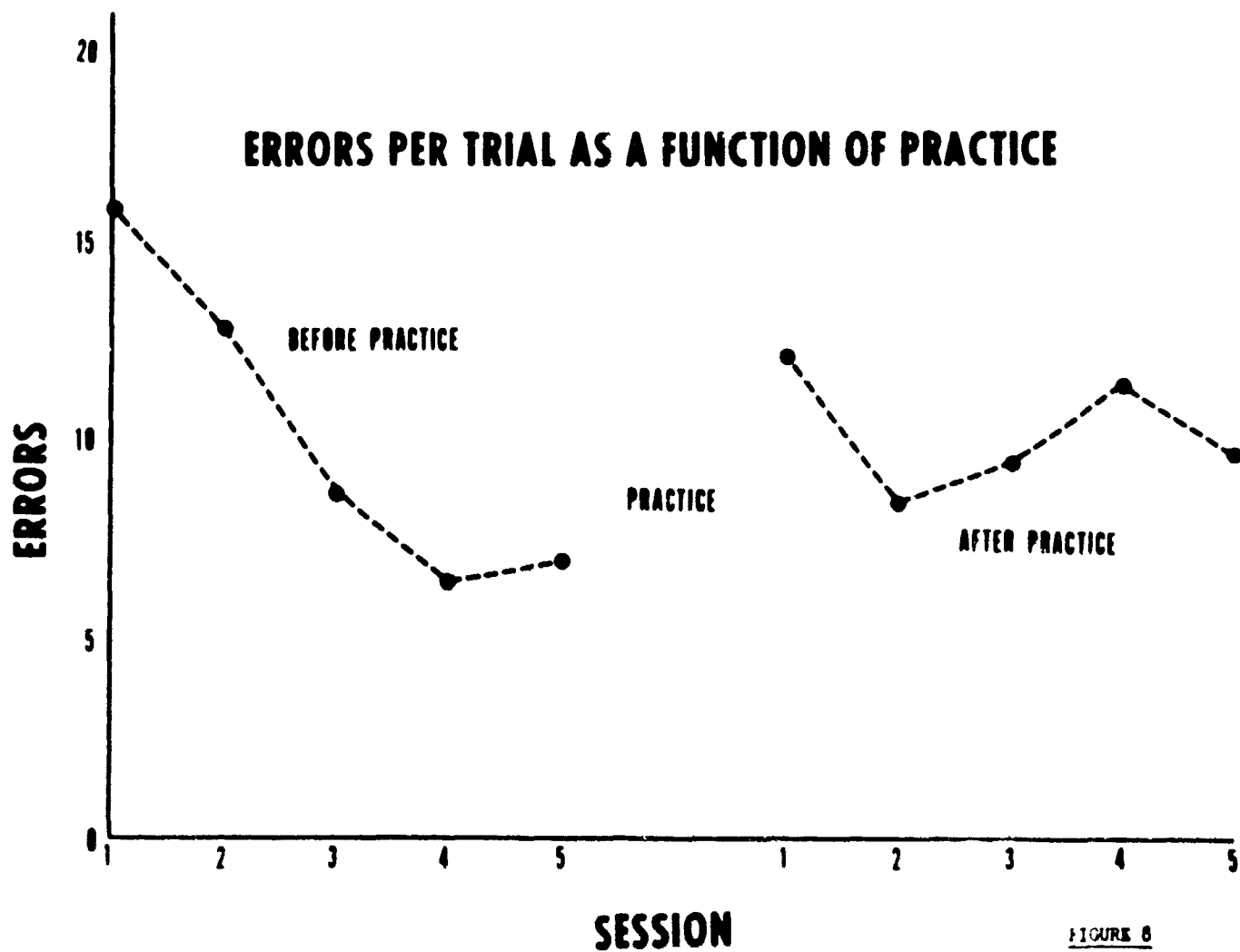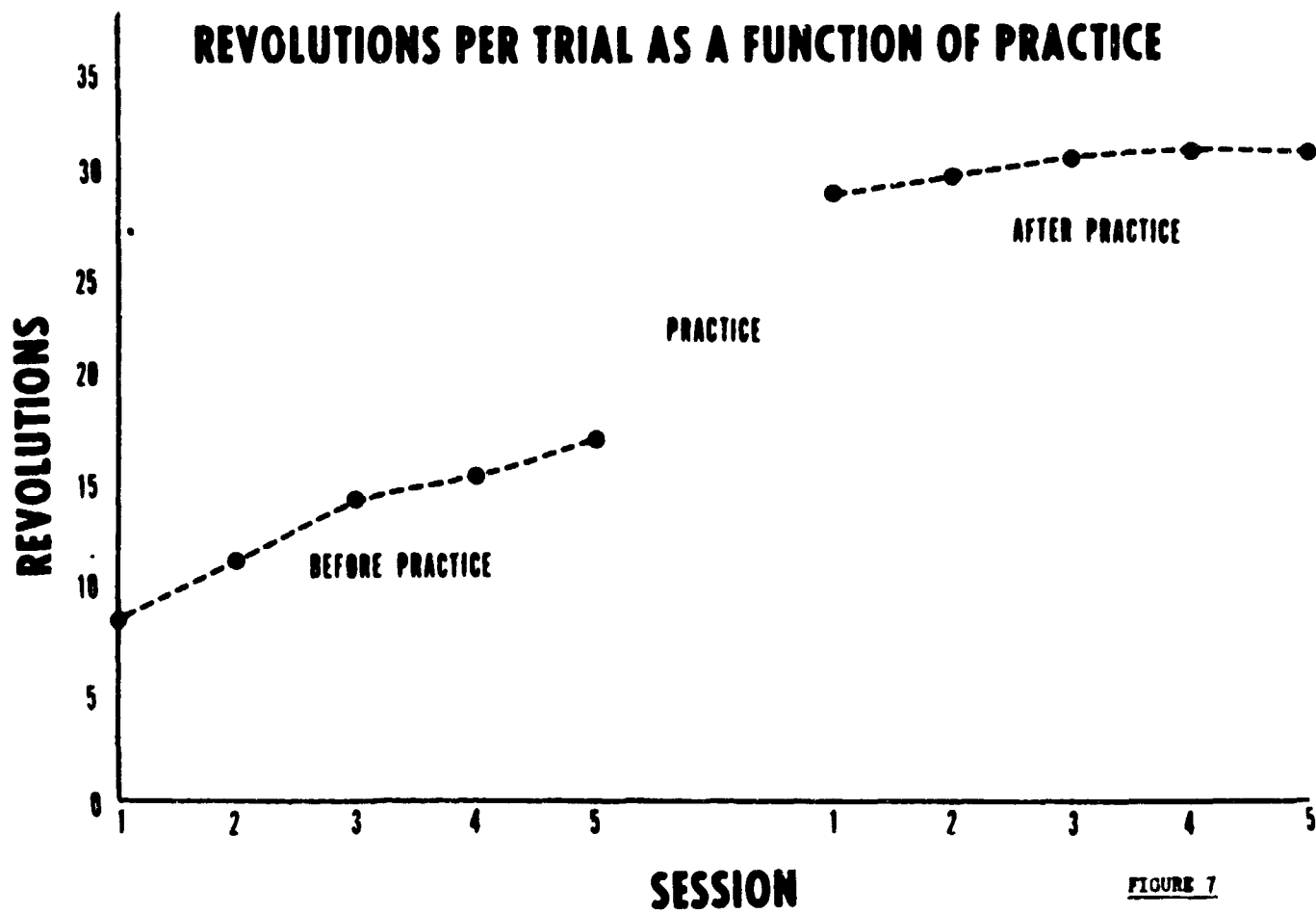pre-practice sessions.

The changes in the performance of the mirror tracing task are shown in
Figures 7, 8, and 9.

The mean number of times that the subjects could trace the outlines of
the geometric forms are presented in Figure 7. As shown in Figure 7, the sub-
jects became progressively more rapid in the performance of the motor task.

As shown in Figure 8, the subjects tended to make progressively fewer errors
as the number of practice sessions increased, although there is a slight rise
in the absolute number of errors during the post-practice sessions (probably
due to the greatly increased speed of performance shown in Figure 7).

Figure 9 clearly illustrates the increased precision in the performance of
the mirror tracing task. Whereas the subjects initially made an average of
1.86 errors per revolution during the first pre-practice session, the post-
practice sessions were much better - with between .26 and .41 errors per revolution

Figure 10 illustrates the changes in the frequency spectrum of the MAP signals
obtained from the extensor digitorum communis muscles of the working arm both
before and after the 34-day confinement-practice period.

-49-

REVOLUTIONS PER TRIAL AS A FUNCTION OF PRACTICE

AFTER PRACTICE

PRACTICE

REVOLUTIONS

BEFORE PRACTICE

SESSION

FIGURE 7

ERRORS PER TRIAL AS A FUNCTION OF PRACTICE

BEFORE PRACTICE

ERRORS

PRACTICE

AFTER PRACTICE

SESSION

FIGURE 8

ERRORS PER REVOLUTION AS A FUNCTION OF PRACTICE
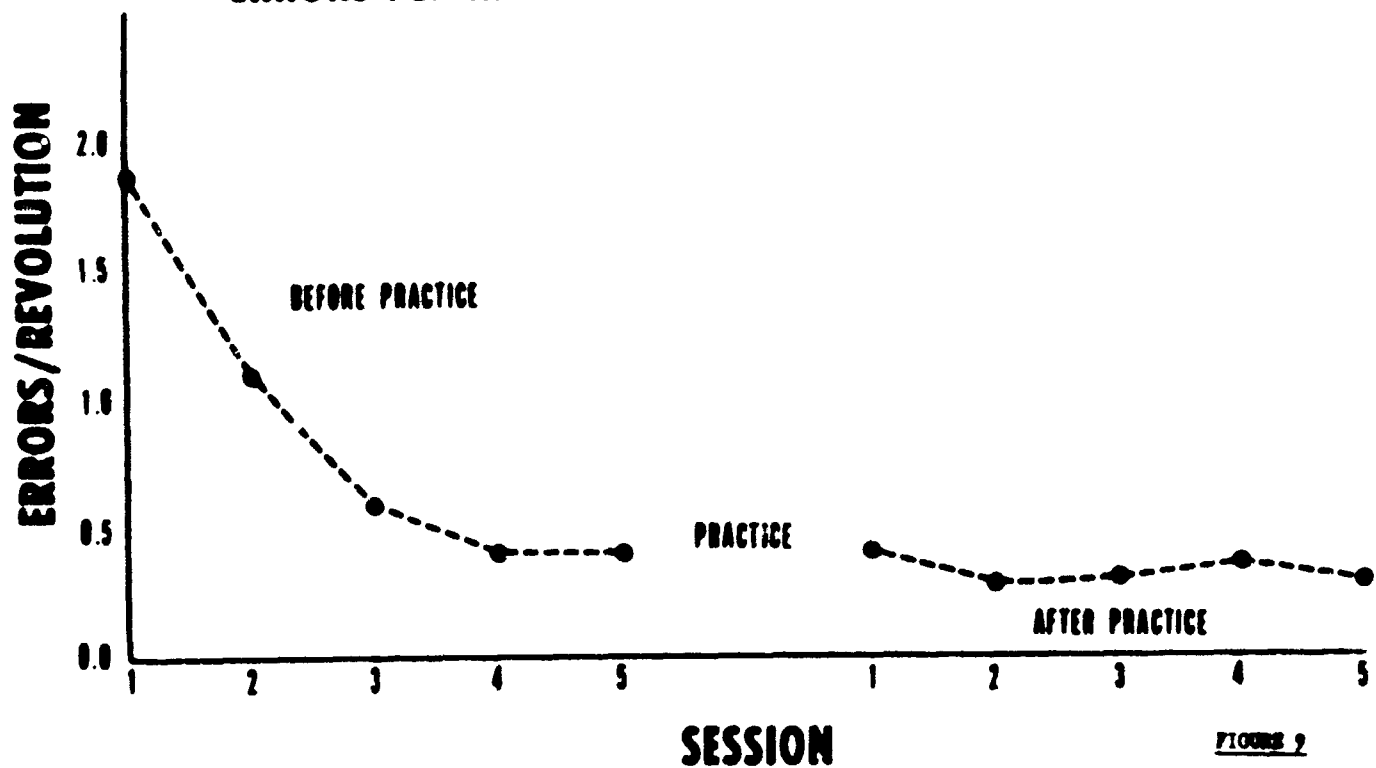
FIGURE 9

CHANGES IN FREQUENCY SPECTRUM OF MAP
AS A FUNCTION OF PRACTICE

FIGURE 10

Curvature After-Effects as a Function of Inspected Material

CURVATURE OF INSPECTED MATERIAL (DIOPTERS)

AFTER-EFFECT (DIOPTERS)
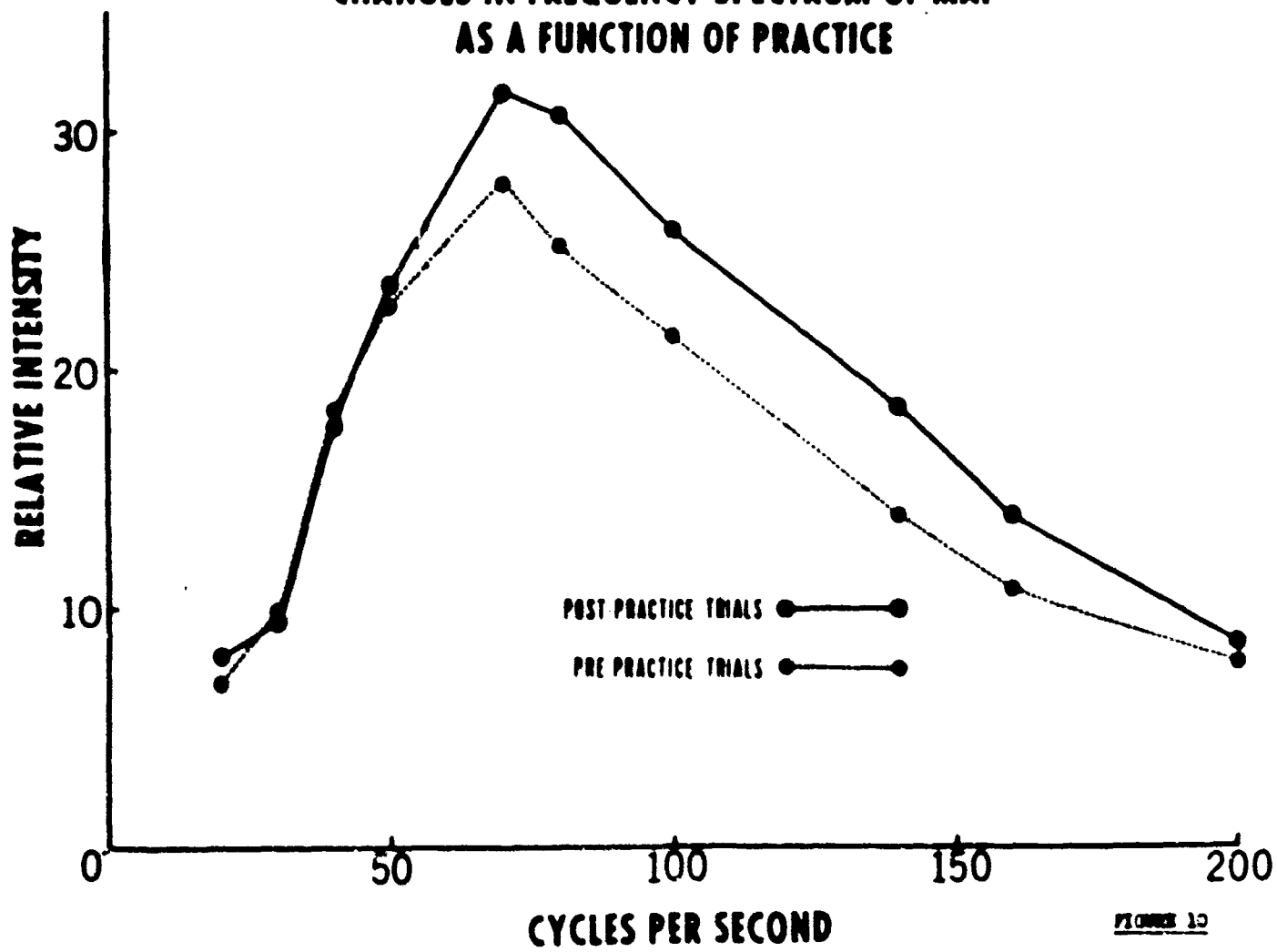
FIGURE 11

As shown in Figure 10, the low frequency components of the MAP signal (i.e. 40 cycles per second and below) do not appear to show any significant change in average energy as a function of practice. On the other hand, the average energy of the high frequency components (i.e., above 50 cycles per second) becomes considerably higher after practice. Thus, the conjecture was partially supported. These changes in the frequency spectrum of the MAP signal suggest that precision of performance in a motor 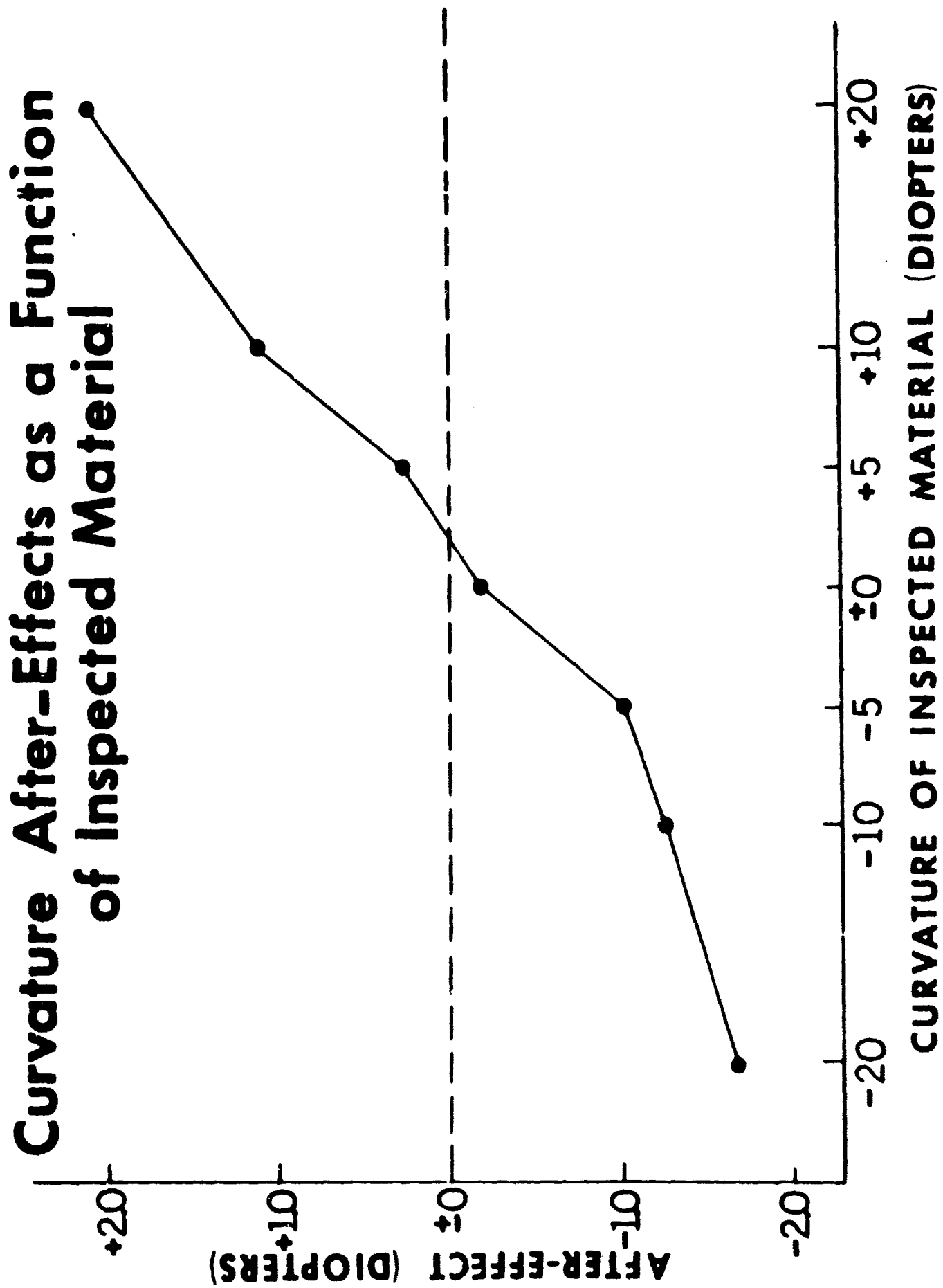task is associated with the frequency-intensity characteristics of the MAP signals produced in the performance of the task, and that the acquisition of a motor skill may be associated with increased activity of the higher frequency components of the performing muscles. Further and more complete data analysis is currently underway. The results of the more complete data analysis will be presented in a subsequent progress report.

An additional finding is also of interest. The total energy of the MAP signals from the various working muscles sampled in the preceding experiment was analyzed. It was observed that the total energy from all working muscles when taken together was less for the post-practice trials than for the pre-practice trials. (This is not apparent in Figure 10, which examined only the extensor digitorum communis.) This finding is in keeping with earlier observations .4j Additional research is required to elucidate this point further.

2. A second study involved an attempted replication and verification of the previous findings .10j In this experiment, each of six subjects was given repeated trials in which he attempted to adjust a luminous rod in a darkened room until he reported that the rod appeared to be vertical. The adjustments were performed under different conditions of muscle loading in which loads were suspended from a helmet on the left side, the right side, both sides, or neither side of the head. The rod measured 24 inches from top to bottom, and was located at distances of 48, 96, or 120 inches from the subjects. Although the data from this experiment is currently under examination, preliminary indications are that our previous findings 10j may not be reproducible.

3. A third study, derived from previous work 12j, 13j, 14j, 15j, was concerned with the relationship between the magnitude of a curvature aftereffect (the amount by which physically straight lines appear to curve when viewed immediately following previous exposure to physically curved lines), and the magnitude of curvature in the previously viewed curved lines. Gibson 12 and Bales and Follansbee 13 have indicated that the magnitude of the curvature aftereffect is not influenced by the magnitude of curvature in the inspected material (previously viewed curved lines). However, these investigators only used single lines both as inspected material and as a test line (line which subject adjusts for apparent straightness). In addition, both Gibson and Bales and Follansbee tested only at two different degrees of curvature in the inspected material - no continuum of curvature was examined.

The current study required each of six subjects to view a grating of optically curved lines through a prism for a period of ten minutes. The amount of optical curvature in the inspected material was adjusted by setting the dioptric power of the prism at 20, 10, and 5 diopters base left (thereby optically curving the lines by different degrees convex to the left), at 0 diopters power, (thereby not optically curving the lines), and at 5, 10, and 20 diopters base right (thereby optically curving the lines by different degrees convex to the right). The results are presented in Figure 11.

As shown in Figure II, the magnitude of the curvature aftereffect is affected by the magnitude of curvature of the inspected material - a finding in contradiction to those of Gibson and Bales and Follansbee. Further work is required to specify the cause for our divergent results. One possible factor of interest is the scanning motions of the eye as the subject views either multiple or single curved lines and as he views lines of different degrees of curvature. Bio-electric techniques (such as the electro-oculogram, EOG) 5] may be of value in this regard.

Future Plans.

The above program will continue to investigate the functional relationships between stressors and stress (as defined by MAP), MAP and performance, MAP and perceptual shifts, and MAP and motor learning.

References.

1] Arnold, M. B.: A study of tension in relation to breakdown. J. Gen. Psychol. 26:315, 1942.

2] Bills, A. G.: Facilitation and inhibition in mental work. Psychol. Bull., 34:286, 1937.

3] Davis, R. C.: Electromyographic factors in aircraft control. The relation of muscular tension to performance. School of Av. Med. Ran. AFB, Tex. Rep. 55-122, 1956.

4] Klein, S. J. Relation of muscle action potentials variously induced to breakdown of work in task-oriented subjects. Percept. Mot. Sk., 1961, 12, 131-141.

5] Klein, S. J., and Cohen, M. M.: Progress Report August 1963. Foundational Research Project No. 19: The Measurement of Stress and its Relationship to and Effects on Performance in Mental and Motor Work. Naval Air Engineering Center, Philadelphia, Pa. 19112.

6] Diggory, J., Klein, S., and Cohen, M.: Muscle action potentials as a function of estimated probability of success. J. Exp. Psychol. 1964, 68, 449-455.

7] Klein, S. J., Cohen, M. M., and Bingham, W. F.: The relationships between muscle action potentials (MAP) and selected parameters of performance in isotonic work. Presented by M. M. Cohen at the 72nd Annual Convention of the American Psychological Association, Los Angeles, California, 4-9 Sep 1964.

8] Klein, S. J., and Cohen, M. M.: Frequency distributions of Muscle Action Potentials during isometric work. Presented at the annual meetings of the Society for Psychophysiological Research, October 1964.

9] Klein, S. J., and Cohen, M. M.: Frequency and amplitude relationships between Muscle Action Potentials (MAP) and fatigue in isometric work. Presented at the annual meetings of the Psychonomics Society, Niagara Falls, Ontario, Canada, October, 1964.

10⌋ Klein, S. J., Wapner, S., Shaw, W. A., Cohen, M. M., and Werner, H.:
The Relationships between Muscle Action Potentials (MAP) and the Perception of
Verticality. Presented at the 72nd Annual Convention of the American Psycho-
logical Association, Los Angeles, California, 4-9 Sep 1964. Submitted
for publication.

11⌋ Klein, S. J., and Cohen, M. M. Progress Report August 1964. Foundational
Research Project No. 19: The Measurement of Stress and its Relationship to
and Effects on Performance in Mental and Motor Work. Naval Air Engineering
Center, Philadelphia, Pa. 19112.

12⌋ Gibson, J. J.: Adaptation, aftereffect and contrast in the perception of
curved lines. J. Exp. Psychol., 16:1, 1933.

13⌋ Bales, J. F. and Follansbee, G. L.: The aftereffects of the perception
of curved lines. J. Exp. Psychol. 18:499, 1935.

14⌋ Cohen, M.: Visual curvature and feedback factors in the production of
prismatically induced curved line aftereffects. Presented at the 34th annual
meetings of the Eastern Psychological Association, April 1963, New York, N. Y.

15⌋ Cohen, M. M.: Curvature aftereffects following exposure under prismatic
viewing conditions. Dissertation, University of Pennsylvania, 1965.

UTILIZATION OF MASER AS A MEANS OF EXCITATION
FOR THE SPECTROGRAPHIC EXAMINATION OF MICROSTRUCTURES OF METALS

JOHN F. DANOVICH AND MELVIN D. SMITH

Background

Although the exact mechanism of structural failure of metals and alloys is still not very well understood, segregation of the alloying constituents is known to play a prominent part. These segregates cannot be examined by conventional spectrographic means because of the minute areas involved, inability to control the electrical discharge, and difference in rates of volatilization. When using the monochromatic light of the laser as a means of excitation, the beam may be optically focused on an area as small as 100 microns in diameter and is not subject to many of the limitations of the electrical discharge.

Objective

Examination of metals by light microscope technique using selected etchants can be used to detect inhomogeneities and phases in the matrices of metals, and to indicate their relative positions in the specimen. After thus locating areas of interest, the laser beam can be focused on specific segregates or phases. Vaporization of these areas by the laser beam can lead to spectral analysis to identify the constituents.

Employing standard calibration curves and internal standard lines, experimental work will be performed to establish techniques using the laser beam as an excitation source for the emission spectrograph in order to perform quantitative analyses of the elements present. These data will make possible the identification of segregates and phase constituents in metals.

Accomplishments

It was previously reported that variation of power output in the laser head made it impossible to perform quantitative analyses. The original laser head was replaced by a redesigned head with a greater power output stability. Subsequently, it was found that variation in power output, other than those occurring in the laser head, were evident. The objective lens system of the microscope, used to select the target area of the specimen and to focus the laser beam, was being damaged progressively by the intensity of the beam. Figure 1 shows photomicrographs of two damaged upper doublets of the lens system. The first (left) shows the damage after 200 shots and the second (right) after only 50 shots. A modified objective (shown on the right side of Figure 2) was designed to overcome this limitation. It has performed well in subsequent investigations. Figure 3 shows photomicrographs of two subjects taken through the standard objective (left) and the modified objective (right). This proved that the field of view at focus was adequate to select the area to be examined.

Qualitative analysis of inclusions in metallic alloys is quite readily accomplished using the laser probe. Figure 4 shows an inclusion in 4340 steel (top). In the bottom photomicrograph, it can be seen that this inclusion has been vaporized by the laser beam. It was determined by spectral analysis to be silicon.

Microphotographs Showing Effects of Laser
Damage to Upper Doublet of Objective Lens
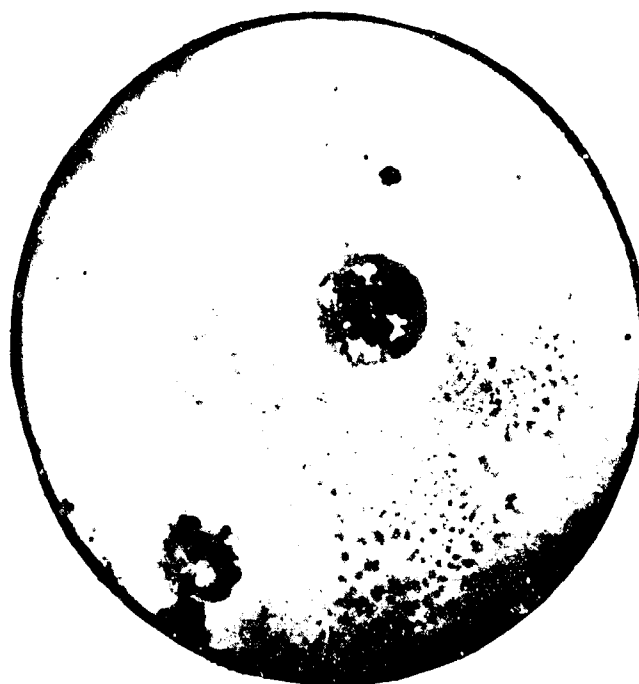
200 Laser Shots   50 Laser Shots

Magnification 20X

FIGURE 1

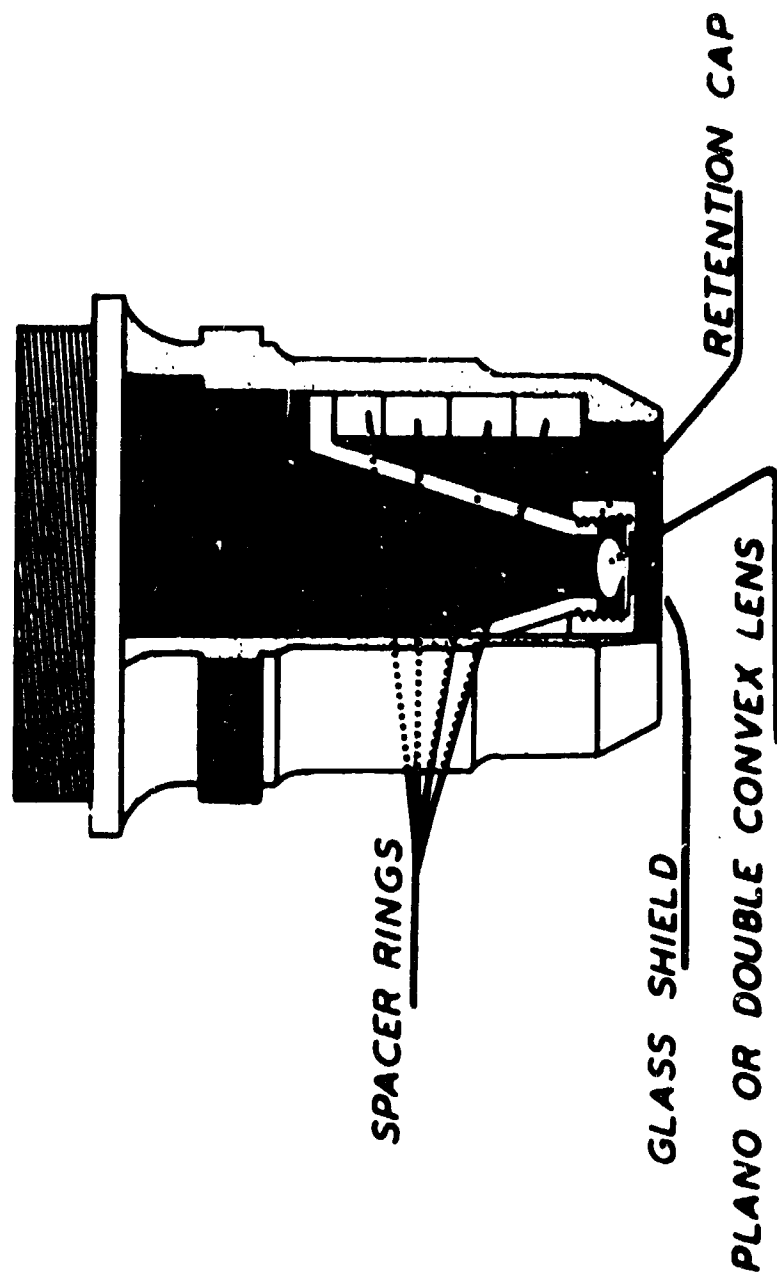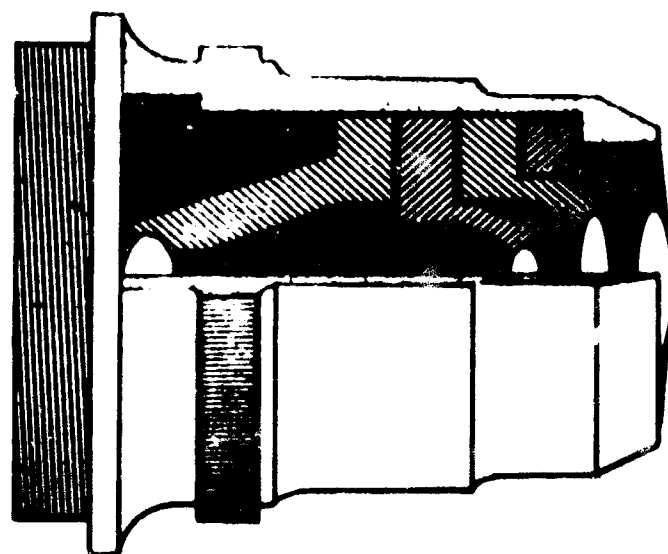STANDARD OBJECTIVE

MAG.   20 X

N.A.   0.25

MODIFIED OBJECTIVE

MAG.   5 TO 25 X

N.A.   VARIED

SPACER RINGS

GLASS SHIELD

PLANO OR DOUBLE CONVEX LENS

RETENTION CAP

COMPARISON OF OBJECTIVES

FIGURE 2

FIGURE 3

BEFORE

AFTER

FIGURE 4
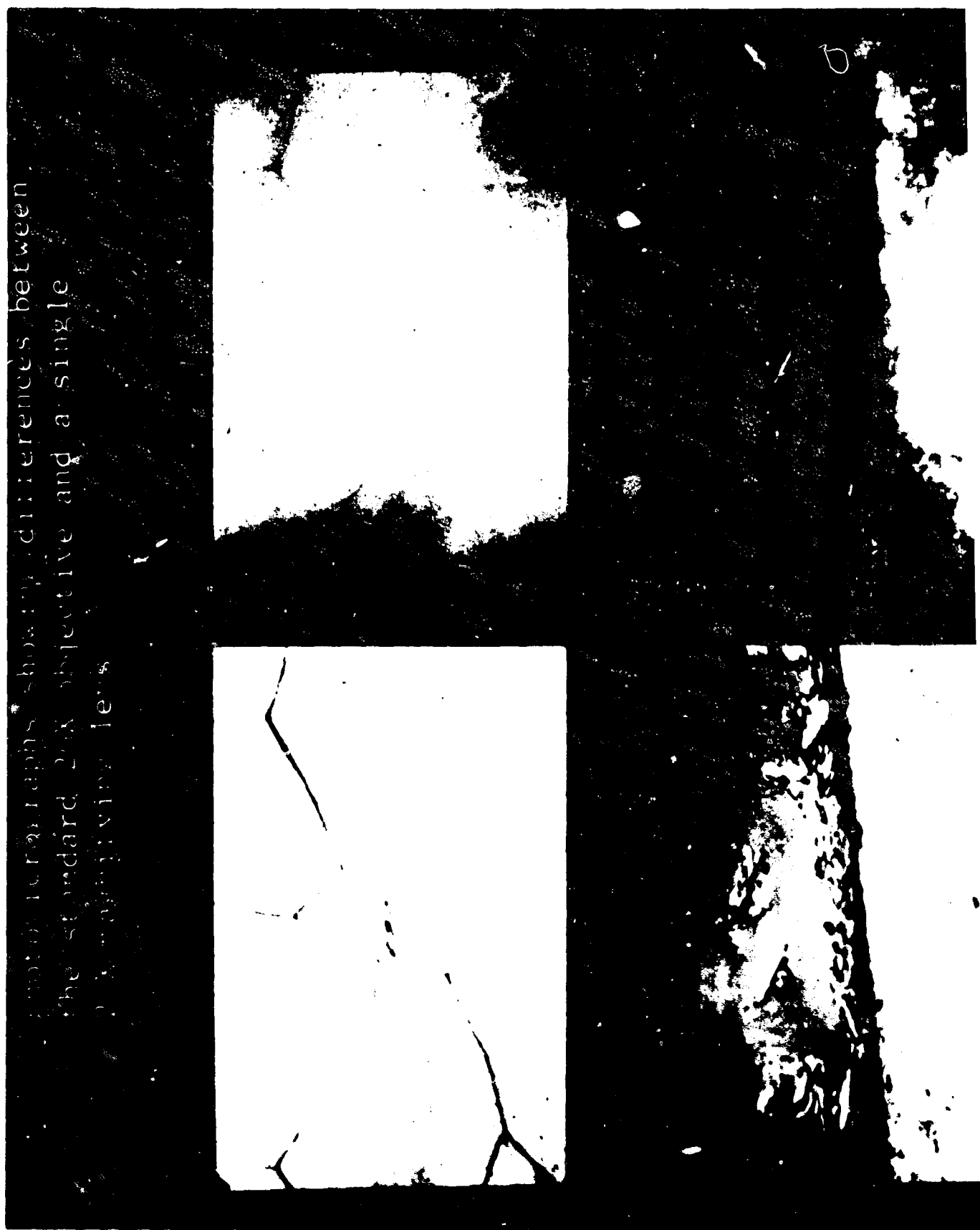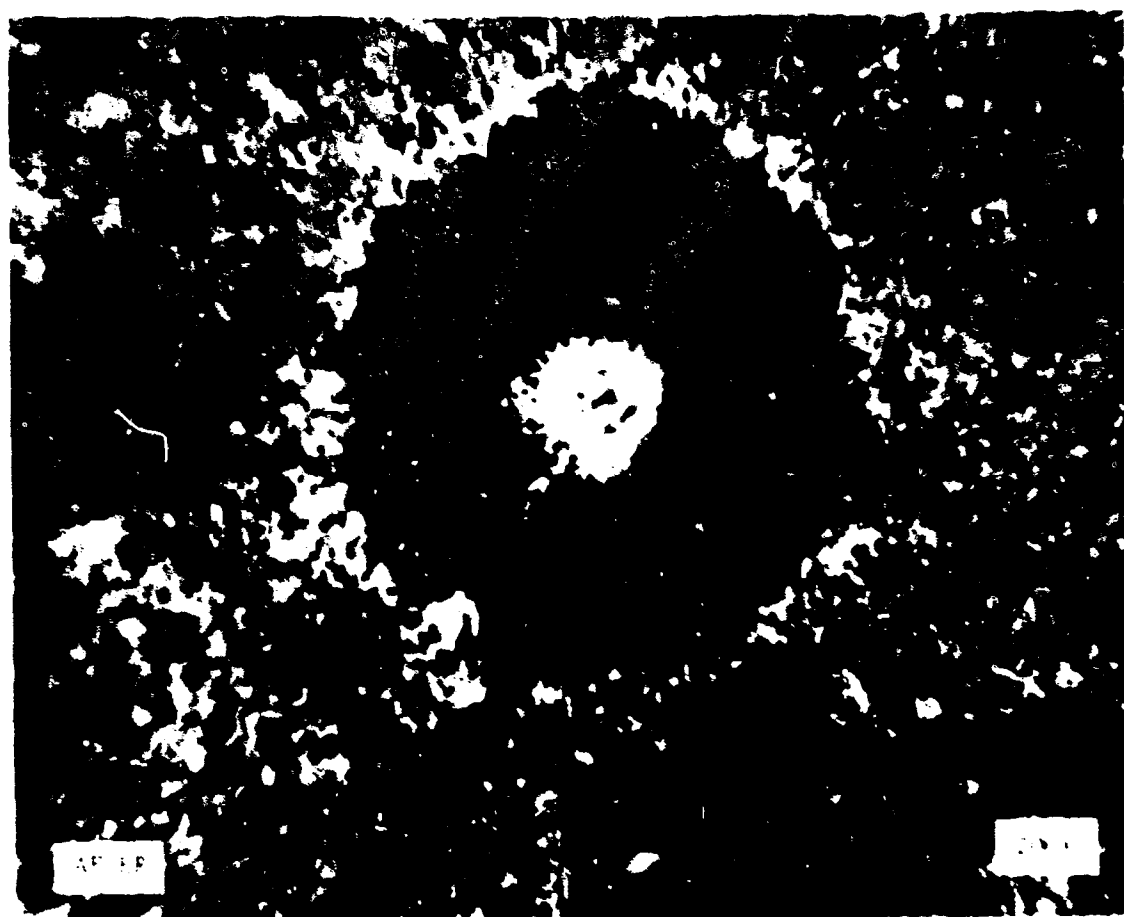
CALIBRATION CURVE FOR SILICON IN AN ALUMINUM ALLOY

Si   2518 A.

Al   3050 A
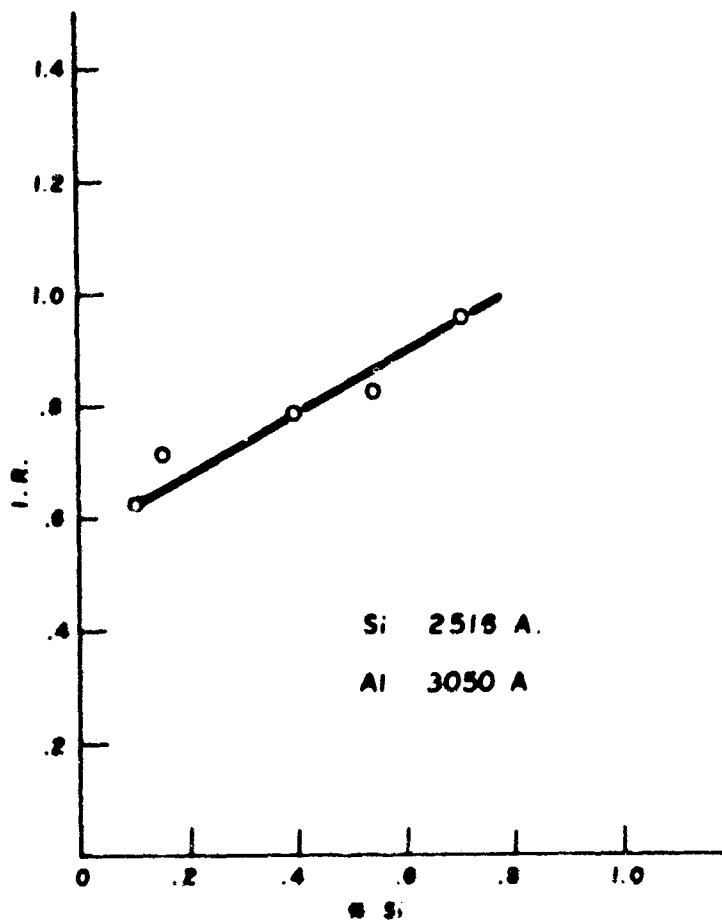
5A

TABULATION OF CRATER DIMENSIONS PRODUCED BY
LASER ENERGY USING THE COATING TECHNIQUE
(NO OR APPROX. 2X* OBJECTIVE)

Coating	Major Diameter (u)	Minor Diameter (u)	M.P. °C	B.P. °C
Alclad*	3400	2300	659	2057
	4200	2500		
Sn-Cd	4800	2100	Sn 231	2260
	3100	2500	Cd 321	767
Cd	4800	3800	321	767
	4800	3100		
Cu-Ni-Cr*	4800	2500	Cu 1083	2336
	5000	2100	Ni 1455	2900
			Cr 1890	2480
Ni-Cr*	4800	2300	Ni 1455	2900
	4800	3100	Cr 1890	2480
Iron	2300	2100	1535	3000
	3100	2900		

5B

As stated in the objective, the establishment of standard calibra
curves and internal standard lines must be made in order that quanti·
studies of segregates can be made. This phase of the investigation
accomplished. Figure 5A shows a representative calibration curve f·
in an aluminum alloy using the silicon line 2516 Angstroms as the e
and the aluminum line 3050 Angstroms as the internal standard line.

It was determined that it was possible to examine metallic coat
qualitatively with the laser probe using no objective or an approxim
2X objective. Figure 5B shows a tabulation of sampling area dimensi   ng
this technique for various metallic coatings.

Future Plans

Work will be performed to investigate segregation in aluminum a
steel alloys, and other materials. The establishment of analytical   e
for metallic coatings will be continued and extended to other inorga   a
organic coatings.

RESEARCH ON CAPTURED AIR

BUBBLE TEST VEHICLE

FRIEDRICH O. RINGLEB* & WALTER A. SIMMONS

BACKGROUND.

The Captured Air Bubble (CAB) vessel concept was conceived at The Naval Air Development Center (NADC) in 1960. The initial theoretical studies indicated that CAB offered great promise of providing efficient high speed naval ships over a wide range of sizes and classes. At this initial stage, discussions with BUSHIPS and David Taylor Model Basin (DTMB) working level personnel were held to ascertain interest in sponsoring a research program on CAB. Reaction was generally negative, except for Dr. Harvey Chaplin of DTMB who strongly endorsed initiating a program.

Response by BUWEPS was more receptive. In July 1961 a project was initiated at NADC and NAEC, under the BUWEPS Foundational Research program, with the objective of confirming that the low drag and favorable seakeeping characteristics indicated by theory for CAB could be achieved in practice.

Theoretical studies and tow tank model research were conducted during 1961 to develop and substantiate smooth water drag theory. Results were promising, and in October 1962 the XR-1 manned vehicle was started at NAEC.

In its initial configuration, the XR-1 had "fixed" fore and aft seals which were suitable for tests to substantiate further the basic smooth water drag theory. Tests of the XR-1 were started in May 1963. As reported in reference 1/, the drag data tests were in good agreement with the drag predicted by theory, and the turning and stability characteristics were satisfactory. In October 1963, a demonstration and program conference was held for RADM Fawkes, BUWEPS; RADM Brown, BUSHIPS; and representatives from various technical divisions of BUSHIPS.

During 1964, tests of 1/7 scale XR-1 models were conducted in waves to develop compliant fore and aft seals, and to demonstrate basic longitudinal stability and wave "platforming" capabilities. The limitations of the NAEC linear tow tank facility restricted these tests to only "head on" wave conditions, and no turning or maneuvering model tests were conducted. In these tests, the models exhibited excellent wave "platforming" characteristics at high model speeds, with little heave and pitch motion. The action of the compliant fore and aft seals in providing this smooth and stable wave "platforming" performance was graphically demonstrated.

---

* During F. O. Ringleb's absence due to sickness, W. A. Simmons acted as principal investigator. He also is essentially the author of this report.

In November 1964, the R&D Division of the Maritime Commission requested performance and basic design data on the CAB, for use in a study to evaluate technical feasibility of various types of Surface Effect Ships (SES) suitable for commercial marine service, and to compare their economic potential. Five concepts were evaluated - Hydrokeep, CAB, Ram Wing, Hovercraft, and Air Foil type. The CAB was selected as being most promising, and a program for development of a 1000 T or larger CAB cargo transport SES is currently being formulated by Maritime Administration for submission to Congress.

OBJECTIVES.

Verification of the rough water capability demonstrated by the 1/7 model test was of prime importance of the 1965 program. Major modifications were made to the XR-1 to provide a suitable test vehicle. Compliant fore and aft seals and associated hydraulic control systems were installed on the XR-1 test vehicle described in reference 1/. Additional modifications included incorporation of a new T53 turboprop main propulsion system, and deeper and thicker sideboards of increased buoyancy and stability.

ACCOMPLISHMENTS.

Operation of the XR-1 conducted after these modifications were of a "shakedown" nature, intended to check the mechanical functioning of the propulsion and seal systems and their associated controls. On 8 December 1964, the XR-1 overturned during a starboard turn which was started at a speed of approximately 35 knots.

The basic cause of the capsizing of the CAB XR-1 test vehicle has not yet been substantiated firmly. Based on analysis conducted to date, it is believed that the cause was lateral instability of the particular configuration of the XR-1, due to a dynamic interaction between roll, pitch, and yaw under the conditions in which the XR-1 was being operated. The instability exhibited by the XR-1 is not considered inherent in the CAB concept, and can be corrected with appropriate design changes.

A model test and computer dynamic analysis program was initiated jointly with the DTMB in early January 1965, to investigate the stability and control characteristics of the XR-1 configuration. It is anticipated that the conditions of the XR-1 accident can be duplicated and then analyzed, using model test data in the computer dynamic analysis. The model tests have been conducted in the DTMB rotating arm facility during May 1965. Model tests will also be conducted with various proposed "fixes", to develop a configuration providing adequate stability and control over the range of conditions under which the XR-1 is expected to be operated. It is then planned to incorporate these "fixes" and continue the "manned" CAB research test program.

FUTURE PLANNING.

1. Tests conducted with the XR-1 from May of 1963 to April of 1964 graphically demonstrated that the CAB concept provided an efficient high speed smooth water vehicle. It is still extremely important that the basic concept with compliant seals be investigated to substantiate scale model results. Of equal importance is the requirement that adequate stability be demonstrated for all operating conditions.

2. The design and construct.on of a small test vehicle is highly desirable to determine modifications that are required to provide stability and rough water capability. Prior to any further effort on the XR-1, successful tests of the sm .ll research vehicle is necessary.

3. A sixteen foot research vehicle is presently being designed. Construction of this craft will be started by mid August 1965, with completion scheduled for early October, 1965.

4. A rotating arm tow facility is presently under construction at NAEC. This facility will be used to determine flow characteristics associated with the CAB scale models. Flow phenomena and the motions of CAB models during turns will be investigated. Results of these tests will be used to formulate design concept of the small research vehicle.

REFERENCES

1/ Foundational Research Programs August 1964
2/ NADC Report WR-6412 of 13 May 1964

INVESTIGATION OF NEW CONCEPTS
FOR THE IN-FLIGHT SUPPRESSION OF JET ENGINE NOISE

R. B. BENHAM

Background

The early work under this project, described in the FR annual report of
August 1964, consisted of studies on circular nozzles only. This was done
for two reasons. Principally, it was desired to gain an insight into the
aerodynamic and acoustic mechanisms at work in suppressor nozzles. Also, the
large number of nozzles studied and the requirements of model fabrication in
the Aeronautical Engine Laboratory (AEL) shop necessitated contours which
could be fabricated quickly and accurately. Overall conclusions resulting
from this work were as follows.

Efficient suppression is obtained in the process of momentum exchange between
the jet and the ambient. Extended plug suppressor nozzles are basically in-
efficient because a significant part of the momentum exchange occurs between
the jet and the plug, resulting in a high drag penalty. Attempts to exchange
momentum with the ambient air at the center of the jet are only effective with
the addition of such quantities of ambient air as are unobtainable with low
drag flight engines.

It was concluded, therefore that lobed nozzles such as the "daisy" were the
most efficient as suppressors. Attention was then directed toward obtaining
a configuration significantly superior to the "daisy", but not requiring the
use of an ejector which, with present suppressors, must be retracted in flight.

A review of the literature revealed that previous investigators had surveyed
extensively such "daisy" parameters as:

    a. Effect of ratio of lobe width to chute width

    b. Effect of depth of chutes

    c. Effect of a centerbody.

However, no studies covering the effect of lobe stagger appeared to have been
made.

Objectives

It was intended, during the present investigation, to conduct parametric
studies of the staggered lobe nozzle to determine the suppression potential
of this concept. In addition, it was planned to test an improved version of
the multi-lobed, staged mixing nozzle discussed in the FY '64 report.
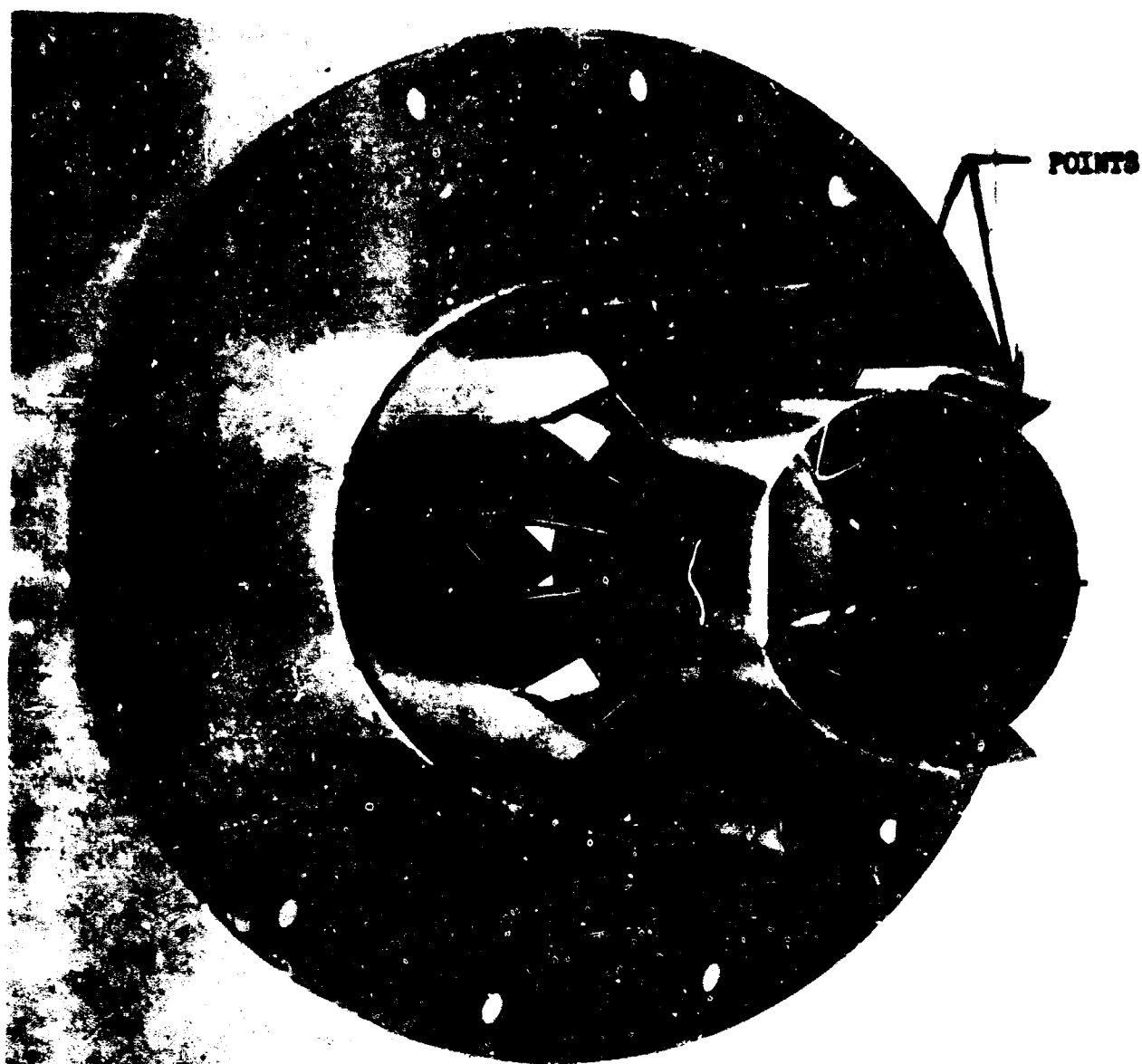
FIGURE 1. REVISED MULTI-LOBED, STAGED MIXING NOZZLE.

PERFORMANCE - MULTI-LOBED, STAGED MIXING NOZZLE

- 71 -

FIGURE 2

DIRECTIVITY
MULTI-LOBED STAGED MIXING NOZZLE

O – REFERENCE CIRCULAR
△ – MULTI-LOBED, STAGED WITHOUT POINTS
▢ – MULTI-LOBED, STAGED WITH POINTS
☆ – "DAISY"

VE = 1275 FPS ← → VE = 1375 FPS

SOUND PRESSURE LEVEL db re 0.0002 μb

FIGURE 3

FIGURE 4

POWER SPECTRUM

MULTI-LOBED STAGED MIXING NOZZLE

FREQUENCY IN CYCLES PER SECOND

SOUND POWER LEVEL IN BAND ~ db re 10^{13} watt

$V_E = 1375$ fps

O - REFERENCE CIRCULAR
△ - MULTI-LOBED STAGED
       WITHOUT POINTS
□ - MULTI-LOBED STAGED
       WITH POINTS
◇ - "DAISY"

FIGURE 5. NOZZLE COMPARISON
REFERENCE CIRCULAR, "DAISY", AND 45-55 STAGGERED LOBE

a. AREA SPLIT

$$\text{AREA SPLIT} =$$
$$\% \text{ OF TOTAL AREA IN } ///,$$
$$\% \text{ OF TOTAL AREA IN } \backslash\backslash$$

b. L/D

c. DENSITY RATIO

$$\text{DENSITY RATIO} = \frac{\backslash\backslash\backslash \text{ ARE}}{/// \text{ ARE}}$$
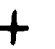
STAGGERED-LOBE NOZZLE PARAMETERS

Accomplishments

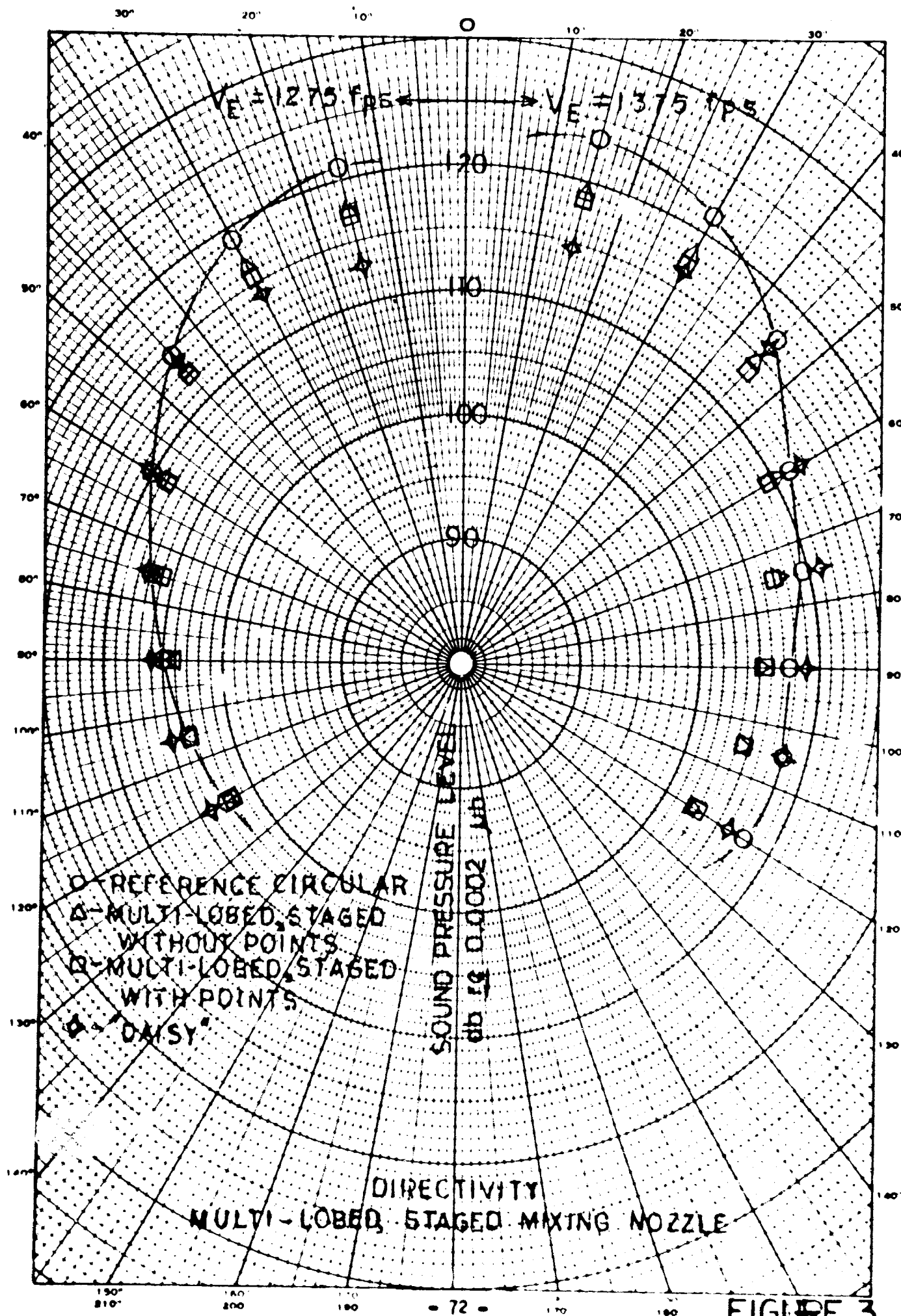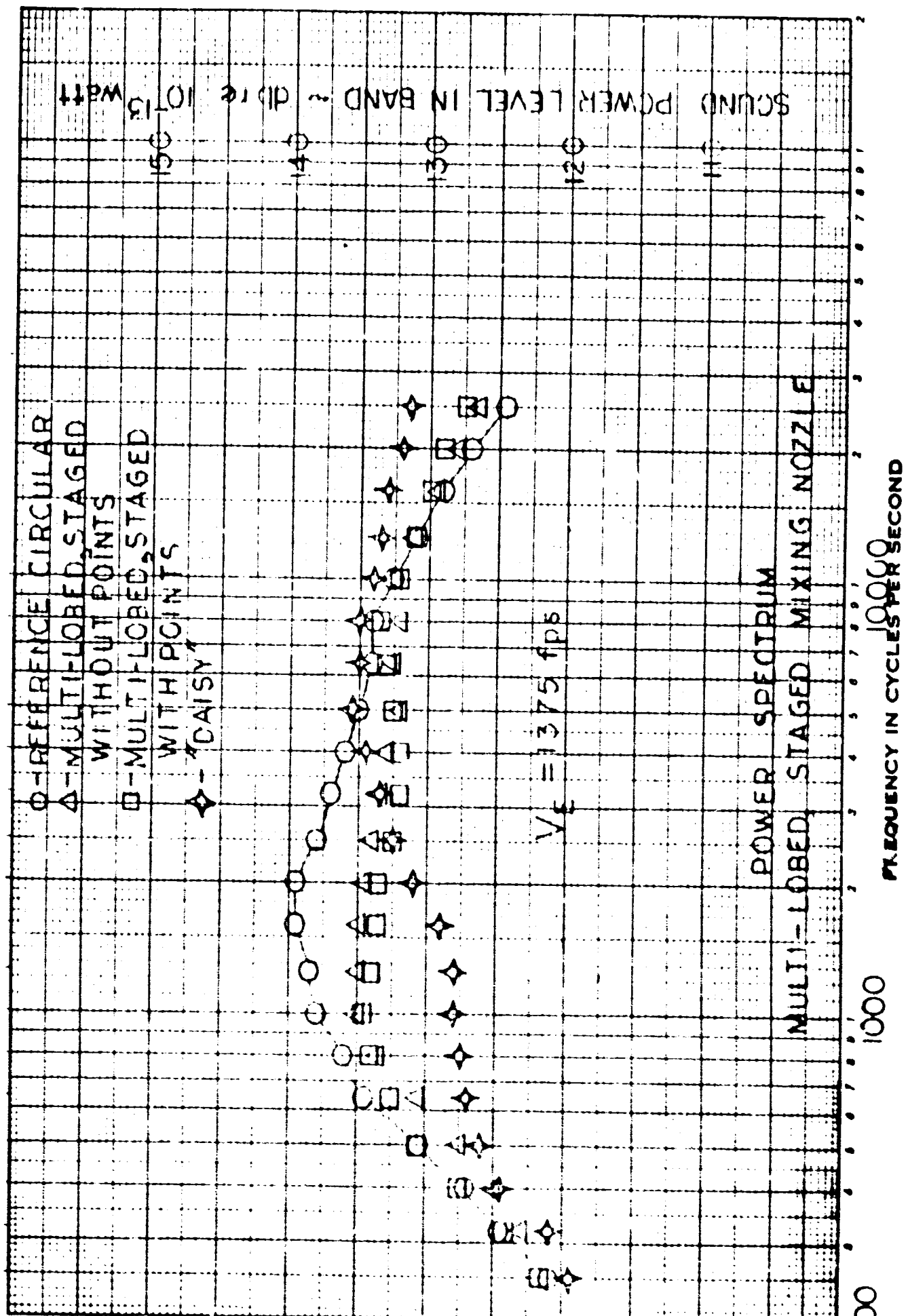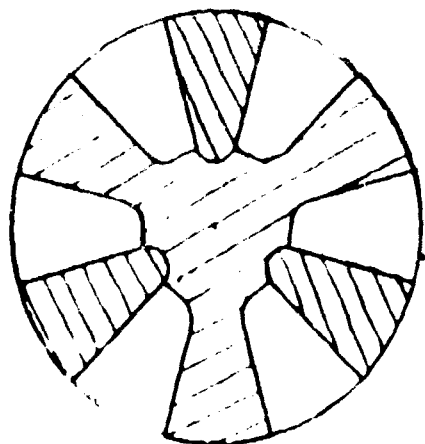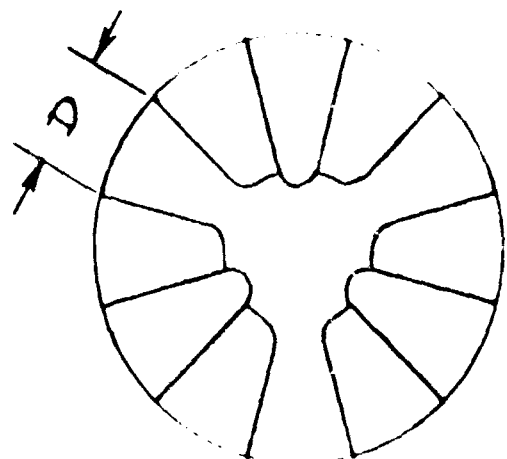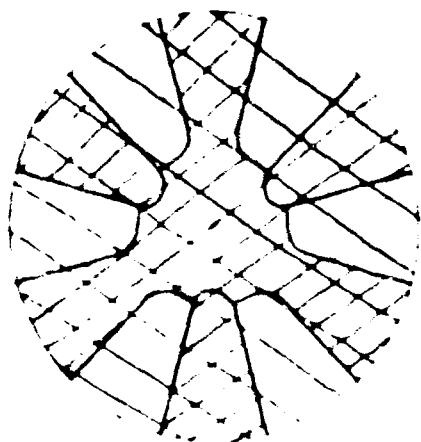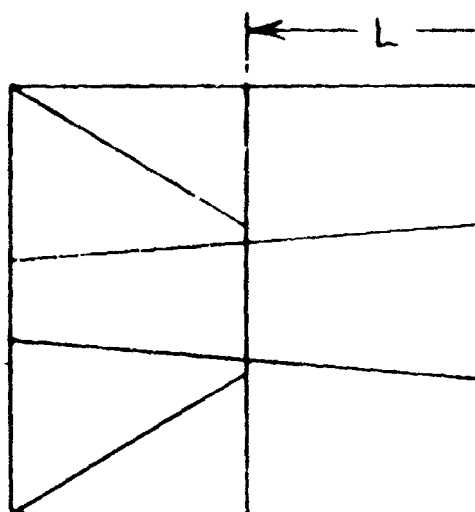Figure 1 shows the revised multi-lobed, staged mixing nozzle. The design was tested both with and without the points shown. Test results are shown in Figures 2, 3 and 4. The parameter V_E is an effective exit velocity obtained by dividing thrust by weight flow. V_E was not employed in previous nozzle comparisons because it requires a more accurate determination of these quantities than was heretofore possible on the model stand. C_D is a measure of nozzle capacity and C_T is basically an indication of efficiency in converting pressure to velocity head. The performance curves show neither version of the suppressor nozzle to be superior to the "daisy." However, the flat-topped spectrum of the multi-lobed, staged design, as compared to that of the "daisy", shows better suppression of the higher frequencies. This type of balanced spectrum is one of the basic goals of the present investigation. Because it did not appear that the concept was capable of significant development, it was not pursued further.

Figure 5 shows a staggered-lobe suppressor nozzle together with the reference circular nozzle and a typical 6-lobe "daisy" model. In the parametric studies, the parameters shown in Figure 6 were varied. The following is a list of pertinent nozzle values.

	Parameter*								
	Area Split			L/D			Density Ratio		
	35,65	45,55	55,45	2.5	4.5	6.5	1.8	2.0	2.2
Symbol	⌂	⌂	◇	+	⌂	◊	✕	⌂	⬡

*Illustrated in Figure 6.

The results of these studies are shown parametrically in the following groups of Figures: Area Split - Figures 7, 8, and 9; L/D - Figures 10, 11 and 12; and Density Ratio - Figures 13, 14, and 15. The fact that C_D and C_T values for the reference circular nozzle lie below those for most of the suppressor nozzles is not an indication that the latter are unusually efficient. The choice of a circular nozzle with a slower taper rate would have made the nozzles more nearly equivalent, both in length and in performance. Two general conclusions can be drawn from the results shown in these Figures.

a. Staggering the lobes of a "daisy" nozzle has no beneficial effect on noise suppression. On the contrary, when compared on an effective velocity basis, the increased wetted areas of staggered lobe nozzles diminish the suppression potential.

b. Staggered lobe nozzles have essentially the same directivity performance as "daisy" nozzles.

AREA SPLIT STUDY, STAGGERED LOBE NOZZLE

FIGURE 7

DIRECTIVITY

AREA SPLIT STUDY, STAGGERED LOBE NOZZLE

- 78 -

FIGURE 8

POWER SPECTRUM
AREA SPLIT STUDY STAGGERED LOBE NOZZLE

FIGURE 9

- 79 -

FIGURE 10

- 80 -

DIRECTIVITY
L/D STUDY, STAGGERED LOBE NOZZLE

Legend:
O — REFERENCE CIRCULAR
O — 6.5 L/D
O — 4.5 L/D
A — 2.5 L/D
◇ — "DAISY"

$V_E = 1275$ fps
$V_E = 1375$ fps

SOUND PRESSURE LEVEL
db re 0.0002 μb

FIGURE II

FIGURE 12

POWER SPECTRUM

L/D STUDY, STAGGERED LOBE NOZZLE

$V_E = 1375$ fps

Legend:

○ — REFERENCE CIRCULAR
◑ — 6.5 L/D
◇ — 4.5 L/D
⬦ — 2.5 L/D
⬧ — "DAISY"

SOUND POWER LEVEL IN BAND ~ dB re 10^{13} watt

FREQUENCY IN CYCLES PER SECOND

- 82 -

DENSITY RATIO STUDY, STAGGERED LOBE NOZZLE

FIGURE 13

FIGURE 14

DIRECTIVITY
DENSITY RATIO STUDY, STAGGERED LOBE NOZZLE

O — REFERENCE CIRCULAR
X — 1.8 DENSITY RATIO
△ — 2.0 DENSITY RATIO
▢ — 2.2 DENSITY RATIO
✧ — DAISY

SOUND PRESSURE LEVEL
db re 0.0002 μb

$V_E = 1275$ fps $\longleftarrow$ $\longrightarrow$ $V_E = 1275$ fps

POWER SPECTRUM

DENSITY RATIO STUDY, STAGGERED LOBE NOZZLE

FIGURE 15

- 58 -

a.

b.

c.

c. Staggered lobe nozzles produce frequency spectrums that are ... ss well balanced than those of "daisy" nozzles. The intent of staggering ha ... een to provide the rear efflux with a moving ambient, thereby reducing mixir ... noise at this point. It was reasoned that, then the only significant noise ... roducer would be the forward efflux, and if this could be made a small percer ... of the overall flow, the resultant noise would be greatly diminished. This ... tent was successful in that the low frequency generating portions of the forwe ... and rea - ward effluxes were better mixed and produced lower noise levels than ... e "daisy" However, the staggering had a deleterious effect on the velocity of t ... air in- duced between the lobes, resulting in greater high frequency noise ge ... ration by the forward efflux.

Future Plans

The studies conducted this year suggest that what is needed is a conf ... uration wherein ambient air is induced into the jet wake without encountering ... arge high-shear jet areas. Conceptually, this could be accomplished by pe ... pheral jets, either few in number or else closely spaced, joining to form an ... ero- dynamic ejector, as in the ring nozzle tested previously. Nozzles of ... is type might appear as shown at "b" and "c" in Figure 16.

A further possibility would be to subject the high frequency peak expe ... ienced with the staggered lobe nozzles to a further splitting, in the hope tl ... t, as before, a reduction in level would accompany the frequency shift. A t ... ree- stage ... le, as shown at "a" in Figure 16, might produce the desired ... esult.

It is customary in both Civil and Military service to ground-run-up je ... engines in aircraft prior to take-off. In order to lower the resultant noise ... levels acceptable to nearby airport and base personnel, ground suppressors ha ... been utilized. However, to date, no such suppressor has been entirely sati ... factory from the dual standpoints of suppression potential and serviceability. ... ecause it is this investigator's belief that the ground run-up suppressor des ... n pro- posed in the FY '64 annual report may well possess improved performanc ... in both these areas, it is proposed to test this concept in FY '66.

POLARIZATION STUDIES OF CORROSION IN NONCONDUCTING
MEDIUMS WHERE ELECTROLYTES EXIST IN A DISCONTINUOUS PHASE

L. J. NESTOR

Background

Fuels used in reciprocating and turbine engine aircraft will dissolve small amounts of water which will be thrown out of the fuel into the dispersed free state by lowering the temperature. For example, a highly aromatic fuel may throw out 3 gallons of water per 100,000 gallons of fuel when cooled from 75°F to 32°F.[1] This ever-present water results in corrosion problems during the production, transport, and storage of petroleum-based fuels. Such corrosion causes degradation of the ground handling facilities, as well as compromising the flight quality of the fuel.[2]

Fuel corrosion problems are combated by the judicious use of additives meeting the requirements of the specification on Fuel Soluble Corrosion Inhibitors, MIL-I-25017. The basic method of inhibitor evaluation is a modification of the ASTM Method D-665, Test for Rust Preventing Characteristics of Steam-Turbine Oil in the Presence of Water.[3] This method is essentially the exposure of a mild steel specimen to a simulated inhibited fuel in the presence of sea water, and visually noting the degree of protection afforded by the inhibitor. Such a subjective evaluation, however, provides only a gross estimate of the inhibiting characteristics of these additives. In addition to the visual interpretations, the analysis is subject to error resulting from the irregular distribution pattern of corrosion which is inherent in such a heterogeneous system; e.g. water dispersed in fuel.

Objectives

a.   Apply the principles of potentiostatic polarization to determine the basic behavior characteristics of oil-soluble corrosion inhibitors.

b.   Determine if these characteristics are typical of all oil-soluble inhibitors, or if they depend upon certain functional groups associated with molecular structure.

Accomplishments

a.   Prior to 30 June 1964

1.   A cell was designed specifically for the application of electrochemical techniques to electrically nonconducting solutions. In principle, it is the analog of actual fuel systems, where water exists in the discontinuous form of suspended droplets. The cell provides for the suspension of a metal
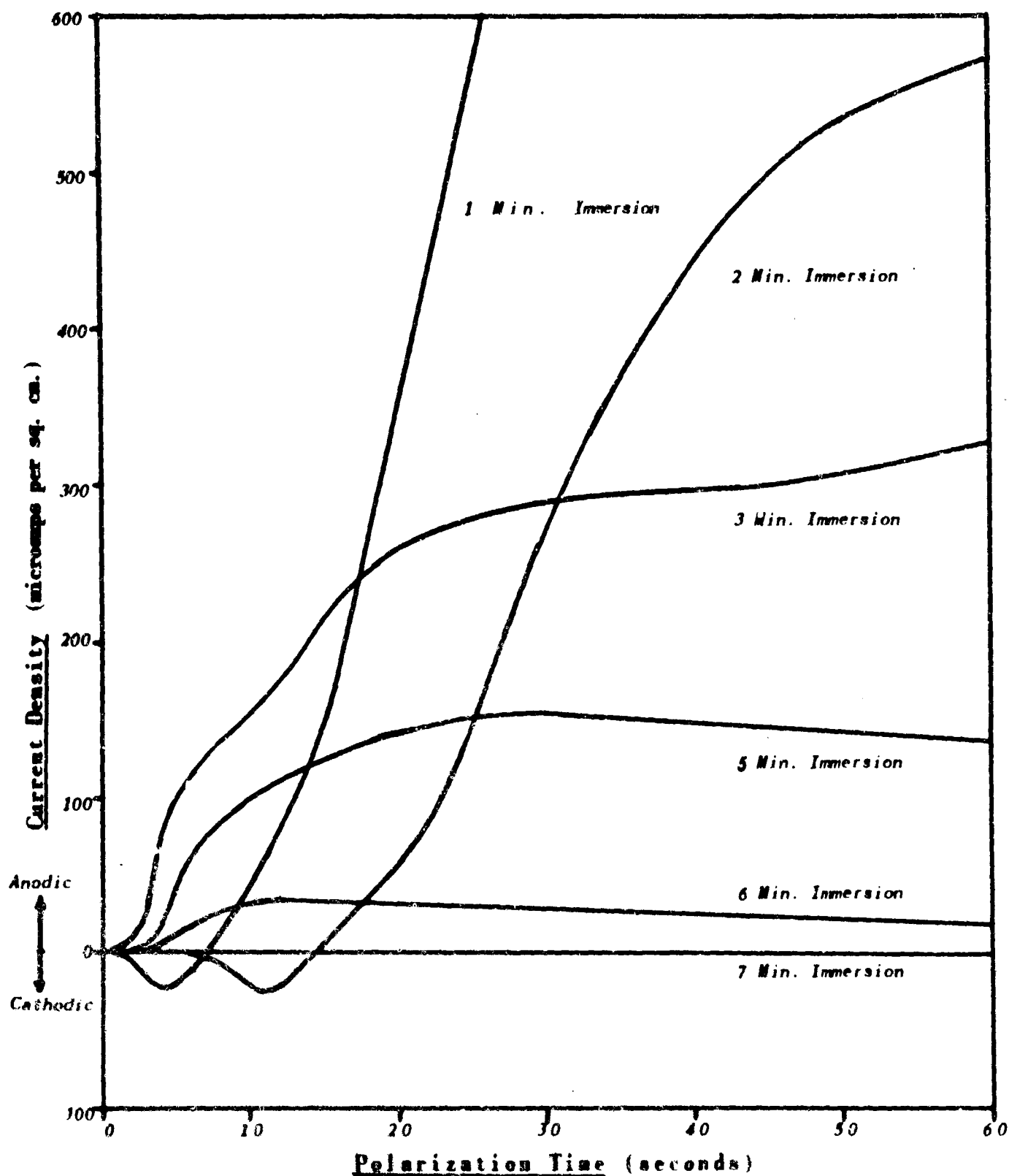
FIGURE 1 – CHARACTERISTIC POLARIZATION CURVES OBTAINED BY VARYING IMMERSION TIMES OF MILD STEEL IN 20 p.p.m. N-LAUROYL SARCOSINE PRIOR TO POLARIZATION AT 0.400 VOLTS(S.C.E.) WITH 0.1 N KCl

specimen (1020 Steel) in the simulated fuel. The corrosive electrolyte is made to impinge onto the metal surface under controlled conditions. By means of a potentiostat and recorder, the transient voltage/current density relationships are determined.

2. It was confirmed that the current measured was a function of the concentration of the oil-soluble inhibitor. By relating the total current versus inhibitor concentration, it was possible to obtain electrochemical data that agreed quite favorably with the minimum effective concentrations determined by the method specified in MIL-I-25017.

3. It was deduced from the experimental data, that the transient current density values obtained initially on contact of the metal specimen by the electrolyte were more strongly influenced by the desorption of the inhibitor than the electrochemical manifestations associated with the corrosion process. With the complications of concentration polarization and limiting diffusion currents reduced to a minimum, it was postulated that the current density measurements could be related to the areas of the metal surface that were free of adsorbed inhibitor.

b. <u>From 1 July 1964</u>

1. One of the major handicaps that plagued our previous experiments was the rather poor reproducibility of the current density measurements. After rather intensive study, the following modifications were made:

(a) Reduced the size of the cell and increased the size of the specimen.

(b) Introduced a specimen design change from multiple to single facet.

(c) Maintained electrode distances constant.

(d) Eliminated electrolyte flow, since this was creating a velocity gradient across the surface of the specimen.

These changes resulted in a significant improvement in repeatability.

2. One of the major benefits obtained from the previously listed modifications, was the capability of maintaining strict control of time in which the specimens were immersed in the simulated inhibited fuel, e.g. N-Lauroyl Sarcosine in Isooctane. By controlling immersion time, it was possible to expand the scope of the entire project. In Figure 1, characteristic curves are shown which depict the rate-controlling desorption of both the solvent and/or inhibitor. The 1-minute immersion time curve shown is typical of curves where no inhibitor is present, in spite of the fact that 20 ppm N-Lauroyl Sarcosine was in the solution. As the immersion time increased, the curves assumed the characteristic shape associated with a strongly adsorbed inhibitor film.

Potential: 0.400 Volts

Electrolyte: 0.1 N KCl

0 p.p.m. N.L.S.

5 p.p.m. N.L.S

10 p.p.m. N.L.S.

20 p.p.m. N.L.S
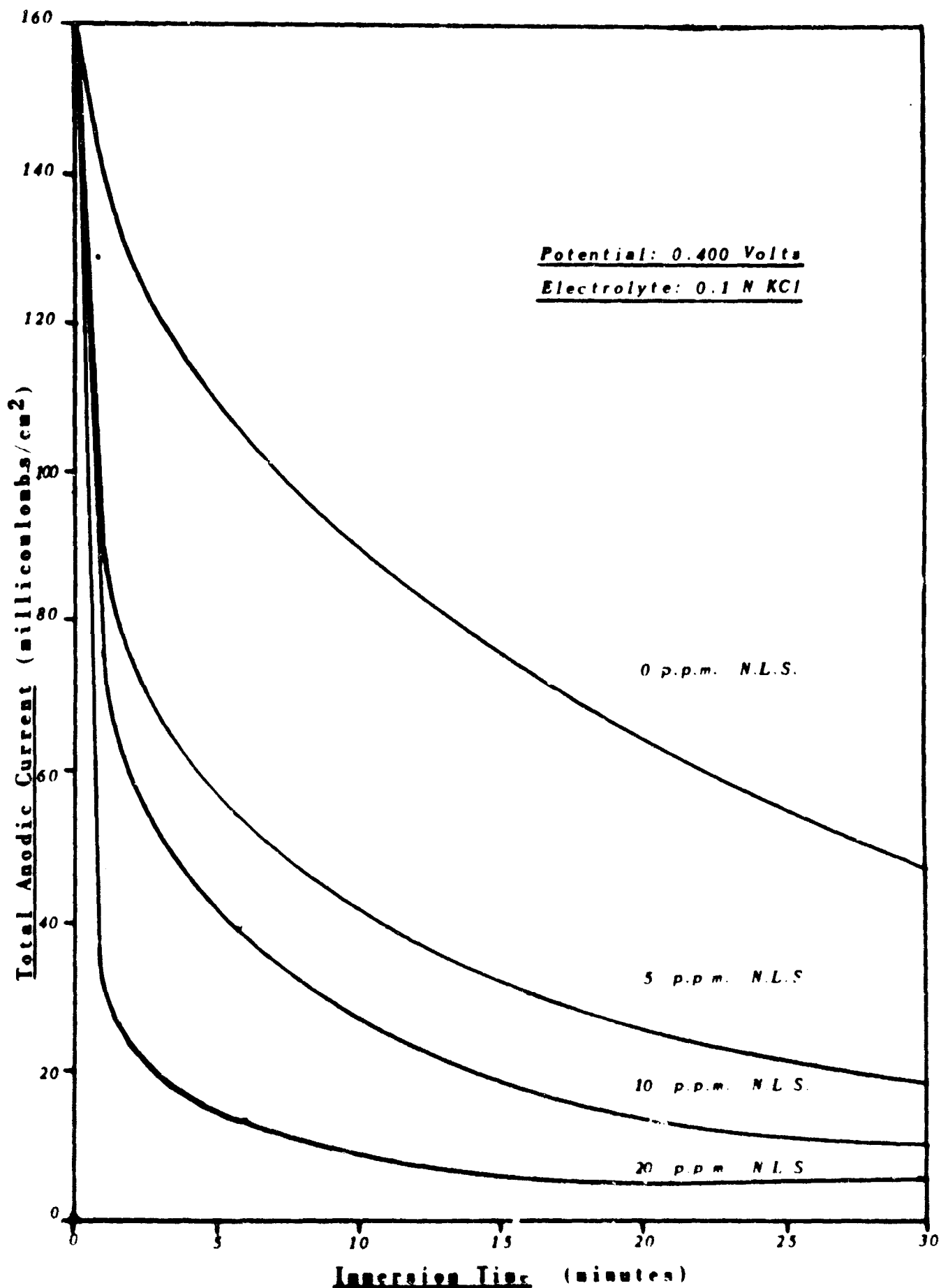
FIGURE 2 - CHANGE OF ANODIC CURRENT WITH VARYING IMMERSION TIMES OF HAND GROUND MILD STEEL IN N-LAUROYL SARCOSINE ISOOCTANE

Potential; 0.400 Volts
Electrolyte; 0.1 N KCl

0 p.p.m. N.L.S.

5 p.p.m N.L.S.

10 p.p.m. N.L.S.

20 p.p.m N.L.S.

Total Anodic Current (millicoulombs/cm^2)

Immersion Time (minutes)

FIGURE 3 – CHANGE OF ANODIC CURRENT WITH VARYING IMMERSION TIMES
OF ALUMINA BLASTED MILD STEEL IN N-LAUROYL SARCOSINE/ISOOCTANE
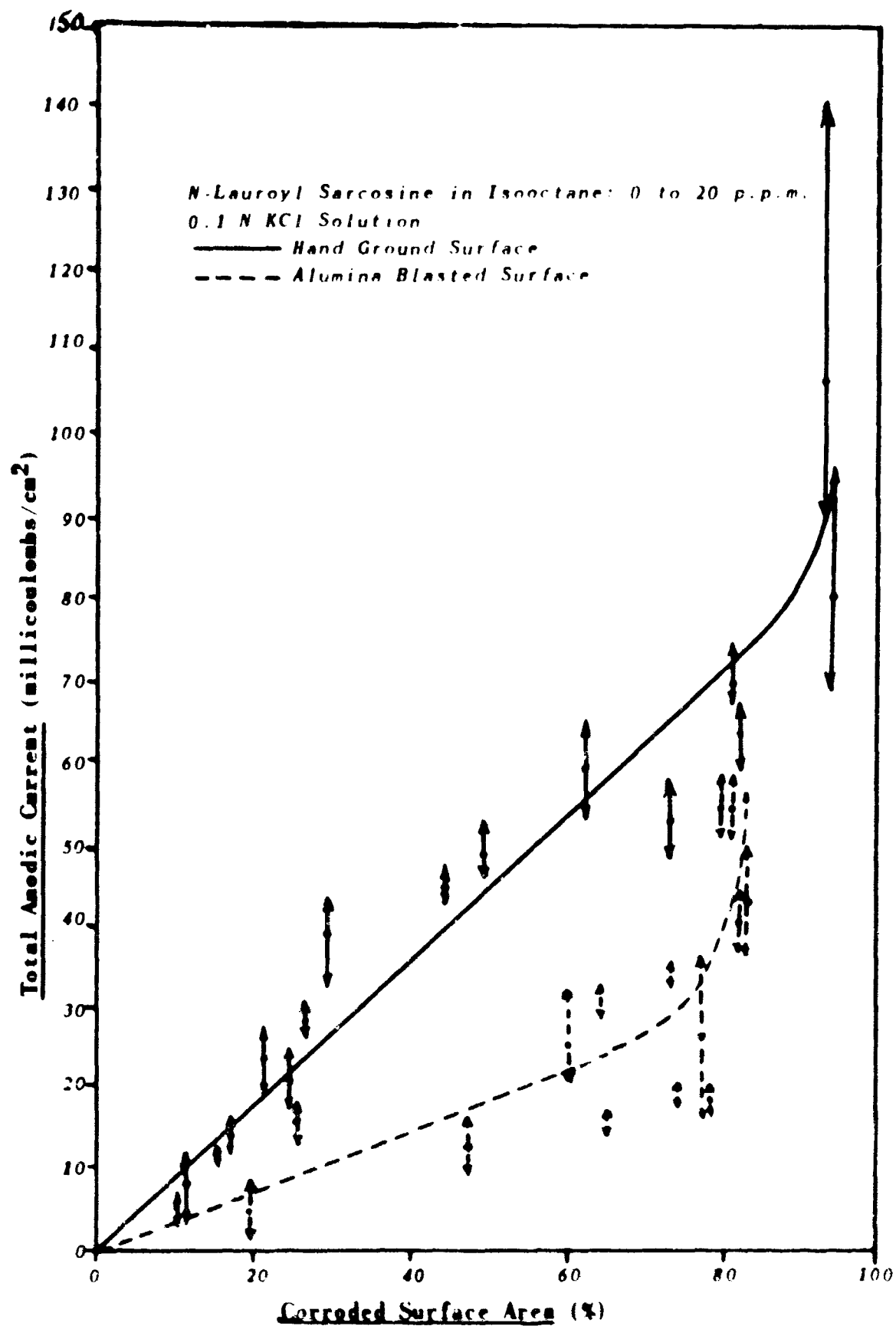
FIGURE 4 - CORRELATION OF TOTAL ANODIC CURRENT WITH MEASURED AREAS OF CORROSION ON MILD STEEL
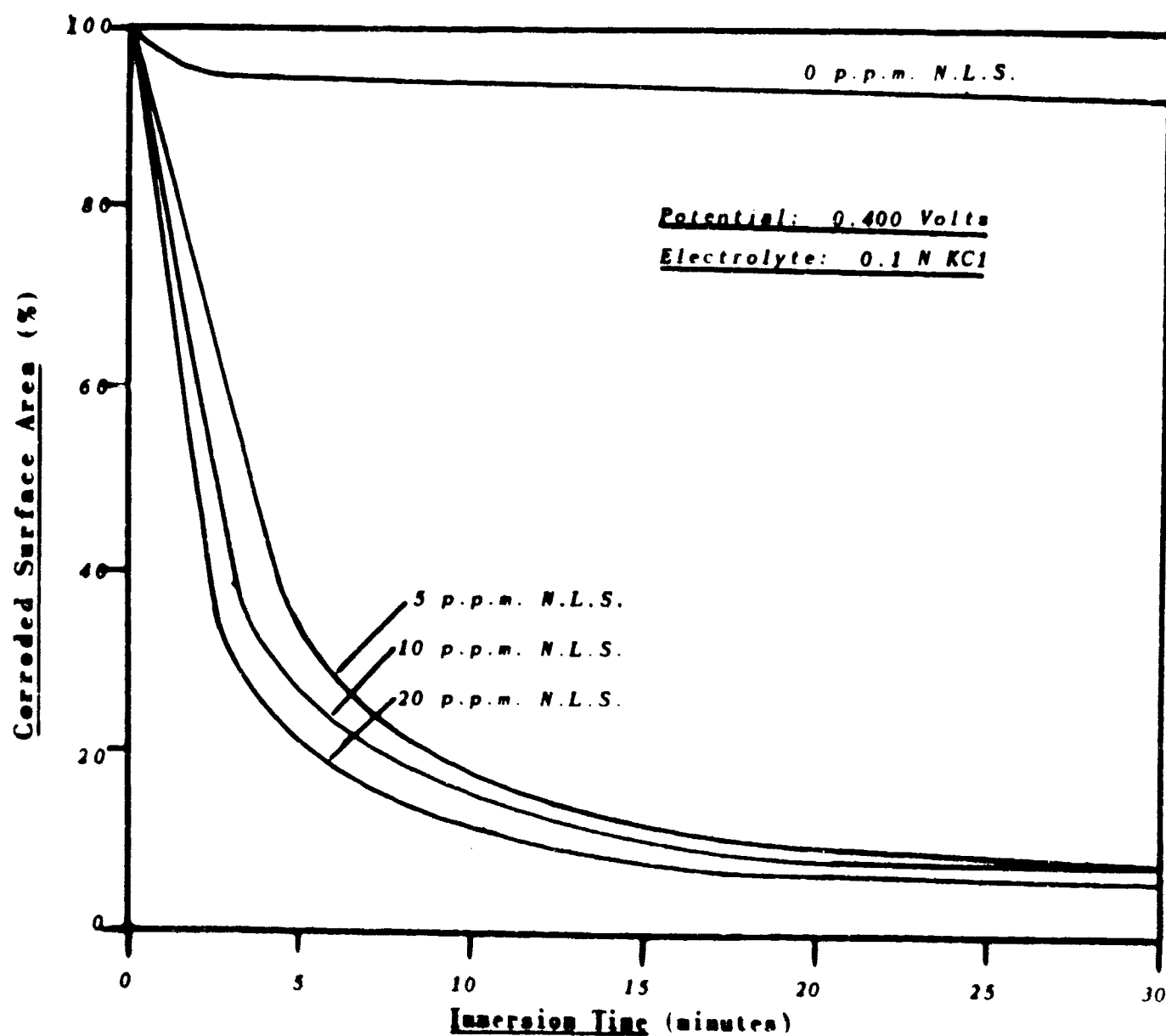
FIGURE 5 - CHANGE OF CORROSION AREAS WITH VARYING IMMERSION TIMES OF HAND GROUND MILD STEEL IN N-LAUROYL SARCOSINE/ISOOCTANE
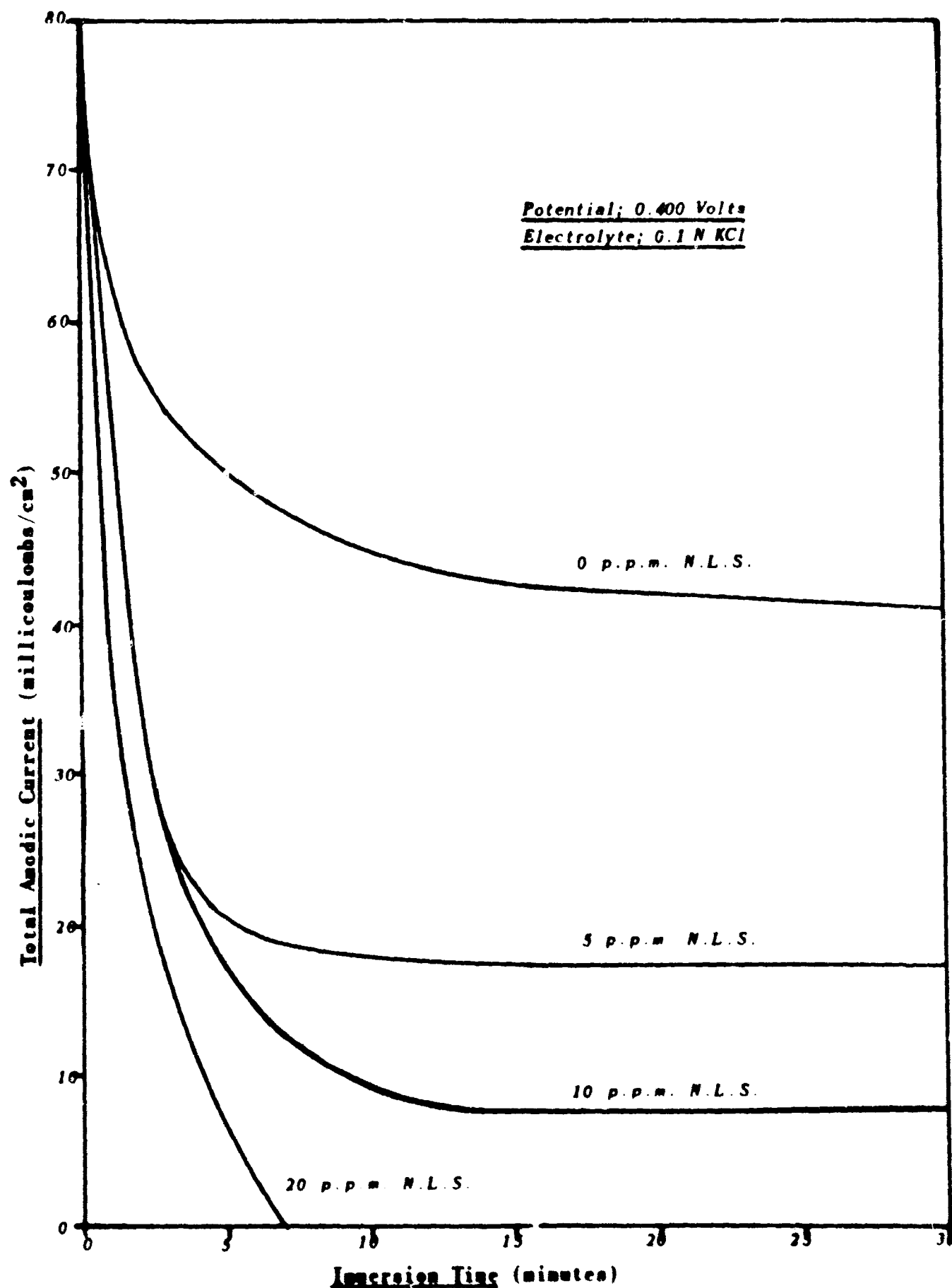
- 95 -
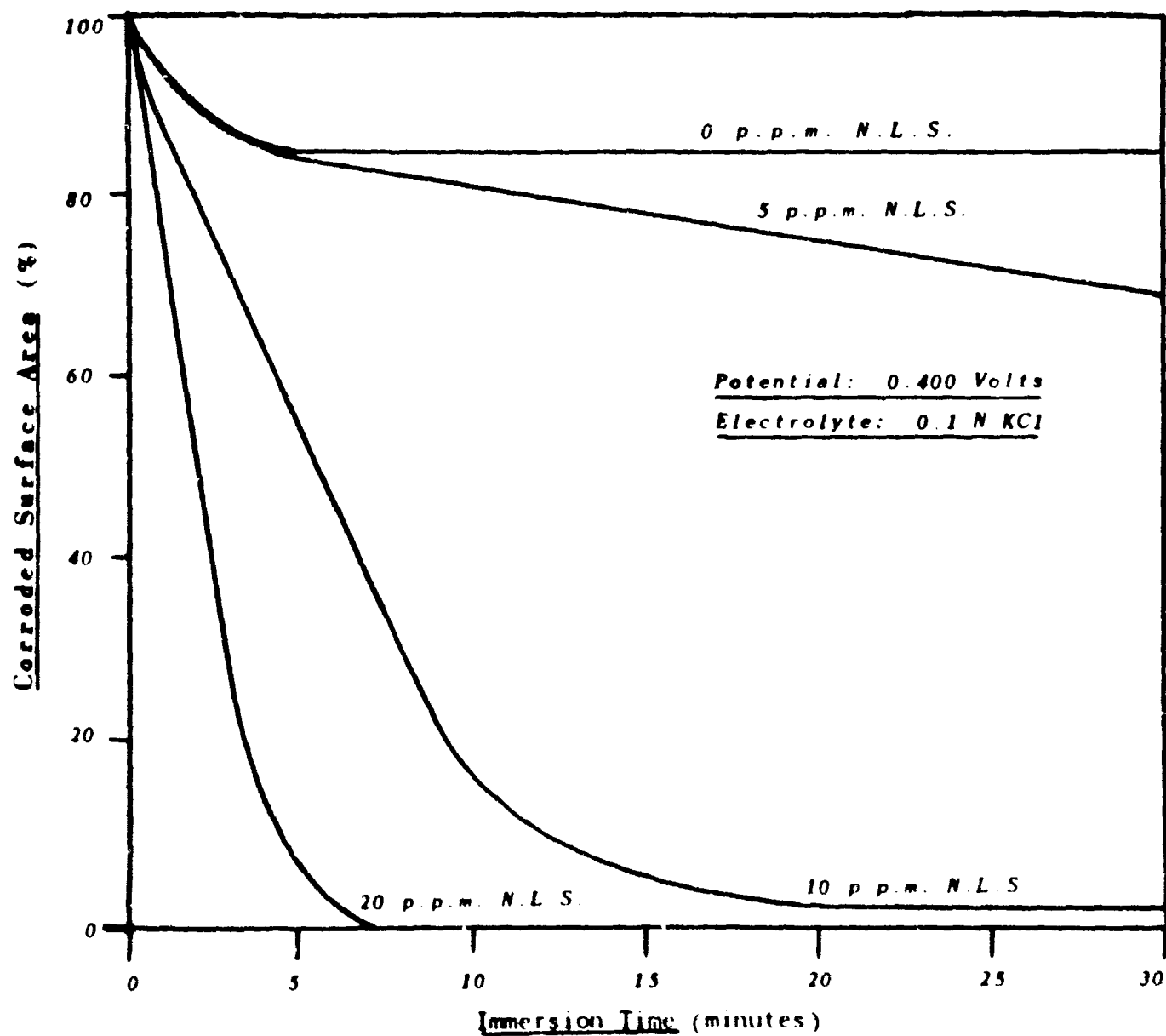
FIGURE 6 - CHANGE OF CORROSION AREAS WITH VARYING IMMERSION TIMES OF ALUMINA BLASTED MILD STEEL IN N-LAUROYL SARCOSINE/ISOOCTANE
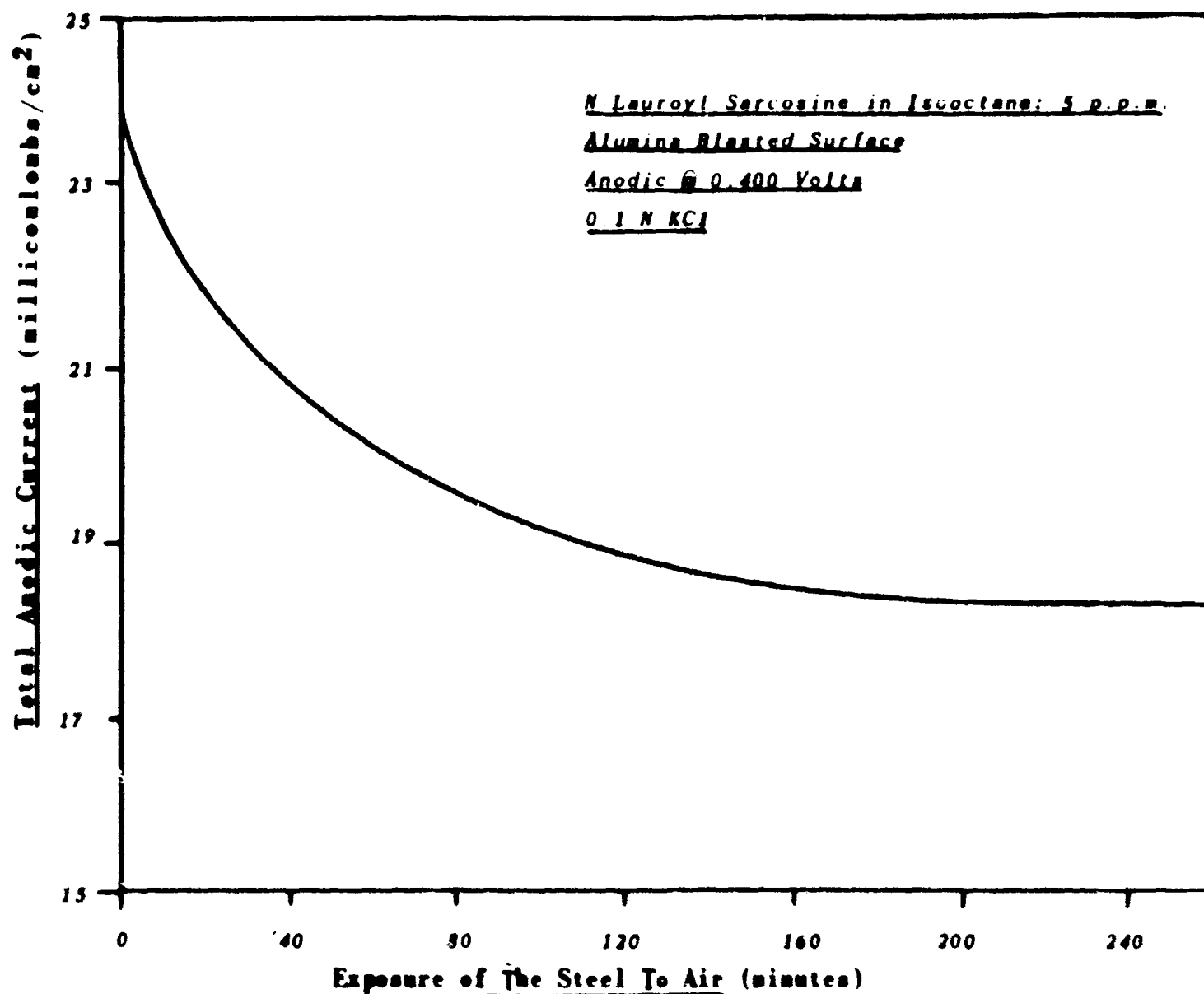
FIGURE 7 - THE EFFECT OF EXPOSURE OF MILD STEEL TO AIR WITH ITS RESULTANT OXIDE FORMATION ON ANODIC POLARIZATION

3   More detailed studies were then made, relating the surface adsorption of N-Lauroyl Sarcosine to immersion time, concentration of the inhibitor, as well as surface preparation of the steel specimen. These results are shown in Figures 2 and 3. The specimen surfaces investigated were designated "hand-ground" and "alumina blasted." The hand-ground specimens were rather rough in appearance, having been prepared by grinding with 2/0 Garnet paper. The alumina blasted specimens were prepared by metallographically polishing the steel to a mirror finish and then scrubbing the surface with 27 micron alumina particles in a high velocity nitrogen stream. It was necessary to scrub the surface with alumina to remove the adsorbed water introduced during the metallographic polishing. By comparing the 0 ppm curves in both Figures 2 and 3, it can be seen that the hand-ground specimen adsorbs isooctane more readily than the alumina-blasted surface. However, by comparing the 20 ppm curves, it becomes apparent that the alumina-blasted surface is the more active of the two to the inhibitor. It should also be noted from Figure 2, that for 20 ppm NLS, it requires 10 to 15 minutes for maximum adsorption to occur, with even longer equilibrium time for lower concentrations. This must necessarily cause us to modify our previous concept on equilibrium requirements, since investigators in the field generally agree that maximum adsorption occurs in the first few minutes.

4.   It was previously postulated that anodic current could be related to areas of the steel specimen lacking an adsorbed film. A partial confirmation of this theory was gained by permitting corrosion to develop on the specimen surface after the electrochemical polarization, then measuring the percent surface corrosion. These results are shown in Figure 4. By plotting observed percent surface corrosion against immersion times, shown in Figures 5 and 6, further evidence was obtained which tends to confirm the electrochemical data shown in Figures 2 and 3

5.   The effects of oxide formation on inhibitor adsorption were also investigated.   This was done by permitting the steel surface to be exposed to dry air for varying times before making polarization measurements. These results are shown in Figure 7, where it can be seen that oxide formation on steel is certainly compatible and synergistic with N-Lauroyl Sarcosine

Future Plans

a.   The nature of this study necessitated concentration of effort on one inhibitor - N-Lauroyl Sarcosine. Duplicate studies will be made on other types of inhibitors, such as the sulfonates, to see if they behave in similar fashion to the acylated sarcosines

b.   Certain further confirmation of the theory relating anodic current density to areas of adsorption. One promising technique is the copper displacement method.   This method is based upon the principle that copper will be displaced from a solution of soluble copper salts onto a steel surface which has no protective insulating adsorbed film.

References

(1)   Aviation Fuels and Their Effects on Engine Performance, NAVAER-   -501,
p. 44.

(2)   E.W. McKelvey, Ultrasonic Detection of Corrosion in Aircraft Fu   Tanks,
Research and Technology Briefs, USAF, Vol. III, No. 6, p. 21, J   1965.

(3)   ASTM Standards on Petroleum Products and Lubricants, ASTM, Phil . Pa.,
1964.

(4)   W.B. Hughes, Copper Ion Displacement Test for Screening Corrosi In-
hibitors, Journal of Petroleum Technology, pp. 54 - 56, June 19 .

(5)   U.L. Stromberg, Effect of Structural Change on the Inhibitor Ef tive-
ness of Amido Acids, Materials Protection, Vol. 4, No. 4, pp. 6(- 64,
April 1965.

ADVANCED POLYMER RESEARCH TO DEVELOP POLYMERS FOR USE IN COATINGS EXPOSED TO EXTREME ENVIRONMENTS

W. W. HOWERTON

Background.

The increased speeds of Navy and other military aircraft have made
it mandatory to develop coating polymers that will withstand high tem-
peratures and have other superior performance characteristics. As no
polymers were available, either commercially or from government research
contracts, to meet these advanced applications, a limited polymer re-
search program was initiated in October 1963 at the Aeronautical Materials
Laboratory to develop such polymers. As one requirement of this program,
an engineering oriented approach is being maintained so that promising
polymers may be put into production more quickly. Also, when possible,
commercially available chemical intermediates are being used.

Work continues to be concentrated primarily on aromatic type struc-
tures for outstanding heat resistance, and more particularly with Bis-
phenol A type polyphenyl ester polymers. To date, modifications of this
type polymer appear to hold the most promise of meeting the many neces-
sary requirements of a high temperature coating polymer.

Objectives.

The principal objectives are as follows:

a. Development of a simple interfacial polymerization process that
consistently will produce the required high molecular weight polymers in
the minimum amount of time.

b. The immediate polymer target is the development of a high tem-
perature resistant coating polymer with the following characteristics:

(1) Ready solubility in relatively non-toxic paint solvents,
such as aromatics and ketones, and capable, after spray-application, of
being usable in a maximum of three days and preferably in one day of am-
bient temperature air drying.

(2) Solutions must be of low viscosity for high solids buildup
during spray application.

(3) Resistance to jet fuels and hot jet lubes (2 hrs. at 250°F)

(4) High temperature resistance to 500°F.

(5) High glass transition temperature (negligible softening at 500°F).

(6) Low temperature resistance to -65°F.

(7) Toughness and abrasion resistance.

(8) Fatigue resistance (non-cracking in fastener areas of aircraft).

(9) Weathering resistance:

    (a) Ultraviolet resistance.

    (b) Moisture and hydrolysis resistance.

    (c) Craze resistance.

(10) Formulated paints should have good package stability for 1 year at 90° - 100°F.

(11) Coatings after application should be glossy.

(12) Good adhesion.

c. Development of a polymer for coatings that is capable of service in the 1000°F range. This coating may be baked to develop optimum properties.

d. A long range target is to develop a series of stable-structure monomers from which stable polymers can be rather quickly made to meet almost any required application, including other than coatings.

Accomplishments.

During the past year, additional process development has been directed to a further improvement of the interfacial polymerization method being utilized in the synthesis of high temperature coating polymers. This has resulted in two primary benefits:

1. Polymerization cycles have been reduced from 3 hours to 15 minutes, giving a greatly increased utilization of personnel and equipment.

2. Molecular weights of polymers have been increased, resulting in a marked improvement in elongation and resistance to crazing, both of which are very necessary for a good coating polymer.

Relative to Bisphenol A type polyphenyl ester coating polymers, a breakthrough has been obtained in high temperature performance, from 500°F to 750°F, by thermal cross-linking. In practice this reaction should occur naturally during aircraft operation at higher speeds, as skin temperatures increase.

New high molecular weight Fluoro-Bisphenol A (Hexafluoroacetone Bisphenol A) polyphenyl ester polymers have been developed which exhibit greatly improved resistance to discoloration at elevated temperature.

A summary describing important phases of the coating polymer research and development work is given below.

a. Interfacial Polymerization.

The resin kettle used for earlier interfacial polymerization has been replaced by a Waring Blender unit. This has resulted primarily in decreased polymerization time, from approximately 3 hours to 15 minutes, and has made possible more efficient utilization of personnel and equipment.

High molecular weight polymers are now more consistently obtained from stoichiometric quantities of reactants in the two immiscible liquid phases. This has been accomplished primarily by using approximately equal volumes of the two liquid phases and also by operating the Blender for a sufficient period of time (15 minutes for the 1 gallon Blender) to exhaust the reactants completely. It has been noted in practice that this has occurred when the pH of the aqueous phase is between approximately 7 and 8.

b. Solubility.

In order for a coating polymer to be used easily, it must be readily soluble in relatively non-toxic usable paint solvents, such as aromatics, ketones, and etc. Until recently, almost all Bisphenol A polyphenyl composition modifications were not sufficiently soluble in paint solvents. Those that gave indication of good solubility in solvents, such as toluene, would usually gell in one to two weeks at higher solids (20%) concentration. This may be seen by an examination of various compositions in Figure 1. It will be noted that all of the polymers are soluble in tetrachloroethane (TCE), but this solvent is highly toxic and was used only to cast films for Instron and other tests.

We have recently developed polymers containing Hexafluoroacetone Bisphenol A (6FK-BPA) with a higher ratio of Isophthalic/Terephthalic (70/30) than the 50/50 used formerly. These have improved solubility particularly in toluene, as may be seen in Figure 1, Runs H-160-2 and H-166. Also, solution viscosities are lower, which allows higher solids build-up during spray application of coatings. These polymers, being thermoplastic, are ready for use as soon as the solvent evaporates.

SOLUBILITIES - BISPHENOL A TYPE POLYPHENYL ESTER POLYMERS

Molal % Composition		Run No.	20% Solution TCE(1)	20% Solution Toluene	Remarks
5 5 40 35 15	Piperazine Bisphenol A 6FK-BPA(2) Isophthaloyl Terephthaloyl	H-167	Soluble and clear	Not completely soluble	None
5 45 35 15	BPA(3) 6FK-BPA Isophthaloyl Terephthaloyl	H-166	Soluble and clear	Soluble and clear	Viscosity of both solutions moderately low
5 45 15 35	BPA 6FK-BPA Isophthaloyl Terephthaloyl	H-162	Soluble and clear	Gelled	None
50 35 15	6FK-BPA Isophthaloyl Terephthaloyl	H-160-2	Soluble and clear	Soluble and clear	Viscosity both solutions moderately low; tough polymer
50 15 35	6FK-BPA Isophthaloyl Terephthaloyl	H-160-1	Soluble and clear	Gelled in 4 days	None
50 10 40	6FK-BPA Isophthaloyl Terephthaloyl	H-160	Not completely soluble	Gelled in 4 days	None
5 45 25 25	BPA 6FK-BPA Isophthaloyl Terephthaloyl	H-158	Soluble, clear, and viscous	Initially soluble, clear, and viscous	After 1 week haze developing in toluene solution

FIGURE 1
PAGE 1 OF 2 PAGES
-104-

SOLUBILITIES - BISPHENOL A TYPE POLYPHENYL ESTER POLYMERS
(Continued)

Molal % Composition		Run No.	20% Solution TCE(1)	20% Solution Toluene	Remarks
50	6FK-BPA	H-157-2	Soluble, clear, and viscous	Slowly gelled in toluene	A 90/10 solution Tol./TCE. originally clear, but slowly gelled in 3 days
25	Isophthaloyl				
25	Terephthaloyl				
10	BPA	H-136	Soluble, clear, but fairly heavy viscosity	Slowly gelled in toluene	None
40	6FK-BPA				
25	Isophthaloyl				
25	Terephthaloyl				
50	6FK-BPA	H-130	Clear and soluble, low viscosity	Slowly gelled	None
25	Isophthaloyl				
25	Terephthaloyl				

(1) Tetrachloroethane solvent

(2) Hexafluoroacetone Bisphenol A, high purity, Allied Chemical Corporation

(3) Bisphenol A, high purity, General Electric Company

FIGURE 1
PAGE 2 OF 2 PAGES
-105-

JET LUBE AND JET FUEL TESTS ON BISPHENOL A TYPE POLYPHENYL ESTER FILMS

Molal % Composition	Run No.	Jet Lubes				Jet Fuels	
		MIL-L-7808		MIL-L-23699		JP-4	JP-5
		48 Hr.-R.T.(1)	2 Hr.-250°F	48 Hr.-R.T.	2 Hr.-250°F	R.T.(1)	R.T.
50 Bisphenol A 25 Isophthaloyl 25 Terephthaloyl	H-150-(3-6)	No change	Slight crazing but film strong	No change	No change	No change	No change
25 Piperazine 25 Bisphenol A 25 Isophthaloyl 25 Terephthaloyl	H-155-1	No change	No change	No change	No change	No change	No change
10 Bisphenol A 40 6FK-BPA(2) 25 Isophthaloyl 25 Terephthaloyl	H-151	No change	Film partly dissolved	No change	Film partly dissolved	No change	No change
50 6FK-BPA 25 Isophthaloyl 25 Terephthaloyl	H-138	No change	Film partly dissolved	No change	Film partly dissolved	No change	No change
5 Bisphenol A 45 6FK-BPA 25 Isophthaloyl 25 Terephthaloyl	H-158	No change	Film partly dissolved	No change	Film attacked but not dissolved	No change	No change
50 6FK-BPA 35 Isophthaloyl 15 Terephthaloyl	H-160-2	No change	Film partly dissolved	No change	Film partly dissolved	No change	No change
5 Bisphenol A 45 6FK-BPA 35 Isophthaloyl 15 Terephthaloyl	H-166	No change	Film partly dissolved	No change	Film somewhat attacked but not dissolved	No change	No change

FIGURE 2
PAGE 1 OF 2 PAGES

-106-

JET LUBE AND JET FUEL TESTS ON BISPHENOL A TYPE POLYPHENYL ESTER FILMS

Molal % Composition	Run No.	Jet Lubes				Jet Fuels	
		MIL-L-7808		MIL-L-23699		JP-4	JP-5
		48 Hr.-R.T.(1)	2 Hr.-250°F	48 Hr.-R.T.	2 Hr.-250°F	R.T.(1)	R.T.
5 Piperazine	H-167	No change	Film at-tacked but not dis-solved	No change	Film at-tacked some but not dissolved	No change	No change
5 Bisphenol A							
40 6FK-BPA							
35 Isophthaloyl							
15 Terephthaloyl							

(1) Room Temperature

(2) Hexafluoroacetone Bisphenol A, Allied Chemical Corporation

FIGURE 2
PAGE 2 OF 2 PAGES

-107-
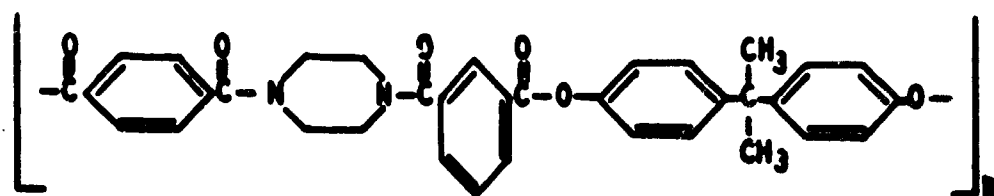
PIPERAZINE — BISPHENOL A POLYPHENYL ESTER POLYMER
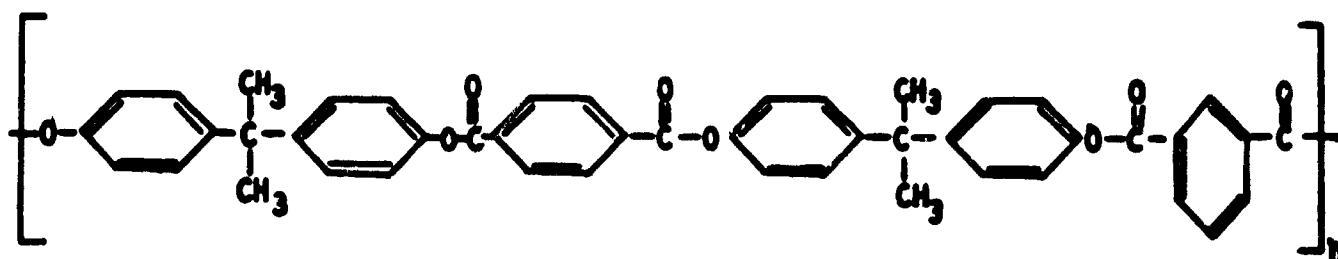
FIGURE 3

BISPHENOL A — POLYPHENYL ESTER POLYMER

FIGURE 4
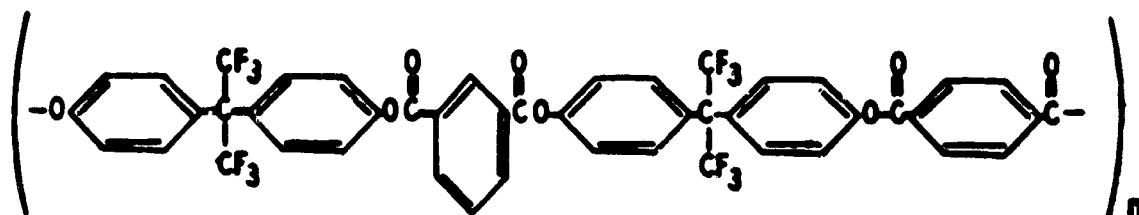
POLYPHENYL ESTER POLYMER WITH BISPHENOL A CONTAINING FLUORO DIMETHYL GROUPS.

FIGURE 5
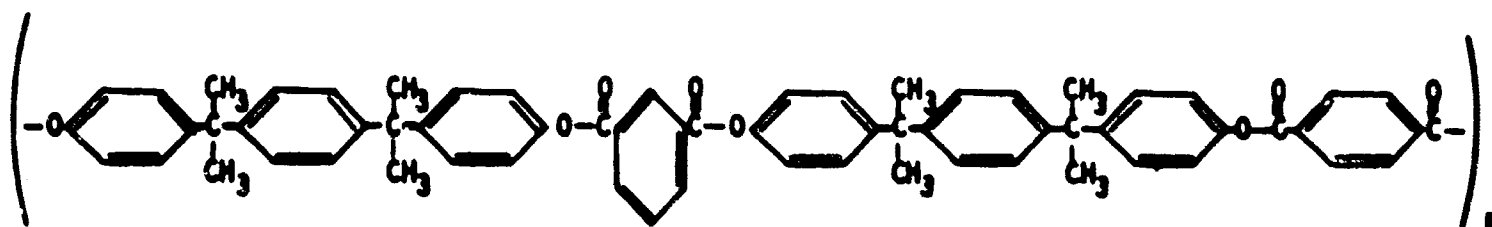
DICUMYL PHENOL POLYPHENYL ESTER POLYMER

FIGURE 6

-108-

c. Jet Lube and Jet Fuel Resistance.

Aircraft coatings must be unaffected by jet lubes and jet fuels, particularly at ambient temperatures. It is desirable that the coatings also resist jet lubes at somewhat elevated temperatures, since leakage or spillage of jet lubes onto aircraft surfaces may occur at times, and with aircraft operating at high speeds, surface temperatures will be somewhat elevated. An exposure of films or coatings to two hours in jet lubes at 250°F has been used as a screening test in an attempt to simulate such conditions. Tests on seven Bisphenol A type polyphenyl ester polymer compositions have been made in jet lubes and fuels at room temperature and also at the elevated temperature (250°F) in jet lubes. Results are given in Figure 2. It will be seen that all polymers resisted any harmful effects at room temperature. At the elevated jet lube temperature, a newly developed polymer containing Piperazine (Run H-155-1) gave best results. The structure of this polymer is shown in Figure 3. It is presently being evaluated for other characteristics. In Figure 2, it will also be seen that the standard Bisphenol A polyphenyl ester polymer (Run H-150-(3-6)) also gave good results in the tests, although there was some slight surface crazing in the MIL-L-7808 jet lube at 250°F.

The fluoro containing polymers, for example, Runs H-138, H-160-2, and H-166 in Figure 2 have not been satisfactory to date in the hot jet lube test. These types of polymers have excellent heat resistance and good solubility in toluene and efforts are being made to improve their hot jet lube resistance. Run H-167 is an illustration in which the addition of a small amount of Piperazine into the structure of the polymer has given some improvement in the lube resistance.

d. High Temperature Resistance.

Comparative heat tests have been run on several promising polyphenyl ester polymers which were synthesized, including the earlier standard one containing Bisphenol A (Run No. 128), whose structure is shown in Figure 4. Included also were polymers containing Fluorodimethyl Bisphenol A (Hexafluoroacetone Bisphenol A) as illustrated by the structural formula in Figure 5 (Run No. 130); polymers containing Dicumyl Phenol as shown in Figure 6 (Run 132); polymers containing P,P'-Biphenol (Run 133) instead of the Bisphenol A shown in Figure 4; and polymers containing Tetrafluorodichloroacetone Bisphenol A (Run No. 135) instead of the Hexafluoroacetone Bisphenol A shown in Figure 5.

For the heat tests, 1 mil clear coatings of the polymers were flow-coated onto 3" x 6" anodized 2024 aluminum panels and allowed to dry. Panels of the various polymer coatings were then subjected to heat cycles in an air-circulating oven for 1 hour each at 600°, 700°, and 800°F, for a total exposure of 3 hours. Photographs were taken of the panels after each hour of exposure to record any color development or other changes which occurred.

FLUORO SERIES

Run No.	Molal % Composition				Remarks
	Bisphenol A[1]	6FK-BPA[2]	Isophthaloyl Chloride	Terephthaloyl Chloride	
128	50	--	25	25	Control
127	40	10	25	25	None
131	30	20	25	25	None
136	10	40	25	25	None
130	--	50	25	25	None

(1) Bisphenol A, high purity, General Electric Company

(2) Hexafluoroacetone Bisphenol A, high purity, Allied Chemical Corporation

FIGURE

- . . -

Composition of the specific polymers tested in the fluorine-co   ining
series of polyphenyl ester polymers is shown in Figure 7. Polymers con   ning
only moderate amounts of Fluoro-Bisphenol A (6FK-BPA) (Runs 1 7 and 131
respectively) did not ag better than the control (Run 128) which conta   i no
fluorine. Those that contained major amounts, or all Fluoro-Bisphenol
(Runs 136 and 130), aged significantly better than the o   r panels in
series. Although not shown in this report, these panels were also aged
900°F for 1 hour. At this temperature all coatings completely evaporat
except for panel in Run 136 on which approximately one-third of a parti   nin
coating still remained. All coatings thr gh 800°F cy   remained as i   gral
and continuous coatings and panels could be bent over ne-quarter inch   -
drels without cracking. It was also observed during this   at test tha
coatings had become thermally cross-linked and were highly resistant to   -
effects of powerful solvents for these type polymers, such as tetrachlo   thane.
The cross-linking mechanism is being investigated further.

Composition of specific polymers tested in the Dicumyl Phenol   ies
is shown in Figure 8. Run 132 contains the maximum amount of Dicumyl P   ol;
i.e., 50 molal percent, or 100% of the dihydroxy intermediate. A compa   n
of panels of Run 132 with standard Bisphenol A - polyphenyl ester (Run
after the 700°F heat test for one hour showed that No. 128 darkens less   an
No. 132. It is believed that the differe   in this particular case ma   ave
been due to some impurity in the Dicumyl Phenol (No. 152) since it was   wn
that the purity was somewhat less than the No. 128 Bisphenol A which is   gnly
purified. A comparison of these two runs after the 800°F - 1 hour test   owed
that the No. 152 had almost completely disappeared from the panel. Thi   as
apparently caused by the very highly thermally cross-linked coating. T   ross-
linking apparently occurs through the -CH₃ groups, and since there is a   n
higher proportion of these in the Dicumyl Phenol intermediate in the No
polymer than in the Bisphenol A intermediate in No. 1 8 polymer, the cr   -
linking density is much greater, rendering it brittle. In No. 14, as
te expected since it contains some of the more stable 6FK-BPA hexa-
fluoroacetone Bisphenol A), the panels more nearly approach No. 130 in
aging characteristics, since this polymer contains the maximum amount o
6FK-BPA.

In the Biphenol series (Figure), No. 113 containing % mola
biphenol and 5% 6FK-BPA was almost as stable in the heat tests as No.
containing the maximum amount of the 6FK-BPA. No. 1 is, of course, t
standard bisphenol A polyphenyl ester polymer control. Polymers contai
the Biphenol were less soluble than those with 6FK-BPA, and additional
polymers will be made with combinations of these two intermediates in a
attempt to get better balance between get lube resistance of polymers a
solubility in common non-toxic paint solvents, as follows.

DICUMYL PHENOL SERIES

Run No.	Molal % Composition					Remarks
	Bisphenol A [1]	Dicumyl Phenol [2]	6FK-BPA [3]	Isophthaloyl Chloride	Terephthaloyl Chloride	
128	50	--	--	25	25	Control
132	--	50	--	25	25	None
134	--	25	25	25	25	None
130	--	--	50	25	25	Control

(1) High purity, General Electric Company

(2) Reasonably high purity, Allied Chemical Corporation

(3) Hexafluoroacetone Bisphenol A, high purity, Allied Chemical Corporation

FIGURE 8

BIPHENOL SERIES

Run No.	BPA[1]	6FF-BPA[2]	Biphenol[3]	Isophthaloyl Chloride[4]	Terephthaloyl Chloride[4]	Remarks
			Molal % Composition			
128	50	--	--	25	25	Control
133	--	25	25	25	25	None
130	--	50	--	25	25	Control

(1) Bisphenol A, high purity, General Electric Company

(2) Hexafluoroacetone Bisphenol A, high purity, Allied Chemical Corporation

(3) P, P' - Biphenol, high purity, Eastman

(4) Isophthaloyl and Terephthaloyl Chloride, high purity, Hooker Chemical Company

FIGURE 9

Polymers were also made containing some chlorine (Run 135, Figure 10) as a partial replacement of some of the fluorine in the 6FK-BPA. Although the heat stability was better than the control with Bisphenol A, Run No. 128, it was not as good as No. 130 with the maximum amount of 6FK-BPA.

The General series gave a relative heat stability comparison of the various groups of polymers discussed above after exposure of one hour each at 600°, 700°, and 800°F for a total exposure of 3 hours. Two panels which contained predominant amounts of the Fluorodimethyl Bisphenol A (6FK-BPA) were superior to all of the other panels in heat resistance.

e. Low Temperature Resistance.

All of the polymers produced have had good low temperature resistance. Films of the most outstanding ones were made and subjected to -65°F exposure, Figure 11. All remained quite flexible at this temperature.

f. Weather Resistance.

Earlier titanium dioxide pigmented standard Bisphenol A polyphenyl ester polymer coatings which were exposed to four months of Florida weathering, exhibited chalking on the surface in much the same manner as epoxy coatings. A close examination of the coating beneath this chalk showed fine cracks and checking. This was also true of the area of the coated panel under the clamps, not exposed to direct sunlight but exposed to the other weathering elements. It thus appeared that moisture was definitely a factor in the aging of these titanium dioxide pigmented polymers, and was probably causing hydrolysis of the ester groups in the polymer structure. Efforts were then made to evaluate and develop polymers of this type with maximum water resistance and maximum resistance to the effects of moisture. A test was set up in which 1 mil clear coatings of polymers of the Bisphenol A type polyphenyl ester polymer on 3" x 5" anodized 2024 aluminum panels were half submerged in water for periods of two or three months to observe any changes that might occur. Results of tests are shown in Figure 12. In general, all of the polymers performed well in this test with the exception of Run H-134 containing 25 mole percent of Dicumyl Phenol. This poor result is believed due to the fairly low molecular weight polymer in this case since the polymer containing 50 mole percent Dicumyl Phenol (Run H-132) resisted any effects of the water test. The 50 mole percent Fluorodimethyl Bisphenol A (6FK-BPA) polymer of Run H-130 had a small amount of crazing but the H-136 polymer containing only 40 mole percent 6FK-BPA did not. The earlier heat aging tests showed H-136 to age as well as H-130, so from these tests it appears that H-136 is a slightly better polymer than H-130 for the coating application.

CHLOROFLUORO SERIES

| Run No. | Molal % Composition | | | | | Remarks |
	BPA[1]	4FK-BPA[2]	6FK-BPA[3]	Isophthaloyl Chloride[4]	Terephthaloyl Chloride[4]	
128	50	- -	- -	25	25	Control
135	- -	50	- -	25	25	None
130	- -	- -	50	25	25	Control

(1) Bisphenol A, high purity, General Electric Company

(2) Tetrafluorodichloroacetone Bisphenol A, high purity, Allied Chemical Corp.

(3) Hexafluoroacetone Bisphenol A, high purity, Allied Chemical Corp.

(4) Isophthaloyl and Terephthaloyl Chloride, high purity, Hooker Chemical Corp.

FIGURE 10

LOW TEMPERATURE TESTS ON
BISPHENOL A TYPE POLYPHENYL ESTER FREE FILMS
AT - 65°C

Molal % Composition	Run No.	Remarks
50 6FK-BPA[1]	H-138	Passed - flexible
25 Isophthaloyl[2]	H-130	Passed - flexible
25 Terephthaloyl[3]	H-142	Passed - flexible
40 6FK-BPA	H-151-1	Passed - flexible
10 BPA[4]		
25 Isophthaloyl		
25 Terephthaloyl		
25 BPA	H-155-1	Passed - flexible
25 Piperazine[5]	H-155-2	Passed - flexible
25 Isophthaloyl	H-155-3	Passed - flexible
25 Terephthaloyl	H-155-5	Passed - flexible
50 BPA	H-150-(3-6)	Passed - flexible
25 Isophthaloyl	H-156	Passed - flexible
25 Terephthaloyl		

(1) Hexafluoroacetone Bisphenol A, high purity, Allied Chemical Corp.

(2),(3) Isophthaloyl and terephthaloyl chloride, high purity, Hooker
         Chemical Corp.

(4) Bisphenol A, high purity, General Electric Company

(5) Piperazine, high purity, Jefferson Chemical Company

FIGURE 11

WATER TEST OF 1 MIL CLEAR BISPHENOL A TYPE POLYPHENYL ESTER COATINGS ON NON-CLAD ANODIZED ALUMINUM PANELS

Molal % Composition	Run No.	Date Start	Date Finished	Remarks
50 Bisphenol A 25 Isophthaloyl 25 Terephthaloyl	H-128	3/1/65	5/25/65	No crazing or other effects
50 6FK-BPA (1) 25 Isophthaloyl 25 Terephthaloyl	H-130	2/15/65	5/25/65	Slight crazing at water-vapor interface
10 Bisphenol A 40 6FK-BPA 25 Isophthaloyl 25 Terephthaloyl	H-136	3/1/65	5/25/65	No crazing or other effects
50 4FK-BPA (2) 25 Isophthaloyl 25 Terephthaloyl	H-135	2/15/65	5/25/65	No crazing or other effects
50 Dicumyl Phenol 25 Isophthaloyl 25 Terephthaloyl	H-132	3/1/65	5/27/65	No crazing or other effects. High mol. wt. polymer
25 Bisphenol A 25 Dicumyl Phenol 25 Isophthaloyl 25 Terephthaloyl	H-134	2/15/65	1 wk.	Badly crazed in one week. Low mol. wt. polymer - brittle as free film
25 P, P' - Biphenol 25 6FK-BPA 25 Isophthaloyl 25 Terephthaloyl	H-133	2/15/65	5/27/65	No crazing - original coating dull as casting solvent poor

(1) Hexafluoro acetone Bisphenol A, Allied Chemical Corporation
(2) Tetrafluorodichloro Bisphenol A, Allied Chemical Corporation

FIGURE 12

g. Other Properties of Polymer.

Other required properties of the coating polymer not specifically discussed in detail above are satisfactory or under study. Toughness and abrasion resistance are outstanding. Glass transition temperatures are high and cross-linking occurs at higher temperatures, so that softening of the polymer coating at elevated temperature is not a problem. Fatigue resistance has not yet been evaluated, but attempts are being made to keep elongations of coatings as high as possible as this is considered a related factor. Adhesion of coatings, without primer, to anodized 2024 aluminum panels is good. Detailed evaluations have not yet been made with other surfaces. Long range heat tests of 168 hours at 500°F are in preparation with silicone coatings being used as a control. Glossy coatings are considered primarily a function of pigmentation volume and titanium pigmentation will be kept to a minimum to help assure this. One-year package stability tests will, of course, have to be made on the final polymer that is developed and formulated into paint for this application.

Future Plans.

In addition to the work which is underway and has been discussed, research and development work will be initiated in the following areas:

a. The possibilities of developing a room temperature cross-linking or curing system will be explored.

b. Process development work will be pursued relative to the feasibility of emulsion interfacial polymerization to polymerize promising intermediates which are not as reactive as some of the present ones, but which would impart important properties.

c. The effect on polymer heat stability and long range aging of end-capping polymer chains with aromatic groups will be investigated.

References.

General references which have been used in this work during the past year are as follows:

1. Sorenson, W. R. and Campbell, T. W., Preparative Methods of Polymer Chemistry, Interscience Publishers, Inc., New York (1961)

2. Gould, R. F. (Ed.), Polymerization and Polycondensation Processes, Advances in Chemistry Series No. 34, American Chemical Society, Washington, D. C. (1962)

3. Schnell, H., Chemistry and Physics of Polycarbonates, Interscience Publishers, New York (1964)

4. Christopher, W. F. and Fox, D. W., Polycarbonates, Reinhold Publishing Corporation, New York (1962)

5. Grassie, N., Chemistry of High Polymer Degradation Processes, Interscience Publishers, Inc., New York (1956)

6. Taylor, C. J. A., Paint Technology Manuals, Part Three, Convertible Coatings, Reinhold Publishing Corporation, New York (1962)

STUDY OF FRACTURE MECHANISMS BY MICROFRACTOGR'PHY

WILLIAM A. SIPES AND JOHN F. DANOVICH

Background.

Failure analysis is effective only insofar as it can determine "the cause of failure." For the materials engineer, the crux of the problem pertains to describing, diagnosing, and explaining the fact of fracture. Unfortunately, materials science has not yet reduced the subtleties of the phenomena to a complete and definitive analysis. Among the many tools used for such investigation is the electron microscope. Electron transmission techniques have proved invaluable in the study of the deformation and plasticity of materials. A newer approach, using replication methods, has now emerged as a means of delineating the final consequences of these processes - fracture.

However, at a very practical level, the success of the instrument in discriminating previously unobserved details of fracture surfaces had led to problems of nomenclature and identification. [1] The commonly used explanations, even theories of fracture, must take account of these new details of fracture topology revealed by the electron microscope.

Objective.

1. The long range goal of this research is to assist in identifying the causes for material failures in high strength materials.

2. The immediate aim of the work reported below is to describe those aspects of hydrogen embrittlement which distinguish it from the other mechanisms of so-called "brittle" fracture.

Accomplishments.

1. The initial task confronting this investigation was the problem of providing fracture surfaces, which, for want of a better phrase, could be described as "pedigreed hydrogen embrittlement" fractures. The consensus of published work [2] indicated that such failures are the result of complicated interactions involving numerous variables, which together might be considered the "failure envelope." These include all those familiar to continuum mechanics as well as those of physical chemistry. Neither atomic mechanisms nor electrochemical effects can be ignored safely. Hence, test methods which involved a piece-meal attack, although informative, would tend to lead to intractable difficulties when attempts are made to correlate the test with information obtained from electron fractographs. An accident which occurred during the investigation of the effect of stress on the permeation rate of hydrogen

Masking Compound:
   Cellulose acetate base

Platinum Anode (or Cathode)

Cell "Window" cut 'n
Masking Compound

D.C. Source:
   Instrumented

Plastic Bottle:
   Electrolyte container

Cathode (or Anode)
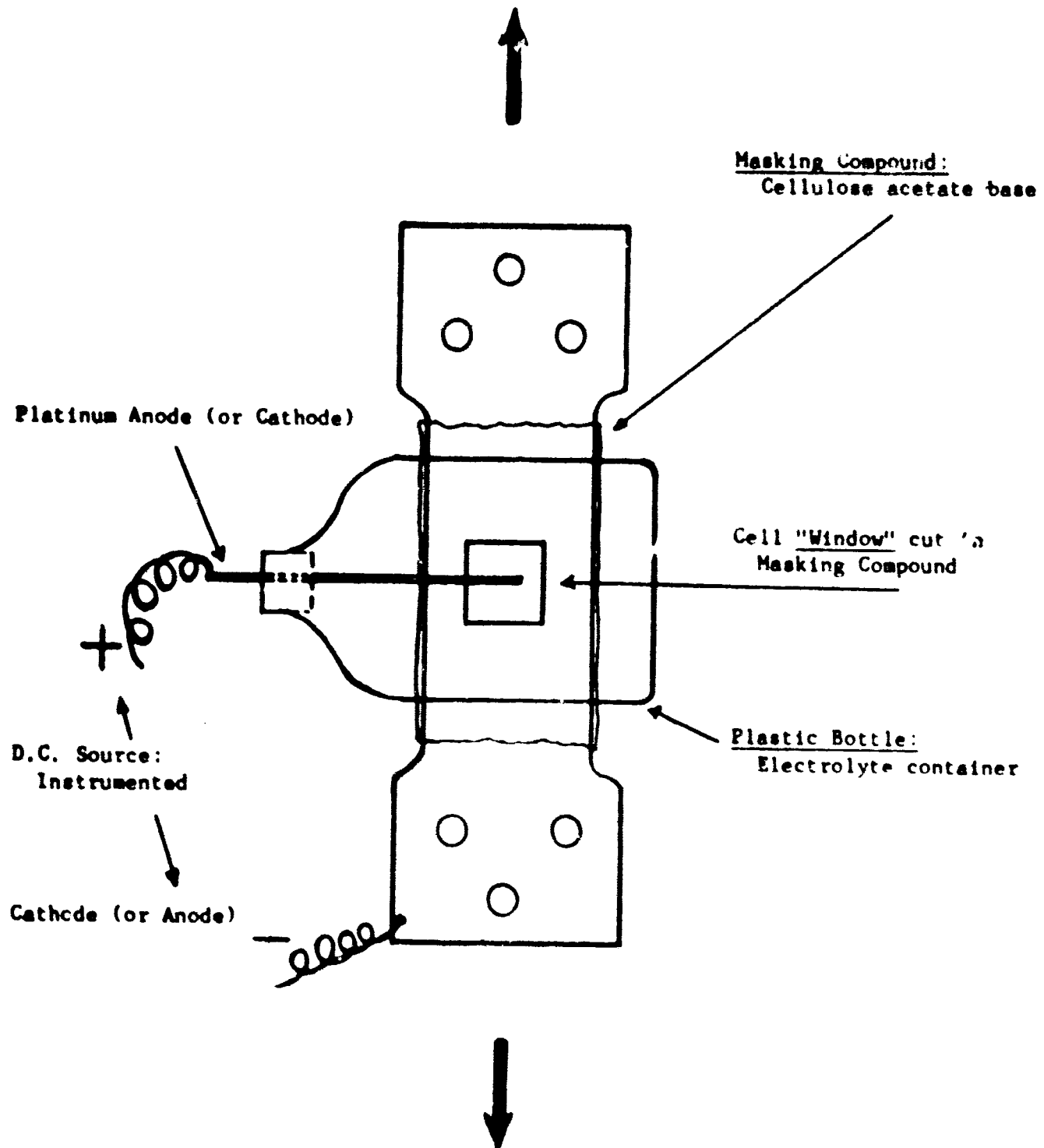
FIG. 1 - SCHEMATIC REPRESENTATION OF FRACTURE TEST SPECIMEN CONFIGURATION

- 126 -
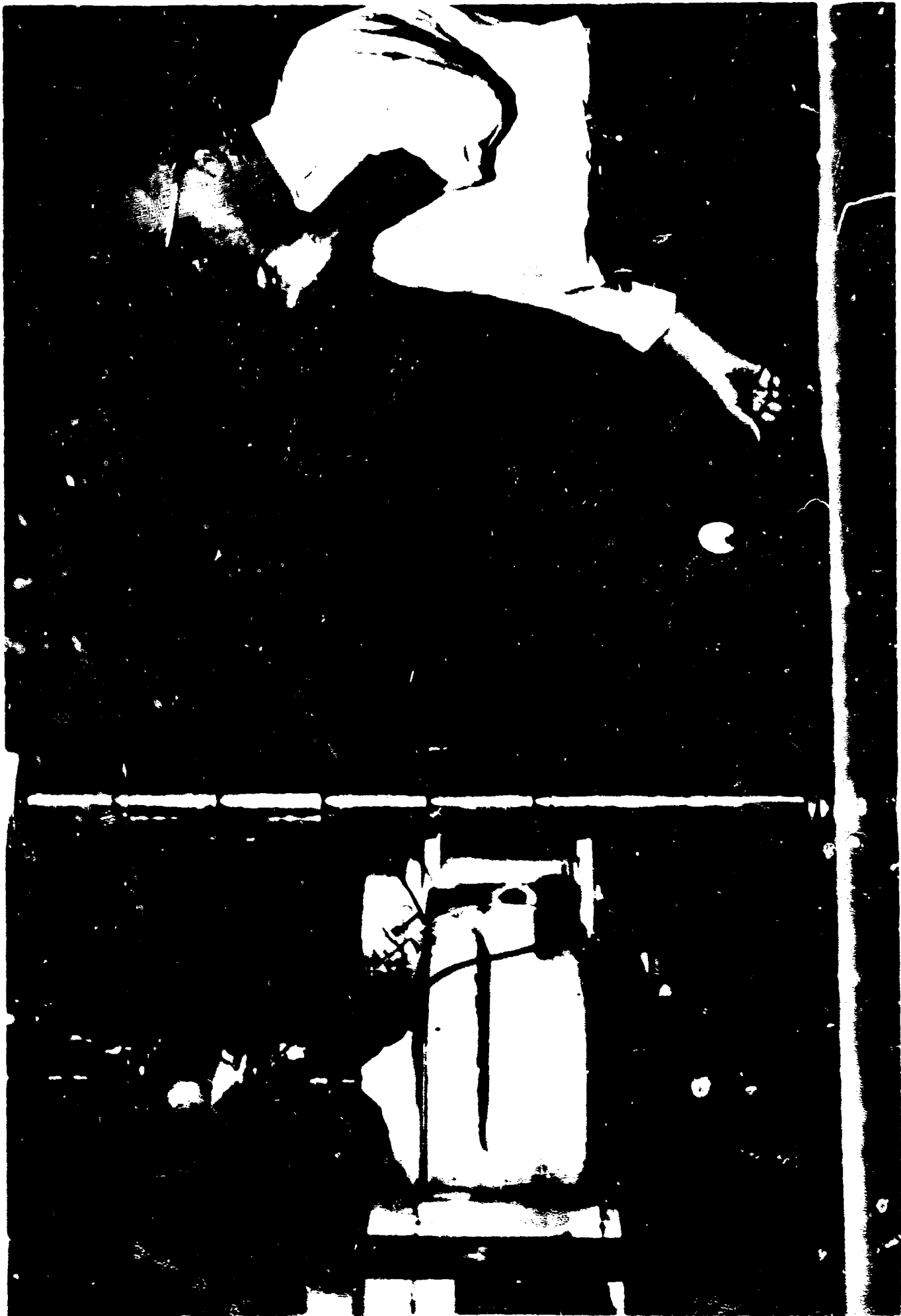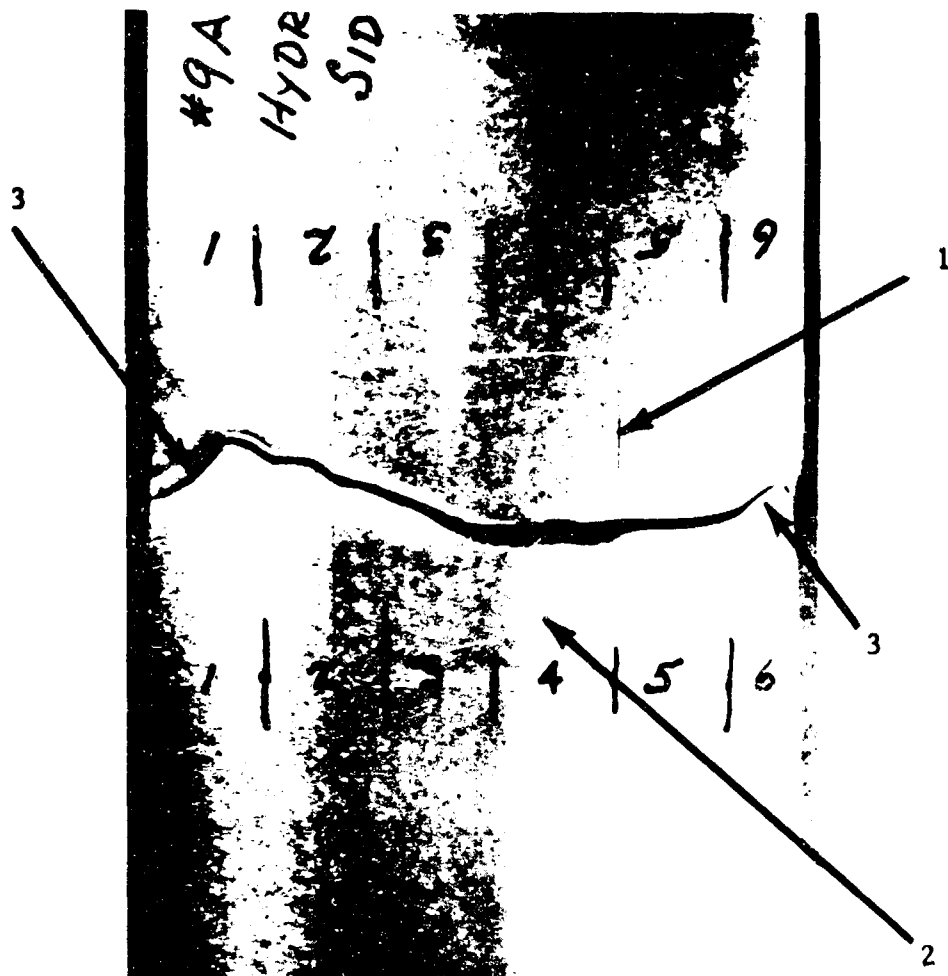
Note: 1. Specimen Gage Section Hydrogen Window -
1" square
2. Note delayed transverse crack indicating
embrittled "notch"
3. At specimen edges, ductile failure is
indicated by shear lip "tongues"

Figure 3   Photograph (1 X) of Hydrogen Embrittlement
Test Specimen, AISI 4340 Steel at 240,000
psi Strength Level
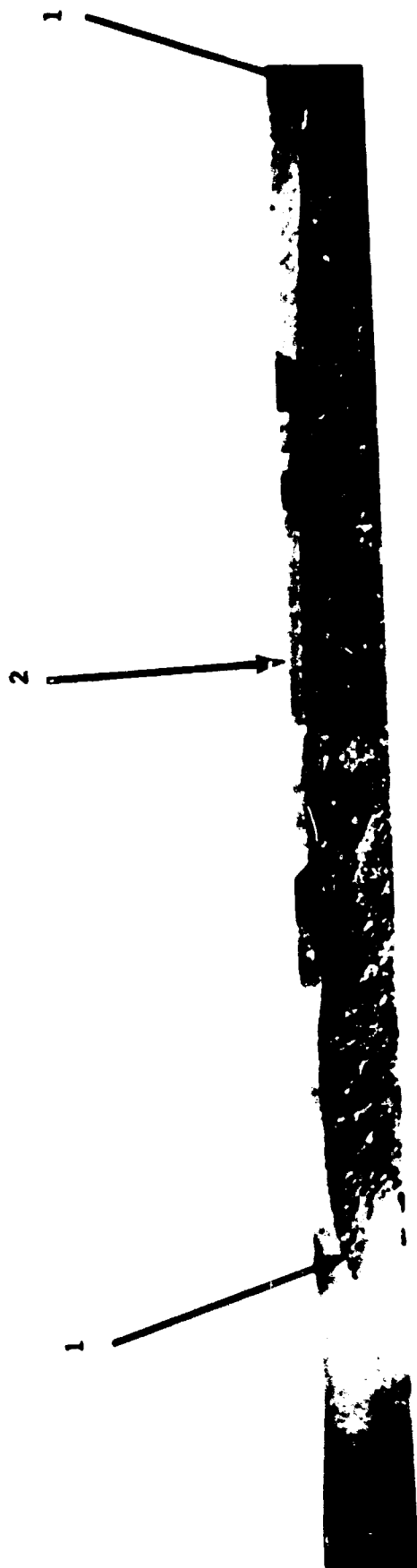
Note: 1. "Tongue" of fracture propagation
      2. Shear lip opposite side of hydrogen area
      3. Brittle fracture zone approximately elliptical

Figure 4 Photo macrograph (6X) of Hydrogen Embrittled
          Notch Area in AISI 4340 Steel Test Specimen Fracture

Figure 6 Electron Fractograph (32,000X) of
Fracture Surface of Test Specimen
AISI 4340 Steel

Appearance of flat crystallites lying in the
"flake sites".

Figure 5 Electron Fractograph (6800X) of
Fracture Surface of Test Specimen
AISI 4340 Steel

Notice "flake sites" interrupting the quasi-
cleavage mode of failure.
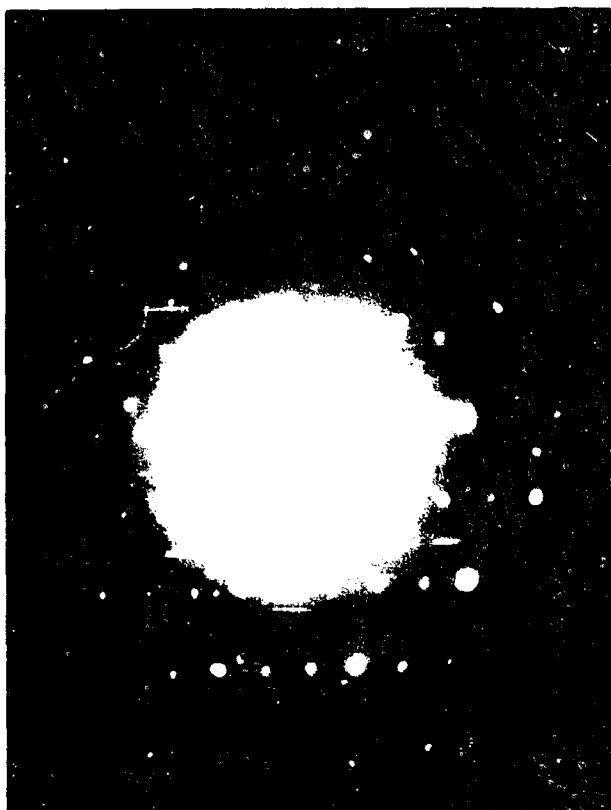
Figure 7   Electron Diffraction Photograph of Crystallite
Found in Hydrogen Embrittled Surface

through a membrane of high strength AISI 4340 steel $\underline{3}^/$ $\underline{4}^/$ fortuitously
suggested a solution to this problem. After certain modifications in
specimen size and cell configuration and preparation, fracture surfaces
of sufficient size for replication were obtained. The successful
production of such fractures indicates that a means of correlating
fracture mechanics, electrochemical effects, and the phenomena associated
with the atomic mechanisms of failure may be possible. This method of
obtaining fracture surfaces suggests that it will be possible to confirm
the hypothesis put forward by Troiano $\underline{5}^/$ to explain the mechanism of
hydrogen embrittlement and delayed fracture. Also, merely by changing
the polarity of the test cell, conditions analogous to stress corrosion
effects may be studied. See Figures 1 and 2.

2. The fracture surfaces obtained, on the macroscopic level, effectively
demonstrated the "notch" effect of hydrogen embrittlement - Figures 3 and
4. However, the most interesting results, considering the differences
among current explanatory theories, were observed in the electron
fractographs - Figures 5 and 6. Besides indicating features of fracture
topology previously unreported, these electron fractographs demonstrate
that it will be possible to correlate the observed phenomena with test
variables. In this regard, recent work has been directed toward confirm-
ing the results so far obtained. Selected area electron diffraction,
Figure 7, has been used in an attempt to identify the crystallite species
observed in the brittle fracture area of the failed surface.

Future Plans.

1. Work will be done to confirm the critical test parameters required
to reproduce the fracture topologies so far observed. The electron
microprobe, now being procured, will be used, as available, to examine
selected features of the hydrogen embrittlement fracture surface.

2. Electron fractographic surveys will be made using "stress corrosion"
fracture surfaces induced in high strength AISI 4340 using a modification
in test procedures.

References.

1/ C. D. Beachem, B. F. Brown, A. J. Edwards, Characterizing Fractures
   by Electron Fractography, Part XII, Illustrated Glossary, Section 1:
   Quasi-Cleavage, NRL Memorandum Report 1432, June 1963, pp 1-2.

2/ Fracture of Solids, D. C. Drucker and J. J. Gilman, Eds., Interscience
   Publishers, John Wiley & Sons, N. Y., N. Y., 1963, Vol. 20 of
   Metallurgical Society Conferences reports papers presented at Maple
   Valley, Washington, August 21-24, 1962.

3/ M.A.V. Devanathan, Z. Stachurski, and W. Beck, "A Technique for the
   Evaluation of Hydrogen Embrittlement Characteristics of Electroplating
   Baths," Electrochemical Society, Journal, V .10, No. 8, August 1963,
   pp. 886-890.

4/ J. McBrean, L. Nanis, and W. Beck, "A Method for the Determination of the Fermcation Rate of Hydrogen Through Metal Membranes," Final Report submitted on Contract No. N156-44134, NAEC.

5/ A. R. Troiano, "The Rate of Hydrogen and Other Interstitials in the Mechanical Behavior of Metals," TRANS ASM, Vol. 52, 1960, pp. 54-80. Edward DeMille Campbell Memorial Lecture.

METABOLIC MECHANISMS OF MAN IN THE FULL PRESSURE SUIT

E. HENDLER and D. W. DERY

Background.

The full pressure suit is an essential piece of life support equipment re-
quired by personnel engaged in flying high-altitude, high-performance aircraft,
as well as manned spacecraft. Since the body is entirely enclosed within a
gas-tight, impermeable garment for prolonged periods of time, provisions must
be made for assuring an environment compatible with a minimum of
performance decrement.

Objective.

The present study has as its objective the quantitative evaluation of the
energy requirements of man during task performance while dressed in the full
pressure suit. Conduct of this study is expected to provide contributions
toward defining life support system requirements in manned aerospace vehicles,
toward improving bioinstrumentation methodology for remote physiological and
psychological monitoring of human subjects, and toward relating performance
capability in the full pressure suit to concurrent physiological changes.

Accomplishments.

As indicated previously, the glass house (chamber in which metabolic measure-
ments will be made) was relocated and reassembled; however, plumbing and
electrical services to make the enclosure functional have not yet been installed.
Consequently, it has not been possible to proceed with the task sequence
as planned.

A small analog computer was purchased and installed, and two of the investi-
gators working on this project were trained in its use and applications.
The computer has been programmed to process data obtained in the course of
the work described below.

A review of the literature was undertaken for the purpose of determining
methods of assessing respiratory function in men, which would also be compatible
with the wearing of the full pressure suit. In addition, it was desired to find
a method which would not necessitate encumbering the subject with excessive gear,
nor interfere with the normal use of the suit. The method of measuring volume-
flow loops appeared promising, and was therefore investigated in some detail,
as indicated in the following discussion.

The volume-flow loop refers to a simultaneous recording of changes in res-
piratory volume and flow which may be obtained while a subject performs certain
respiratory maneuvers. Such loops contain a relatively large amount of information
pertaining to a subject's respiratory capability, as will be shown, while at
the same time presenting this information in a compact and convenient manner.
The configuration of these loops is quite consistent in size and shape for a
given individual, and therefore may reflect subtle changes in respiratory function

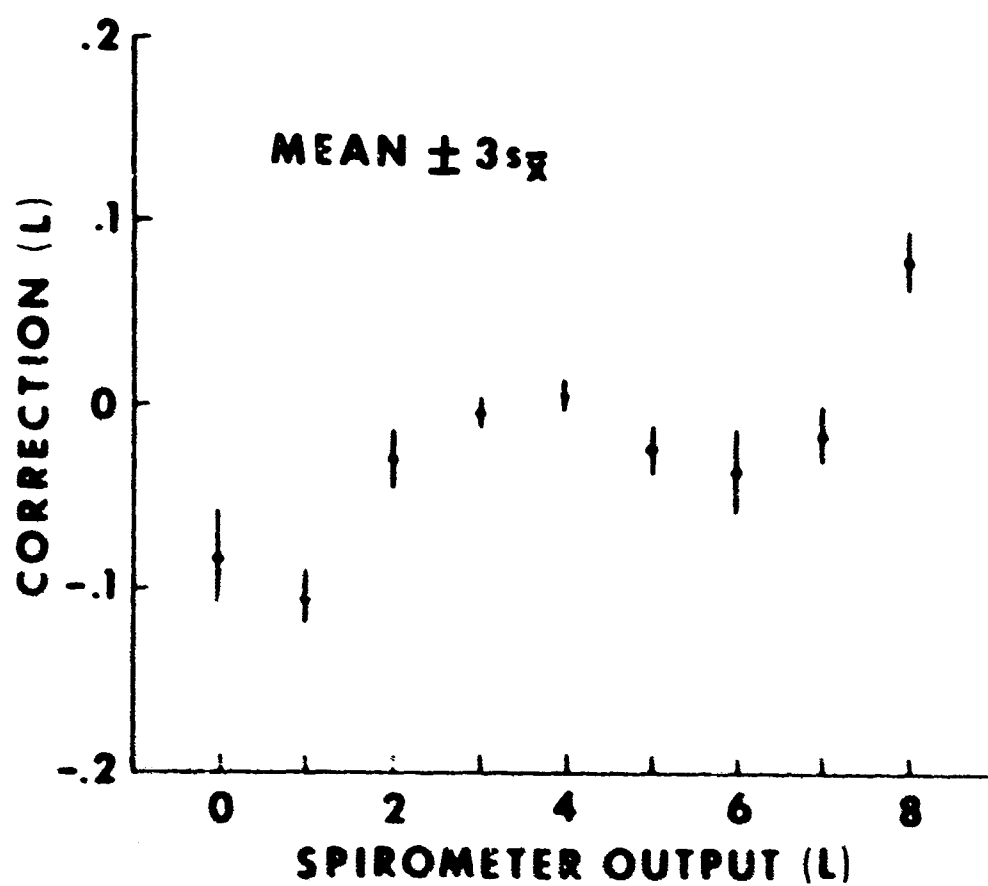Fig. 1   Arrangement of apparatus to measure respiratory function

Fig. 2   Correction factors for NEBLE spirometer

as a result of imposed stress. Another important advantage of this method of presentation is that respiratory dysfunctions of many kinds are easily recognized. This is in contrast to the rather tedious graphical analyses required to obtain equivalent information from the usual spirograms.

Fig. 1 indicates the procedure followed in obtaining volume-flow loops. Seated subjects breathed into a waterless WEDGE spirometer (Med-Science Electronics, Inc.) through a mouthpiece connected to a short length of wide-bore tubing. Two electrical outputs from the WEDGE spirometer, one proportional to volume and the other proportional to flow, were amplified and fed into an X-Y plotter. As shown in Fig. 1, the spirometer outputs could also be fed into an oscilloscope capable of retaining the trace so obtained on the tube face. The latter was used for monitoring and training purposes. A number of subjects were instructed to deliver tidal volumes (TV) and forced vital capacities (VC) into the spirometer, and these maneuvers were practiced until consistent loops were produced. Since one of the prime purposes of this study was to evaluate the accuracy of this method of measuring respiratory functions, the subjects repeated these procedures using a standard 13.5-liter Collins respirometer from which records of volume as a function of time were obtained.

Calibration of the WEDGE spirometer and its associated recording equipment was accomplished in two ways. First, measured volumes of air were delivered to the spirometer by manually expressing this air from beneath the bell of the Collins respirometer. Changes in air volumes of the latter were recorded by a stylus mechanically linked to the bell, which provided a record of volume change as a function of time. Simultaneous volume changes thus induced in the WEDGE spirometer were recorded as pen movements along the x-axis of the X-Y plotter. Tangents drawn along the steepest slopes of the respirometer volume-time records were used as measures of peak flow. These were compared to corresponding peak flow records from the WEDGE spirometer, which appeared as pen movements along the y-axis of the X-Y plotter. Second, a mechanical breathing machine (Scott Aviation Corp., No. P/N 23575) cyclically injected and withdrew preset volumes of air, at predetermined frequencies, into and out of the spirometer. The resultant spirometer outputs of volume and flow, both as functions of time, were recorded on a Sanborn Model 150 strip chart recorder, as well as the plotter.

Fig. 2 shows the mean corrections (plus and minus three standard errors of the mean) for volumes recorded from the WEDGE spirometer on the X-Y plotter. The spirometer is generally used in a partially filled condition, to allow for either deep inspiration or deep expiration as the initial respiratory movement. In our tests, the starting position of the spirometer was adjusted to approximately 4 liters, at which volume no voltage output was fed to the X-Y plotter. As the volume in the spirometer decreased below 4 liters, an increasingly positive voltage was applied to the plotter pen; for volumes greater than 4 liters, the applied voltage was negative in sign. It is evident from Fig. 2 that the smaller corrections were applied in the usual working range of the spirometer. Respirometer readings, which served as the standard for calibrating the WEDGE spirometer, could not be read closer than ± 0.02 liters, a value comparable in magnitude to the correction factors from about 2 to 7 liters. All volumes recorded on the X-Y plotter were corrected in accordance with the values shown in Fig. 2; corrections for intermediate values of recorded volumes were calculated on the basis of linear changes between adjacent corrections.

TABLE 1

COMPARISON OF CORRESPONDING PEAK FLOW RATE DETERMINATIONS

Peak Flow Rate (LPS)

Collins Respirometer	WEDGE Spirometer
1.73	1.69
1.65	1.69
1.52	1.50
2.37	2.30
2.19	2.18
1.73	1.78
2.92	2.78
3.42	3.54
4.30	4.38
5.49	5.38

TABLE 2

MEAN VALUES OF RESPIRATORY FUNCTION MEASUREMENTS MADE IN TWO WAYS

Subject	Tidal Vol. (ml)		Expir. Res. (ml)		Inspir. Res. (ml)		Vital Cap. (ml)		Max. Brea. Cap. (LPM)		Peak Exp. Flow (LPS)		Peak Insp. Flow (LPS)	
	C*	W**	C	W	C	W	C	W	C	W	C	W	C	W
A	863	774	2230	2790	3420	2650	5805	6220	156	147	9.6	7.8	5.7	9.1
B	829	1060	2490	2420	3480	3500	5960	5920	1??	122	7.1	8.3	5.7	7.4
C	1040	906	2650	2390	3015	3325	5760	5700	?7	167	7.4	8.8	5.1	9.0
D	805	988	2510	2265	3330	3550	5870	5840	202#	-	12.1	8.8	6.6	11.4
E	810	980	1020	902	2880	2910	3890	3790	116	120	7.0	7.7	4.8	6.8
F	780	828	1705	1380	2540	2840	4250	4210	161	185	8.4	7.8	4.4	7.7
G	820	734	2800	2250	2790	3310	5200	5580	192#	-	8.9	8.6	6.0	10.3
H-1	1180	851	1870	1920	2830	2745	4960	4990	87	93	-	5.0#	5.0	6.9
H-2	1200	1100	2010	1960	3150	3400	5160	5360	-	-	-	6.7#	-	9.0#
I	742	760	1200	925	4180	3895	5380	4820	177	139	6.0	8.4	6.5	9.4
J	741	803	989	723	2990	3325	4010	4090	136	117	5.3	7.2	8.8	7.5
K	771	712	1490	1790	3770	3660	5230	5450	-	-	5.1	8.4	8.5	9.0
L	478	670	1180	1360	3170	3140	4290	4500	169	144	6.2	8.7	10.3	9.2
Mean	850	859	1860	1775	3195	3320	5060	5110	150	137	7.6	8.2	6.4	8.6
No. Indiv. Dets.	351	39	351	39	351	39	351	39	27	27	33	33	36	36

* Measurements made using 13.5L Collins Respirometer
** Measurements made using WEDGE spirometer
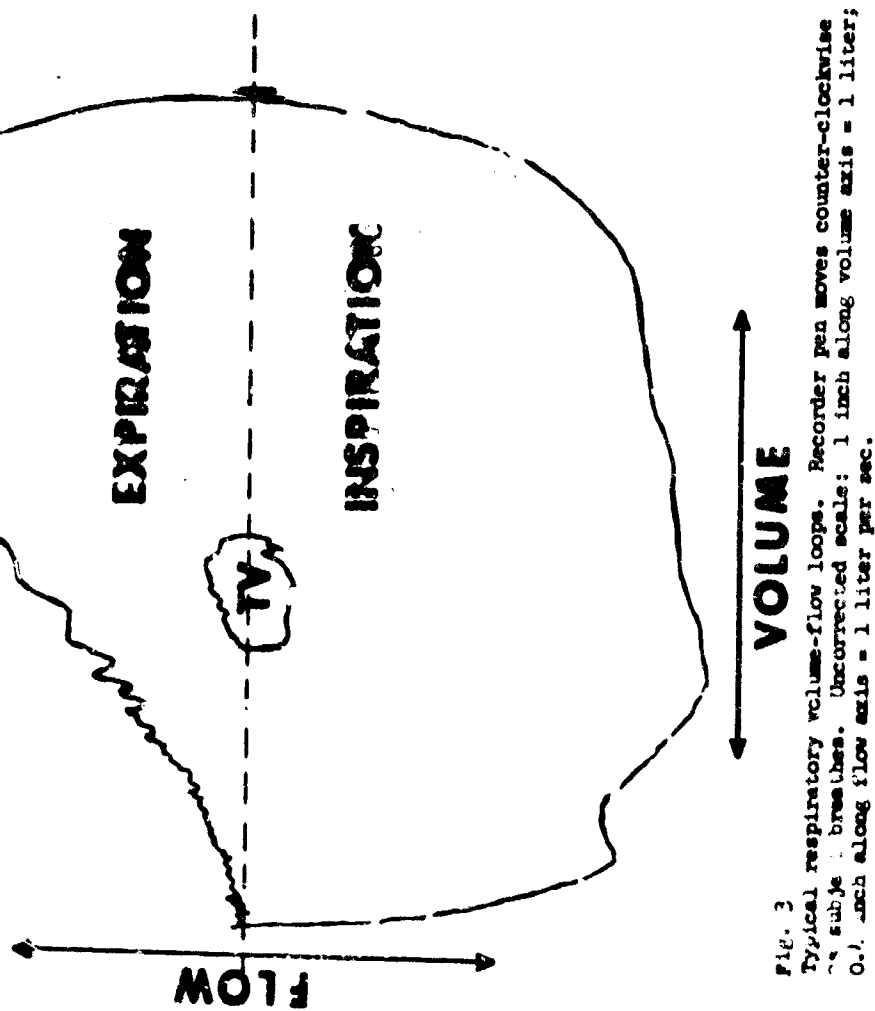# This value not included in computing column mean

Fig. 3

Typical respiratory volume-flow loops. Recorder pen moves counter-clockwise on subject breaths. Uncorrected scale: 1 inch along volume axis = 1 liter; 0.1 inch along flow axis = 1 liter per sec.
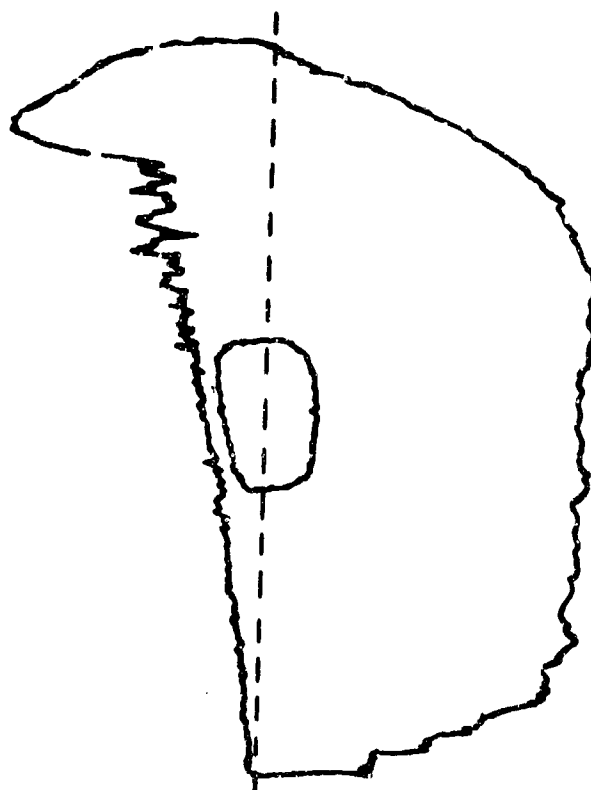

Fig. 4
Volume-flow loops of subject showing decrease in expiratory flow. Uncorrected scale as in Fig. 3.

Peak flows determined graphically from volume-time curves obtained with the respirometer compared favorably with corresponding peak flows measured on the WEDGE spirometer flow recordings (Table 1). In addition, electronic integration of spirometer flow signals, using the computer, resulted in volumes essentially the same as those indicated directly by the respirometer. Spirometer volumes obtained directly, and by integrating the flow rate, remained unchanged when produced by the breathing machine over the frequency range of 5 to 60 cycles per minute, with peak flows of approximately 350 liters/min.

Typical VC and TV volume-flow loops are shown in Fig. 3. These loops were traced directly from a plotter record, and indicate the usual relationship and shape of the VC and TV configurations. Loops of maximum breathing capacity were superimposed on the volume-flow loops. A comparison of means of repeated measurements of tidal volume, expiratory reserve, inspiratory capacity, vital capacity, maximum breathing capacity, peak expiratory flow, and peak inspiratory flow for twelve subjects, using both the Collins respirometer and the volume-flow technic, is shown in Table 2. All of the values shown were measured at ambient (sea-level) temperature and pressure conditions. When tested statistically, no differences could be found between the values obtained for each of the above pulmonary function measurements using the Collins respirometer and those obtained using the WEDGE spirometer, except for peak inspiratory flow. The latter was found to be significantly higher when measured using the WEDGE spirometer. The reason for this difference is not immediately apparent, and further efforts will be devoted to examining this phenomenon.

Fig. 4 is presented to illustrate the point, previously mentioned, that volume-flow loops may serve to indicate deviations from the more usual respiratory patterns in a most striking manner. The subject in this case was a young naval aviator, selected as a potential astronaut candidate, who appeared to be in excellent physical condition. From his volume-flow loops, one of which is shown as Fig. 4, it is quite apparent that when executing a forced vital capacity maneuver, his expiratory flow is reduced throughout much of his functional lung volume. This finding was much more difficult to visualize in the usual spirograms, and could have easily escaped detection.

Initial procedures were worked out for measuring pressure suit leakage by using the computer to calculate continuously the difference between integrated inlet and outlet flows through mass flowmeters.

Future Plans.

It is planned to complete installation of plumbing and electrical services, in order to have a functional facility for carrying out the principal objectives of this study. The computer will continue to be utilized to handle data analysis, and further work will be done to evaluate the volume-flow technic for measuring pulmonary function. An attempt will be made to calibrate a pneumotachograph for obtaining volume-flow loops from subjects within the full pressure suit. Models incorporating cyclic volume changes with controlled leakage rates will be tested in the glass house. Unoccupied and occupied pressure suits will be statically and dynamically evaluated; metabolism and other physiological functions of men in full pressure suits will be determined for the resting, exercising, and psychomotor task performance situations.

It is intended to prepare a paper describing the work performed with the volume-flow technic for presentation at the 18th Annual Conference in Engineering in Medicine and Biology.

Publications.

Hendler, E., D. W. Dery, and N. Miller: Heart rate during performance of a complex physical task. Fed. Proc. 23:522, 1964.

THE DEVELOPMENT OF ELECTROCHEMICAL AND METALLURGICAL MEASURING TECHNIQUES FOR SIMULATED DEEP SEA CONDITIONS

JOHN J. DE LUCCIA AND EDWARD TAYLOR

Background.

The deterioration of materials exposed to seawater has been investigated by a number of researchers, and much is contained in the literature concerning shallow water exposure. Until a few years ago, very little deep water testing (beyond 500 feet) of structural materials had been accomplished. A project titled, "Oceanographic Effects on Materials," was initiated at that time, and the Aeronautical Materials Laboratory (AML) has since exposed several thousand specimens of about 100 different varieties of engineering materials to depths of 2300 and 5640 feet. So far, the exposure of about 25% of these specimens has been completed and the determination of physical and chemical changes is underway.

Some researchers have maintained that deep water testing of metals is unnecessary since little oxygen is available to assist in the corrosion reaction. This viewpoint invited scientific curiosity, and the determination perhaps, by deep sea simulation equipment, of any possible correlation of corrosion rate with depth and oxygen concentration.

Recently, identical materials which were exposed at two different depths for similar periods were examined and found to exhibit more severe corrosion at the greater depth where the oxygen concentration happened also to be greater. This result, as well as vermiform (worm-like) corrosion of stainless steels due to water flow over its geometry, has convinced these investigators that laboratory simulation of deep ocean corrosion is extremely necessary in order to cope with these problems.

Objective.

The specific aim of the program is to develop electrochemical and metallurgical instrumentation techniques suitable for monitoring chemical, physical, and mechanical changes of metals exposed to pressurized sea water simulating various ocean depths.

Accomplishments.

A. A controlled environment system (Figures 1 and 2) for deep sea simulation has been procured and is being fitted with numerous accessories which are corrosion resistant. The system consists of a pressure vessel, a cooling unit and a high pressure pump. The pressure vessel is capable of achieving 20,000 psi and 0°C; conditions which are the maximum known for any ocean. Because a flow of up to 6 gal./hr. is possible, currents found at ocean depths can also be simulated.
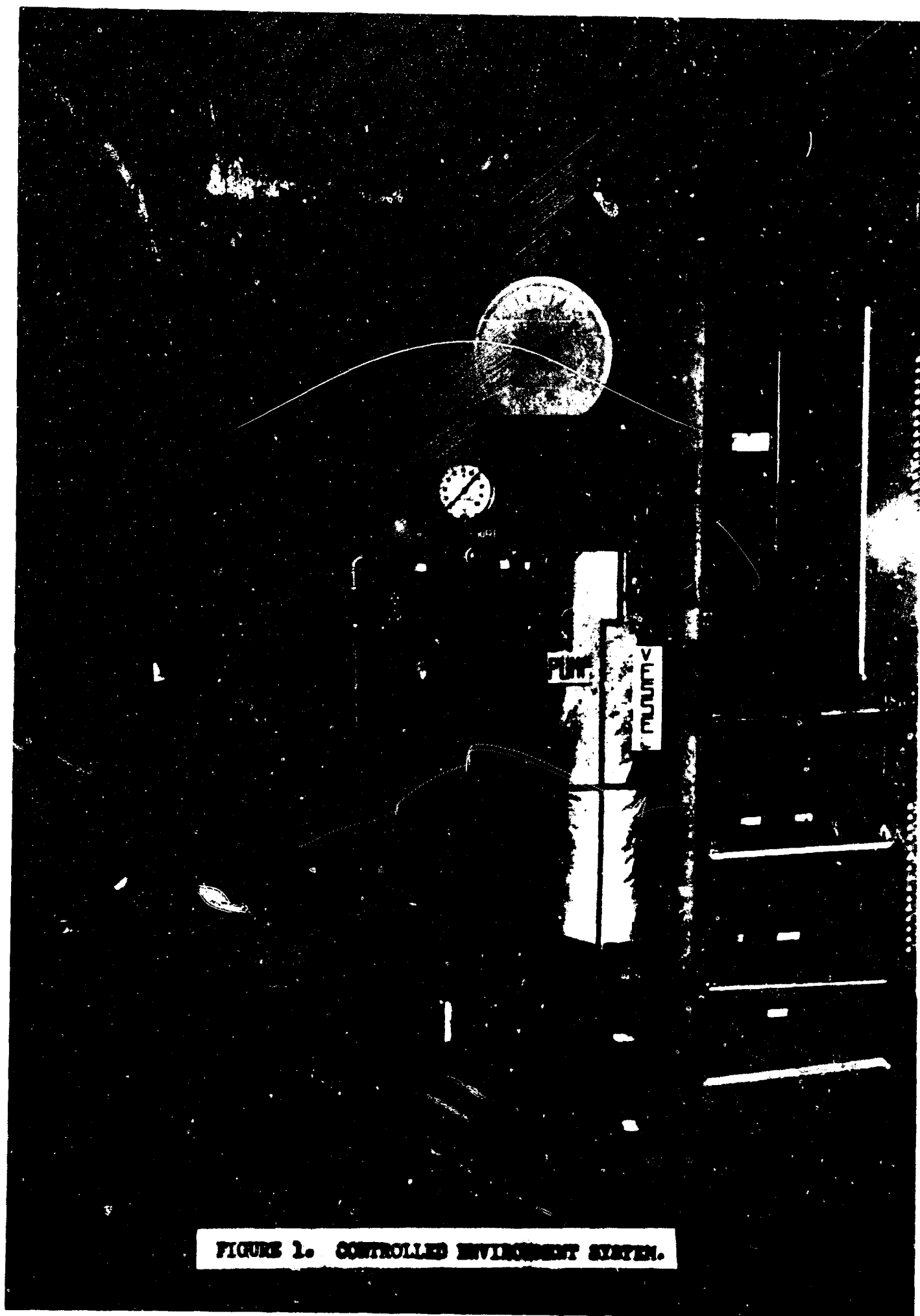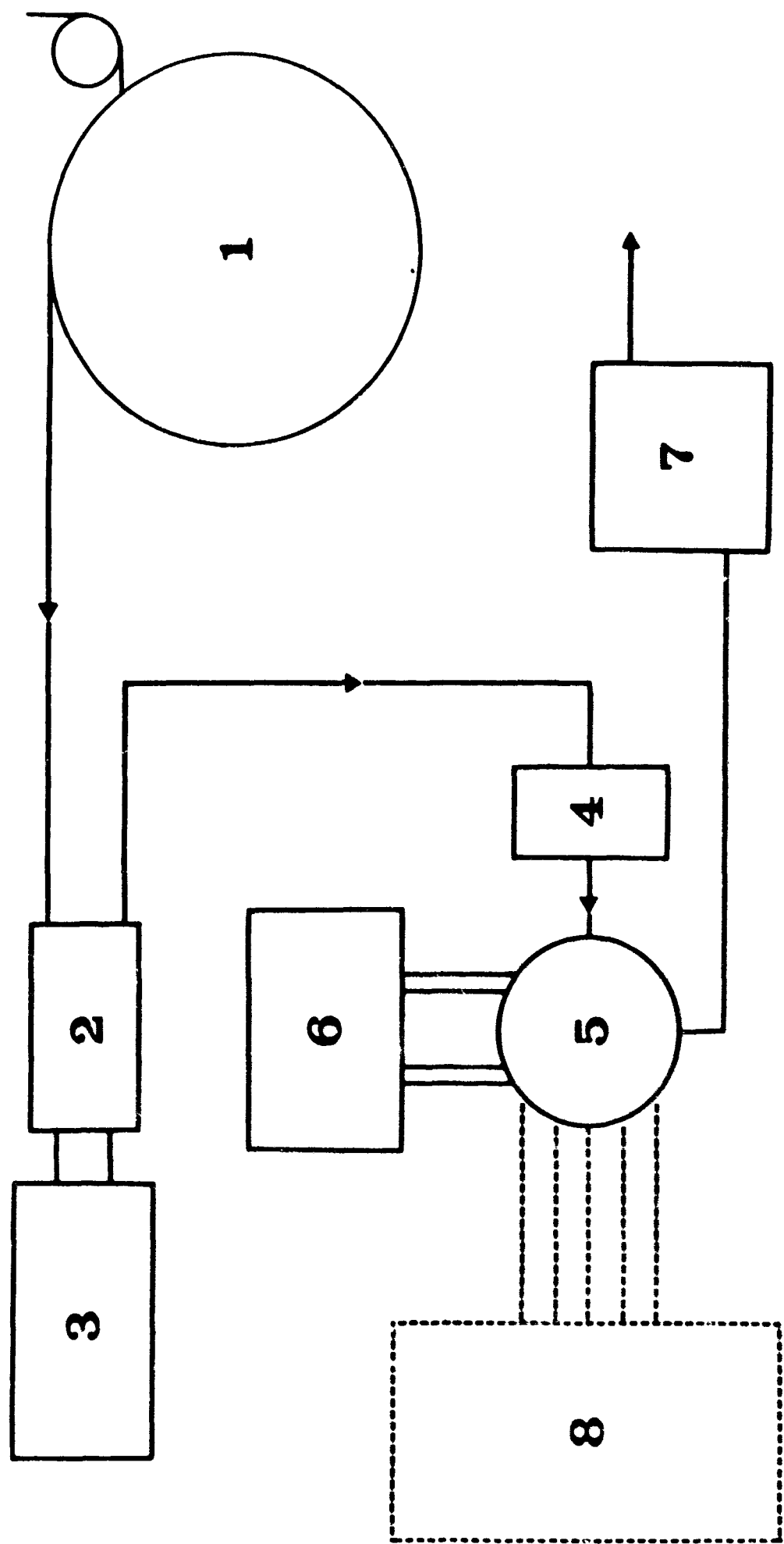
FIGURE 1. CONTROLLED ENVIRONMENT SYSTEM.

DEEP-SEA SIMULATION SYSTEM

① STORAGE VESSEL ② CONTROLLED RESERVOIR ③ O₂ AND pH METERS ④ PRESSURE PUMP

⑤ PRESSURE VESSEL ⑥ COOLING SOURCE ⑦ ATM. PRESSURE VESSEL ⑧ DATA ACQUISITION

FIGURE 2.

FIGURE 3. HIGH PRESSURE HYDRODYNAMIC SEAL

The head of the vessel contains 8 electrical feed-throughs, so that any transducing devices mounted on the electrochemical cell inside the vessel will be able to deliver their signals through it. A fabricated plastic jig (high pressure electrochemical cell) Figure 3) has been designed and constructed to facilitate the measurement of electrode potentials of metals with or without stressing. Silver-silver chloride electrodes are being constructed with established techniques [1] to provide pressure insensitive electrode potential measurements.

A data recording system is now being procured which will monitor and store at least 25 channels of information for periods up to 3 days. The data will be printed voltages with polarity, decimal point and channel identification also printed.

B. While the controlled environment system was being procured, a hydro-static testing unit was designed and assembled by AML personnel using aircraft hydraulic parts. Metal specimens were fastened to a plastic frame, stressed with wedges and enveloped by a sealed polyethylene bag containing fresh seawater. The bag was placed in an aircraft accumulator pressurized to approximately 3000 psi for 5 weeks.

Upon examination after this exposure, the high strength steel, stainless steel, and titanium were still bright and free of corrosion, whereas the magnesium had severely corroded. It was concluded that the magnesium, being more active than the other metals, consumed all of the available oxygen in order to corrode, thus leaving almost none for the steel which severely "rusts" in contact with oxygen.

The lesson from this experiment drove home the fact that oxygen plays a key role in deep sea corrosion, and close monitoring and controlling of a flowing system under pressure is highly desirable.

C. Mr. DeLuccia presented a paper on the deteriorative effects of the sea on materials at the First Naval Advisory Council on Materials sponsored Navy Meeting on Corrosion (Review and Analysis of the Navy's Deep Sea Corrosion and Deterioration Program) held at the Naval Civil Engineering Laboratory (NCEL), Port Hueneme, California. Inspection of NCEL's simulation equipment and subsequent discussion of this field brought new ideas to this laboratory. He also participated in a committee during June 1965, which will evaluate the Navy's current program on marine corrosion and deterioration in the light of requirements, and then recommend additions, deletions, and changes in emphasis in order to formulate integrated and balanced Navy Program in Marine Corrosion and Deterioration which will support adequately the Navy s commitment to deep ocean engineering ventures.

Future Plans.

Natural seawater purchased under contract from a local aquarium will be compared with artificial seawater and solutions of metal salts to determine the pressure insensitivity and other pertinent physical and electrochemical characteristics of reference electrodes to be custom made in the laboratory.

A plastic liner and diffuser will be constructed for the vessel to minimize the diffusion of copper ions from the monel walls to the metallic surfaces under investigation. Fresh filtered seawater will always first flow past the reference electrode in this system, with the specimens receiving the water next, and finally contacting the outer wall before being ejected.

The orientation of the specimens with relation to the direction of water flow will be studied to duplicate oxygen concentration cells which were found on several panels exposed to the ocean. Crevices will be intentionally formed and potential measurements will monitor the corrosion rate.

The primary effect to be studied depends somewhat on the above "subordinate" results but is concerned specifically with the effect of pressure on corrosion reactions. The effect of pressure (p) on the emf (E) of a galvanic cell can be predicted from the classical relations.

$$\left(\frac{d \Delta G}{d p} \right)_{m, T} = \Delta V \tag{1}$$

$$\left(\frac{d E}{d p} \right)_{m, T} = \frac{- \Delta V}{nF} \tag{2}$$

where ΔG is the change in free energy, ΔV the volume change when n Faradays (F) are passed through the cell at constant molal concentration (m) and temperature (T). From these equations, one finds that pressure does have an effect on corrosion reactions: this effect can be measured in situ by the simulation apparatus and compared with predicted values.

References.

1/ Reference Electrodes, Ives & Janz, Ac. Press (1961).

DEVELOPMENT OF MEASURING TECHNIQUE
FOR THE ACCURATE INDICATION OF TURBINE INLET TEMPERATURE

P. L. HOSTED

Background

This project was undertaken to develop a temperature measuring system capable
of providing accurate temperature data at the turbine inlet stations of a gas
turbine engine. To obtain an accurate indication of temperature in this en-
vironment, an averaging technique must be used because of the extreme temper-
ature gradients that exist in the area of the turbine inlet. Average temperature
techniques of measurment used at present have been found unsuitable, particularly
at altitude operating conditions where large discrepancies have been observed
between T5 measured and T5 calculated thermodynamically.

Objectives

The object of this program is to develop a new instrumentation technique or system
capable of providing accurate temperature data at the turbine inlet of a gas
turbine engine. This technique or system must be capable of yielding an accurate
temperature profile in the turbine inlet at all engine operating conditions.

Accomplishments

As the result of a literature review conducted last year, three techniques of
temperature measurement were thought to be applicable in the environment of the
turbine inlet.

      (1) Radiation Measuring Technique

      (2) Gas Density Measuring Technique

      (3) Shielded Thermocouple Measuring Technique

1. Radiation Measuring Technique

Infra-red radiation was investigated and the following conclusions
were drawn. The temperature of a hot gas stream can be determined
if the senser sees only the gas and not the walls of the containing
duct. However, the gas products of combustion are transparent over
the greater part of the spectrum; there are only a few discrete wave
bands where the gas products of combustion absorb and emit radiant
energy. Sensers have been designed which filter out all radiation,
except that being emitted from a gaseous target in a well defined
spectral band. For example, a senser has been designed that collects

radiation in wavelength band in which the CO_2 in the gas stream absorbs and emits radiation. However, since the emissivity of the gas is a function of the concentration of the CO_2 molecules, concentration or density would have to be obtained before meaningful temperature data could be taken. Considering the cost of equipment and problems involved, this method of temperature measurement was dropped from consideration.

2. Gas Density Measuring Technique

Research during the first 6 months of fiscal year 65 was primarily concerned with the investigation of an alpha particle gas density measuring technique. The distance which an ionised particle travels in a gaseous absorbing media is a function of the initial and final energy of the alpha particle and the density of the gaseous absorber. As the alpha particle traverses the gas stream it loses energy, primarily due to the coulomb interaction with the electrons of the absorbing media. Assuming classical coulomb interaction behavior, one computes the amount of energy transferred to an electron in a single collision, and then sums up all electrons in the alpha particle path to arrive at the total energy dissipated by the alpha particle. Knowing the amount of energy lost, the range of travel, and the molecular properties of the gaseous absorber, the density of the absorber can be determined. This technique of density measurement appears suitable in high altitude environments where average gas density at the turbine inlet is in the order of 0.6 kgms/ $m.^3$ (35,000 ft.). However, as sea level conditions are approached, density at this station increases and range measurements can not be made due to the extreme energy attenuation of the alpha particle. Table 1 lists density at the turbine inlet for various altitudes.

Table 1

density (kgms/.m.3)	altitude (ft.)
1.77	10,000
1.46	15,000
1.19	20,000
0.96	25,000
0.77	30,000

This method of measurement does appear to have merit in the study of high temperature rarefied gas flows, and a summary of this phase of the investigation has been prepared. This summary includes a deviation of the range-energy equation from stopping power considerations, and an example problem illustrating a method of solving the derived range-energy equation.

HIGH TEMPERATURE THERMOCOUPLE PROBE DOUBLE SHIELDED
ASPIRATED FOR TURBINE INLET ENVIRONMENT

5/16" DIAMETER INLET

22 GAGE CHROMEL ALUMEL WIRE 1/4" LONG

1/4" O.D X 0.020 WALL INCONEL TUBE WELDED TO THERMOCOUPLE INSERT

5/16" O.D X .031" WALL INCONEL TUBE

8"

8 HOLES 0.031" DRILL

0.014" INCONEL GUIDE FINS SPOT WELDED TO INSERT

THERMOCOUPLE INSERT SWAGED CONSTRUCTION INCONEL TUBING 0.125" FINAL O.D.

FIGURE 1

FIGURE 1

SCHEMATIC 9W TEST FACILITY WITH
J-79 COMBUSTOR TEST SECTION INSTALLED
IN SOUTH COMBUSTION LEG

EXPANSION JOINT

WATER SPRAY

EXPANSION JOINT

ORIFICE

1.- ONE THERMOCOUPLE I.C.

2.- FOUR FLANGE TAP STATIC PRESSURE
PROBES

3.- 1 TOTAL PRESSURE PROBE
3 TOTAL TEMPS (I.C.)

4 - 1 TOTAL PRESS.
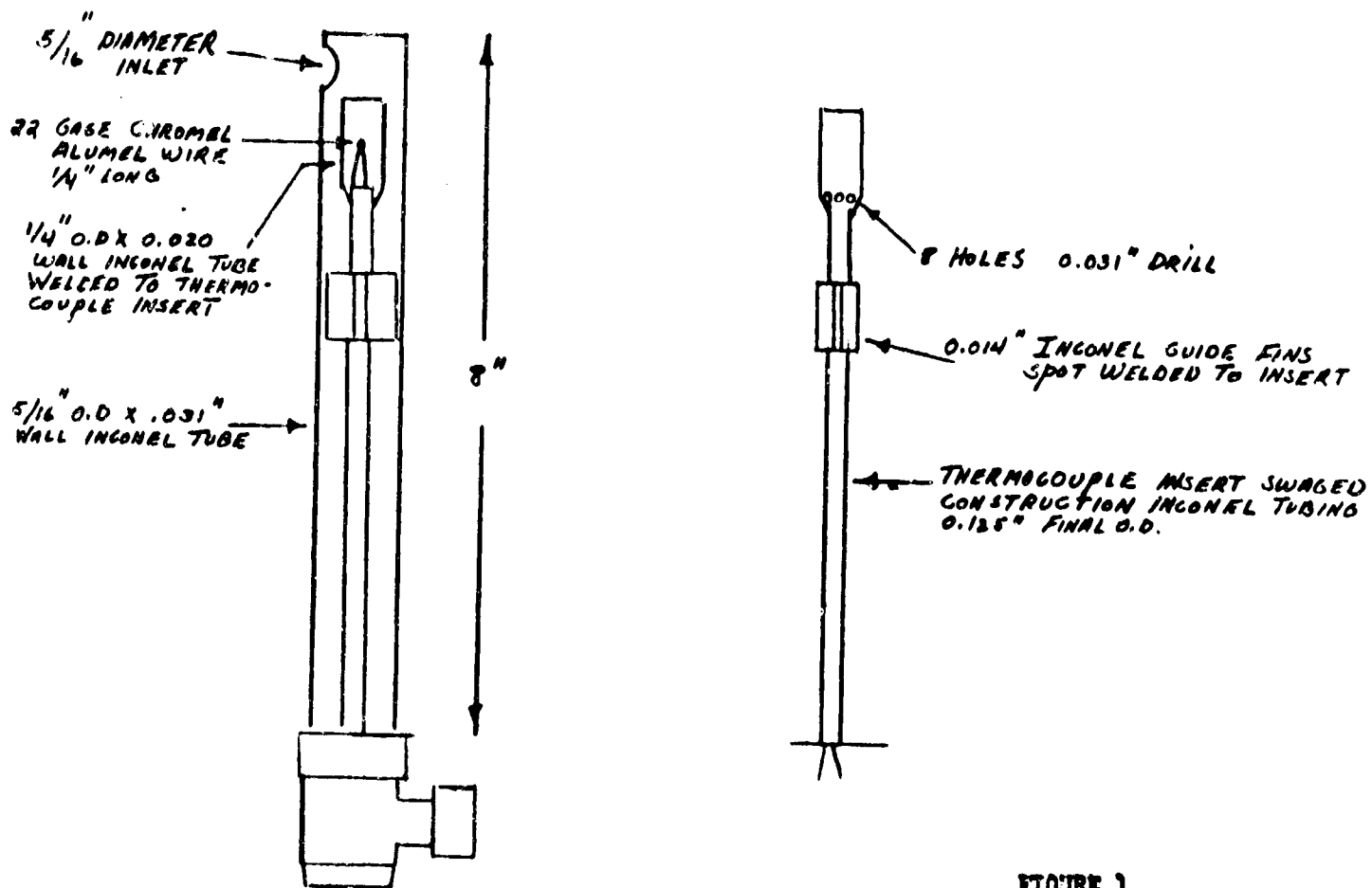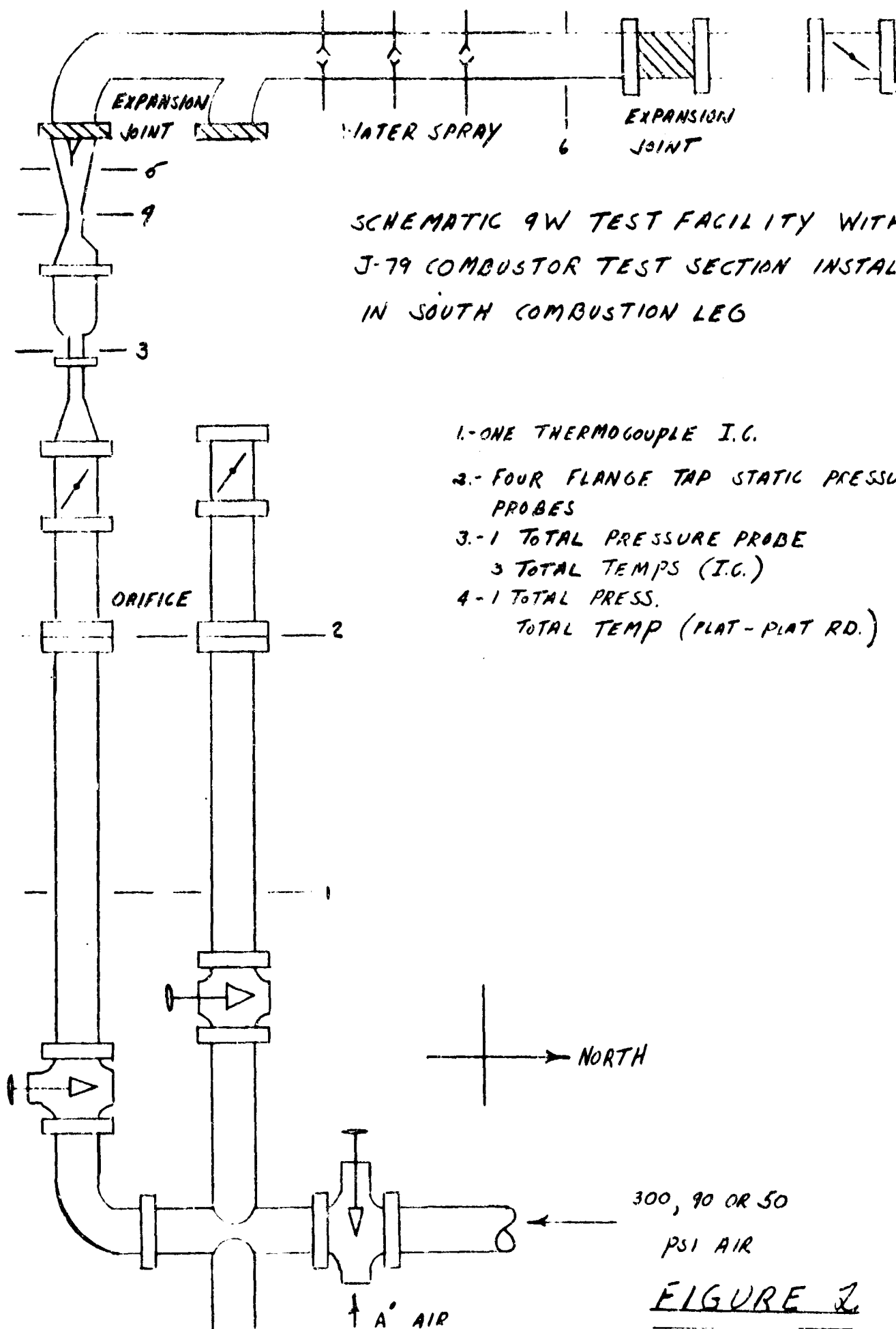TOTAL TEMP (PLAT - PLAT RD.)

NORTH

300, 90 OR 50
PSI AIR

FIGURE 2

A' AIR

3. Shielded Thermocouple Measuring Technique

The shielded thermocouple is the temperature measurement sensor
universally employed throughout the aircraft industry to measure
turbine inlet and discharge temperatures. To design a thermocouple
probe for a particular engine location, accuracy, speed of response,
temperature magnitude, and the various modes of heat energy transfer
must be considered. In a high temperature, high velocity gas stream,
some compromise must be made between speed of response and accuracy
of indication. Since this project is concerned with the accurate
indication of turbine inlet temperature, this criteria was deemed of
primary importance. Accordingly, a shielded and aspirated probe has
been fabricated as shown in Figure 1. This probe is a double shielded
temperature sensor designed for high temperature environments where
radiation is the significant mode of heat energy transfer. This probe
is to be used as the absolute temperature standard in the calibration
of all future test probe designs.

In order to simulate the environment of the turbine inlet a test rig
has been fabricated and instrumented and is now operational in 9W
test cell (Figure 2). Mass flows up to 3#/sec at inlet pressures of
30" to 70" HgA can be generated with temperatures ranging from 1000°F
to 2500°F. The above test conditions simulate altitude operating
environments for a single combustor can of a gas turbine engine.

Future Plans

Future plans include the design and test of various shielded probes, as well as
operation in test facilities capable of generating higher mass flows and pressures.
In this manner, test probes can be evaluated in the turbine inlet environment at
all engine operating conditions.

INVESTIGATION OF THE RESIDUAL STRESS FIELD
AROUND FILLED AND UNFILLED HOLES

R. VINING

BACKGROUND.

Recent fatigue investigations performed with the use of full-scale
and simulated structures have demonstrated that current fatigue
hypotheses for application to structures are not valid in the high-
stress low-life range. These hypotheses are all based on a non-
varying stress distribution (except for magnitude) in the region
being investigated. To substantiate the fatigue behavior obtained
in the current Aeronautical Structures Laboratory (ASL) tests, one
must hypothesize that the stress field varies throughout the test
life.

OBJECTIVE.

The objective of this investigation is to study the behavior of
the applied and residual stress fields around both filled and un-
filled holes in an "infinite" aluminum sheet for various cyclic
loading conditions.

ACCOMPLISHMENTS.

The special strain transducers, which have been developed in
miniature form to measure strains up to 30% near the periphery of
the hole, have been received. A technique has been developed for
using these transducers, which are miniature differential trans-
formers. One is shown in Figure 1, mounted on a simple test coupon.
The transducers and the signal-conditioning equipment to adapt their
output to the existing recording equipment have undergone check-out.

The test fixture has been designed and its erection has been completed,
as shown in Figure 2. Test specimen 1 has been fabricated, instru-
mented, and installed in the test fixture; it can be seen in Figure 2.
A closeup view of the test specimen is shown in Figure 3; the elaborate
strain gage instrumentation can be seen clearly.

For specimen 1, a loading cycle consisted of an increase in load to
140,000 pounds and a decrease in load to 18,800 pounds. The maximum
load is a value approximately two-thirds of the ultimate failing load

FIG. 1. STRESS TRANSDUCER MOUNTED ON TEST SPECIMEN
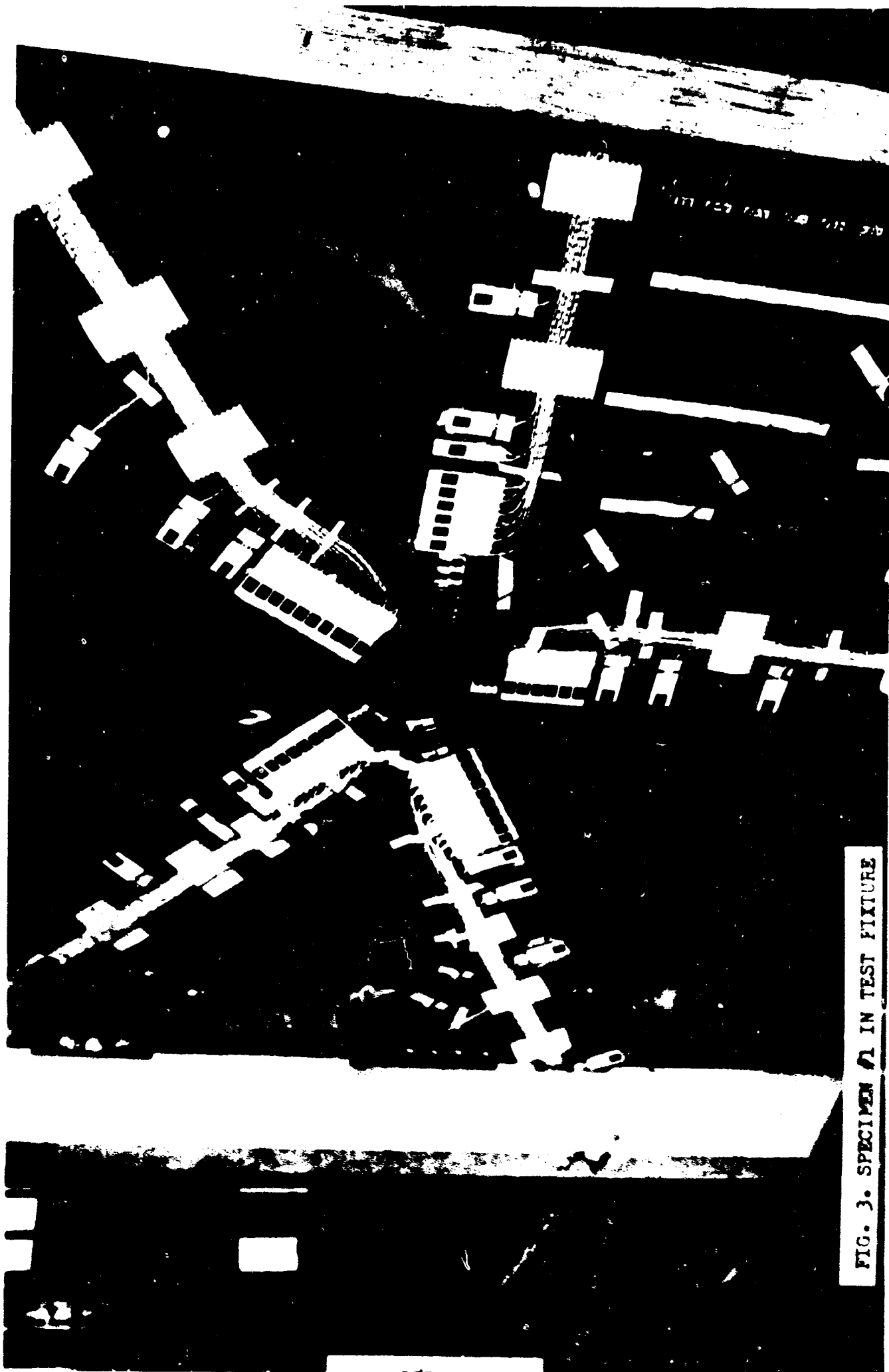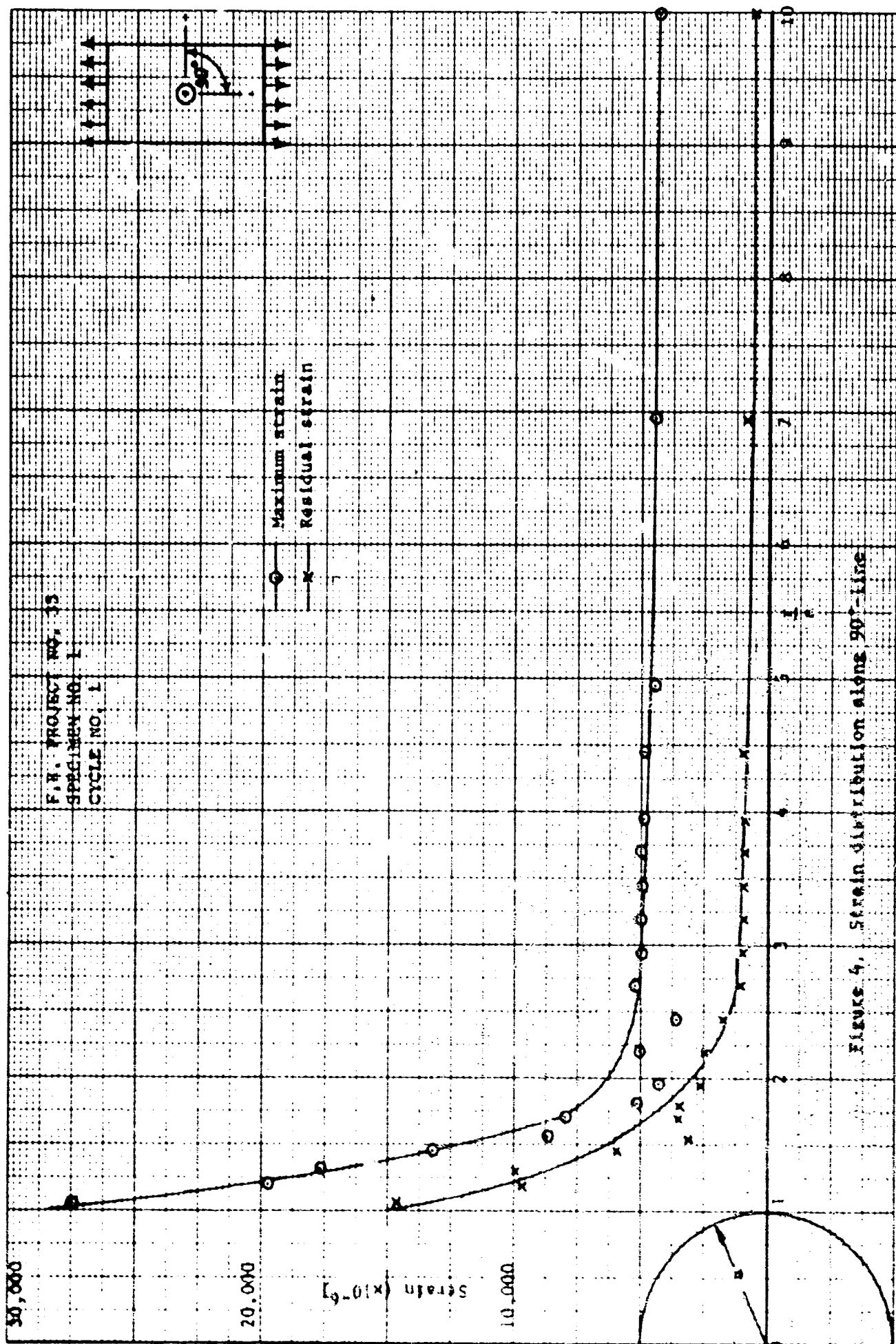

FIG. 2. TEST FIXTURE WITH SPECIMEN #1.

FIG. 3. SPECIMEN *Ω* IN TEST FIXTURE

Figure 4. Strain distribution along 90°-line

of the aluminum sheet. This load was assumed to represent what is termed "limit load" in airplane design terminology, where limit load is defined as a load which establishes the strength level for design purposes. The minimum load represents a fictitious level-flight condition load. The strain at maximum load and the residual strain at minimum load for the first cycle along a line normal to the direction of load are shown in Figure 4. Additional cycling of specimen 1 has been performed and the data which have been obtained are being studied.

FUTURE PLANS.

In the coming year, additional test specimens will be loaded with a high initial preload to be followed by cycling at lower loads. The peak and residual strains will be measured. Some specimens will be cycled with a spectrum-type of loading after the preload, in an effort to determine how this type of loading affects residual stress and strain, as opposed to constant-magnitude cyclic loading. By taking the time history of strain measured at some point near the hole and duplicating this time history on a simple tensile test coupon, an attempt will be made to determine the variation of residual stress around the hole under cyclic loading.

UTILIZATION OF GAMMA RADIATION TO ENHANCE PROPERTIES OF POLYMERS
AND TO INITIATE POLYMERIZATION OF MONOMERS

G. HARGREAVES

Background

The use of ionizing radiation to initiate chemical changes offers a number of unique advantages over conventional chemical techniques. Certain reactions can be induced which are not possible, or convenient, by other means. The control over reaction conditions is extended; the temperature is not a limiting factor, since many radiation-induced changes are only slightly affected by temperature changes. Modification of long-chain polymers by radiation has aroused considerable interest in recent years. The sometimes marked changes produced in such polymers by radiation do not depend on any special chemical effect that is different from those obtained in smaller organic molecules, but do result from the fact that the physical properties of such polymers are easily modified by small changes in molecular arrangement.

Objectives

1. To develop a capability in the use of gamma radiation to process polymers, their composites, and monomers, and to enhance their properties. Desirable improvements would be increased flexural strength, abrasive resistance, hardness, and resistance to higher temperatures.

2. To polymerize relatively stable monomers by gamma radiation to produce new and unusual polymers.

Accomplishments

1. The Gammacell 220 was returned to the manufacturer and rejuvenated. It contains 12,586 curies of cobalt 60. The measured dose rate in the center of the irradiation chamber is now about 1.0×10^6 rads per hour of gamma radiation. The half life of cobalt 60 is 5.26 years.

2. An irradiation helix is connected with the system for emulsion or solution polymerization. This is a closed system with temperature, atmosphere and amount of radiation under controlled conditions. Figure 1 is a diagram of the system, the reservoir(1) holds the material (in liquid form) to be irradiated. Several openings in the reservoir provide for the entrance of solvent, monomer, nitrogen or other gas into the system, or it may be attached to a vacuum line. A circulating pump(2) forces the liquid through the system. It passes through a flow meter(3) and then through a heating or cooling unit(4). Next the liquid material is forced through the helix in the gamma cell irradiation chamber(5). After leaving the irradiation chamber the pressure can be measured(6). Samples may be withdrawn at(8) then the remainder returns to the reservoir and repeats the cycle. This equipment may also be used for vapor phase polymerization.

3. Objective 1 has been realized. Styrene has been polymerized in an emulsion to produce a film forming polymer. Styrene has been grafted onto nylon fabric to produce a fabric with improved tearing strength, and other
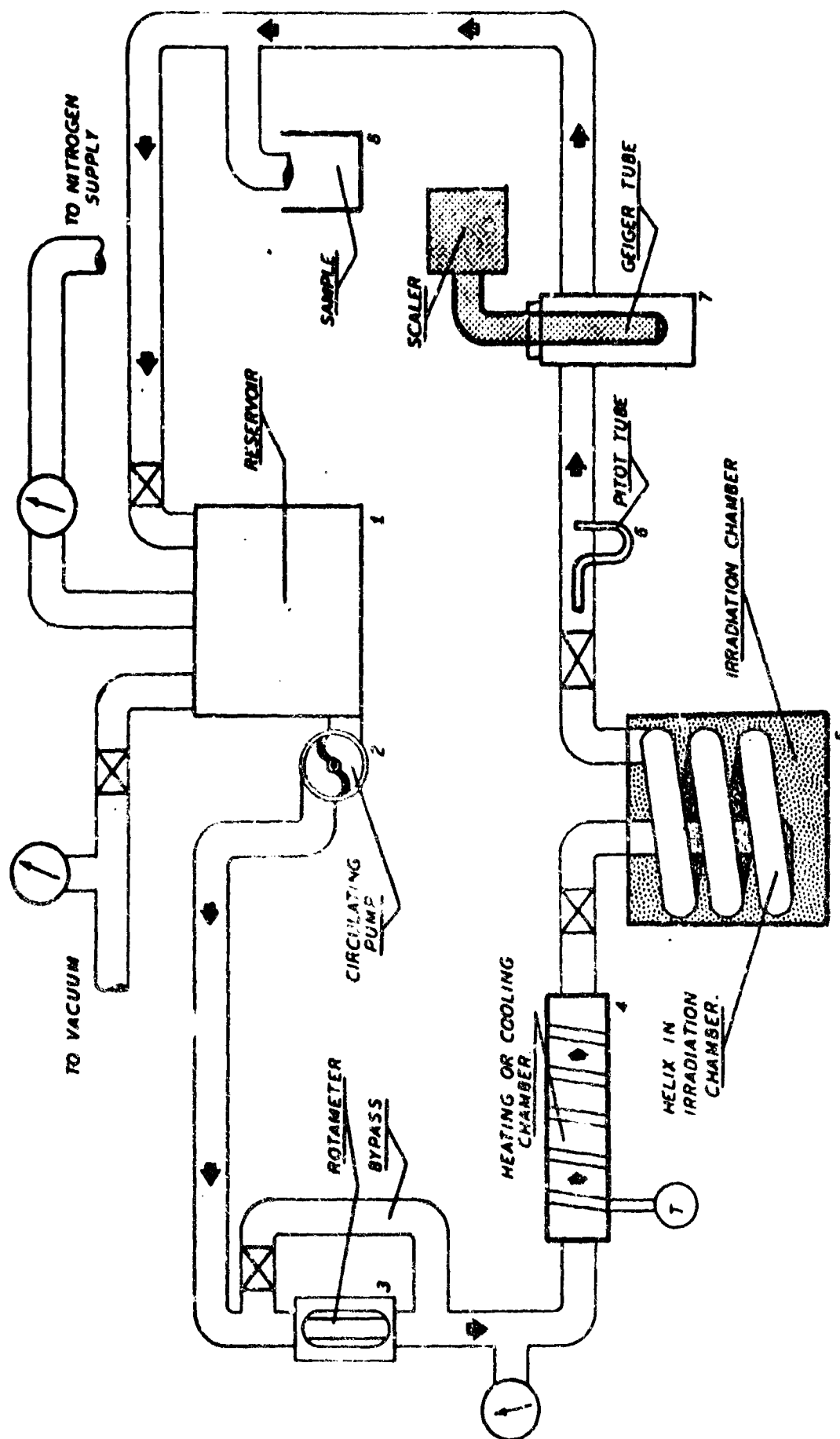
-..-

FIGURE 1. FLOW DIAGRAM FOR RADIATION POLYMERIZATION OF LIQUID MATERIALS

FLOW DIAGRAM FOR RADIATION POLYMERIZATION OF LIQUID MATERIALS

properties for "outdoor" use.

    4. Some adhesives for laminates have been irradiated in situ. This
work shows promise but has not been explored further due to the lack of
personnel.

    5. Benzophenone (⬡-C-⬡ with O double bonded) has been dissolved in a number of
solvents-acetone, benzene, chloroform, ethanol, methanol, and irradiated to
various levels. Benzophenone in ethanol produced a crystalline material
which melted at 150-180°C, benzophenone melts below 50°C. When dissolved in
chloroform and irradiated with a dose of 4.8×10^7 rads, an orange-red precipitate
was formed. This material does not melt or decompose below 300°C.

Future Plans

    Since the work with benzophenone and similar monomers seems to have
possibilities for successful polymerization by irradiation, more work with
these monomers is planned. There are also many aliphatic structures as
well as aromatic, which have excellent potential as polymers which should be
explored. The estimated completion date at this time is 1 July 1967.

STUDY OF THE MECHANISM OF WATER COALESCERS

R. H. SHERTZER AND H. LINDENHOFEN

Background

Aircraft fuels contain appreciable amounts of dissolved, and, under certain conditions, emulsified water. The emulsified or "free" water present in the fuel system can have an adverse effect upon the in-flight operation of the aircraft 1/. To control this problem, filter separators have been inserted into the fuel dispensing system to remove emulsified water prior to aircraft fueling. These filter separators contain coalescer elements composed of glass fibers which coalesce the emulsified water in the fuel. This coalescence process is a phenomenon which depends upon the energetics of the surfaces of the solid, water, and hydrocarbon present in the system. The service life of the coalescers is affected by the type of system they are operating in; i.e. in some systems elements remove the emulsified water satisfactorily for a long period of time, whereas in other systems the elements fail quickly and the emulsified water passes through the coalescer element. An explanation of this problem can only be obtained by a better understanding of the variables which affect this water separation process. The present trend of thought indicates that surface active (surfactant) material present in the fuel, in the form of additives or contaminants, drastically reduces the efficiency of the coalescer by being adsorbed on the fibers 2/. Certain experimental techniques, viz. the drop volume - experiment, also support this hypothesis 3/. The present phase of this investigation is directed toward the study of the effect of surfactants present in the hydrocarbon phase on the fibers used in the coalescer.

Objectives

The purpose of the present investigation is to determine if fibers used in the coalescers will quantitatively adsorb an acid from a non-aqueous solvent. This would enable the investigators to obtain an estimate of the surface area of the fibrous material, in order to develop a method by which adsorption on fibers could be observed in the hydrocarbon fuel system presently in use.

This information would give the investigators a method whereby they would be able to estimate the surface area being poisoned by the additives or contaminants present in the fuel. By the addition of known surface active agents into an uncontaminated fuel, the relative adsorption strength of the additives may be obtained by the method described above.

In addition to the acid adsorption experiment, the surface energies of certain solid - water - hydrocarbon systems will be investigated to support the adsorption theory, and to study the effects of certain solids on the energetics of their surfaces.

Accomplishments

An intensive literature search, which was undertaken, led to the following conclusions:

(1) The process of coalescence is a much neglected and complex field. Some of the studies of coalescence found in the literature could not be applied to the problem at hand, since they delt only with systems where two phases were present - (e.g.) water, hydrocarbon 4/ - excluding the solid phase from the system completely. Since the solid phase (fiberglass) is present in the coalescer elements in use, the foregoing method would not shed much light on the problem.

(2) An attempt has been made to construct an instrument which would give an indication as to the separation properties of a small scale coalescer 5/. This method rates a fuel or hydrocarbon system by a photometric estimation of the amount of emulsified water passing through the coalescer element. This instrument is calibrated by adding trace amounts of surfactant to a standard fuel. However, the method does not explain how the surface active agents affect the coalescence of water in the system.

(3) Another approach to the problem which has merit is the study of the wettability of certain solids by water in different hydrocarbon media by contact angle and interfacial surface tension measurements 3/. This method will be used in future investigations.

(4) The method that has been pursued since April 1965 is one in which we are attempting to show that surface active material is adscrbed on the glass fibers, rendering them unable to coalesce the emulsified water in the system. If we can accomplish this, then a method could be devised to evaluate the adsorption of additives that are present in the fuels and the constituents present in the base fuels themselves. Specifically, a method is being developed to measure the surface area of glass fibers by the adsorption of palmitic acid $(CH_3(CH_2)_{14}COOH)$ from a dry benzene solution. Harkin, et al 6/, 7/ have used this method to determine the apparent surface area of fine powders. The method used is a titration of the palmitic acid before and after exposure to the fiberglass. The amount of acid adsorbed is calculated from the difference in the amount of alcoholic KOH used to titrate the sample and the blank. A specific problem encountered to date is the fact that the fibers have a much smaller surface area per unit weight than the powders hitherto used. The fiberglass is supposed to have a surface area from 1 - 3 square meters per gram as opposed to a much larger area for the powders 8/. The success of the method depends upon the accuracy with which the acid present in the solution is determined. Initially, it was believed that a colorimetric titration with phenolphthalein as indicator would suffice 9/.

FIG. 1.

ADSORPTION RATE of
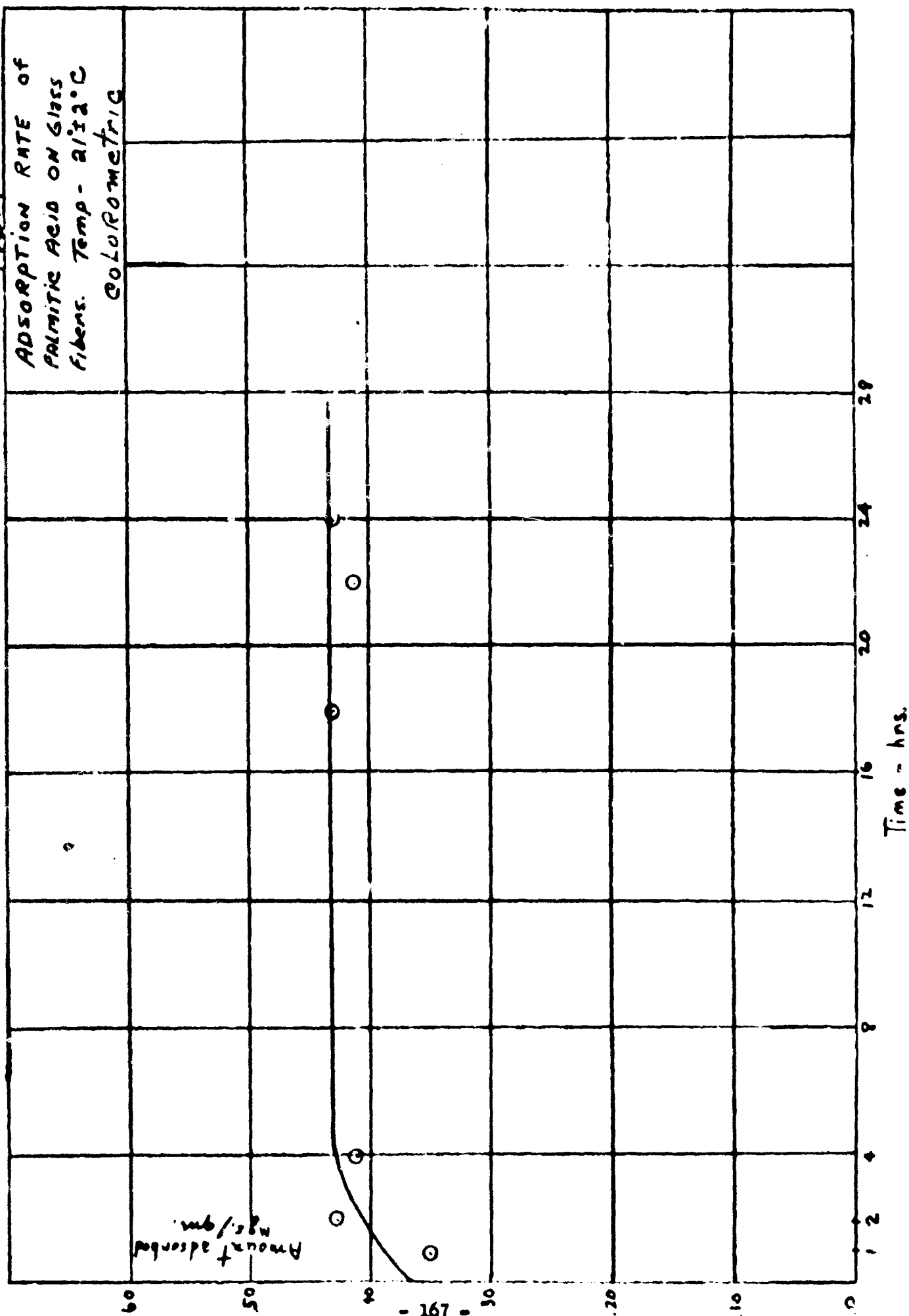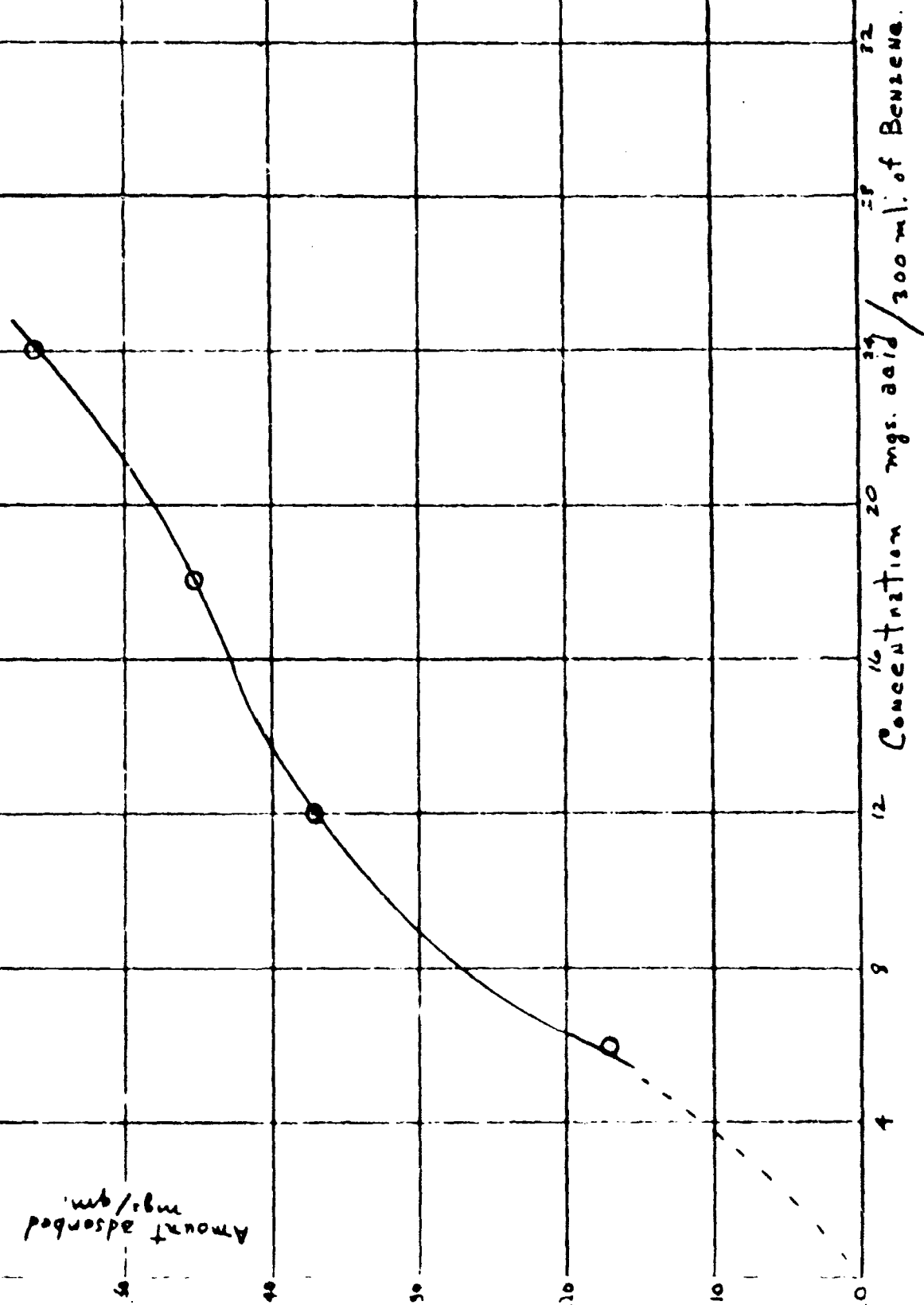PALMITIC ACID ON GLASS
fibers. Temp - 2/22°C
Colorometric

Time - hrs.

Amount adsorbed
mgs./gm.

FiG 2.

ADSORPTION ISOTHERM
PALMITIC ACID ON
Glass Fibers Temp 18±2°C
Potentiometric.

Amount adsorbed mg/gm.

Concentration mgs. acid/300 ml. of Benzene.

Difficulties were encountered due to the fact that the color change was very weak because the concentration of the KOH is about 0.01 Normal. However, same data of value were obtained by this method. Figure 1 shows the rate of adsorption of Palmitic acid onto glass fibers. To increase the accuracy of the method, an electrometric titration was used to construct the adsorption isotherm (figure 2). The amount of acid adsorbed per unit weight of fiber is plotted against varying concentrations of acid. It can be seen from figure 2 that multilayer adsorption is occurring. In order to obtain an estimate of the surface area, the isotherm should be horizontal in some concentration range. If an isotherm of this type is obtained, the amount adsorbed corresponding to the horizontal portion of the plot, is taken as the value at which a monomolecular layer of acid is covering the surface. Knowing the amount of acid adsorbed and the area occupied by each molecule 10/ the surface area of the fibers may be calculated. The multilayer adsorption found on the fibers may be due to a number of factors 11/. Some of these are the cleaning procedure and quality of reagents used in the experiment, and the method of contact of the solid with the acid solution.

Future investigations will include development of better methods of drying the fibers and solvent, search for a more accurate procedure for the determination of the amount of acid adsorbed, and an experimental setup which would allow more intimate contact between the fibers and the acid solution. Once the feasibility of the method is established, this procedure may be employed to study the interaction of fuel constituents with the fibers.

Future Plans

(1) Continue the study of adsorption of organic acids onto glass fibers in an effort to determine their surface areas, and to apply this method to certain fuels.

(2) Investigate the surface energies of glass and other solids by contact angle and Interfacial Tension measurements on water, hydrocarbon, and solid systems.

(3) Consider the feasibility of radiochemical tracer studies on a full scale or scaled down filter separator unit. If certain surface active agents were tagged, their migration through the system could be monitored continuously. It is my belief that this method would give information as to what is actually happening in the dynamic full scale system.

References

1/ Esso Laboratories, Standard Oil Development Co., Research Division Memorandum, "Factors Affecting the Water Content of Aviation Fuels" by R.F. Finn, W.E. Lifson, Sept., 1953

2/ Coordinating Research Council #(C.A. 35-61) "Development of Research Technique for Assessing the Water Seperation Characteristics of Fuels Containing Surfactants" Oct., 1963, pg. 3

3/ Ethyl Corporation, Ferndale 20, Michigan, "Jet Fuel Decontamination Studies", by H.A. Beatty and C. Walcutt, March 1965, pg 42

4/ Gillespie,T., Rideal, E.K., Trans. Faraday Soc. 52, 173 (1956)

5/ Federal Test Method 3256T, Sept., 1963, Fed. Test Method Std. No. 791a

6/ Harkin, W.D., Gans, D.M., J. Am. Chem. Soc. 53, 2804 (1931)

7/ Smith, H.A., Fuzek, J.K., J. Am. Chem. Soc. 68, 229 (1946)

8/ Private Communication, Corning Glass Works, Corning New York

9/ Mitchell, J., Kolthoff, I.M., Proskauer, E.S., Weissberger, A., "Organic Analysis" Vol. III, pg 18, New York. Interscience Publishers Inc., 1956

10/ Adam, N.K., "The Physics and Chemistry of Surfaces", 3rd edition, pg 51, Table III, London, Oxford Press 1941

11/ Hirst, W., Lancaster, J.K., Trans. Faraday Soc. 47, 318 (1951)

CONDUCTIVE TRANSPARENT THERMOPLASTIC FILMS

I. H. CUSTIS

Background

The accumulation and retention of an electrostatic charge on the surface of materials have been known for some time. The presence of this charge introduces a potential hazard where missiles are involved. Previously, very little work had been done to eliminate this static buildup. This was due to the lack of effective antistatic agents and methods of evaluating their performance. Two methods of evaluation are presently being used; they are the cigarette ash test and the soot chamber test. The latter is being used by the industry to evaluate the electrostatic properties of plastic bottles. Both of these methods are qualitative and only indicate the presence of a charge. A more definitive test method requiring a circular coulometer was used to evaluate the electrostatic properties of the materials studied.

Objectives

The purposes of this program are to develop conductive transparent thermoplastic materials through the use of internal antistatic agents, and to develop a test method which will evaluate accurately their performance in improving the electrostatic properties of materials.

Accomplishments

The electrostatic properties of five materials were evaluated using the coulometer test method. These consisted of three films and two materials which can be applied to films resulting in a transparent coating. The evaluation is listed in Figure 1. An analysis of these data indicates that thermoplastic materials, which are insulators, can also be made conductive through the use of chemical agents. As noted, the hydroxyaquochromium diphenyl phosphinate, which is a new resin, exhibited good electrostatic properties. Polyethylene with an internal antistatic agent, and polyurethane with carbon filaments embedded in the resin, exhibited poor electrostatic properties. The effectiveness of the transparent coatings which are applied to the films, are dependent upon thickness. When a 2% solution of Zelec DP was applied to polyethylene and nylon the electrostatic properties of polyethylene were somewhat improved, as noted by the reduction in the charge retained. For the nylon film, the electrostatic properties were greatly improved. The application of a 4% solution of Zelec DP further improved the electrostatic properties of both the polyethylene and nylon. Two and 4% concentrations of Zelec DX exhibited no effect on the electrostatic properties of the polyethylene; whereas, the properties of nylon were greatly improved.

Therefore, it is believed that the electrostatic properties of thermoplastic material can be improved to the point that the material will be conductive and prevent a static charge buildup. Further, it is believed that this can be accomplished through the use of the proper antistatic agent. No one antistat appears to meet the requirement for all resins.

References

1/ Essc Laboratories, Standard Oil Development Co., Research Division Memorandum, "Factors Affecting the Water Content of Aviation Fuels" by R.F. Finn, W.E. Lifson, Sept., 1952

2/ Coordinating Research Council #(C.A. 35-61) "Development of Research Technique for Assessing the Water Seperation Characteristics of Fuels Containing Surfactants" Oct., 1963, pg. 3

3/ Ethyl Corporation, Ferndale 20, Michigan, "Jet Fuel Decontamination Studies", by H.A. Beatty and C. Walcutt, March 1965, pg 42

4/ Gillespie,T., Rideal, E.K., Trans. Faraday Soc. 52, 173 (1956)

5/ Federal Test Method 3256T, Sept., 1963, Fed. Test Method Std. No. 791a

6/ Harkin, W.D., Gans, D M., J. Am. Chem. Soc. 53, 2804 (1931)

7/ Smith, H.A., Fuzek, J.K., J. Am. Chem. Soc. 68, 229 (1946)

8/ Private Communication, Corning Glass Works, Corning New York

9/ Mitchell, J., Kolthoff, I.M., Proskauer, E.S., Weissberger, A., "Organic Analysis" Vol. III, pg 18, New York. Interscience Publishers Inc., 1956

10/ Adam, N.K., "The Physics and Chemistry of Surfaces", 3rd edition, pg 51, Table III, London, Oxford Press 1941

11/ Hirst, W., Lancaster, J.K., Trans. Faraday Soc. 47, 318 (1951)

CONDUCTIVE TRANSPARENT THERMOPLASTIC FILMS

I. H. CUSTIS

Background

The accumulation and retention of an electrostatic charge on the surface of materials have been known for some time. The presence of this charge introduces a potential hazard where missiles are involved. Previously, very little work had been done to eliminate this static buildup. This was due to the lack of effective antistatic agents and methods of evaluating their performance. Two methods of evaluation are presently being used; they are the cigarette ash test and the soot chamber test. The latter is being used by the industry to evaluate the electrostatic properties of plastic bottles. Both of these methods are qualitative and only indicate the presence of a charge. A more definitive test method requiring a circular coulometer was used to evaluate the electrostatic properties of the materials studied.

Objectives

The purposes of this program are to develop conductive transparent thermoplastic materials through the use of internal antistatic agents, and to develop a test method which will evaluate accurately their performance in improving the electrostatic properties of materials.

Accomplishments

The electrostatic properties of five materials were evaluated using the coulometer test method. These consisted of three films and two materials which can be applied to films resulting in a transparent coating. The evaluation is listed in Figure 1. An analysis of these data indicates that thermoplastic materials, which are insulators, can also be made conductive through the use of chemical agents. As noted, the hydroxyaquochromium diphenyl phosphinate, which is a new resin, exhibited good electrostatic properties. Polyethylene with an internal antistatic agent, and polyurethane with carbon filaments embedded in the resin, exhibited poor electrostatic properties. The effectiveness of the transparent coatings which are applied to the films, are dependent upon thickness. When a 2% solution of Zelec DP was applied to polyethylene and nylon the electrostatic properties of polyethylene were somewhat improved, as noted by the reduction in the charge retained. For the nylon film, the electrostatic properties were greatly improved. The application of a 4% solution of Zelec DP further improved the electrostatic properties of both the polyethylene and nylon. Two and 4% concentrations of Zelec DX exhibited no effect on the electrostatic properties of the polyethylene; whereas, the properties of nylon were greatly improved.

Therefore, it is believed that the electrostatic properties of thermoplastic material can be improved to the point that the material will be conductive and prevent a static charge buildup. Further, it is believed that this can be accomplished through the use of the proper antistatic agent. No one antistat appears to meet the requirement for all resins.

RESULTS OF ELECTROSTATIC PROPERTY EVALUATION
(Volts Retained)

	Untreated	Zelec DP 2%	Zelec DP 4%	Zelec DX 2%	Zelex DX 4%
Hydroxyaquochromium Diphenyl Phosphinate	30	---	---	---	---
Polyurethane with Carbon Filaments	0-200	---	---	---	---
Polyethylene with Internal Antistatic Agent	>300	---	---	---	---
Polyethylene	>300	165	50	>300	>300
Nylon	>300	80	Negligible	85	Negligible

FIGURE 1

Future Plans

Equipment to evaluate the charging, saturation, and decay rate of an induced charge has been purchased, and will be assembled to continue this investigation. Antistatic agents will be incorporated in the material by solvent casting or milling processes and their performance evaluated. Information obtained will be applied on pilot plant equipment.

NEUTRON ACTIVATION ANALYSIS

EDWIN S. TANKINS AND ALFRED L. GLASS

Background.

Neutron activation analysis is a relatively new research tool which offers unprecedented sensitivity in the detection of more than half of the elements in the periodic Table. The sample, as well as a standard, is bombarded with neutrons from a neutron generator, which converts them to an unstable radioactive form. The irradiated samples are then identified and measured quantitatively by means of gamma ray spectroscopy. This method is nondestructive in that the specimen can be reused. It has a sensitivity far better than most chemical or spectrographic techniques. This method of analysis is extremely sensitive, free from reagent contamination, and is a very rapid method of analysis.

Objectives.

A. In the various studies of mechanical properties of materials, it is very important to have alternate gas analysis. Certain metals and ceramic materials are difficult to analyze for gas contents. Nitrogen analysis is difficult in most metals by any method other than the Kjeldahl. The first aim will be to establish a method of oxygen and nitrogen analysis in ceramics and metals, and to correlate these results with physical and mechanical properties. The authors are on ASTM Committees and will be involved in round robin programs involving neutron activation analytical procedures.

B. Lubricating oil, hydraulic oil, and greases will be examined quantitatively to determine accurately minute particles and how they vary with time and tests. These analyses will be involved in programs to investigate wear and to make correlation with a theoretical model

C. Trace quantities of materials in metals, due to diffusion, will be investigated. This will be related with metal-to-metal wear.

Accomplishments.

A. Detailed plans have been made for setting up the site for the system of equipment necessary to perform neutron activation analysis.

B. A survey of pertinent literature is underway.

Future Plans.

Purchase of the equipment is in progress. As soon as the equipment has been delivered and installed, personnel will familiarize themselves with the equipment and the first phase of the program will get underway.

STUDY OF SYNTHETIC FIBER CLOTH VARIABLES, ACCELERATED WEATHERING VARIABLES AND THEIR INTERACTION

WARREN T. KELLY

Background.

The differences in degradation experienced with various fibers and in atmospheric contaminants at various test locations, have prevented complete agreement in magnitude of degradation or method of assessment for weathering determinations. The deterioration produced by exposures in moist humid air has always been reported as greater than tests in dry air. However, tests performed on Aeronautical Materials Laboratory accelerated weathering apparatus, to evaluate deterioration of nylon cloths exposed without the water spray operating, indicated greater deterioration when moisture was omitted.

Objective.

The accelerated weathering equipment, while conforming to government and commercial test procedures, does not control adequately temperature and humidity conditions or prevent contamination by materials in the atmosphere. To determine if this anomaly is caused by operating conditions, the equipment manufacturer is exposing specimens prepared from available fabrics in a research type accelerated weathering apparatus. Analysis of these preliminary samples may indicate that differences in expected deterioration are due to nylon properties. Based on this analysis, the investigation will be continued. Cloths specially prepared to control significant variables will be used, and exposed in equipment that can control all known variables to determine optimum materials, test procedures, and operation instructions for textiles for sea survival equipment.

Accomplishments.

Test specimens for accelerated weathering exposure were prepared from five nylon cloths of known history for six test conditions at Atlas Electric Devices and three test conditions at the Aeronautical Materials Laboratory. The planned exposure at the Aeronautical Materials Laboratory- 30 hours of light with standard, continuous, and no water spray - has been completed. One set has been exposed at Atlas Electric Devices and is being returned for strength tests.

Future Plans.

Upon completion of present exposure tests and analysis, the data will be reviewed and detailed plans developed. The approximate completion date is 1 July 1967.

HEAT TRANSFER AND SURFACE WEAR STUDIES ASSOCIATED WITH FRICTION TYPE CLUTCH AND BRAKE ASSEMBLIES

S. BRITTINGHAM

BACKGROUND

Present day and future high capacity clutch and brake requirements imposed by Small Airfield Tactical Support (SATS) catapult systems make it neces-sary to determine design criteria for development of reliable, long life clutch and brake systems. It was concluded, from contacts with organiza-tions connected directly with high capacity clutch and brake system design, that empirical approaches are primarily being used in the design phase, and that an analytical approach is needed for future clutch and brake design studies. Consequently, this study was initiated to develop a method of de-termining thermodynamic, lubrication, and wear characteristics of friction surfaces rubbing together; and to utilize the resulting methods as design criteria for present day aircraft launching and arresting systems, using friction surfaces to translate or dissipate energy.

OBJECTIVES

An electronic digital computer will be programmed to simulate conditions anticipated at the surface of two unlike materials rubbing together and generating heat, and studies made to determine the thermodynamic charac-teristics at the surface and within the configuration selected. Computer programs will be developed to analyze one, two, and three-dimensional con-figurations; as progress is made, parameters such as lubrication and wear will be added.

A one-dimensional configuration is used when the temperature gradient is one-dimensional or can be represented as one-dimensional with insignifi-cant error. The transient temperature can be determined for rubbing sur-faces and surfaces exposed to cooling media. Consequently, the one-dimensional program can be used to approximate: (1) the surface tempera-tures of dry clutch and brake systems; and (2) the temperature distributions in lubricated or liquid-cooled configurations at regions remote from cool-ing fluid grooves, where one-dimensional analysis applies.

The two-dimensional program is developed primarily to analyze cooling fluid groove shape and thin film cooling. The two-dimensional physical model represents two rubbing surfaces with a network of cooling fluid grooves. With this configuration, the cooling fluid groove will be varied in size to determine an optimum cooling fluid area to bearing area ratio and groove size

Finally, a three-dimensional configuration, incorporating the experience and technique gained in one and two-dimensional analysis, will be developed to analyze thermodynamic characteristics, cooling fluid dynamics, wear pheno-mena, and lubrication of rubbing surfaces. Emphasis is placed on clutch and brake systems; however, the programs developed are applicable to any problem area where surfaces rub or are exposed to cooling fluid.

The ultimate goals of this study are to:

1. Provide design criteria to develop clutch and brake systems applicable to the present day and future generation high-capacity aircraft launcher and arresting systems.

2. Develop a method of predicting transient temperature distributions at the surface and within two materials generating heat by rubbing together.

3. Examine the mechanism of wear and develop a criteria for predicting wear based on surface pressure, temperature, and relative motion of the bearing or contacting surfaces.

4. Examine the effects of various cooling and lubricating fluids and cooling fluid groove design to establish an optimum configuration for minimum wear maximum cooling efficiency.

PROCEDURE

The difficulty anticipated in the solution of the three-dimensional wave equation

$$\nabla^2 T \propto \partial T / \partial t$$

advocates the use of numerical methods of solution. Consequently, the mathematical model or models used in this study consists of nodal networks applicable to the forward difference numerical method, which reduces the three-dimensional wave equation to the form

$$\left(\sum_2 T_2 - \lambda T_o \right) / \delta^2 \propto \partial T / \partial t$$

Where T_1 is the temperature of nodes adjacent to the primary node T_o and λ a dimensional factor.

At nodal points representing surfaces adjacent to cooling media the Nusselt relation

$$N_{NU} = .023 \, N_{Re}^{.8} \, N_{Pr}^{.3} \left(\frac{\mu_m}{\mu_w} \right)^{.14}$$

will be used. However, during the preliminary phase of this investigation, a constant Nusselt number and corresponding convection coefficient will be used. The convection coefficient will be varied over a wide range of values to determine the effect of this parameter on overall performance.

The unit nodal dimension is selected for proper subdivision of the cooling fluid groove. The groove depth is divided into a number of equal parts and the length of one division is used as the unit dimension and thickness of the two-dimensional physical model. The physical model is subdivided into cubic subvolumes with the length of each side of the cube equal to the unit dimension. The physical properties of the unit cubes are considered concentrated at the geometric center of the cubic subvolume, and each subvolume

or node is connected by a heat transmission path whose resistance to heat flow is related to thermal conductivity k, area normal to flow direction A and distance between nodes L by the relation,

$$R = kA/L$$

The time increment over which thermal change occurs is not an arbitrary parameter and must be related to the nodal dimension such that particular coefficients in the equations describing nodal temperatures are positive or zero. Consequently, the time increment selected must be computed for each unit nodal dimension used and is not an independent variable.

SUMMARY OF PROGRESS
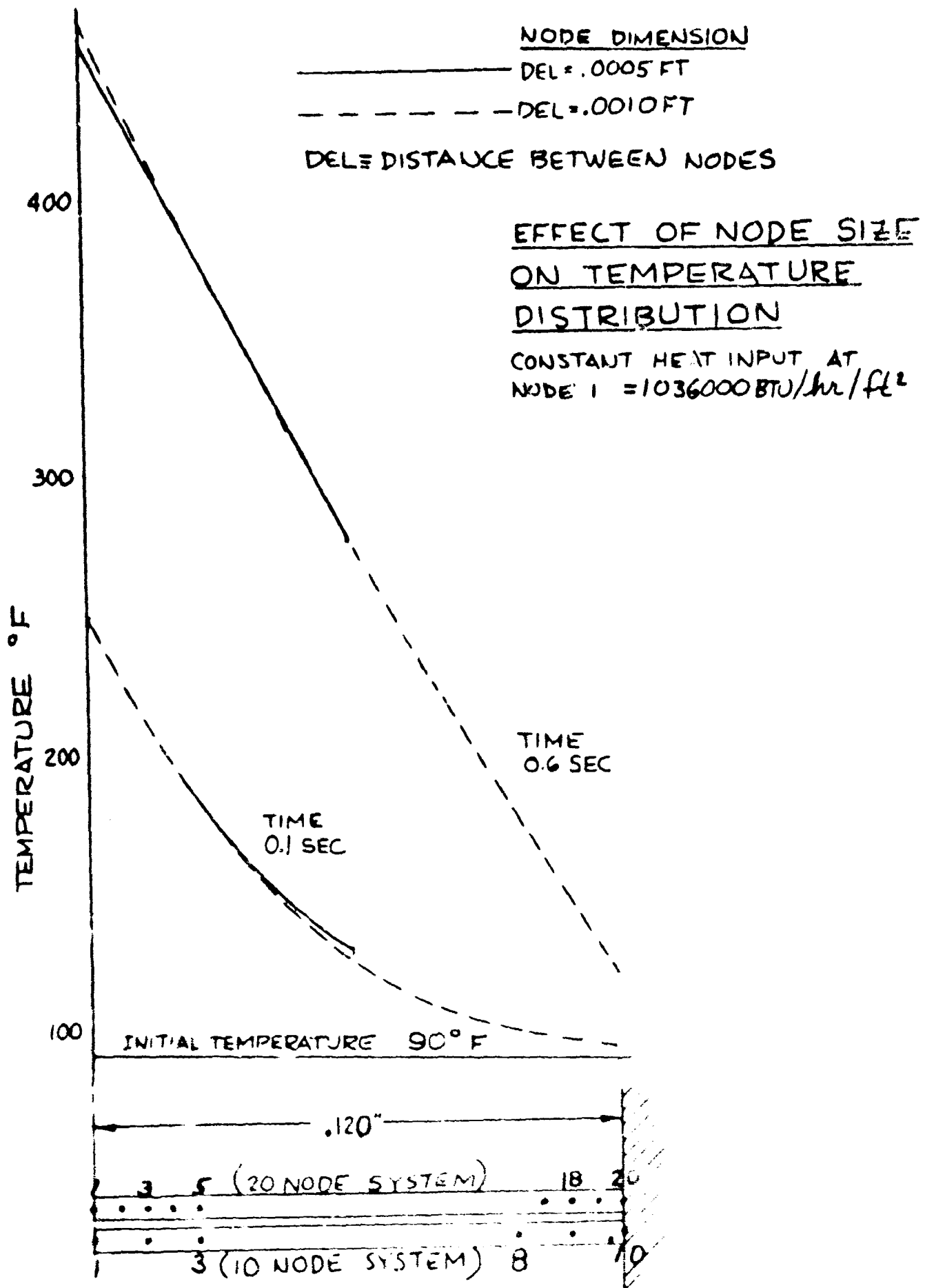
A. One-Dimensional System

A preliminary investigation was conducted to determine the effect of node size variation and violation of the condition imposed by the Fourier number. The transient temperature distributions were determined for a one-dimensional system consisting of a thin 0.120 inch long ray of material imbedded in a perfect insulator, and having a heat source at one end as shown by Figure 1.

To determine the effect of node size variation, the material ray shown on Figure 1 is divided into ten and twenty subvolumes, and the transient temperature distribution computed for each configuration. The temperature distribution after .1 and .6 seconds with a constant heat input of 1,036,000 BTU/hr/ft^2 for nodal dimension of .0005 and .0010 feet are shown on Figure 1. It is concluded from the results of this study that, in this case, node size variation has insignificant effects on temperature distribution.

A study was conducted to determine the effect of exceeding the time increment imposed on the program by the Fourier modulus. For the configuration shown a modulus of .5 or less was required. The temperature at node 1, the surface node, is computed as a function of time using moduli of .43, .55 and .59 and plotted on Figure 2. The results indicate that the Fourier modulus restriction is a critical factor and care should be exercised in studies of higher dimension to ensure that the imposed conditions are satisfied.
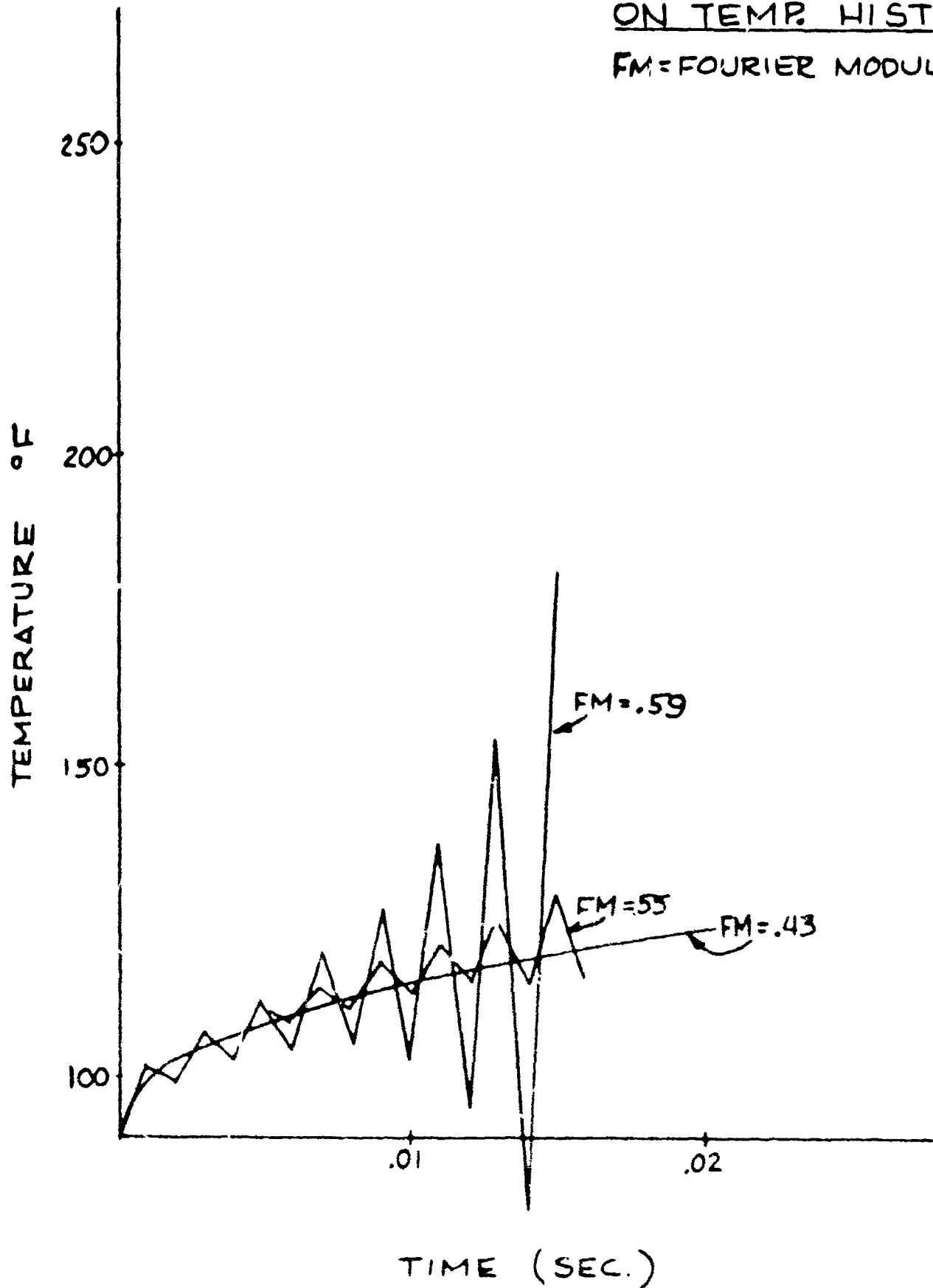
The one-dimensional program is expanded to analyze two surfaces rubbing together by adding, to the existing one-dimensional configuration, a mirror image ray of material with different physical properties, resulting in the configuration shown by Figure 3. Node 1 of the resulting configuration is composed of two different materials and a heat source. The heat rate history and corresponding temperature history are also shown on Figure 3. The transient temperature distribution as a function of penetration depth is shown by Figure 4.

From the results presented, it is concluded that the one-dimensional program for analyzing the thermodynamic characteristics of two surfaces is complete, and an attempt to correlate calculated values with test data will be initiated as part of the next phase of this study.
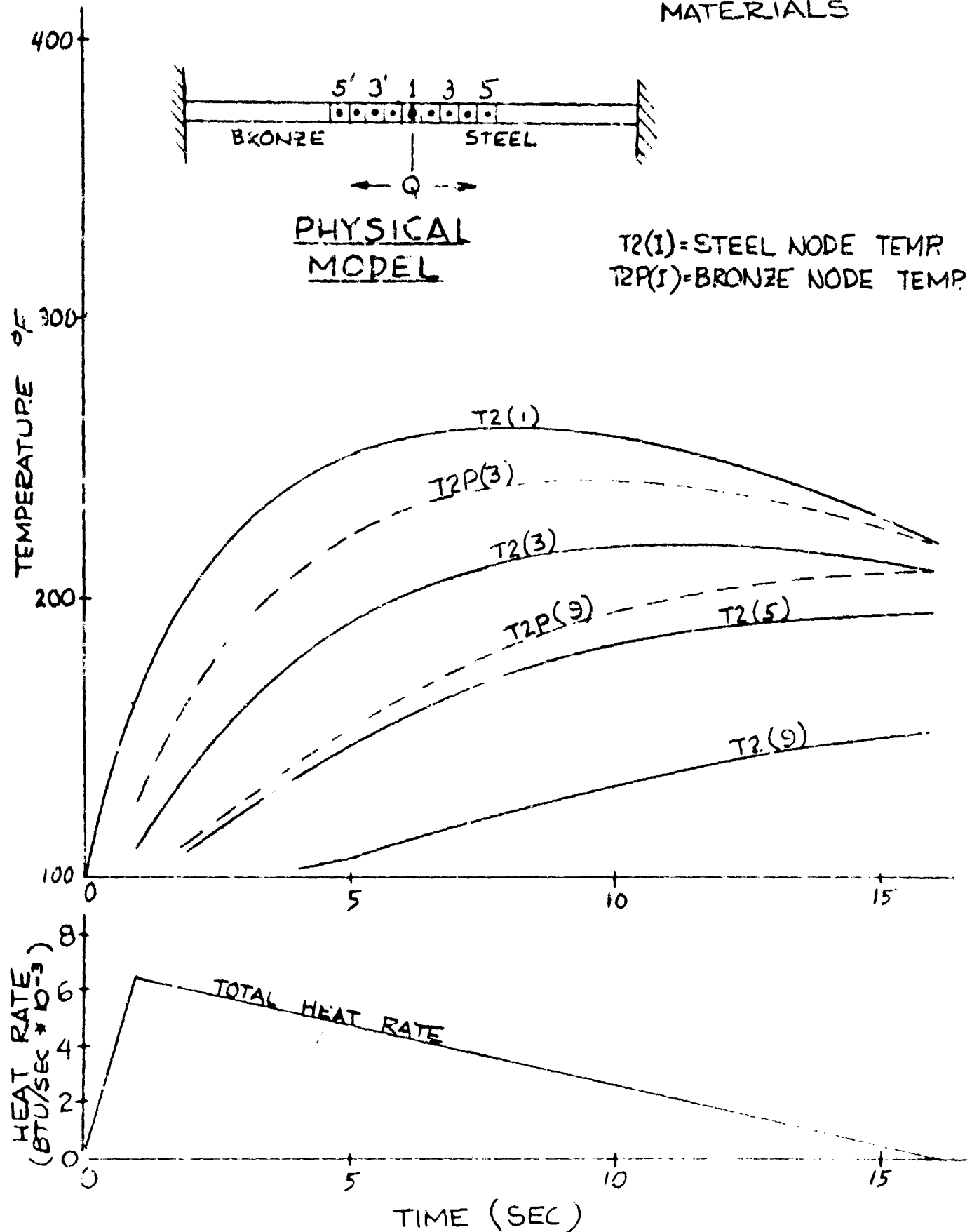
NODE DIMENSION

—————————— DEL = .0005 FT

— — — — — — DEL = .0010 FT

DEL = DISTANCE BETWEEN NODES

EFFECT OF NODE SIZE
ON TEMPERATURE
DISTRIBUTION

CONSTANT HEAT INPUT AT
NODE 1 = 1036000 BTU/hr/ft²

TIME
0.6 SEC

TIME
0.1 SEC

INITIAL TEMPERATURE 90° F

.120"

3 5 (20 NODE SYSTEM) 18 20

3 (10 NODE SYSTEM) 8 10

FIGURE 1

EFFECT OF FOURIER
MODULUS VARIATION
ON TEMP. HISTORY

FM = FOURIER MODULUS

FM = .59

FM = 55

FM = .43

TEMPERATURE °F

250

200

150

100

TIME (SEC.)

.01   .02

FIGURE 2

ONE DIMENSIONAL
HEAT TRANSFER
HEAT GENERATING
SURFACE BETWEEN
TWO DIFFERENT
MATERIALS

PHYSICAL MODEL

T2(I)=STEEL NODE TEMP.
T2P(I)=BRONZE NODE TEMP.

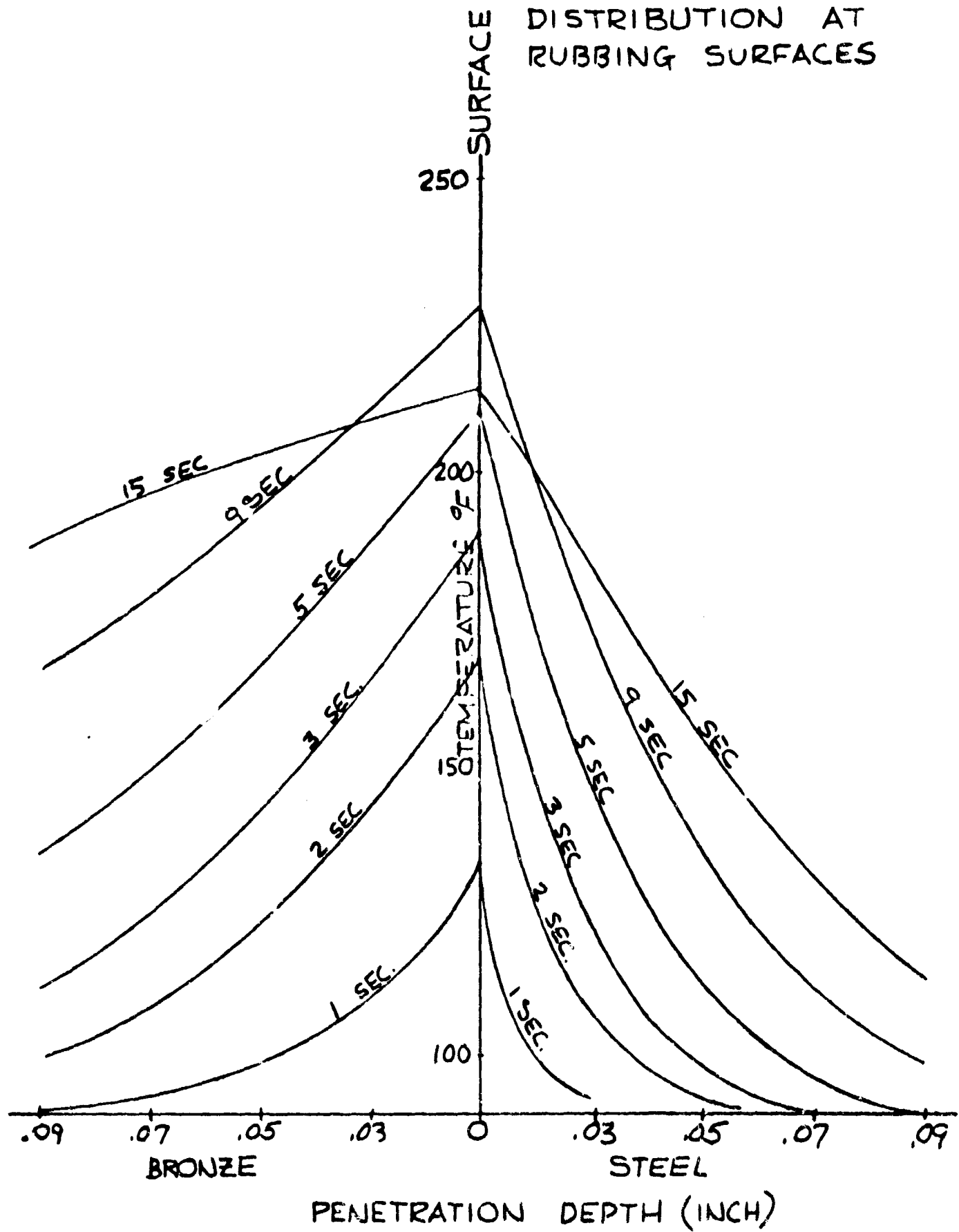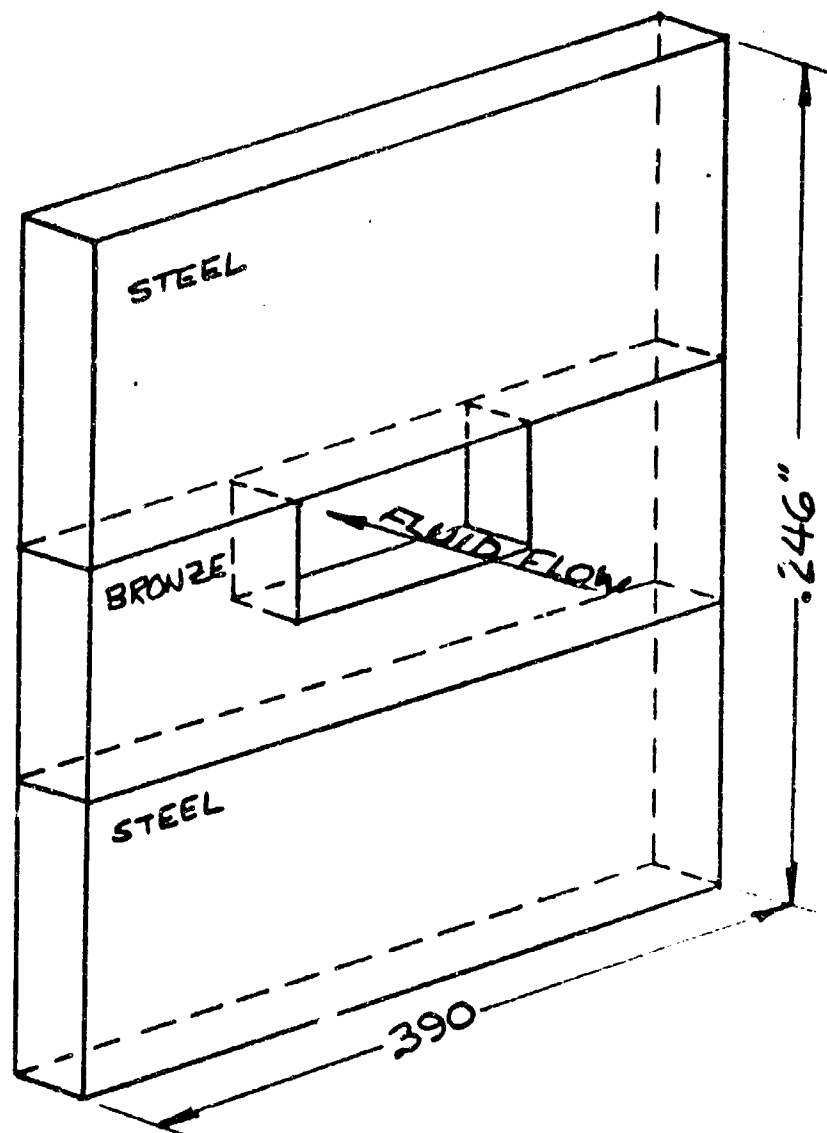FIGURE 3

TRANSIENT TEMPERATURE DISTRIBUTION AT RUBBING SURFACES

FIGURE 4

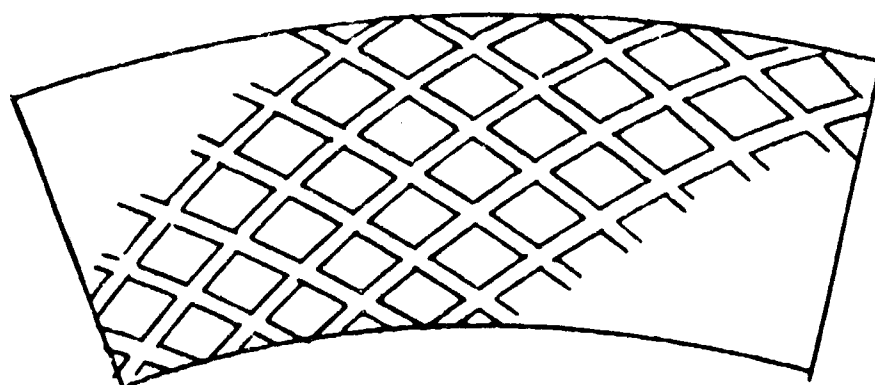2·DIMENSIONAL PHYSICAL
MODEL

FIGURE 5

THERMOCOUPLE

CLUTCH DISC

ACTUATING PISTON

INPUT
SHAFT

OUTPUT
SHAFT
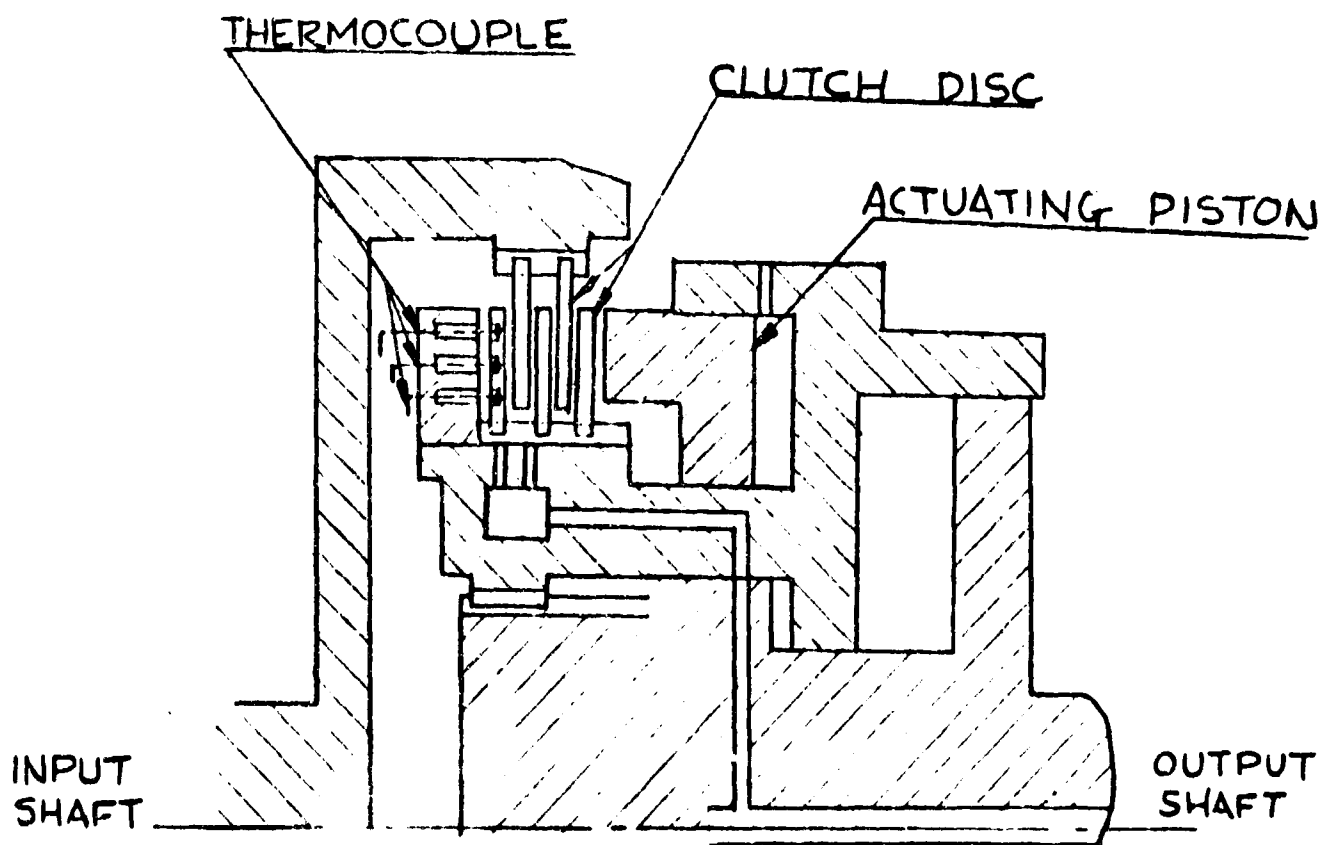
FRICTION DISC
TEST APPARATUS

FIGURE 6

BRONZE DISC SURFACE
GROOVE DESIGN PATTERN

FIGURE 7

TYPICAL LOCATION
OF THREE DIMENSIONAL
PHYSICAL MODEL

.394"

.394"

FLUID FLOW

TYPICAL LOCATION
OF TWO DIMENSIONAL
PHYSICAL MODEL

FLUID FLOW

FLUID GROOVES

.0469"

FLUID GROOVE

STEEL

BRONZE

STEEL

.123"

.50"

.25"

.0735"

STEEL
DISC

BRONZE
STL. DISC

SECTION SHOWING
LOCATION OF TWO
DIMENSIONAL MODEL
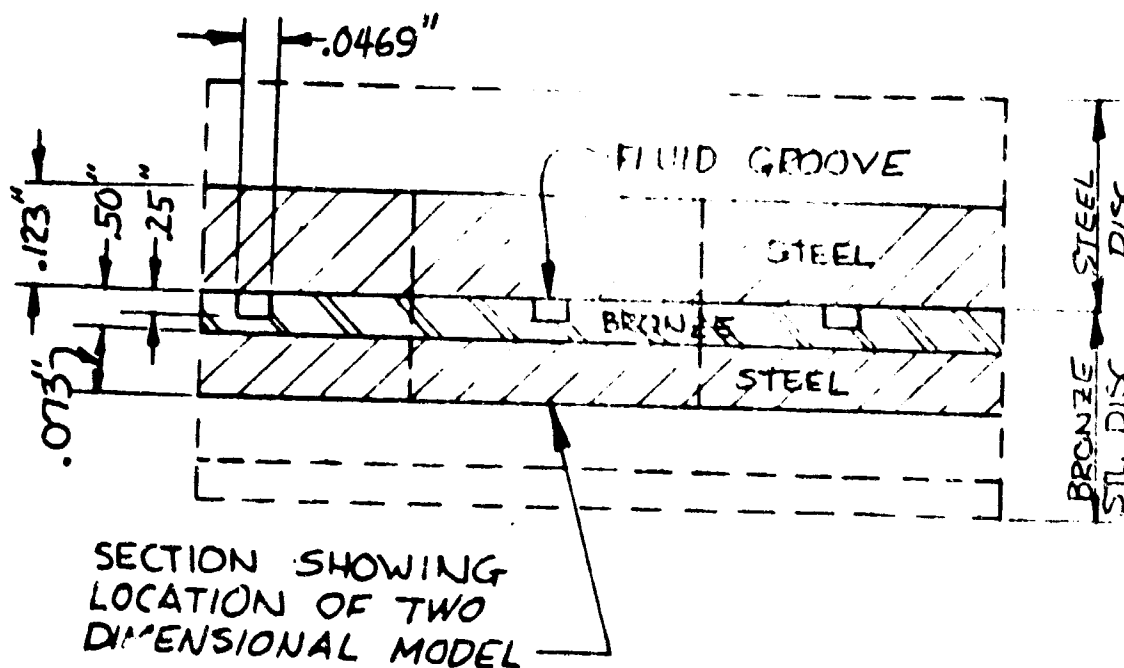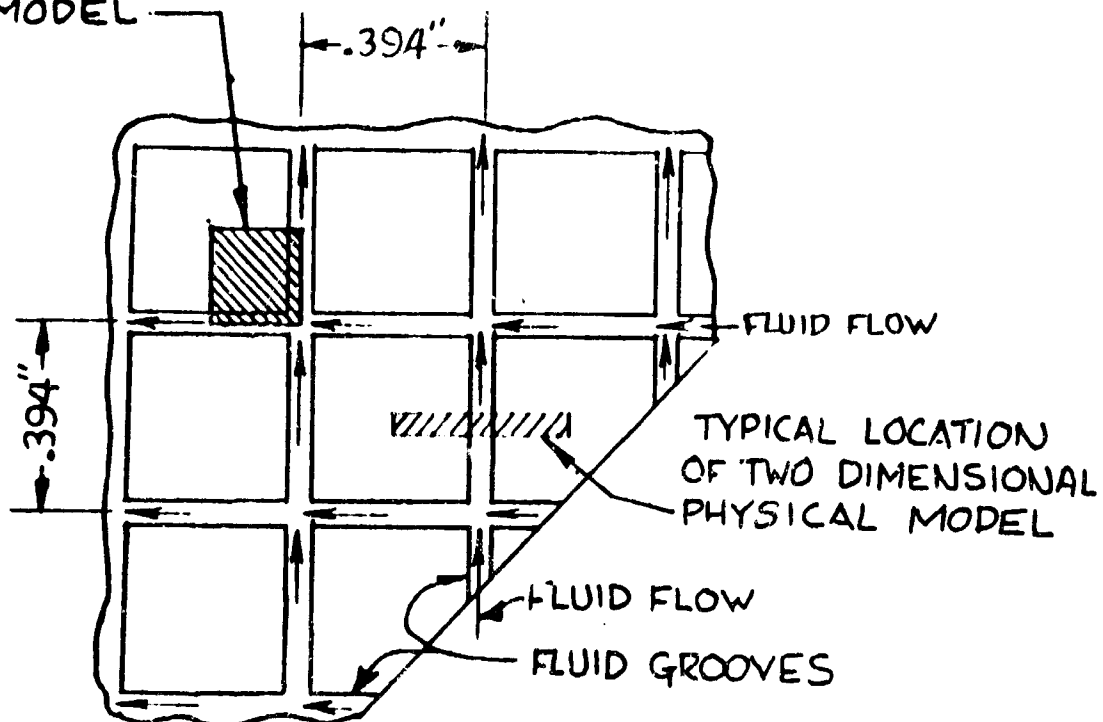
IDEALIZED FRICTION DISC

FIGURE 8

ONE DIMENSIONAL ARRAY

II   IM

STEEL

KL

BRONZE

GROOVE

TI(6,13)

KM

TI(3,11)

KK

TYPICAL
INTERIOR NODE

STEEL
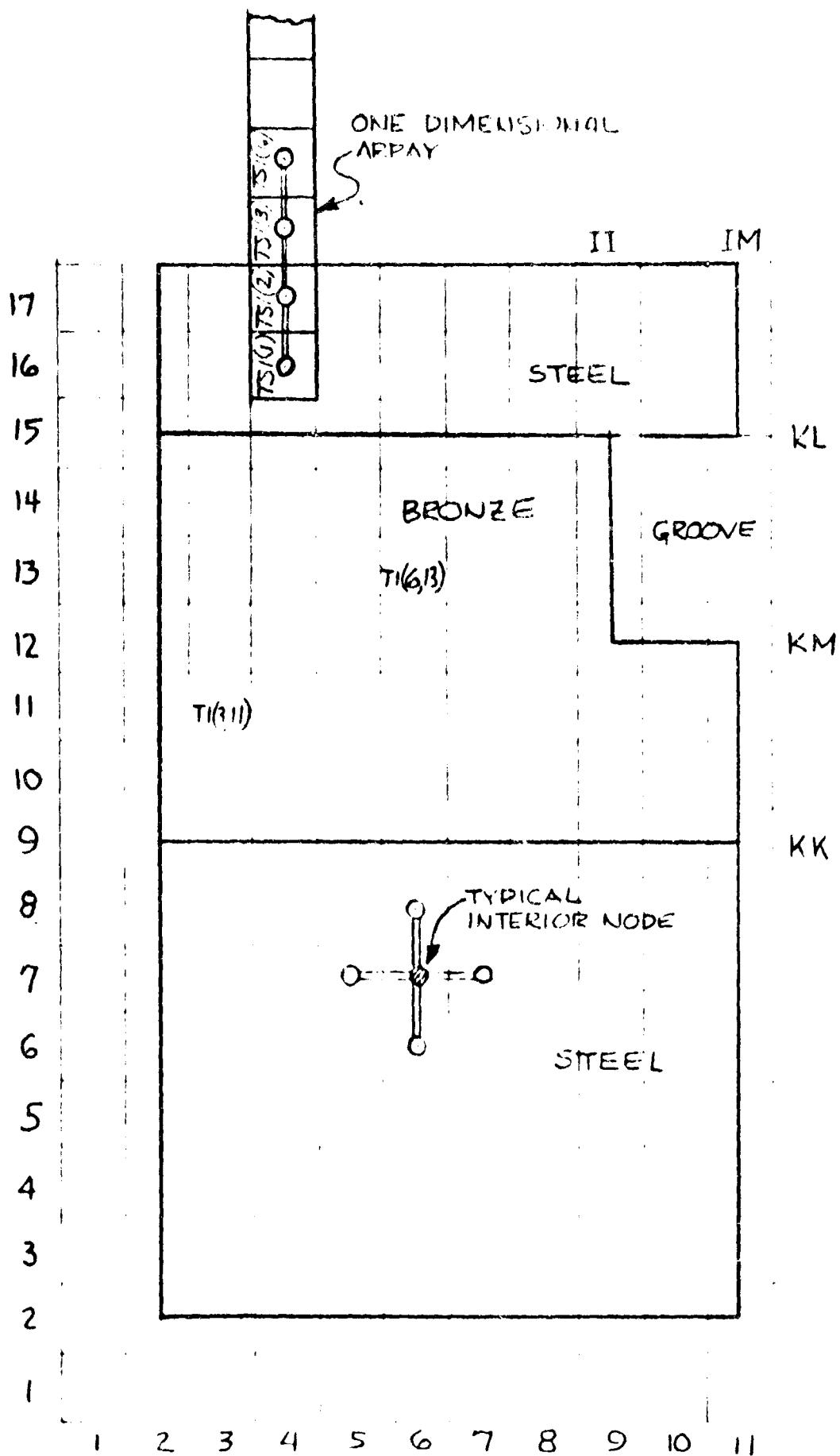
TWO DIMENSIONAL
MATHEMATICAL MODEL

FIGURE 9

MODEL USED FOR THREE
DIMENSIONAL ANALYSIS

FIGURE 10

B. Two-Dimensional System

Since this study was initiated primarily to analyze friction discs used in high capacity clutch and brake designs, emphasis will be directed toward this area. A prototype of a typical clutch or brake system, shown schema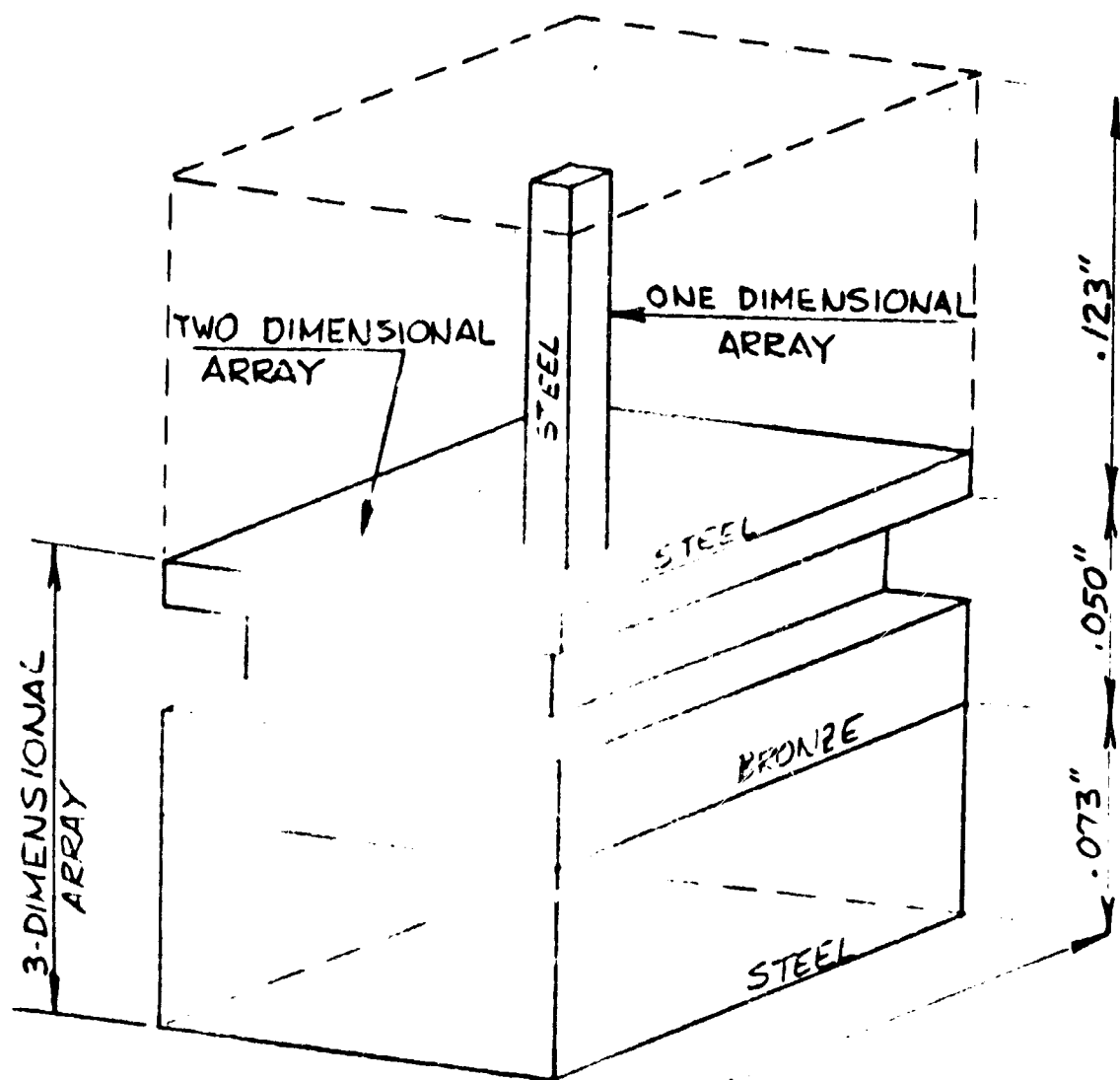tically by Figure 6, is available for testing, and a two-dimensional model is constructed to facilitate analysis of this system. A section of the clutch plate shown by Figure 7 is idealized on Figure 8, and the two-dimensional physical model, shown by Figure 5, is taken from the shaded region of Figure 8.

Early in the two-dimensional programming phase, it was found advantageous to construct the mathematical model in a one and two-dimensional array. The one-dimensional array is used to describe the thermodynamic characteristics of the surface that is in motion relative to the cooling fluid grooves. By virtue of this motion the nodal position is continually changing, and an averaging process is indicated for analysis of temperature distribution associated with the moving surface. To this end, the temperature of all nodes in the KL+1 layer, shown by Figure 9, are computed with the two-dimensional array then averaged. The average temperature is then used as the temperature of the first node in the one-dimensional array.

For a complete analysis of the two-dimensional system the IBM 1620 scientific computer is impractical and a computer with larger core capacity must be used. A limited version of the two-dimensional program was analyzed with the 1620 computer and found to be in working order. Conversion of the program for the larger computer is readily accomplished and will be completed in the near future.

C. Three-Dimensional System

The three-dimensional program is an extension of the two-dimensional program. Development of the three-dimensional program will be in steps of increasing flexibility and complexity. The first three-dimensional program will be designed to determine the transient temperature distribution, using a constant Nusselt number at the fluid boundries. A second program will add to the above analysis the effects of fluid dynamics and groove design. Finally, the mechanism of wear will be included in the final analysis, and the analytical results of all parameters compared with empirical results.

The three-dimensional program is in the preliminary development phase and completion of the preliminary program is related to progress of the two-dimensional program results.

The problem of relative motion between the steel and grooved bronze discs is present in the three-dimensional case, and a method must be developed to include relative motion as was done in the two-dimensional case. To this end, the physical three-dimensional mathematical model is divided into a one, two and three-dimensional array as shown by Figure 10. The K layer notion used in the two-dimensional model, shown by Figure 9, is used to describe nodal locations in horizontal planes. Each layer is then

divided into a grid or matrix of I by J subdivisions, and the layers are
thereby reduced to a network of cubic subvolumes which are readily reduced
to a three-dimensional nodal network. Individual nodal temperatures are
described with the three-dimensional matrix notation $T(I,J,K)$.

The temperature of the moving surface is computed by combining the
KL+1 layer with the three-dimensional array and using standard three-
dimensional methods. The temperatures of the KL+1 layer are then averaged,
and the average temperature is used as the temperature of the first node of
a one-dimensional array.

D. Wear

When consideration is given to surface roughness on a microscopic level,
the material surface is not well defined. The surface is composed of a
large number of asperities or protuberances, and the actual surface bearing
area ranges from zero to the apparent area as pressure is applied. Physi-
cally, only a small area is on contact and considerable localized pressure
is anticipated. It is theorized that the bearing asperities are plastically
deformed and are free to move on surface without apparent damage. This
asperity motion could possibly be used to describe friction, and when an
adequate theory is developed information available on friction forces could
be used to substantiate the theory. The results of a library search leads
to the conclusion that a statistical approach would best be suited to des-
cribe wear based on asperities.

E. Future Plans

1. Complete two-dimensional heat transfer program.

2. Develop three-dimensional heat transfer program.

3. Incorporate lubrication and wear theory in three-dimensional heat
transfer program.

4. Undertake optimization studies (as noted herein) of clutch and brake
configuration.

DYNAMIC SYSTEMS BEHAVIOR DURING CATAPULT OPERATION

N. GOODIS

BACKGROUND.

The need to define accurately the performance of newer generation catapults requires improved theoretical and quantitative definitions of the complex dynamic behavior of aircraft caused by interaction of aircraft with the launcher, matting, and soil subgrade. Soil and matting elastic and roughness characteristics, interacting with aircraft and catapult tow force histories, produce complex aircraft dynamic behavior, which must be described accurately to define structural and stability characteristics of aircraft during launch. To obtain the optimum catapult design, a mathematical theory of interaction between the aircraft and soil matting combination must be developed to define quantitative effects of the soil matting interaction on aircraft stability and structure.

This mathematical theory will apply also to less complex situations involving aircraft and soil matting interaction without the catapult, under taxiing and take-off conditions.

OBJECTIVE.

Once the basic motion equations of a complex dynamic system are determined, along with their auxiliary kinematic and coupling equations which would allow dynamic interaction and geometric coupling, the question of method of mathematical solution and numerical methods in computer programming is of utmost importance. Previously, dynamic systems have been of moderate complexity or purposefully simplified, and selection mathematical and computer methods was not overly difficult. These systems, by nature of their mathematical solution, were not capable of higher mode vibrations, so that inefficiencies in numerical methods were not detrimental to the computer solution time for a prescribed accuracy. The systems were, in general, of a low frequency nature and dynamically uncoupled so that they could be treated as isolated events. When existing numerical methods are applied to a complex dynamic system and approximate solution time extrapolated, it becomes evident that method inefficiencies not only account for hours of additional computation time and undue cost but also produce mathematical instabilities that invalidate the solution.

It is unlikely that a general method of solution can be found for complex dynamic systems that would fulfill the requirements of optimized computer solution time and accuracy. It is necessary, therefore, to establish separate solution methods for individual components, and modify these methods to account for dynamic coupling. The general scheme is solution

of representative sections of the system that reflect distinctive dynamic characteristics by applying selected mathematical and computer methods that will allow immediate optimization of computer solution time and accuracy. It is doubtful that the "best" method can be found after a brief study; however, a significant achievement would be to develop a feasible method that would allow complex dynamic system investigation while constant improvement of mathematical and computer methods is attempted.

Capabilities and techniques developed in this research effort would greatly advance the stability and structural understanding for both shipboard and land-based launch operations. Practical application of these knowledges would permit:

a. Definition of safer launch operations for both stability and structural considerations.

b. Redesign and improvement of existing launch systems to improve both characteristic features.

c. Develop criteria for needs of refurbishing launch sites and matting installation.

d. Auxiliary studies to describe instrumentation behavior on the aircraft to properly correlate test results with theory.

e. Aircraft ground matting phenomena interaction studies to provide an improved definition of present power spectrum analysis techniques.

ACCOMPLISHMENTS.

The study was conducted in the following phases:

    (1)   literature search and error study;

    (2)   synthesis of theory;

    (3)   development of computer numerical methods and programs; and

    (4)   correlation of mathematical model performance with test and R&D catapult performance.

1. .Literature Search and Error Study.

a. Literature Search. The literature search revealed that the "State of the Art" of numerical analysis is at a saturated level; in that the new advances in the field are actually sophistications and combinations of previously established methods. A large proportion of the work of interest has been solution of differential equations by approximate numerical methods and tabulation of results for accuracy and stability. The differential

- 199 -

equations investigated were linear with constant coefficients
and therefore capable of integration in closed form. Exact
mathematical solutions were used for comparative purposes.
While this work is useful from an academic viewpoint, the
complex dynamic system under consideration cannot be defined
in this manner.

It is unfortunate that the formal mathematical methods
presented in the literature, mask understanding of the physical
problem needed to allow anticipation of system complexities
and subsequent effects. The matrix technique of solution of
dynamic system equations typifies this by obscuring the physical
problem in influence or elastic coefficients. While numerical
solution is important, an equally important aspect is the
"insight" into the mechanism of the problem.

The computer techniques developed in the literature
are direct translations of the methods of numerical analysis
into efficient computer language. While some programming
techniques may be useful, the existing computer programs cannot
be used for the reasons stated above. It is necessary, there-
fore, to use the literature as a loose guide and to establish
independent methods for mathematical solution and computer
programming.

b. Error Study. The criteria for selection of the best
method for solving this complex dynamic system is optimization
of computer solution time and accuracy. Secondary consideration
is given to adjusting methematical methods to computer storage
capacity.

The dynamic system under consideration is defined by
second degree non-linear, ordinary or partial differential
equations with variable coefficients. Because equations of
this type cannot be integrated in closed form, an exact mathe-
matical solution cannot be obtained. It is necessary, therefore,
to generate an "exact" solution that can be used to judge the
accuracy of the solutions obtained from the mathematical methods
to be developed.

The "exact" solution generated must have a minimum
error. Literature shows that error criteria is lacking in theory
and error type magnitudes can be misleading in that they vary
for the type of problem evaluated and the computer used.

Errors are classified into three categories:

(1) truncation

(2) round off

(3) inherent

Truncation error is usually expressed as a factor of the function, and is the magnitude of the highest order term neglected.

Round off error is associated with the last significant digit that is retained by the computer. It is impossible to determine the magnitude of this error by deterministic means, the only solution being of a statistical nature.

Inherent error is a combination of error generation by the process itself or the function. The process generates errors due to previous erroneous information which is used to predict new information. This is analogous to electrical feedback. The function will generate errors due to non-analytical points (Ex. coulomb friction).

Since the round off and inherent error are elusive in their evaluation, it seems safest to generate an "exact" solution on the basis of the truncation error only.

The Taylor series is selected for this purpose since its accuracy in the neighborhood of the origin is determinable. It has the general form:

$$f(a + x) = f(a) + (x - a) f^1 (a) + \frac{(x - a)^2}{2!} f + \ldots \frac{(x - a)^m}{m!} f^m$$

The last term omitted in the series will be classified as the truncation error. Since the origin may be shifted from interval to interval, as (x - a) approaches zero for a given number of series terms, a mean deviation or change in the system should approach zero also.

2. Synthesis of Theory.

a. Dynamic System Model. The general method of solving the dynamic equations which describe an aircraft and associated launching equipment, is applied to both shipboard and shore-based systems, when applicable components are selected for system analysis. To define adequately a system and its interacting dynamic characteristics, each component must be modeled in a sufficient degree of freedom to produce accurate response to parametric influence. A generalized dynamic system model will be composed of the following components:

(1) Dynamic model of aircraft in six degrees of freedom; pitch, roll, yaw, laterial, longitudinal and vertical motions.

(2) Dynamic model of launching dolly in five degrees of freedom; same as aircraft with omission of roll motion.

(3) Dynamic model of matting-soil system.

(4) Dynamic model of catapult with multi-degree of freedom cable dynamics.

The above components would be dynamically interrelated to produce singular or resonant type dynamic histories.

b. Classification of Dynamic System Components. As a model of all system components would be unnecessary for an initial system dynamic analysis, only those components contributing principally to the high and low frequency dynamics were selected for model synthesis. This model, composed of these principal components, is adequate for proper system mathematical definition and development of numerical methods for use in programming. When the feasibility of this analysis scheme is demonstrated, the complete system model will be developed.

The frequency spectrum is divided into high and low bands. The high band includes the bridle and holdback members of the aircraft attachment system, matting-soil system, tow cable system, instrumentation (accelerometers), and aircraft landing gear systems. The low band includes the catapult system and the aircraft system.

(1) Low Frequency Components. These system components may be sub-divided into two categories exhibiting distinctive characteristics:

(a) Corrective Dynamics. Here, there is a dynamic motion that exhibits a corrective nature resulting from a predictable process. This is accomplished by a low estimation at a dynamic interval, which in turn produces a higher estimation at the following interval and vice versa. This results in the following type curve:
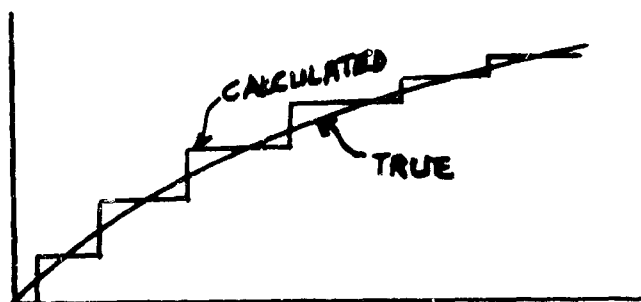
(b) Non-Corrective Dynamics. Here, there is a dynamic motion that exhibits divergent characteristics resulting from an unstable analytical solution. The error generated is accumulative, and the deviation increases with solution time.
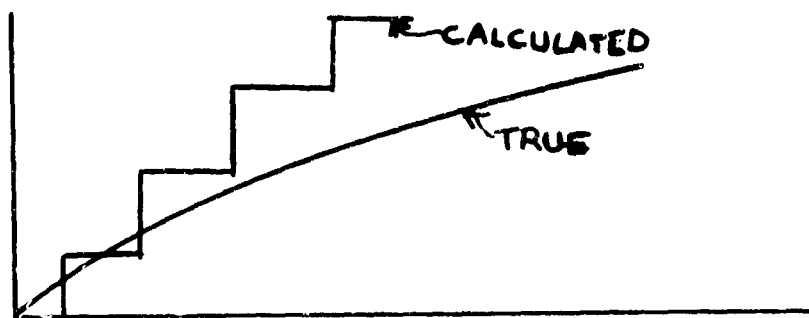
This divergent system is typified by the aircraft in yaw, which is influenced by lateral tire force of a non-linear nature.

(2) High Frequency Components. These system components may also be sub-divided into two categories exhibiting distinctive characteristics:

(a) Distributed Mass. This is characterized by the tow cable system. Since the cable media can be excited by a high frequency component, the frequency response must be allowed for analytically. This can be accomplished by a distributed mass technique in which the inertial characteristics of the system is maintained.

(b) Lumped Mass. The characteristics of these systems are low inertia and high frequency. While the inertial characteristic can be adequately described by the consideration of concentration or omission, special methods must be used to preserve the vibrational integrity. These systems are typically classified by the bridle and holdback members of the aircraft, aircraft landing gears, and matting-soil systems.

3. Development of Computer Numerical Methods and Programs.

a. Numerical Methods. Solution of the general equations of motion which take the form of second order non-linear differential equations, is classified typically as an initial value problem. This type problem can generally be solved by two numerical methods·

(1) Generation of a mathematical series that describes the dynamic process. By direct substitution at suitable intervals, a time history evolves. This is of the form $y = a + bx + cx^2 + dx^3 + \ldots$ This is a complete polynomial approximation and is valid for dynamic systems of small displacement only.

(2) Prediction of unknown dynamic points by polynomial approximation through known pivotal values.

(Given x^1, t^1); $(x^2, \quad t^2)$

Solution $(x^3, \quad t^3)$
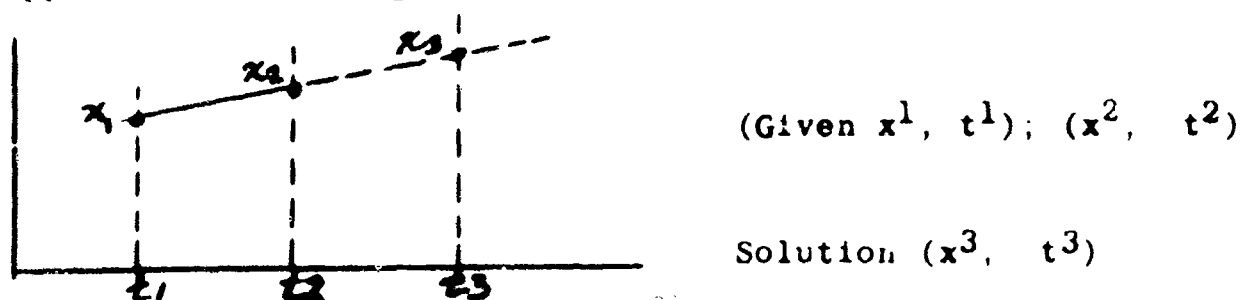
Relation of the variations and modifications of these
two basic methods is beyond the scope of this project.
However, a basic method is used with deviations as necessary
to satisfy the characteristics of each particular problem.

The initial series of numerical methods investigated fall
in the category of function approximation. A function can be
approximated by passing a polynomial through known pivotal
points. The future value is assumed to lie on the curve
generated by the previous values of the function. Subsequent
integration is performed in accordance with the degree of
the function assumed. The integration error will depend upon
the deviation of the polynomial approximation from the true
function for the finite time differential.

Polynomials of degrees one to three were considered for
function generation. The functions operated on are the
first and second derivatives with respect to time, velocity,
and acceleration.

For a general nth degree polynomial (n + 1), pivotal
points must be known to predict a future value. The values
for formulas below are for equally spaced intervals. The
predicted values for the polynomials are in general form:

$$n = \text{degree of polynomial}$$

$$Y_{n+2} = Ay_{n+1} + By_n + Cy_{n-1} + Dy_{n-2}$$

Polynomial Degree	A	B	C	D
1°	2	-1	0	0
2°	3	-3	1	0
3°	4	-6	4	-1

The subsequent integration is of the general form:

$$Y_{n+2} = Y_{n+1} + t (A\,y^1_{n+2} + By^1_{n+1} + Cy^1_n + Dy^1_{n-1}$$

Polynomial Degree	A	B	C	D
1°	1/2	1/2	0	0
2°	5/12	8/12	-1/12	0
3°	9/24	19/24	-5/24	1/24

A general type sub-program was devised which allowed for maximum flexibility in polynomial approximation. The program permits selection of derivative order to be extrapolated, and also selection of the polynomial degree. Initial pivotal points for the polynomial approximation are controlled by an iterative process. Their exactness is controlled by either a tolerance on the function itself or a predetermined number of iterations.

b. Programs.

(1) Generalized Aircraft Description Program.

(a) Pitch Plane. The aircraft is described in two rigid modes - vertical translation and rotation. The airframe is considered to be rigid. The landing gears are treated as standard oleo pneumatic shock struts. The dynamic analysis considers hydraulic friction forces, which can be adequately represented by a non-linear dashpot, non-linear spring, and coulomb damping. The unsprung mass represents the strut and tire-axle assembly. The tire deflections are represented by a non-linear spring constant. This complete assembly is elastically connected to a rigid air frame coupled by a linear spring constant.
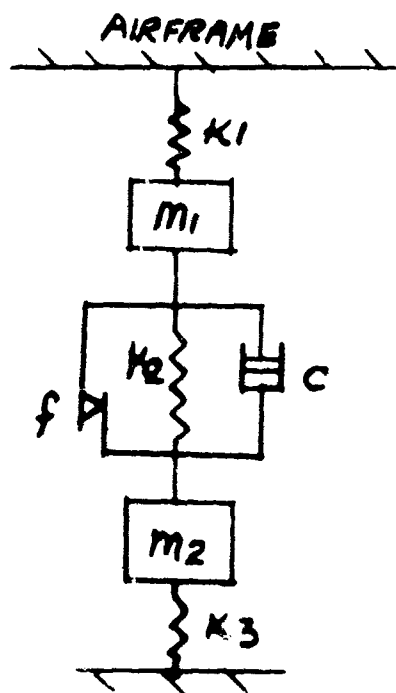
k_1 Structural spring constant

k_2 oleo spring constant

c   oleo viscous damping

f   coulomb damping

m_1 oleo housing mass

m_2 unsprung mass (oleo, tire wheel)

k_3 tire spring constant

AIRCRAFT IN LAUNCH - DYNAMIC PITCH

R1 - NOSE WHEEL LOAD
R2 - MAIN WHEEL LOAD
ΘΕΘ - PITCH ANGLE
1G - C.G HEIGHT
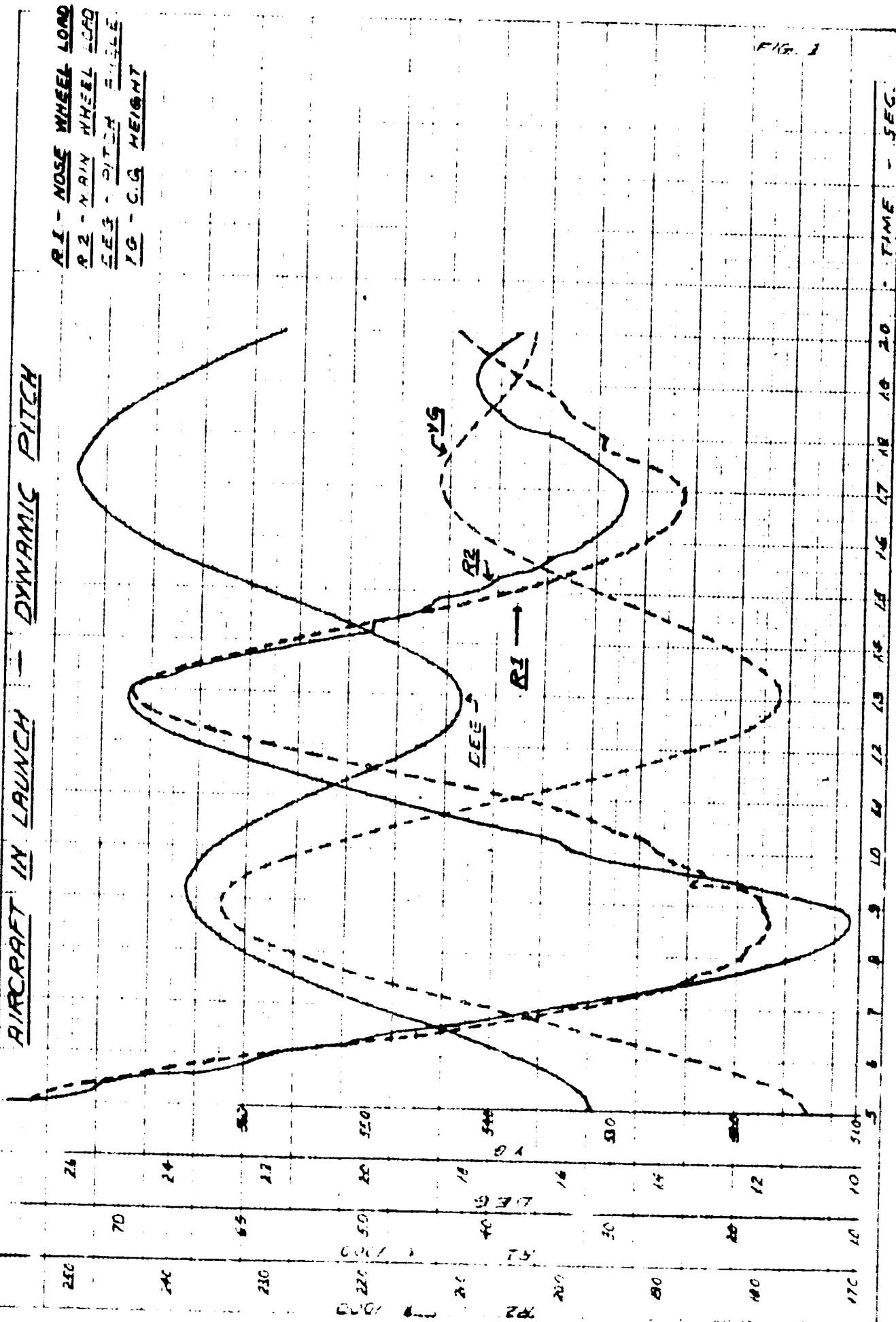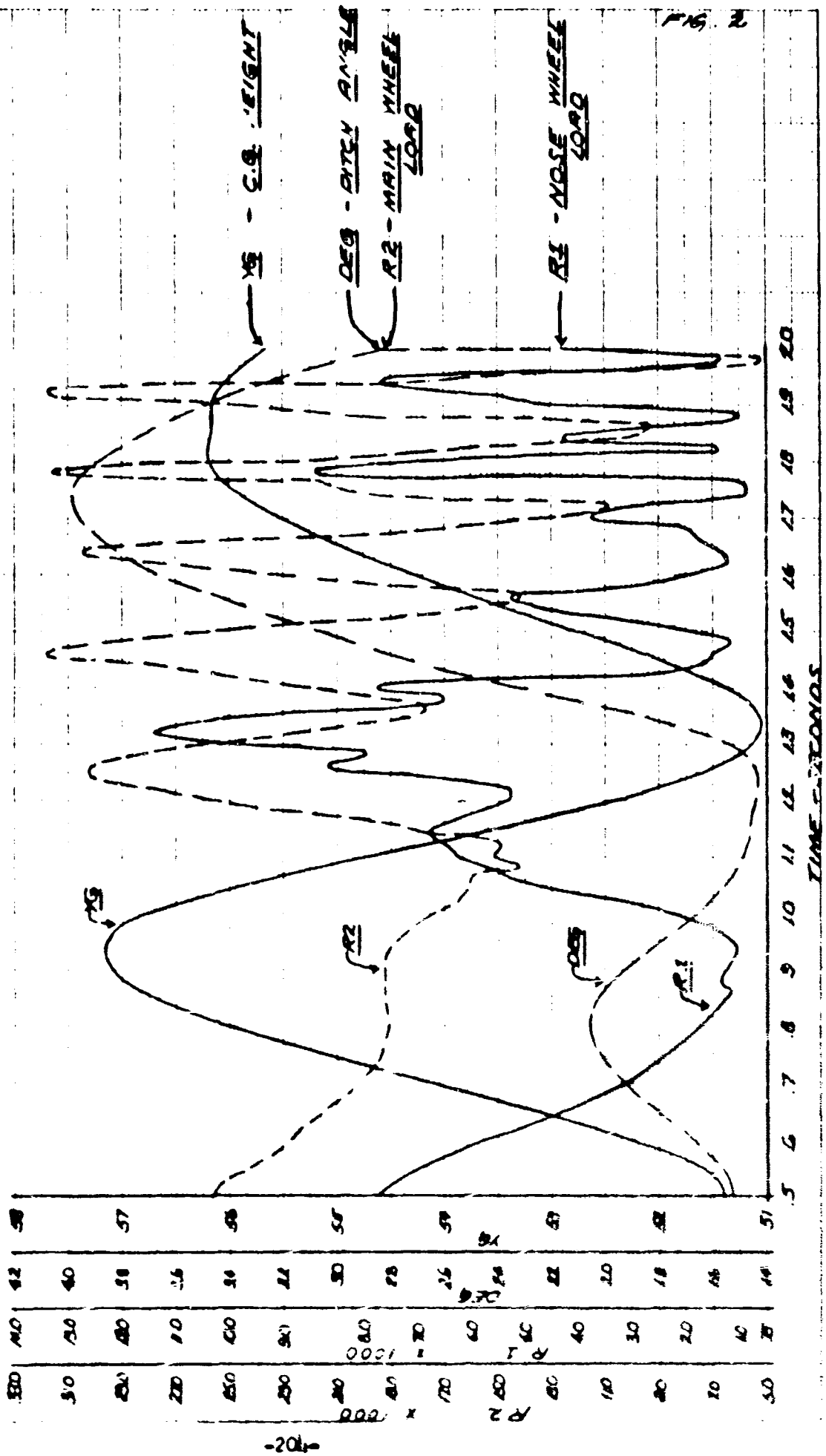
TIME - SEC.

FIG. 1

AIRCRAFT IN LAUNCH — DYNAMIC PITCH

FIG. 2

Y5 — C.G. HEIGHT

DEG — PITCH ANGLE

R2 — MAIN WHEEL LOAD

R1 — NOSE WHEEL LOAD

TIME SECONDS

-207-

AIRCRAFT IN LAUNCH - DYNAMIC YAW
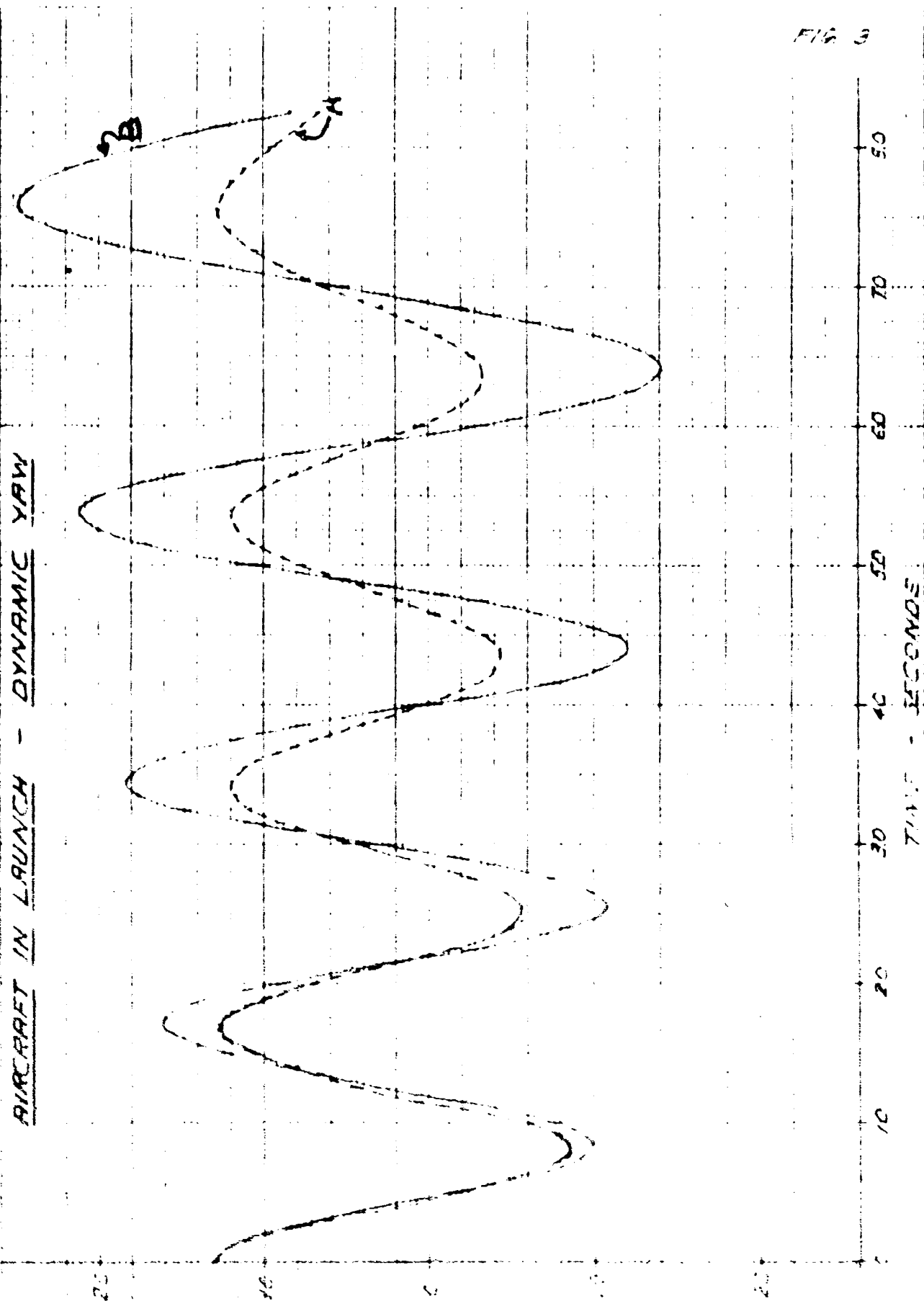
FIG. 3

TIME - SECONDS

This representation is adequate to describe dynamic actions that result from forcing functions produced by surface roughness of a static or dynamic nature.

The generalized aircraft pitch motion was programmed for a digital computer and preliminary series of computer studies were initiated. An aircraft in launch was exposed to surface conditions at zero roughness, and also to a measured survey roughness that was favorable utilizing the criteria of the power spectra method. These computer studies showed no adverse results, and the gear motions and pitch angle of attack were not excessive. A typical result is shown in Figure 1.

To investigate more intensified dynamic landing gear action and also stability of computer technique and mathematical stability, a ten foot wave length of two inch amplitude was imposed during the aircraft launch. The results are shown in Figure 2. A quasi-dynamic matting-soil system was used in the above analysis to account for load deflection characteristics.

The generalized sub-program of integration technique has been written and programmed for this section of the system, and investigations are being made concerning the stability and accuracy of the highly vibrating landing gear system.

(b) Yaw Plane. Initial studies, utilizing mathematical methods described, were applied to the aircraft model in a yaw plane. This system, under the environment of a vibratory landing gear load history, produces a resonant type instability or escalating yaw angle history. This system is further complicated by a non-corrective integration characteristic which accumulates the error of integration.

This characteristic can be seen in Figure 3, Curve B, which exhibits a rapid rate of yaw angle escalation. Utilizing a polynomial approximation under the same time differential, and the same computational time, curve A was generated. The dynamic values agree to within 6 significant figures with results obtained utilizing the method that was used to generate curve A, but with a time interval reduction of 1/100. The final result was a six significant figure accuracy with a computational time reduction of approximately 20 to 1.

Since the yaw studied was a duplication of an actual launch, a small initial displacement angle was imposed. In order to verify the numerical techniques, a series of computer studies were made with an initial displacement angle of 10 degrees which would correspond to a large displacement system. Comparative results were obtained for solution time and accuracy.

(2)   Additional Programs.

Dynamic coupling of the aircraft in the pitch and yaw planes of motion are being programmed for a digital computer. This coupling is achieved by a series of sub-programs with control options that would allow a mode to be either coupled or uncoupled. Additional flexibility is achieved by the predetermined selection of mathematical technique for each characteristic dynamic member of the composite system.

Investigations into computer techniques were made for the tow cable system. Utilizing previous work that allows for mass distribution criteria, a series of computer studies were made with techniques that minimized errors in significant digit arithmetic. A satisfactory method of solution was obtained that allowed for minimum error and mathematical stabili* of the system. The criteria for mass distribution was reven.fied.

FUTURE PLANNING.

1. Numerical Methods.   Further investigation of the stability of integration and optimization of solution time-accuracy will be made, utilizing other numerical methods which can be class-ified as:

    a   Semi-iterative - predictor-corrector.

    b.   Iterative.

    c.   Function prediction utilizing a prior error history.

2. Synthesis of Complete Launch System.   Each dynamic component of the system will be developed and programmed for a digital computer. The system will be flexible in that any combination can be dynamically coupled. Each section will operate independently with respect to its most efficient solution technique.

3. Computer Technique. Development of computer techniques needed for efficient and flexible operation of programmed components.

4. Matting-Soil System.

    a. Synthesis of dynamic model utilizing wave form genera-tion.

    b. Investigation of parametric effects of:

    (1) Soil variations.

    (2) Water leakage.

(3) Soil erosion or degeneration.

(4) Runway roughness variations.

5. Cable dynamics studies into non-linear damping and elasticity characteristics

6. Correlation of mathematical model to test results.

7. Continued effort to accomplish previously specified objectives.

MISSILE LAUNCHING CONCEPTS FOR DEEP DEPTH OPERATIONS

E. T. BUTKIEWICZ

BACKGROUND.

The participation of the Naval Air Engineering Laboratory (SI) (NAEL(SI)) in the Advanced Sea-Based Deterrence (ASBD) Long Range program has been documented in publications (references 1 thru 7) encompassing the four year period from 1960 to 1964. Authorization has been under reference (8) up to the 1964 Summer Study Program (Project SEABED), as convened during June-July 1964 at the U. S. Naval Postgraduate School, Monterey, California. The NAEL(SI) efforts were directed toward obtaining as much timely information as possible to provide the Study Group with technical inputs for ASBD missile launching systems evaluation. At this point, NAEL(SI) tasks were terminated.

In an attempt to bridge the remaining gaps, this project has been initiated under the Foundational Research Program. Phase I of this effort, as reported here in a preliminary manner, involves (1) the investigation of current literature to determine the feasibility of pursuit (FOP), and (2) the formulation of program objectives to be fulfilled within the Phase II time frame.

OBJECTIVES.

1. To determine the FOP of missile launching systems concepts for future sea-based deterrence operations, by means of a continuing literature search.

2. To formulate the program objectives to be considered within the next phase of effort.

3. To establish the tentative implementation plan for the conduct of research for the development of computer techniques.

4. To review the program status and overall data completeness to determine remaining gaps and avoid duplication of effort.

ACCOMPLISHMENTS.

The pioneering literature search efforts well underway prior to the construction of a realistic feasibility study is unquestionably extensive. A broad base has been laid during the past five years in an attempt to encompass all technological inputs directed toward defining the 1970-era ASBD Weapons Complex. As a result, over 1,000 reports, proposals, etc. have emanated from both private industry and Government activities. Within this period, the sifting process of several of these publications has been conducted in an attempt to determine the overall program status and data completeness so that the FOP of this program may be established.

-202-

In this sifting process of ASBD literature, several noteworthy aspects stand out. Of the studies conducted elsewhere within the area of ASBD missile launching systems, the relationship to previous NAEL(SI) investigations does exist; however, the analytical approach relationship is not evident. The primary reason for this omission appears to lie in the intended application of these ASBD concepts. Significant departure from the analytical techniques, therefore, as to be adapted under this phase of effort, is possible. As a result, the data obtained from these other studies (for example, solid propellant density, molecular weight, burning rate exponents, etc.) may be applied as inputs to the computer programs to be initiated during the next phase of effort.

The ASBD missile launching concept converged upon at NAEL(SI) up to the 1964 Summer Study Program (Project SEABED) is termed the Hybrid Powered Flotation and Solid Propellant Launcher Concept (Variant D). This concept (references 4 and 6) could not be treated in the detail of some of the other concepts in time for Project SEABED; however, in comparing the launcher power-plant sizing characteristics for this concept, significant distinguishing features were readily seen. Continued exploitation of this concept for detailed evaluation is necessary to determine its relative "worth", limitations, sensitivity, etc., as a candidate missile launching concept for deep depth (6,000-20,000 ft.) operations.

As indicated in references 9 and 10, hybrid missile launching concepts as considered comprise the basic configuration utilizing the secondary injection of a liquid monopropellant in the launch cycle. The combined flotation/solid propellant system as envisaged here has not been revealed through this literature search thus far. Direct contact with several of the key participating activities would provide additional insight into the methodology adopted there during their course of study, so that technical inputs may be derived and updated information obtained. There are many promising directions, and the logical cyclic spin-off will evolve during the next phase of effort.

FUTURE PLANS.

The following plan defines and describes the logical implementation envisaged under the Foundational Research Program to be conducted during the period from 1 July 1965 to 30 June 1967:

1. To explore the literature constantly to determine current state of the art developments for solid propellants and collateral studies relevant to advanced under-sea missile launching concepts.

2. To exercise the existing Solid Propellant Gas Generator and Flotation computer programs with updated inputs. An estimated total of six (6) computer programs is involved.

3. To revise and execute the "Theoretical Launch Performance" Solid Propellant Gas Generator (G.G. Mod -6E) computer program by incorporating a non-iterative analytical technique. This revision will result in generating a new computer program capable of faster computer running time, and will serve as the guideline in the analytical approach for the solid propellant performance portion of the Variant "D" hybrid missile launching concept.

4. To contact the pertinent participating government and contractor activities through short visits as necessary to obtain definitive inputs, such as capsule/missile weights, solid propellant density, molecular weight, burning rate characteristics, etc., to execute the mathematical model computer programs.

5. To incorporate the necessary additions and conversions to the key computer programs, so that compilation and execution may be performed on the faster, larger-capacity computer equipment available at commercial data centers on a rental basis.

6. To document the computer programs to systemize the orderly flow of analytical effort to be applied in the next stage of program development.

7. To develop the analytical techniques directed toward developing the computer programs for the theoretical evaluation of the Variant "D" hybrid ASBD missile launching concept.

8. To exercise this newly developed program with specific inputs to arrive at the theoretical launch history profile. With definitive inputs, a thorough, detailed evaluation resulting in the measurement of the relative "worth" of this concept in comparison to other candidates may be derived.

It should be noted that the above merely provides the preliminary planning for this task in order to establish some procedural criteria, and it is possible that sharp deviations therefrom may evolve during the course of the study as a result of the many considerations involved. As a result, recommendations for program segmentation into other funded programs to provide additional study requirements may be specified.

REFERENCES.

1 NAEF-ENG-6781 "Launch Systems Investigations for Advanced Fleet Ballistic Missiles" 29 March 1961 (SECRET)

2. NAEL-ENG-6918 "Theoretical Evaluation of the High Temperature High Pressure Launching System (HTHP) Relative to Long Range Research and Development for Advanced Sea Based Deterrence", 1 August 1962 (CONFIDENTIAL)

3 NAEL-ENG-7107 "Developmental Studies of a High Temperature High Pressure Launching System, Phase I", 8 April 1964

REFERENCES (Continued)

4   NAEL-ENG-7179 "Rationale and Criteria for Advanced Sea
    Based Deterrent Systems", 8 June 1964 (CONFIDENTIAL)

5   NAEL-ENG-7180 "Theoretical Evaluation of Static Sea
    Pressure Missile Launching Concept for Advanced Sea Based
    Deterrent Systems (Captive Sabot Concept)", 8 June 1964
    (CONFIDENTIAL)

6   NAEL-ENG-7181 "Theoretical Evaluation of Solid Propellant
    Gas Generator Missile Launching Concepts for Advanced Sea
    Based Deterrence", 14 August 1964 (CONFIDENTIAL)

7   NAEL-ENG-7182 "Theoretical Evaluation of Tubeless Simple
    Flotation Concepts for Advanced Sea Based Deterrence"
    16 June 1964 (CONFIDENTIAL)

8   Authorization: WEPTASK N.. RMLG-30-006/200-1/F009-01-016
    of 9 August 1960

9   NOTS IDP 2074 "State of the Art for Underwater Launch for
    Advanced Sea Based Deterrent Systems (C)", United States
    Naval Ordnance Test Station, Pasadena, California, 3 May 1964
    (CONFIDENTIAL)

10 WEC ASE TN-343 "Preliminary Calculations on Fixed Program
    Ejection Systems for Deep Depth", Westinghouse Electric
    Corp., Sunnyvale, California, 22 August 1962 (CONFIDENTIAL)

HYDROGEN EMBRITTLEMENT OF METALS AND ALLOYS

WALTER BECK AND EDWARD J. JANKOWSKY

Background.

During the past ten years, many reports on hydrogen embrittlement have been published, including several generated from the work conducted at the Aeronautical Materials Laboratory. These reports have dealt with the mechanism, testing, alleviation, and generation of hydrogen embrittlement induced in metals by a variety of procedures. Their content is frequently confusing and attempts to gather the information together have been very limited in scope. A book in which the useful procedures are separated from the ineffective, a critical analysis made of the various suggested mechanisms, and all the practical aspects of testing for and minimizing hydrogen embrittlement are set forth, would be of great value to materials engineers, aircraft designers, corrosion engineers, and metallurgists.

Objective.

The objective of this project is to review all the reports on hydrogen embrittlement published during the past ten years and present the information in the form of a book.

Accomplishments and Future Plans.

The project was started in June 1965. All the reports, papers, and other publications on hydrogen embrittlement are being gathered together and cataloged for future reference. Work on the section on testing procedures will begin immediately after the cataloging is complete.